

March 2019

HYBRIDIZED POLYMERIC NANO-ASSEMBLIES: KEY INSIGHTS INTO ADDRESSING MDR INFECTIONS

Ryan Landis
University of Massachusetts Amherst

Follow this and additional works at: https://scholarworks.umass.edu/dissertations_2



Part of the [Alternative and Complementary Medicine Commons](#), [Bacterial Infections and Mycoses Commons](#), [Biochemistry Commons](#), [Food Chemistry Commons](#), [Medicinal Chemistry and Pharmaceutics Commons](#), [Nanomedicine Commons](#), [Other Immunology and Infectious Disease Commons](#), [Pathogenic Microbiology Commons](#), [Skin and Connective Tissue Diseases Commons](#), and the [Therapeutics Commons](#)

Recommended Citation

Landis, Ryan, "HYBRIDIZED POLYMERIC NANO-ASSEMBLIES: KEY INSIGHTS INTO ADDRESSING MDR INFECTIONS" (2019). *Doctoral Dissertations*. 1522.
<https://doi.org/10.7275/13190278> https://scholarworks.umass.edu/dissertations_2/1522

This Open Access Dissertation is brought to you for free and open access by the Dissertations and Theses at ScholarWorks@UMass Amherst. It has been accepted for inclusion in Doctoral Dissertations by an authorized administrator of ScholarWorks@UMass Amherst. For more information, please contact scholarworks@library.umass.edu.

**HYBRIDIZED POLYMERIC NANO-ASSEMBLIES:
KEY INSIGHTS INTO ADDRESSING MDR
INFECTIONS**

A Dissertation Presented

By

RYAN F. LANDIS

Submitted to the Graduate School of the
University of Massachusetts Amherst in partial fulfillment
Of the requirements for the degree of

DOCTOR OF PHILOSOPHY

February 2019
Chemistry

© Copyright by Ryan F. Landis 2019
All Rights Reserved

HYBRIDIZED POLYMERIC NANO-ASSEMBLIES: KEY INSIGHTS INTO ADDRESSING MDR INFECTIONS

A Dissertation Presented

By

RYAN F. LANDIS

Approved as to style and content by:

Vincent M. Rotello, Chair

Richard W. Vachet, Member

Dhandapani Venkataraman, Member

Gregory N. Tew, Member

Richard W. Vachet, Department Head
Department of Chemistry

DEDICATION

To my mother and father who never gave up on me.

ACKNOWLEDGEMENTS

I am grateful to my research advisor, Prof. Vincent M. Rotello, for allowing me to join his group for the duration of my PhD studies. His laboratory resources and research staff were very helpful to accelerate the pursuit of my thesis intentions. Notably, his insights into his unique scientific writing style has improved my writing capacity and I am most thankful for that.

I sincerely appreciate my thesis committee members, Professors Richard W. Vachet, Dhandapani Venkataraman, and Gregory N. Tew. Their immense insight and valuable advice was fundamental during my PhD period. I truly hope that during my progression through each qualifier examination, I demonstrated not only improvements, but competency as a chemist.

Completion of my PhD work would not have been possible without some of the most profound collaborations I could ever hope to be a part of. I wish to thank Dr. Bradley Duncan and Dr. Xiaoning Li for their efforts in laying the foundational work for antimicrobial testing. Furthermore, I am most grateful to two of my co-workers: Akash Gupta and Cheng-Hsuan 'Ian' Li. Their expertise in bacteria biologics, assays, and data analysis coupled with immense "elbow-grease" was fundamental to completing my PhD work. My hope is that in the future, I can repay them in a manner that I deem suitable (Not just simply words, publications and/or patents). Thank you, Akash. Thank you, Ian.

I consider myself fortunate to have done my PhD work during when such incredible individuals were employed in the chemistry department at the University of

Massachusetts Amherst. My sincerest thanks to Carol Greene, J.M. Stowe, Robert Sabola, Ryan Feyrer, Dennis Glick, Marvin Ellin, Deirdre McDaniel, Vicki Hubby, Kay Fenlason, Kristina Knight, Glenda Pons, and the entire chemical delivery staff. Thank you everyone, truly.

ABSTRACT

HYBRIDIZED POLYMERIC NANO-ASSEMBLIES: KEY INSIGHTS INTO ADDRESSING MDR INFECTIONS

FEBRUARY 2019

RYAN F. LANDIS

B.Sc., UNIVERSITY OF PITTSBURGH

Ph.D., UNIVERSITY OF MASSACHUSETTS AMHERST

Directed by: Professor Vincent M. Rotello

Multidrug-resistant (MDR) bacteria contribute to more than 700,000 annual deaths world-wide. Millions more suffer from limb amputations or face high healthcare treatment costs where prolonged and costly therapeutic regimens are used to counter MDR infections. While there is an international push to develop novel and more powerful antimicrobials to address the impending threat, one particularly interesting approach that has re-emerged are essential oils, phytochemical extracts derived from plant sources. While their antimicrobial activity demonstrates a promising avenue, their stability in aqueous media, limits their practical use in or on mammals. Inspired by the versatility of polymer nanotechnology and the sustainability of traditional medicine, I employed a hybridization approach to improve the stability and subsequently the antimicrobial activity of phytochemical extracts. This approach was accomplished through a crosslinked Nano-emulsification templating strategy, generating a highly robust and reproducible library of potent oil-in-water Nano-assemblies. These assemblies, stabilized using synthetic or natural polymers, demonstrated long-term shelf life, high stability in serum-containing aqueous environments, and most

notably, were demonstrated to penetrate highly refractory biofilm infections, eliminating a broad-spectrum of pathogenic bacteria where accumulated resistance towards these materials were not observed during the course of laboratory experiments. Taken together, the technology presented herein, offers key insight into addressing MDR-associated infections with hopes that future platforms can be built from to tackle the rising dangers of MDR infections.

TABLE OF CONTENTS

	Page
ACKNOWLEDGEMENTS	v
ABSTRACT	vii
LIST OF TABLES	xv
LIST OF FIGURES	xvi
CHAPTER	
1. ORIGIN, CHALLENGES, AND STRATEGIES TO ADDRESS MULTIDRUG-RESISTANCE	1
1.1. Origin and Evolution of Antibiotic-Mediated MDR	1
1.1.1 MDR Origin	1
1.1.2 MDR Evolution.....	3
1.1.3 Enzyme-Mediated Resistance	5
1.1.4 Efflux Pump-Mediated Resistance	5
1.1.5 Gene Transfer-Mediated Resistance	6
1.1.6 Target Site Modification-Mediated Resistance	7
1.2. Multidrug-Resistance in Biofilm Microcolonies	7
1.2.1 Antibiotic Penetration Paradox	8
1.2.2 Antibiotic-Modifying Enzyme.....	8
1.2.3 Extracellular DNA	9
1.2.4 Biofilm Infections in Hospitals.....	10
1.3. Challenges of Current Methods in Treating MDR	10
1.3.1 Antibiotics.....	10
1.3.2 Debridement.....	12
1.4. Emerging Strategies to Counter MDR.....	13
1.4.1 Host-Defense Peptides	13
1.4.2 Phage Therapy	15
1.4.3 Antibodies	16
1.4.4 Quorum Sensing Inhibitors	17
1.4.5 Essential Oils / Phytochemical Extracts	18
1.4.6 Limitations	20

1.4.7 Encapsulation Strategies	21
1.5. Dissertation Overview	22
1.6. References.....	24
2. CROSSLINKED POLYMER-STABILIZED NANOCOMPOSITES FOR THE TREATMENT OF BACTERIAL BIOFILMS	31
2.1. Introduction.....	31
2.2. Results.....	33
2.2.1 Generation and Characterization of Nanocomposites.....	33
2.2.2 X-NCs Penetration into Biofilms.....	36
2.2.3 Antimicrobial Activity of X-NCs Against Biofilms.....	37
2.2.4 Eradication of Biofilms in a Co-culture Model	38
2.2.5 Serum Stability of X-NCs.....	39
2.3. Conclusions.....	40
2.4. Experimental Protocols.....	41
2.4.1 Materials and Methods.....	41
2.4.2 Synthesis of PONI-GAT	41
2.4.3 Preparation of Nanocomposites	42
2.4.4 Fluorescamine Assay	42
2.4.5 Biofilm Formation	42
2.4.6 Biofilm – 3T3 Fibroblast Cell Co-culture.....	43
2.5. Supporting Figures.....	44
2.5.1 Shelf life of X-NCs	44
2.5.2 Synthesis of PONI-GAT	44
2.5.3 Zeta Potential	50
2.5.4 Attenuated Total Reflectance Fourier Transform Infrared Spectroscopy (ATR-FTIR).....	51
2.5.5 Serum Stability of Non-Crosslinked NCs.....	53
2.6. References.....	54
3. DYNAMICALLY CROSSLINKED POLYMER NANOCOMPOSITES TO TREAT MULTIDRUG-RESISTANT BACTERIAL BIOFILMS	59
3.1. Introduction.....	59
3.2. Results.....	61

3.2.1	Generation and Characterization of DCPNs	61
3.2.2	Stability and pH Responsiveness of DCPNs	63
3.2.3	DCPNs Penetration into Biofilm	65
3.2.4	DCPNs Antibiofilm Activity	66
3.2.5	Cytotoxicity Assessment of DCPNs Against Fibroblast Cells	68
3.3.	Conclusions.....	69
3.4.	Experimental Protocols.....	70
3.4.1	Chemicals and Reagents	70
3.4.2	Fabrication of DCPNs.....	70
3.4.3	MIC Measurements.....	71
3.4.4	Antibiofilm Activity Measurements	71
3.4.5	Cytotoxicity Evaluation of DCPNs Against Fibroblast Cells.....	72
3.4.6	TEM, Dynamic Light Scattering (DLS), Confocal Scanning Laser Microscopy (CSLM), and SEM Methods.....	72
3.4.7	Evaluate DCPNs Imine Bond Displacement	73
3.5.	Supporting Figures.....	73
3.5.1	Synthesis and Characterization of Crosslinker 1,3,5,7-Tetrakis(4- formylphenyl) adamantane (ATA)	74
3.5.2	Synthesis and Characterization of DCPNs	76
3.5.3	Dynamic Light Scattering (DLS) of DCPNs	76
3.6.	References.....	80
4.	BIODEGRADABLE NANOCOMPOSITE ANTIMICROBIALS FOR THE ERADICATION OF MULTIDRUG-RESISTANT BACTERIAL BIOFILMS WITHOUT ACCUMULATED RESISTANCE.....	83
4.1.	Introduction.....	83
4.2.	Results.....	85
4.2.1	Generation and Characterization of Nanocomposites.....	85
4.2.2	Stability and Degradability of X-BNCs.....	87
4.2.3	Antimicrobial Activity of X-BNCs Against Biofilms	88
4.2.4	Selective Killing of Biofilms in a Co-culture Model.....	91
4.2.5	Bacterial Resistance Towards Antibiotics Vs. X-BNCs.....	92

4.3. Conclusions.....	95
4.4. Experimental Protocols.....	95
4.4.1 Materials and Methods.....	95
4.4.2 Preparation of Nanocomposites.....	95
4.4.3 Biofilm Formation.....	96
4.4.4 Biofilm – 3T3 Fibroblast Cell Co-culture.....	96
4.4.5 Membrane Disruption Study <i>via</i> PI Staining.....	97
4.4.6 Synthesis of DTDS (3).....	98
4.4.7 Synthesis of PONI-GMT.....	100
4.4.8 Synthesis of TAMRA-PONI-GMT.....	105
4.5. Supporting Figures.....	105
4.5.1 DTDS Storage Stability.....	106
4.5.2 Zeta Potential of X-BNCs.....	106
4.5.3 Long-Term Storage of X-BNCs.....	106
4.5.4 Serum Stability of NX-NCs.....	107
4.6. References.....	109
5. NATURE-DERIVED CROSSLINKED NANOCOMPOSITES FOR A SUSTAINABLY-RELAVENT TREATMENT OF MULTIDRUG-RESISTANT BIOFILMS.....	114
5.1. Introduction.....	114
5.2. Results.....	116
5.2.1 Generation of GEL-XCs.....	117
5.2.2 Morphology of GEL-XCs.....	118
5.2.3 Chemical Identification of GEL-XCs.....	120
5.2.4 Stability of GEL-XCs.....	122
5.2.5 Biological Activity of GEL-XCs.....	123
5.2.6 Scalability of GEL-XCs.....	125
5.3. Conclusions.....	127
5.4. Experimental Protocols.....	127
5.4.1 Materials and Methods.....	127
5.4.2 Preparation of GEL-XCs.....	128
5.4.3 Biofilms Formation.....	128

5.5. References.....	129
6. ENGINEERED POLYMER NANOPARTICLES WITH UNPRECEDENTED ANTIMICROBIAL PROPERTIES FOR THE TREATMENT OF MULTIDRUG- RESISTANT BACTERIAL AND BIOFILMS INFECTIONS	132
6.1. Introduction.....	132
6.2. Results.....	134
6.3. Conclusions.....	143
6.4. Experimental Protocols.....	144
6.4.1 Synthesis of Grubbs 3 rd Generation Catalyst.....	144
6.4.2 Determination of Antimicrobial Activities of Cationic Polymers	144
6.4.3 Determination of Hemolysis of Cationic Polymers	144
6.4.4 Macrophage Cell Studies and TNF-alpha Secretion.....	145
6.4.5 Polymer Nanoparticles and LPS Treatment.....	146
6.4.6 Propidium Iodide Staining Assay	146
6.4.7 Biofilm Formation and Treatment	146
6.4.8 Biofilm – 3T3 Fibroblast Cell Co-culture.....	147
6.4.9 Resistance Development.....	148
6.5. Supporting Figures.....	148
6.5.1 Oxanorbornene Monomer Synthesis.....	148
6.5.2 Oxanorbornene Polymer Synthesis.....	150
6.5.3 Synthesis of 5 Quaternary Ammonium Polymers	150
6.5.4 FRET NP Formation	151
6.5.5 TEM Characterization of Polymeric Nanoparticles.....	152
6.5.6 Biofilm Penetration Studies Using Confocal Laser Scanning Microscopy	152
6.5.7 Mammalian Cell Viability Assay.....	154
6.5.8 Therapeutic Indices Against Biofilms	155
6.5.9 Critical Micelle Concentration Study	156
6.6. References.....	159
7. HYBRIDIZED NANO-ASSEMBLIES: A PARADOX IN BIOFILM PENETRATION.....	164
7.1. Antimicrobial Nanocomposites	164
7.1.1 Electrostatic Argument Doesn't Hold with Biofilms.....	165

7.1.2 Consider Mechanical Dynamics	166
7.1.3 Consider Biochemical-Mediated Mechanical Dynamics.....	167
7.2. Antimicrobial Polymeric Nanoparticles	169
7.2.1 Looking Beyond Amphiphilic Balance and Membrane Disruption	169
7.2.2 Further Analysis into Polymeric Nanoparticle Biofilm Dynamics.....	171
7.2.3 Optimization to Prevent Protein Fouling	172
7.3. References.....	174
BIBLIOGRAPHY.....	176

LIST OF TABLES

Table	Page
1.1. List of common antibiotic classes, their action mechanism, and common bacterium resistant towards their mode of action	3
1.2. List of common “Superbugs”, common infection sites, and common antibiotics they are resistant towards.....	4
1.3. List of common Phytochemicals and their structure, plant sources, and some biological activities	20
3.1. MICs of the 5wt%DCPN against different strains of bacteria.....	79
6.1. Minimum inhibitory concentrations and therapeutic indices of P5 NPs against multiple uropathogenic clinical isolate bacterial strains.....	138

LIST OF FIGURES

Figure	Page
1.1. Common routes of acquired resistance	5
1.2. ‘Hockey-Stick Projection’ indicates resistance continues to rise exponentially while antibiotic discovery in industry drops to zero in the late 1980s	12
2.1. Strategy used to generate antimicrobial composites.....	33
2.2. Physical and chemical characterization of X-NCs.....	36
2.3. Confocal image stacks of <i>E. coli</i> DH5 α biofilm after 3 h treatment with 10 wt% X-NCs	37
2.4. Viability of 1 day-old biofilms	38
2.5. Viability of 3T3 fibroblast cells and <i>P. aeruginosa</i> biofilms in the fibroblast – biofilm co-culture model after 3 h treatment with 10 wt% X-NCs at different emulsion concentrations (v/v % of emulsion)	39
2.6. Stability of X-NCs in 10% fetal bovine serum (FBS)	40
2.7. DLS size of X-NCs	44
2.8. ¹ HNMR spectra of a) protected and b) deprotected PONI-GAT.....	50
2.9. Zeta potential of X-NCs with varying wt% of p-MA-alt-OD.....	51
2.10. ATR-FTIR analysis before and after emulsification	52
2.11 Fluorescamine calibration curve.....	53

2.12. DLS size of a) 10% fetal bovine serum only and b) non-crosslinked nanocomposites	53
3.1. Schematic depiction of the strategy to generate DCPNs along with the chemical structures of ATA crosslinker and PONI-GAT	60
3.2. Confocal micrographs of the corresponding micron-sized counterparts of DCPNs...	63
3.3. DLS curves of DCPNs	65
3.4. Representative 3D views of confocal image stacks of RFP-expressing DH5 α <i>E. coli</i> biofilms	66
3.5. Viability of 1 day-old biofilms	68
3.6. Viability of 3T3 Fibroblast cells after treated with 5 wt% DCPN at different emulsion concentrations for three hours	69
3.7. ¹ HNMR spectrum of ATA with CDCL ₃ as the solvent.	75
3.8. Attenuated Total Reflectance Fourier Transform Infrared Spectroscopy (ATR-FTIR) spectrum of ATA	76
3.9. ATR-FTIR spectra of DCPN and NonPN	76
3.10. DLS curves monitoring imine-oxime displacement in PBS	77
3.11. Variation of DLS curves detected after incubated half an hour in serum media for DCPN	77
3.12. DLS curves monitoring the shelf life of DCPN and the NonPN control.....	78
3.13. SEM micrographs of pathogenic planktonic bacteria.....	79

4.1. (a) Crosslinked PONI-GMT-DTDS structure showing linkage points reactive to endogenous biomolecules	85
4.2. Stability and degradability of X-BNCs	88
4.3. Confocal image stacks and penetration profile of <i>E. coli</i> DH5 α biofilm after 1-hour treatment with X-BNCs loaded with DiO.....	89
4.4. Viability of one-day-old Gram-negative/positive biofilms after a three-hour treatment with X-BNCs	90
4.5. Viability of 3T3 Fibroblast cells and <i>P. aeruginosa</i> biofilms in the coculture model after treating X-BNCs at different emulsion concentrations for three hours.....	92
4.6. Accumulated resistance of pathogenic <i>E. coli</i> (CD-2) in both plankton and biofilm settings	94
4.7. Storage of DTDS.....	106
4.8. Zeta potential of X-BNCs	106
4.9. Size distribution of X-BNCs stock solution in PBS after 1 year of storage	107
4.10. DLS size distribution	107
4.11. Percentage of <i>P. aeruginosa</i> stained by propidium iodide (PI) following treatment with X-BNCs or ciprofloxacin.....	108
5.1. a) Schematic depiction of GEL-XCs generation	118
5.2. a) Confocal of isolated GEL-XCs emulsion indicated a composite morphology, in addition to hydrogel-like appendages found external to the oil-water interface	119
5.3. ATR-FTIR spectra	122

5.4. GEL-XC stability	123
5.5. Activity of GEL-XCs against pathogenic biofilms.....	125
5.6. Image of 2 L scale GEL-XC production.....	127
6.1. Molecular structures of a) oxanorbornene polymer derivatives	135
6.2. Graph showing minimum inhibitory concentrations (MIC) and structure details of oxanorbornene derivatives with different hydrophobicity of the cationic headgroups ...	137
6.3. Confocal micrographs.....	139
6.4. Biofilm viability towards P5 NPs	140
6.5. Viability of 3T3 fibroblast cells and <i>E. coli</i> biofilms in the coculture model after 3 h treatment with P5 NPs	142
6.6. Molecular structures of P5 polymer derivatives used for FRET NP studies	151
6.7. TEM image of polymer nanoparticles	152
6.8. Penetration of Rhodamine Green labelled PONI-C11-TMA nanoparticles into DsRed expressing <i>E. coli</i> biofilms.....	154
6.9. Cytotoxicity of PNPs against NIH – 3T3 Fibroblast cells.....	155
6.10. Therapeutic indices of PNPs against four bacterial biofilms.....	156
6.11. Critical micelle concentration of P5 NPs.....	158

CHAPTER 1

ORIGIN, CHALLENGES, AND STRATEGIES TO ADDRESS MULTIDRUG-RESISTANCE

1.1. Origin and Evolution of Antibiotic-Mediated MDR

1.1.1 MDR Origin

The discussion of antibiotic resistance and multidrug-resistant (MDR) bacteria have become a “hot topic” issue in recent decades. However, antibiotic resistance determinants have been circulating within the microbial genome for millennia and largely predates the manufacture and use of antibiotics by humans.¹ This observation was observed by D’Costa et al.² who authenticated ancient DNA from 30,000-year-old permafrost sediments. The study confirmed a diverse collection of encoded resistant genes towards some of the most common antibiotics used world-wide, including β -lactam, tetracycline, and glycopeptide classes. Furthermore, these genetics were found to be remarkably similar to genes currently expressed by bacteria found in healthcare-associated infections. Given that current databases indicate the existence of more than 20,000 potential resistance genes (r genes) of nearly 400 different microbial species,³ medical experts are severely concerned about the possibility of a return to the preantibiotic era, a time where even simple skin laceration infections could result in a quick death.⁴

Understanding how these microbial infections develop resistance to certain antimicrobials, like antibiotics, is best viewed from first understanding antibiotic

development during the 1900s. Since the first introduction of the sulfonamide antibiotic class in 1937,⁵ along with many other naturally or synthetically derived classes in the coming decades, so too was introduced the Modern Medicine paradigm. Without question, antibiotics have revolutionized medicine in many respects, saving countless lives ever since their first medical implication. Table 1.1 provides a wide range of antibiotic classes and subsequently, their mode of action, and mechanisms which pathogenic microorganisms develop resistance towards therapeutic intervention.⁶ Notably, in some cases, these antibiotic classes or through finite chemical modifications, can be repurposed beyond antibacterial targets, creating a significant number of additional therapeutic applications, including antiviral, antitumor, or anticancer agents.⁷ Two significant examples of their nonantibiotic effects include cardiovascular disease and immunosuppressive treatments. The dire tradeoff of these benefits is that since their introduction, millions of metric tons of antibiotics have been produced with limited regulation use world-wide. Furthermore, production improvements over the decades have created less expensive agents and have been branded as non-prescription or off-label products. Numerous studies have concluded that the sharp rise in antibiotic-resistant microbes and their global distributions are a direct result of an unremitting selection pressure of antibiotic use by humans. The overuse, underuse, and misuse of antibiotics in healthcare, and in fact, largely (~80% of all antibiotics) in agriculture is responsible for the rapid development of MDR bacteria.⁸ It is clear that this process is not natural, but a man-made event brought upon nature and is arguably the best example of Darwinian notions of selection and survival. The review of antimicrobial resistance, published in 2016, has concluded that if great lengths are not taken to mitigate the dangers of MDR, by 2050, 10

million lives will be lost each year with incurring healthcare costs reaching beyond \$100 trillion.⁹

Antibiotic Class	Mode of Action	Resistant Microorganisms
β-Lactams	Bacteria Cell Wall Inhibition	Methicillin-Resistant <i>Staphylococcus aureus</i>
Aminoglycosides	Protein Synthesis Inhibition	<i>Pseudomonas aeruginosa</i>
Glycopeptides	Bacteria Cell Wall Inhibition	Enterococcus Bacteria
Quinolones	Bacteria DNA Replication Interference	<i>Escherichia coli</i>
Lipopeptides	Cell Membrane Function Disruption	<i>Klebsiella Pneumoniae</i>
Sulfonamides	Growth Prevention	<i>Escherichia coli</i>
Macrolides	Protein Synthesis Inhibition	<i>Streptococcus pyogenes</i>
Tetracyclines	Protein Synthesis Inhibition (Growth Prevention)	<i>Neisseria gonorrhoeae</i>

Table 1.1. List of common antibiotic classes, their action mechanism, and common bacterium resistant towards their mode of action.

1.1.2 MDR Evolution

Given their rapid reproductive cycles and robust capacity to develop resistance from external threats, prokaryotes such as bacteria have successfully evaded extinction prior to man’s discovery of antibiotics and most notably after their large-scale manufacturing and global implementation.¹⁰ Bacterial microbes capable of resisting a range of antibiotic classes via multiple genetic mutations have coined the name “superbugs” and exacerbate the difficulty in treating against these pathogens as the number of therapeutic options are limited and increase the duration of hospital care, dramatically increasing financial burden in both developing and developed countries.¹¹ Table 1.2

provides a list of these superbugs and their associated infections, along with a list of antibiotics they are resistant towards.¹² Although it is clear there is a positive correlation within a bacterial population between resistance to one drug and resistance to one or more other drugs, it is unknown whether each bacterial taxon has inherent resistant mechanisms or the extent at which pathways to accumulation of multiple resistances are shared among pathogens.¹³ Figure 1.1 highlights the most common routes of acquired resistance.

“Superbug”	Associated Infection	Resistant Towards:
<i>Methicillin-Resistant Staphylococcus aureus</i>	Skin Infections	β -Lactam Antibiotics
<i>Acinetobacter baumannii</i>	Respiratory Tract Infections	Carbapenem Antibiotics
<i>Pseudomonas aeruginosa</i>	Pneumonia Urinary Tract Infections	Aminoglycoside Antibiotics
<i>Enterobacteriaceae</i>	Lower Respiratory Tract Infections	Carbapenem Antibiotics
<i>Enterococcus faecium</i>	Catheter-Related Infections	Vancomycin

Table 1.2. List of common “Superbugs”, common infection sites, and common antibiotics they are resistant towards.

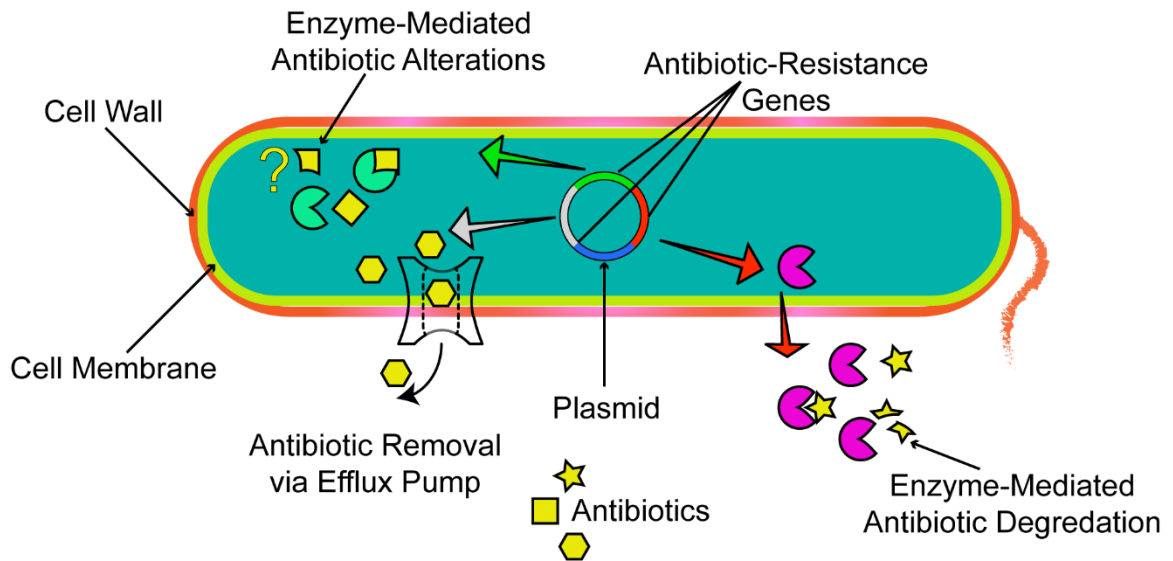


Figure 1.1. Common routes of acquired resistance.

1.1.3 Enzyme-Mediated Resistance

One of the most common forms of resistance involve the degradation or modification of antibiotics, in particular, the β -lactamases.¹⁴ Endogenously produced by pathogens such as *K. pneumoniae*, these enzymes are highly effective at degrading ampicillin, preventing the agent from reaching cells buried within. Furthermore, chromosomally encoded AmpC β -lactamase secreted into the matrix of *P. aeruginosa* are additionally capable of lactam antibiotic degradation.¹⁵ Interestingly, this has been identified as an important and clinically relevant determinant of β -lactam resistance in *P. aeruginosa*. These are only but two examples, where almost 600 class A β -lactamases were reported in 2011.¹⁶ Most concerning however, is the rapid emergence in clinics of carbapenemase found in *K. pneumoniae*. Carrying over to other pathogenic infections such as Enterobacteriaceae, *P. aeruginosa*, and *A. baumannii*, this antibiotic degrading enzyme continues to spread worldwide.¹⁷

1.1.4 Efflux Pump-Mediated Resistance

Another common resistance mechanism found in pathogenic infections are acquired efflux pumps on their cellular membranes. Efflux pumps are transmembrane proteins designed to simply 'Pump' out intracellular antibiotic agents, preventing them from reaching their active site and ultimately killing the pathogen.¹⁸ Interestingly, efflux pumps can aid certain pathogen species like *Pseudomonas putida*, to grow at a liquid interface of water and toluene, extruding the toluene solvent through their TtgABC pump.¹⁹ This resistance mechanism is responsible for protecting pathogens from antibiotics like fluoroquinolones, chloramphenicol, florfenicol, streptomycin, sulfonamide classes, and tetracycline.²⁰

1.1.5 Gene Transfer-Mediated Resistance

Although typically observed to occur at a faster rate (x10,000) in a biofilm setting, planktonic pathogens are also capable of transferring plasmids between cells via conjugation.²¹ This plasmid transfer process is by far the most common mechanism of Horizontal Gene Transfer (HGT). Most disturbing, however, is that although the most common transfer mechanism is plasmid-mediated, it wasn't until the rise of the 'antibiotic era' that these r genes began to appear.²² This is supported further by bacterial pathogens isolated before the 'antibiotic era', while possessing plasmids, rarely had any r gene association.²³ This discovery further indicates the strongly positive correlation of antibiotic use and subsequent resistance. Given that the rate of this gene transfer-mediated resistance process occurs more frequently in large bacterial populations, (e.g. biofilms found in hospitals, food processing equipment, and even the human gut microbiome) so too rises the severity of acquired resistance and therefore decreases the chances of successful removal/treatment with any therapeutic intervention.²⁴

1.1.6 Target Site Modification-Mediated Resistance

The most common form of target site modification of bacterial pathogens is fluoroquinolone resistance genes of the *qnr* family.²⁵ These *qnr* genes encode proteins to bind onto bacterial DNA gyrase, effectively preventing fluoroquinolone antibiotics from interacting with its target. This mechanism has proven to be highly successful at transferring between vastly different species. One example of this transfer has been observed in Enterobacteriaceae that derived its *qnrA* genes from the chromosomes of *Shewanella algae*, a species found predominately in marine and freshwater bodies.²⁶ It has been suggested that the reason for this gene migration is in response to the man-made induced antibiotic pressure, especially antibiotic usage in livestock settings. Furthermore, given the building evidence of *qnr*-type gene transfer is heavily derived from phylogenetically distant bacterial species, (e.g. *Shewanella*, *Stenotrophomonas*, *Vibrio*, *Enterococcus*, *Serratia*, and *Citrobacter*) the role of this antibiotic mechanism is likely ancestral.²⁷

1.2. Multidrug-Resistance in Biofilm Microcolonies

While MDR bacteria in their planktonic or ‘free-flowing’ pose a threat to human health, their threat is further exacerbated when they colonize onto surfaces.²⁸ Given the term, biofilms, these surface-attached microbial cells secrete a highly complex and heterogenous extracellular matrix. This matrix severely compromises antimicrobial agent’s penetration and subsequently their effectiveness.²⁹ From a physical perspective, this extracellular polymeric substance (EPS) is comprised of proteins, nucleic acids, phospholipids, and DNA which act like a protective shield, preventing antimicrobial

penetration and instead adsorb onto the outer matrix shell.³⁰ Additionally, an external extracellular polysaccharide shell creates a hydration shell, preventing key immune response cells within a host from recognizing MDR pathogens buried deep within the matrix.³¹ Together, this matrix dramatically reduces the chance of eliminating the threat, regardless of the therapeutic used to treat the threat. Furthermore, given the fact that biofilms are a highly regulated process that heavily depends on numerous environmental and genetic factors that vary from species to species, accurate diagnosis and therefore treatment is often erroneous, catalyzing the chance to further increase MDR-associated infections.

1.2.1 Antibiotic Penetration Paradox

Suggesting poor antimicrobial penetration is the reason for ineffective treatment would be a gross simplification. For example, previous studies indicated that the antibiotic tetracycline penetrated uropathogenic *Escherichia coli* biofilms within 10 minutes of exposure without any compromise to bacterial cellular viability.³² This has also been seen in other antibiotic-biofilm combinations such as ampicillin-*Klebsiella pneumoniae* and rifampin-*Staphylococcus*. Alternatively, it has been previously demonstrated that antibiotics like oxacillin, cefotaxime, and vancomycin (a drug of last resort) was limited in their penetration capabilities onto *Staphylococcus aureus* biofilms, suggesting that in some cases, the penetration barrier does contribute to the reduced susceptibility of biofilms to certain antibiotic classes.³³ Therefore, it has been proposed that slower antibiotic penetration may increase the opportunity for adaptive phenotypic responses, potentially increasing tolerance.

1.2.2 Antibiotic-Modifying Enzyme

Another advantage the EPS matrix provides is the localization of antibiotic-modifying enzymes throughout the biofilm. For instance, *K. pneumoniae* biofilms secrete β -lactamase and has been demonstrated to effectively degrade ampicillin, preventing the antibiotic from even reaching pathogenic cells.³⁴ Furthermore, certain pathogenic biofilms, such as *P. aeruginosa* grow faster than their counterparts, increasing the total amount of β -lactamase enzymes within the matrix, further impairing the therapeutic relevance of antibiotics.³⁵

1.2.3 Extracellular DNA

A particularly interesting resistance mechanism of MDR biofilms is their ability to incorporate extracellular DNA (eDNA) throughout the EPS matrix, dramatically enhancing both resistance and tolerance of antimicrobials.³⁶ This observation has been best studied in *P. aeruginosa* biofilms. In fact, previous studies have showed that *P. aeruginosa* biofilms can sequester DNA from exogenous sources, resulting in an increased level of resistance towards tobramycin by 3-fold and 2-fold for gentamicin.³⁷ One proposed mechanism for eDNA's effect on resistance/tolerance of MDR biofilms is through the alteration of the EPS environment. eDNA has been demonstrated to chelate ions such as magnesium (II).³⁸ Decreasing levels of magnesium leads to the trigger of PhoPQ and PmrAB pathways, two processes that contribute to antibiotic resistance. In a similar fashion, eDNA can create acidic microdomains throughout the matrix has been observed synergistically with magnesium chelation, additionally activating PhoPQ and PmrAB pathways, further conferring antimicrobial resistance.³⁹ However, this is one but many observed mechanisms, eDNA has been observed to be directly involved in sequestering polyamines such as spermidine that localizes on the matrix surface, compromising certain cationic

antimicrobial treatment. Finally, eDNA has been observed to contribute directly to horizontal gene transfer, a well-known mechanism for transferring resistance genes to nearby microbial cells.⁴⁰

1.2.4 Biofilm Infections in Hospitals

Armed with these powerful and creative avenues of defense against antibiotics and other antimicrobial agents, numerous MDR biofilm-associated infections have infiltrated hospitals on a global scale, imparting high healthcare costs in addition to patient suffering and mortality.⁴¹ Overall, around 80 percent of hospital-acquired infections are associated in one form or another with biofilm formation.⁴² These infections occur commonly on inert surfaces such as indwelling medical devices or inflamed tissues where an injury or incision is already present. In particular, *P. aeruginosa* biofilms cause chronic lung infections in cystic fibrosis patients, while pacemaker devices commonly colonize *S. aureus* biofilms, resulting in pacemaker replacement and further patient anguish.^{43, 44} This challenge is further exacerbated by the unavailability of diagnostic techniques capable of distinguishing infections as MDR biofilm variants.

1.3. Challenges of Current Methods in Treating MDR

1.3.1 Antibiotics

Given the ‘large bag of tricks’ MDR-associated infections have to circumvent therapeutic intervention, current antibiotic methods continue to demonstrate marginal effect. In some cases, MDR infections are beginning to evolve to become completely resistant to any therapeutic admission. Recently, strains of drug-resistant tuberculosis (TB) have evolved to be extremely drug-resistant (XDR-TB) to any antibiotic medications such

as rifampicin and isoniazid, two first line TB drugs.⁴⁵ While new derivatives or classes of antibiotics could be in theory produced, numerous microbiologists argue against this notion. As pointed out by Professor Bob Hancock⁴⁶ at the University of British Columbia, “If we come up with new antibiotics, we’re still going to have those same pressures for development of resistance. The drugs that we are producing today are just going to keep us in the game; they’re not going to get us ahead of the game. In my opinion, we need to change the game.” Professor Hancock is not alone with this notion as experimentalists and theoreticians both conclude that rates of antibiotic resistance continue to rise exponentially along with a severe reduction in the number of newly discovered antibiotic classes (Figure 1.2). Furthermore, the antibiotic paradigm, regardless if the correct antibiotic is chosen, long-term antibiotic regimens will continue to incur major financial burden for patients and hospitals and increase the probability of killing the patient as the concentration of antibiotics reach far beyond the safe therapeutic dose.⁴⁷

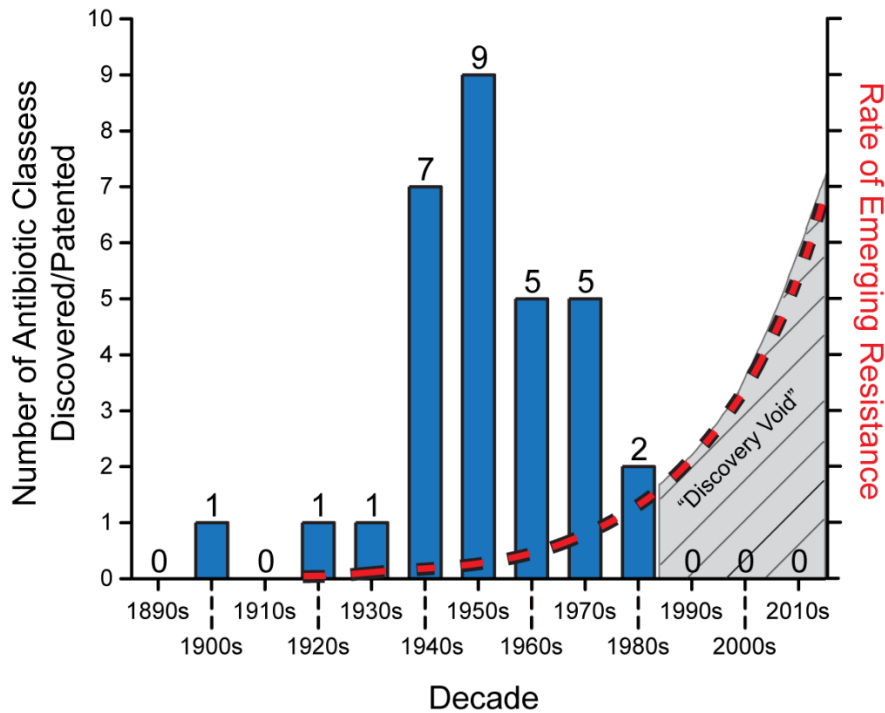


Figure 1.2. ‘Hockey-Stick Projection’ indicating resistance continues to rise exponentially while antibiotic discovery in industry drops to zero in the late 1980s.

1.3.2 Debridement

Chronic wounds are typically wounds that cannot heal within a 2 week time-frame because of influence factors such as infection and foreign objects.⁴⁸ Some of the most common examples of chronic wounds in the category of ulcers include diabetic foot ulcers, pressure ulcers, arterial ulcers, venous ulcers, and fungus-infected wounds.⁴⁹ Additionally, chronic wounds encompass healthcare-associated infections and further complicate treatment derived from chronic diseases, vascular insufficiency, diabetes, neurologic defects, nutritional deficiency, advanced age, and local factors like pressure, infection, and edema. Taken together, these factors severely impair wound healing. A critical tactic to enhance wound healing is to perform debridement at the infection site.⁵⁰ Debridement is a general terminology given to the removal of necrotic tissue and foreign objects from a

wound to expose viable tissue to both promote and expedite the healing process. Various debridement strategies have been implemented including autolytic (self-digestion via hosts own enzymes), enzymatic, biodebridement, mechanical, and conservative sharp and surgical. In recent decades, new debridement methods have been introduced including Versajet technology, ultrasound debridement therapy, hydrosurgery debridement, and WoundVac technologies.⁵¹ These methods vary in overall effectiveness as comprehensive analysis of these techniques is not well establish. While there are an array of reports indicating that these debridement methods improve both the rate of healing and overall wound healing, accurately determining which method to implement to maximize healing is not universally possible. Furthermore, the choice in debridement method largely rests on the clinician's experience coupled with the patient preferences to pain and ethics, the clinical context, and overall healthcare costs.⁵² Detailed contrast studies between all these methods are greatly needed as it is unclear which technique offers the greatest chance of wound healing capacity.

1.4. Emerging Strategies to Counter MDR

1.4.1 Host-Defense Peptides

Host-defense peptides (HDPs), also named antimicrobial peptides (AMPs), is an evolutionarily ancient component of a hosts innate immune system.⁵³ In fact, more than 2,700 HDPs have be described thus far in six host Kingdoms (bacteria, archaea, protists, fungi, plants, and animals).⁵⁴ Currently, these HDPs are classified as: 1) α -helical peptides, 2) peptides containing β -sheet elements, 3) peptides combining both α and β structures,

and 4) peptides free of α and β structures and are unusually rich with proline, arginine, tryptophan, or histidine residues. Furthermore, HDPs fall into two major mammalian antimicrobial peptide classes, defensins and cathelicidins (LL-37 is the only member of cathelicidins at the time of this thesis work). In general, HDPs generally contain less than 50 residues, possess net cationic charge, and contain particularly interesting dynamics regarding their hydrophobic and cationic domains, coined “amphiphilic balance”.⁵⁵

HDPs offer many advantages over traditional antibiotic agents. HDPs display a broad-spectrum activity, killing Gram-negative and Gram-positive pathogens.⁵⁶ Additionally, HDPs wide-range mechanisms of action (observed as membrane disruption, promoting immune responses via regulating DNA, RNA, and protein synthesis, altering gene expression, and stimulating wound healing.) suggest pathogenic microorganisms rarely become resistant to them.⁵⁷ Notably, HDPs have been observed to penetrate biofilms, produce synergistic effects with conventional antibiotics, and possess activity towards bacteria, viruses, and fungi. Taken together, HDPs offer a promising strategy to address MDR-associated infections. However, only a couple examples of HDPs namely Gramicidins derived from *Bacillus brevis*, Polymyxin B isolated from *P. polymyxa*, caspofungin extracted from echinocandin fungi, and iseganan from pig protegrin have reached clinical trials.⁵⁸ The reason for the limited number of current clinical trials comes from HDPs poor selectivity, adverse hemolytic (lysis of red blood cells) and host toxicity, insufficient stability via protease degradation *in vivo*, low hydrosolubility and other biodistribution challenges, and significant cost of production on a large-scale consideration. *However, it is of the opinion of this PhD candidate that, excluding his thesis work, HDPs is the most promising strategy that has emerged to counter MDR infections.*

1.4.2 Phage Therapy

For nearly a century, phage therapy, the use of bacterial viruses (phages), has been used to treat bacterial infections. Interestingly, phages are the most abundant biological entity world-wide and play a crucial role in regulating bacterial populations, responsible for killing 20%-40% of all marine surface bacteria every 24 hours.⁵⁹ The first successful use of phage therapy in a clinical setting was documented in 1919, where four pediatric cases of bacterial dysentery were effectively treated. Serious considerations towards phage therapy has occurred over the past few decades as the rise of antibiotic resistance became apparent. Phages action mechanism is derived from its ability to bind to specific receptors on a bacterial cell surface, followed by injecting their genetic material into the host pathogen that integrates the material into the bacterial genome.⁶⁰ An alternative mechanism involves the compromise of bacterial replication process and instead produce next-generation progenies that lyse the host cell. In contrast to lytic phages, lysogenic phages undergo a different process. Upon integrating their genetic material within the hosts chromosome, these endogenous prophage (a separate plasmid capable of transmitting across bacterial generations) can be beneficial to bacterial hosts and impart numerous virulence factors that enhance their pathogenicity towards competing microbes or mammals.⁶¹ Therefore, phage therapy strictly relies on lytic phages combined together as a “phage cocktail” which has proven *in vitro* efficacy against target pathogens. Notably, there are a couple examples of lytic phages effectively penetrating biofilms, a remarkable capability by any means.⁶²

While phages have been demonstrated to eliminate key pathogenic bacteria such as *Clostridium difficile*, *E. faecium*, *E. coli*, *P. aeruginosa*, *S. aureus*, and *Enterococcus* spp,

currently, there are no phage therapy products approved for human use in the EU or United States.⁶³ However, there are a couple instances of phage preparations for biocontrol in the food industry and have been approved by the FDA under the classification of “generally considered as safe.” Regardless of these apparent advantages, phage cocktails can induce the possibility of intestinal barrier dysfunction, known as “leaky gut” and significantly varies between individuals and the types of phage strains used.⁶⁴ Although it is unclear of the severity of this action, compromised intestinal barrier function has dire downstream effects including Crohn’s disease, inflammatory bowel disease, and type 1 diabetes. Despite their ease of production, purification, and storage, it is unclear of the universal success of these phage cocktails as recent reports indicate potential resistance accumulation via horizontal gene transfer.⁶⁵ It is clear however that additional studies involving the interactions between phage, microbiome, and human host are needed before any clinical trial considerations are made.

1.4.3 Antibodies

Another emerging method to counter MDR infections is to use pathogen specific monoclonal antibodies (mAbs).⁶⁶ Prior to the introduction of antibiotics, mAbs had marginal success in the form of serum therapy, performed in the 1940s. However, given the inconclusive data on toxicity, high cost, and poor purification methods, antibiotics were the chosen cheaper alternative. Following the discovery of murine hybridoma technology in the 1970s, biotech and pharmaceutical industries have expanded their antibody profiles.⁶⁷ Prior limitations such as purification, adverse toxicity, and poor scalability were eliminated, and the promise of mAb-based therapies have garnered more attention in recent decades. Currently, only one mAb treatment, Palivizumab (treatment of respiratory

syncytial virus) is licenced in the US, along with several other mAb candidates in advanced clinical trials to treat other infectious diseases including HIV, *Clostridium difficile*, rabies prophylaxis, and *Staphylococcus aureus*. Antibodies offer great advantages over antibiotics.⁶⁸ Their remarkably high specificity prevents adverse off-target effects and improved circulation time ensures a more effective treatment. However, antibodies are currently best suited for high-risk patients and further work is needed to determine their effectiveness as a therapeutic agent when the infection is already present.⁶⁹ Furthermore, antibody therapies heavily rely on rapid diagnostic outputs to enhance the feasibility of their use. Currently, diagnostic methods must be improved to ensure the maximum therapeutic capacity of antibody therapies.

1.4.4 Quorum Sensing Inhibitors

Quorum sensing inhibitors (QSIs), while not considered a direct therapeutic, is a fundamentally unique approach to reduce the dangers of MDR biofilm infections.⁷⁰ Quorum sensing small molecules are used in a variety of bacteria such as *Aliivibrio*, *Escherichia*, *Pseudomonas*, and *Staphylococcus*. QS is a signaling mechanism that enables bacteria to adapt their gene expression machinery according to the population density in a local environment (e.g. biofilms).⁷¹ QS is a critical component to organize light-emitting reactions (bioluminescence), to form biofilms, produce antibiotics, express virulence factors, and transfer/trade genetic material like HGT. First identified in *Vibrio fischeri* bacterium, these QS molecules are traditionally called autoinducers (AI) and give significant advantage to bacterium survival.⁷² It should be noted, however, that Gram-negative and Gram-positive use different classes of AI. Gram-negative rely on N-acyl L-homoserine lactones (AHLs) with conjugated fatty acid chains, while Gram-positive use

cyclic thioester peptides. These AIs are either actively transported within the intracellular environment (Gram-positive) or passively diffuse through the membrane (Gram-negative), although there are some reports of Gram-negative bacterium using active transportation. Currently, there are four main methods to block QS: 1) Suppress AI synthesis, 2) target AIs through enzymatic degradation reactions, 3) antagonize the QS regulator, and 4) hinder the regulator protein from binding to DNA.⁷³ While there are numerous examples of successfully using QSI tactics to address MDR infections, significant research gaps still remain. First, it is unclear if all molecular components of QS and their respective regulators have been discovered.⁷⁴ Second, only a few clinical trials are underway involving QS inhibitors. Third, a better understanding of the complex intricacies of the QS system needs to be performed as to avoid adverse effects such as unexpected resistance to QS inhibitors. Finally, improved scalability and cost structure of these components must be improved before commercial viability is feasible.⁷⁵

1.4.5 Essential Oils / Phytochemical Extracts

Essential oils (EOs) and their separated EO compounds (Phytochemicals) have received a renewed interest in the areas of antimicrobials, cosmetics, food, and textiles.⁷⁶ These compounds are typically obtained from plant materials including flowers, buds, seeds, leaves, twigs, bark, herbs, wood, fruits, and roots and represent a small fraction of plant composition (~5% dry vegetation). Table 1.3 provides a list of common phytochemicals, their molecular structure, their plant source, and some biological activities.⁷⁷ Nearly every EOs available on the market are obtained by hydro-distillation although other classical methods such as organic solvent extraction and cold pressing along with innovative methods such as supercritical fluid extraction and solvent-free microwave

extraction processes are implemented in certain cases.⁷⁸ The value of EOs has been well documented as antibacterial, antifungal, antiviral, pest, and insect repellent agents found across biomedical, food, and textile industries. In fact, numerous studies have even highlighted EOs value to treat multidrug-resistant bacteria such as *Staphylococcus aureus* and *P. aeruginosa*.⁷⁹ Furthermore, EOs offer a viable option against nosocomial infections, showing promise as a cleaning liquid for disinfecting medical equipment and surfaces. Interestingly, it has been suggested that EOs use on hospital patients offer a feeling of psychic comfort thanks to their inherent pleasant odors. Given EOs possess high biocompatibility, low-cost, and potent physicochemical properties with respect to their environment, EOs have been used in important food preservative applications to fight against dangerous food poisoning bacteria such as *Listeria monocytogenes*, *Salmonella typhimurium*, *Clostridium perfringens*, *Pseudomonas putida*, and *Staphylococcus aureus*.⁸⁰ Notably, EOs are gaining traction as health and growth promoters in livestock. The reason for this dramatic change is in response to the dramatic rise of MDR pathogens, causing the European Union to prohibit synthetic antibiotics in livestock in 2006 and the recent Veterinarian Feed Directive implemented by United States Food and Drug Administration (FDA).⁸¹ The FDA recognizes EOs as safe substances according to Code of Federal Regulations, with many compounds approved for use as antibacterial additives. Taken together, EOs and phytochemical extracts offer an immense advantage over antibiotics and other emerging strategies to combat MDR infections.


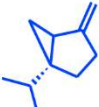
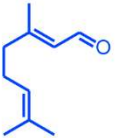

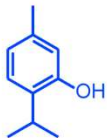
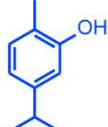
Phytochemical	Molecular Structure	Plant Source	Biological Activities
D-Limonene		<i>Citrus limon</i>	Antifungal Antioxidant
Sabinene		<i>Quercus ilex</i>	Antifungal Antioxidant Anti-Inflammatory
Citral		<i>Aloysia citrodora</i>	Antifungal Antibacterial Painkiller
Camphor		<i>Lavendula stoechas</i>	Antispasmodic Antifungal Antimicrobial
Thymol		<i>Thymus vulgaris</i>	Strong Antimicrobial Antiseptic
Carvacrol		<i>Thymus polybractea</i>	Strong Antimicrobial Anti-Inflammatory

Table 1.3. List of common phytochemicals and their structure, plant source, and some biological activities.

1.4.6 Limitations

While there are clear advantages to supplement current antimicrobials with EOs, a variety of fundamental limitations prevent their universal adoption.⁸² The first limitation is in their name, Essential *Oils*. These compounds, typically liquid oils at room temperature have almost no solubility in water, causing phase separation and an ineffective delivery avenue in aqueous environments. Second, EOs are unstable and in some cases are highly volatile, and can be easily degraded by oxidation, volatilization, heating, and light.⁸³ Finally, depending on the external environment plants are subjected to, the ratio of phytochemical extracts across different plant batches can vary marginally and, in some

cases, significantly. Strict isolation of EOs into phytochemical extracts can resolve this, however in some cases, manufacturing costs often increase, limiting applications that require substantial plant oil material. Therefore, it is critical to develop avenues of encapsulating these EOs and phytochemical extracts to not only improve their stability and solubility but enable their universal application in aqueous-based products, such as those found in biomedical and agriculture industries.

1.4.7 Encapsulation Strategies

Encapsulation of EOs and phytochemical extracts has been well-documented in recent decades and are compartmentalized into microparticles, nanoparticles, and liposomes.⁸⁴ These vehicles have demonstrated dramatic improvement in release profiles, enhanced activity, improved thermal stability, and prolonged activity.⁸⁵ Carefully selected materials are chosen to stabilize the oil in a water matrix, otherwise known as oil-in-water emulsions. In the context of this thesis, polymeric materials will be discussed, although there are examples in literature of using micron and nano-sized particles such as iron oxide, and silica-cored materials.^{86,87,88} Most literature articles discussing EO encapsulation rely on nature-derived materials such as chitosan, Alginates, and starches.⁸⁹ In particular, one valuable synthetic polymer stabilizer, poly lactic-*co*-Glycolic Acid (PLGA) has been used in some cases due to its high biocompatibility and biodegradability.⁹⁰ Although a wide-range of applicable EO delivery vehicles have been created, fundamental challenges regarding their commercial feasibility still remain unaddressed. First, while current stabilizers do improve EO stability in aqueous environments, long-term shelf-life demonstration remains to be seen across every EO formulation. In particular, carvacrol, an immensely potent antimicrobial agent suffers from vehicle aggregation, leading to Ostwald

ripening (emulsion size growth) and phase separation between oil and water.⁹¹ Second, research into crosslinking these emulsions after oil-temptation is scarce, with only a few examples of in-situ polymerization found in literature.⁹² Addressing this second point will additionally improve the chances of resolving the first challenge. Third, while there are examples of encapsulated EOs eliminating MDR pathogens, these cases are typically performed with planktonic pathogens, with almost zero examples of these EO vehicles capable of penetrating and eliminating MDR biofilms.⁹³ Once these three challenges are resolved, the final consideration will be to reproducibly generate EO vehicles demonstrating *in vivo* or field trial success that can be appropriately scalable for their intended application whether its target application is biomedical, agriculture, food, or textile industries.

“It is the opinion of this PhD candidate that if the following considerations can be effectively addressed, coupled with their impressive physiologic properties and the chance to mitigate drug-resistance without harming hosts or the environment, EO vehicles will almost certainly become valuable platforms to build additional formulations to combat MDR infections found world-wide.”

1.5. Dissertation Overview

The fundamental goal of this thesis is to address three of the four key challenges preventing the commercialization of phytochemical encapsulated vehicles in the areas of biomedical and other easily translatable industries found in agriculture. Therefore, chapter 2 starts with creating a suitable polymeric stabilizer that can be reproducibly crosslinked at an oil-water interface, generating nanocomposite-type phytochemical vehicles along

with reporting its characterization, activity (biofilm penetration and elimination of pathogens within), and viability as a wound-healing agent. Chapters 3 and 4 focus on engineering this polymeric stabilizer to include responsive chemical moieties to degrade in the presence of biologically relevant stimuli including pH, small molecule, and enzymatic processes. Furthermore, careful consideration into their characterization, activity, and application viability are monitored to ensure cross-platform applicability. Chapter 5 discusses the use of combining nature-derived stabilizers with a biocompatible crosslinking strategy to generate phytochemical emulsion platforms easily scalable for commercial industries like biomedical and agriculture. Additionally, their cross-platform characteristics and application capabilities is confirmed. Chapter 6 begins to explore engineering strategies to develop synthetic polymeric nanoparticles as alternative candidates to host-guest peptides. These polymeric particles were found to have impressive therapeutic indices that improve upon current peptides and their synthetic analogs. Additionally, these polymers were also capable of penetrating and eliminating biofilms and show promise as a wound-healing agent. Chapter 7 concludes with a discussion on why phytochemical emulsion vehicles and engineered polymeric nanoparticles penetrate and easily distribute throughout the entire biofilm's matrices generated by pathogenic bacterium and offers experimental suggestions going forward.

1.6. References

- (1) Davies, J.; Davies, D. Origins and Evolution of Antibiotic Resistance. *Microbiol. Mol. Biol. Rev.* **2010**, *74*, 417-433.
- (2) D'Costa, V. M.; King, C. E.; Kalan, L.; Morar, M.; Sung, W. W.; Schwarz, C.; et al. Antibiotic resistance is ancient. *Nature* **2011**, *477*, 457-461.
- (3) Liu, B.; Pop, M. **2009**, ARDB – Antibiotic Resistance Genes Database. *Nucleic Acids Res.* *37*, D443-D447.
- (4) Antibiotic / Antimicrobial Resistance. (**2018**, March 05). Retrieved from <https://www.cdc.gov/drugresistance/about.html>
- (5) Bryskier, A. (ed.) **2005**, Antimicrobial Agents: Antibacterials and Antifungals. *ASM Press*, Washington, DC.
- (6) Morar, M.; Wright, G. D. The Genomic Enzymology of Antibiotic Resistance. *Annu. Rev. Genet.* **2010**, *44*, 25-51.
- (7) Demain, A. L.; Sanchez, S. Microbial Drug Discovery: 80 Years of Progress. *J. Antibiot.* **2009**, *62*, 5-16.
- (8) Boeckel, T. P. V.; Glennon, E. E.; Chen, D.; Gilbert, M.; Robinson, T. P.; Grenfell, B. T.; Levin, S. A.; Bonhoeffer, S.; Laxminarayan, R. Reducing Antimicrobial Use in Food Animals. *Science* **2017**, *357*, 1350-1352.
- (9) Tackling Drug-Resistant Infections Globally: Final Report and Recommendations, May 19, 2016, <https://amr-review.org/Publications> (accessed Aug 2018).
- (10) Gullberg, E.; Cao, S.; Berg, O.; Ilback, C.; et al. Selection of Resistant Bacteria at Very Low Antibiotic Concentrations. *PLoS Pathog.* **2011**, *7*, e1002158.
- (11) Levy, S. B.; Marshall, B. Antibacterial Resistance Worldwide: Causes, Challenges and Responses. *Nat. Med.* **2004**, *10*, S122-S129.
- (12) Mataseje, L. F.; Neumann, N.; Crago, B.; Baudry, P.; Zhanel, G. G.; Louie, M; Mulvey, M. R. Characterization of Cefoxitin-resistant *Escherichia coli* isolates from Recreational Beaches and Private Drinking Water in Canada Between 2004 and 2006. *Antimicrob. Agents Chemother.* **2009**, *53*, 3126-3130.
- (13) Link-Gelles, R.; Thomas, A.; Lynfield, F.; Petit, S.; Schaffner, W.; Harrison, L.; Farley, M. M.; Aragon, D.; Nicols, M.; et al. Geographic and Temporal Trends in Antimicrobial Nonsusceptibility in *Streptococcus Pneumoniae* in the Post-Vaccine Era in the United States. *J. Infect. Dis.* **2013**, *208*, 1266-1273.
- (14) Bush, K.; Fisher, J. F. Epidemiological Expansion, Structural Studies, and Clinical Challenges of New Beta-Lactamases from Gram-Negative Bacteria. *Annu. Rev. Microbiol.* **2011**, *65*, 455-478.

- (15) Scotta, C.; Juan, C.; Cabot, G.; Oliver, A.; Lalucat, J.; Bennasar, A.; Alberti, S. Environmental Microbiota Represents a Natural Reservoir for Dissemination of Clinically Relevant Metallo-beta-Lactamases. *Antimicrob. Agents Chemother.* **2011**, *55*, 5376-5379.
- (16) Bush, K.; Jacoby, G. A. Updated Functional Classification of β -Lactamases. *Antimicrob. Agents Chemother.* **2010**, *54*, 969-976.
- (17) Horrevorts, A. M.; Borst, J.; Puyk, J. T.; Ridder, R. D.; Dzoljic-Danilovic, J. E.; et al. Ecology of *Pseudomonas aeruginosa* in Patients With Cystic Fibrosis. *J. Med. Microbiol.* **1990**, *31*, 119-124.
- (18) Poole, K. Efflux-Mediated Multiresistance in Gram-Negative Bacteria. *Clin. Microbiol. Infect.* **2004**, *10*, 12-26.
- (19) Mosqueda, G.; Ramos, J. L. A Set of Genes Encoding a Second Toluene Efflux System in *Pseudomonas Putida* DOT-T1E is Linked to the Tod Genes for Toluene Metabolism. *J. Bacteriol.* **2000**, *182*, 937-943.
- (20) Piddock, L. J. Multidrug-Resistance Efflux Pumps – Not Just for Resistance. *Nat. Rev. Microbiol.* **2006**, *4*, 629-636.
- (21) Norman, A.; Hansen, L. H.; Sorensen, S. J. Conjugative Plasmids: Vessels of the Communal Gene Pool. *Philos. Trans. R. Soc. Lond. B. Biol. Sci.* **2009**, *364*, 2275-2289.
- (22) Datta, N.; Hughes, V. M. Plasmids of the Same Inc Groups in Enterobacteria Before and After the Medical Use of Antibiotics. *Nature* **1983**, *306*, 616-617.
- (23) Davies, J. Vicious Circles: Looking Back on Resistance Plasmids. *Genetics* **1995**, *139*, 1465-1468.
- (24) Costerton, J. W.; Stewart, P. S.; Greenberg, E. P. Bacterial Biofilms in Nature and Disease. *Annu. Rev. Microbiol.* **1987**, *41*, 435-464.
- (25) Rodriguez-Martinez, J. M.; Cano, M. E.; Velasco, C.; Martinez-Martinez, L.; Pascual, A. Plasmid-Mediated Quinolone Resistance: an Update. *J. Infect. Chemother.* **2011**, *17*, 149-182.
- (26) Poirel, L.; Rodriguez-Martinez, J. M.; Mammeri, H.; Liard, A.; Nordmann, P. Origin of Plasmid-Mediated Quinolone Resistance Determinant QnrA. *Antimicrob. Agents Chemother.* **2005**, *49*, 3523-3525.
- (27) Jacoby, G. A.; Griggin, C. M.; Hooper, D. C. *Citrobacter* spp. As a Source of *qnrB* Alleles. *Antimicrob. Agents Chemother.* **2011**, *55*, 4979-4984.
- (28) Hall, C. W.; Mah, T.-F. Molecular Mechanisms of Biofilm-Based Antibiotic Resistance and Tolerance in Pathogenic Bacteria. *FEMS Microbiol. Rev.* **2017**, *41*, 276-301.

- (29) Suci, P. A.; Mittelman, M. W.; Yu, F. P.; et al. Investigation of Ciprofloxacin Penetration into *Pseudomonas aeruginosa* Biofilms. *Antimicrob. Agents. Ch.* **1994**, *38*, 2125-2133.
- (30) Byrd, M. S.; Sadovskaya, I.; Vinogradov, E.; et al. Genetic and Biochemical Analyses of the *Pseudomonas aeruginosa* Psl Exopolysaccharide Reveal Overlapping Roles for Polysaccharide Synthesis Enzymes in Psl and LPS Production. *Mol. Microbiol.* **2009**, *73*, 622-638.
- (31) Domenech, M.; Ramos-Sevillano, E.; Garcia, E.; Moscoso, M.; Yuste, J. Biofilm Formation Avoids Complement Immunity and Phagocytosis of *Streptococcus pneumoniae*. *Infect. Immun.* **2013**, *81*, 2606-2615.
- (32) Stone, G.; Wood, P.; Dixon, L.; et al. Tetracycline Rapidly Reaches all the Constituent Cells of Uropathogenic *Escherichia coli* Biofilms. *Antimicrob. Agents. Ch.* **2002**, *46*, 2458-2461.
- (33) Singh, R.; Ray, P.; Das, A.; et al. Penetration of Antibiotics Through *Staphylococcus aureus* and *Staphylococcus epidermidis* Biofilms. *J. Antimicrob. Chemoth.* **2010**, *65*, 1955-1958.
- (34) Anderl, J. N.; Franklin, M. J.; Stewart, P. S. Role of Antibiotic Penetration Limitation in *Klebsiella pneumoniae* Biofilm Resistance to Ampicillin and Ciprofloxacin. *Antimicrob. Agents Ch.* **2000**, *44*, 1818-1824.
- (35) Bowler, L. L.; Zhanel, G. G.; Ball, T. B.; et al. Mature *Pseudomonas aeruginosa* Biofilm Prevail Compared to Young Biofilms in the Presence of Ceftazidime. *Antimicrob. Agents Ch.* **2012**, *56*, 4976-4979.
- (36) Chiang, W.-C.; Nilsson, M.; Jensen, P. O.; et al. Extracellular DNA Shields Against Aminoglycosides in *Pseudomonas aeruginosa* Biofilms. *Antimicrob. Agents Ch.* **2013**, *57*, 2352-2361.
- (37) Chiang, W.- C.; Pamp, S. J.; Nilsson, M.; et al. The Metabolically Active Subpopulation in *Pseudomonas aeruginosa* Biofilms Survives Exposure to Membrane-Targeting Antimicrobials via Distinct Molecular Mechanisms. *FEMS Immunol. Med. Mic.* **2012**, *65*, 245-256.
- (38) Mulcahy, H.; Charron-Mazenod, L.; Lewenza, S. Extracellular DNA Chelates Cations and Induces Antibiotic Resistance in *Pseudomonas aeruginosa* Biofilms. *PLoS Pathog.* **2008**, *4*, e1000213.
- (39) Wilton, M.; Charron-Mazenod, L.; Moore R.; et al. Extracellular DNA Acidifies Biofilms and Induces Aminoglycoside Resistance in *Pseudomonas aeruginosa*. *Antimicrob. Agents Ch.* **2015**, *60*, 544-553.

- (40) Marks, L. R.; Reddinger, R. M.; Hakansson, A. P. High Levels of Genetic Recombination During Nasopharyngeal Carriage and Biofilm Formation in *Streptococcus pneumoniae*. *mBio*. **2012**, *3*, e00200-e00212.
- (41) Ito, A.; Taniuchi, A.; May, T.; Kawata, K.; Okabe, S. Increased Antibiotic Resistance of *Escherichia coli* in Mature Biofilms. *Appl. Environ. Microbiol.* **2009**, *75*, 4093-4100.
- (42) Romling, U.; Balsalobre, C. Biofilm Infections, Their Resilience to Therapy and Innovative Treatment Strategies. *J. Intern. Med.* **2012**, *272*, 541-561.
- (43) Marrie, T. J.; Nelligan, J.; Costerton, J. W. A Scanning and Transmission Electron Microscopic Study of an Infected Endocardial Pacemaker Lead. *Circulation* **1982**, *66*, 1339-1341.
- (44) Sauer, K.; Camper, A. K.; Ehrlich, G. D.; et al. *Pseudomonas aeruginosa* Displays Multiple Phenotypes During Development as a Biofilm. *J. Bacteriol.* **2002**, *184*, 1140-1154.
- (45) Shah, N. S.; Wright, A.; Bai, G. H.; Barrera, L.; Boulahbal, F.; et al. Worldwide Emergence of Extensively Drug-Resistant Tuberculosis. *Emerg. Infect. Dis.* **2007**, *13*, 380-387.
- (46) Hrvatin, V. Combating Antibiotic Resistance: New Drugs or Alternative Therapies? *CMAJ* **2017**, *189*, E1199.
- (47) Schulz, M.; Iwersen-Bergmann, S.; Andresen, H.; Schmoldt, A. Therapeutic and Toxic Blood Concentrations of Nearly 1,000 Drugs and Other Xenobiotics. *Crit. Care* **2012**, *16*, R136-R139.
- (48) Hu, A. L.; Zheng, M. C.; Li, W. J. Modern Clinical Nursing Practice of Wound and Stoma. *Peking Union Medical College Press* **2010**, *11*.
- (49) Singh, A.; Halder, S.; Menon, G.R.; et al. Meta-analysis of Randomized Controlled Trials on Hydrocolloid Occlusive Dressing Versus Conventional Gauze Dressing in the Healing of Chronic Wounds. *Asian J. Surg.* **2004**, *27*, 326-332.
- (50) Madhok, B. M.; Vowden, K.; Vowden, P. New Techniques for Wound Debridement. *Int. Wound J.* **2013**, *10*, 247-251.
- (51) Mosti, G.; Labichella, M. L.; Picerni, P.; Magliaro, A.; Mattaliano, V. The Debridement of Hard to Heal Leg Ulcers by Means of a New Device Based on Fluidjet Technology. *Int. Wound J.* **2005**, *2*, 307-314.
- (52) Elraiyyah, T.; Domecq, J. P.; Prutsky, G.; Tsapas, A.; et al. A Systematic Review and Meta-Analysis of Debridement Methods For Chronic Diabetic Foot Ulcers. *J. Vasc. Surg.* **2016**, *63*, 37S-45S.

- (53) Dennison, S. R.; Harris, F.; Mura, M.; Morton, L. H. G.; Zvelindovsky, A.; Phoenix, D. A. A Novel Form of Bacterial Resistance to the Action of Eukaryotic Host Defense Peptides, the Use of a Lipid Receptor. *Biochemistry*, **2013**, *52*, 6021-6029.
- (54) Wang, G.; Li, X.; Wang, Z. APD3: The Antimicrobial Peptide Database as a tool for Research and Education. *Nucleic Acids Res.* **2016**, *44*, D1087-D1093.
- (55) *Handbook of Biologically Active Peptides*, Kastin, A. J. (Ed.) Academic Press: San Diego, CA, USA, **2006**.
- (56) Furci, L.; Baldan, R.; Bianchini, V.; et al. New Role for Human Alpha-Defensin 5 in the Fight Against Hypervirulent *Clostridium difficile* Strains. *Infect. Immun.* **2015**, *83*, 986-995.
- (57) Mishra, C.; Reiling, S.; Zarena, D.; Wang, G. Host Defense Antimicrobial Peptides as Antibiotics: Design and Application Strategies. *Curr. Opin. Chem. Biol.* **2017**, *38*, 87-96.
- (58) Seo, M. -D.; Won, H. -S.; Kim, J. -H.; Mishig-Ochir, T.; Lee, B. -J. Antimicrobial Peptides for Therapeutic Applications: A Review. *Molecules* **2012**, *17*, 12276-12286.
- (59) Wittebole, X.; De Roock, S.; Opal, S. M. A Historical Overview of Bacteriophage Therapy as an Alternative to Antibiotics for the Treatment of Bacterial Pathogens. *Virulence* **2014**, *5*, 226-235.
- (60) Delbrück, M. The Growth of Bacteriophage and Lysis of the Host. *J. Gen. Physiol.* **1940**, *23*, 643-660.
- (61) Hatfull, G. F.; Hendrix, R. W. Bacteriophages and their Genomes. *Curr. Opin. Virol.* **2011**, *1*, 298-303.
- (62) Abedon, S. T. Ecology of Anti-Biofilm Agents I: Antibiotics Versus Bacteriophages. *Pharmaceuticals* **2015**, *8*, 525-558.
- (63) Monk, A. B.; Rees, C. D.; Barrow, P.; Hagens, S.; Harper, D. R. Bacteriophage Applications: Where are we now? *Lett. Appl. Microbiol.* **2010**, *51*, 363-369.
- (64) Tetz, G.; Tetz, V. Bacteriophage Infections of Microbiota can Lead to Leaky Gut in an Experimental Rodent Model. *Gut Pathog.* **2016**, *8*, 33.
- (65) Hodyra-Stefaniak, K.; Miernikiewicz, P.; Drapala, J.; et al. Mammalian Host-Versus-Phage Immune Response Determines Phage Fate *in vivo*. *Sci. Rep.* **2015**, *5*, 14802.
- (66) Babb, R.; Pirofski, L. -A. Help is on the Way: Monoclonal Antibody Therapy for Multi-Drug Resistant Bacteria. *Virulence* **2017**, *8*, 1055-1058.
- (67) Reichert, J. M. Antibodies to Watch in 2015. *MAbs* **2015**, *7*, 1-8.

- (68) DiGiandomenico, A.; Sellman, B. R. Antibacterial Monoclonal Antibodies: The Next Generation? *Curr. Opin. Microbiol.* **2015**, *27*, 78-85.
- (69) Buchwald, U. K.; Pirofski, L. Immune Therapy for Infectious Diseases at the Dawn of the 21st Century: The Past, Present, and Future Role of Antibody Therapy, Therapeutic Vaccination, and Biological Response Modifiers. *Curr. Pharm. Des.* **2003**, *9*, 945-968.
- (70) Reuter, K.; Steinbach, A.; Helms, V. Interfering with Bacterial Quorum Sensing. *Perspectives in Medicinal Chemistry* **2016**, *8*, 1-15.
- (71) Eberhard, A.; Burlingame, A. L.; Eberhard, C.; et al. Structural Identification of Autoinducer of *Photobacterium Fischeri* Luciferase. *Biochemistry* **1981**, *20*, 2444-2449.
- (72) Lupp, C.; Ruby, E. G. *Vibrio fischeri* uses Two Quorum-Sensing Systems for the Regulation of Early and Late Colonization Factors. *J. Bacteriol.* **2005**, *187*, 3620-3629.
- (73) Scutera, S.; Zucca, M.; Savoia, D. Novel Approaches for the Design and Discovery of Quorum-Sensing Inhibitors. *Expert Opin. Drug. Discov.* **2014**, *9*, 353-366.
- (74) Miller, M. B.; Bassler, B. L. Quorum Sensing in Bacteria. *Annu. Rev. Microbiol.* **2001**, *55*, 165-199.
- (75) Kalia, V. C. ed. *Quorum Sensing vs Quorum Quenching: A Battle with No End in Sight*. Springer, New Delhi, India; **2014**.
- (76) El Asbahani, A.; Miladi, K.; Badri, W.; Sala, M.; et al. Essential Oils: From Extraction to Encapsulation. *Int. J. Pharm.* **2015**, *483*, 220-243.
- (77) Singh, P.; Shukla, R.; Prakash, B.; Kumar, A.; et al. Chemical Profile, Antifungal, Antiaflatoxigenic and Antioxidant Activity of *Citrus maxima* Burm. And *Citrus sinensis* (L.) Osbeck Essential Oils and their Cyclic Monoterpene, DL-Limonene. *Food Chem. Toxicol. Int. J. Publ. Br. Ind. Biol. Res. Assoc.* **2010**, *48*, 1734-1740.
- (78) Vian, M. A.; Fernandez, X.; Visinoni, F.; Chemat, F. Microwave Hydrodiffusion and Gravity, a New Technique for Extgraction of Essential Oils. *J. Chromatogr. A* **2008**, *1190*, 14-17.
- (79) Burt, S. Essential Oils: Their Antibacterial Properties and Potential Applications in Foods – A Review. *Int. J. Food Microbiol.* **2004**, *94*, 223-253.
- (80) Oussalah, M.; Caillet, S.; Saucier, L.; Lacroix, M. Inhibitory Effects of Selected Plant Essential Oils on the Growth of Four Pathogenic Bacteria: *E. coli* O157:H7, *Salmonella typhimurium*, *Staphylococcus aureus* and *Listeria monocytogenes*. *Food Control* **2007**, *18*, 414-420.
- (81) Castanon, J. I. R. History of the use of Antibiotic as Growth Promoters in European Poultry Feeds. *Poult. Sci.* **2007**, *86*, 2466-2471.

- (82) Hong, K.; Park, S. Melamine Resin Microcapsules Containing Fragrant Oil: Synthesis and Characterization. *Mater. Chem. Phys.* **1999**, *58*, 128-131.
- (83) Patravale, V. B.; Mandawgade, S. D. Novel Cosmetic Delivery Systems: An Application Update. *Int. J. Cosmet. Sci.* **2008**, *30*, 19-33.
- (84) Wang, L.; Weller, C. L. Recent Advances in Extraction of Nutraceuticals from Plants. *Trends Food Sci. Technol.* **2006**, *17*, 300-312.
- (85) Abreu, F. O. M. S.; Oliveira, E. F.; Paula, H. C. B.; de Paula, R. C. M. Chitosan/Cashew Gum Nanogels for Essential Oil Encapsulation. *Carbohydr. Polym.* **2012**, *89*, 1277-1282.
- (86) Talelli, M.; Rijcken, C. J. F.; Lammers, T.; Seevinck, P. R.; Storm, G.; et al. Superparamagnetic Iron Oxide Nanoparticles Encapsulated in Biodegradable Thermosensitive Polymer Micelles: Toward a Targeted Nanomedicine Suitable for Image-Guided Drug Delivery. *Langmuir* **2009**, *25*, 2060-2067.
- (87) Duncan, B.; Li, X.; Landis, R. F.; Kim, S. T.; Gupta, A.; Wang, L. -S.; et al. Nanoparticle-Stabilized Capsules for the Treatment of Bacterial Biofilms. *ACS Nano* **2015**, *9*, 7775-7782.
- (88) Duncan, B.; Landis, R. F.; Jerri, H. A.; Normand, V.; et al. Hybrid Organic-Inorganic Colloidal Composite 'Sponges' via Internal Crosslinking. *Small* **2015**, *11*, 1302-1309.
- (89) Fernandes, R. V.; Borges, S. V.; Botrel, D. A. Gum Arabic Starch, Maltodextrin, and Inulin as Wall Materials on the Microencapsulation of Rosemary Essential Oil. *Carbohydr. Polym.* **2014**, *101*, 524-532.
- (90) Iannitelli, A.; Grande, R.; Di Stefano, A.; Di Giulio, M.; et al. Potential Antibacterial Activity of Carvacrol-Loaded Poly(DL-Lactide-co-Glycolide) (PLGA) Nanoparticles Against Microbial Biofilm. *Int. J. Mol. Sci.* **2011**, *12*, 5039-5051.
- (91) Chang, Y.; McLandsborough, L.; McClements, D. J. Physicochemical Properties and Antimicrobial Efficacy of Carvacrol Nanoemulsions Formed by Spontaneous Emulsification. *J. Agric. Food Chem.* **2013**, *61*, 8906-8913.
- (92) Hwang, J. S.; Kim, J. N.; Wee Y. J.; Yun, J. S.; Jang, H. G.; Kim S. H.; Ryu, H. W. Preparation and Characterization of Melamine-Formaldehyde Resin Microcapsules Containing Fragrant Oil. *Biotechnol. Bioproc. E* **2006**, *11*, 332-336.
- (93) Landis, R. F.; Gupta, A.; Lee, Y. -W.; et al. Cross-Linked Polymer-Stabilized Nanocomposites for the Treatment of Bacterial Biofilms. *ACS Nano* **2017**, *11*, 946-952.

CHAPTER 2

CROSSLINKED POLYMER-STABILIZED NANOCOMPOSITES FOR THE TREATMENT OF BACTERIAL BIOFILMS

2.1. Introduction

Multidrug-resistant (MDR) bacterial infections are a rapidly emerging health challenge.¹ MDR bacterial infections are responsible for 700,000 deaths each year worldwide, with more than 10 million predicted deaths per year by 2050.² A key threat is provided by biofilm infections³ of wounds and indwelling systems such as catheters,⁴ joint prosthesis,⁵ and other medical implants.⁶ Biofilms secrete extracellular polymeric substance⁷ (EPS), acting as a protective barrier against antibiotics and limiting the efficacy of drugs including vancomycin,⁸ teicoplanin,⁹ and colistin¹⁰ deemed as, “drugs of last resort”. Excising infected tissues/implants¹¹ and long-term antibiotic therapy¹² are currently the best treatments for combatting biofilm-based infections but these invasive approaches have obvious limitations, including patient suffering and inconvenience and extensive health care costs.¹³

Phytochemical^{14,15} extracts from plants are responsible for their self-defense against microbial agents,¹⁶ making them promising tools to combat MDR bacteria.¹⁷ These essential oils are of particular interest as “green” antimicrobial agents¹⁸ due to their low cost,¹⁹ biocompatibility,^{20,21} and potential anti-biofilm properties.²² Previous studies have

demonstrated that many essential oils are cytotoxic towards pathogenic bacteria,^{23,24} however poor solubility²⁵ and stability²⁶ in aqueous media has substantially limited their therapeutic application. Essential oils can be encapsulated into surfactant²⁷ and nanoparticle-stabilized²⁸ colloidal delivery vehicles to enhance their aqueous stability and antimicrobial activity against bacteria with applications in food and beverage industries.²⁹ However, these carriers can be colloidally unstable,³⁰ significantly impairing practical use, particularly in complex media such as serum.

We hypothesized that using a polymer-stabilized essential oil platform would enable us to generate nano-sized emulsions to improve the delivery of the payload,³¹ and to increase its stability³² by incorporating crosslinking strategies. Herein, we report an essential oil-in-water crosslinked polymer nanocomposite (X-NC) for the treatment of bacterial biofilms (Figure 2.1). These nanocomposites exhibit high stability in storage (Supporting Figure 2.7) and serum, and rapidly penetrate into biofilms as evidenced by confocal experiments. Most importantly, X-NCs efficiently eradicate multiple pathogenic biofilms including methicillin-resistant *Staphylococcus aureus* (MRSA). The therapeutic potential of this system demonstrated using a fibroblast-biofilm co-culture wound infection model that demonstrated essentially complete elimination of bacteria while maintaining high fibroblast cell viability.

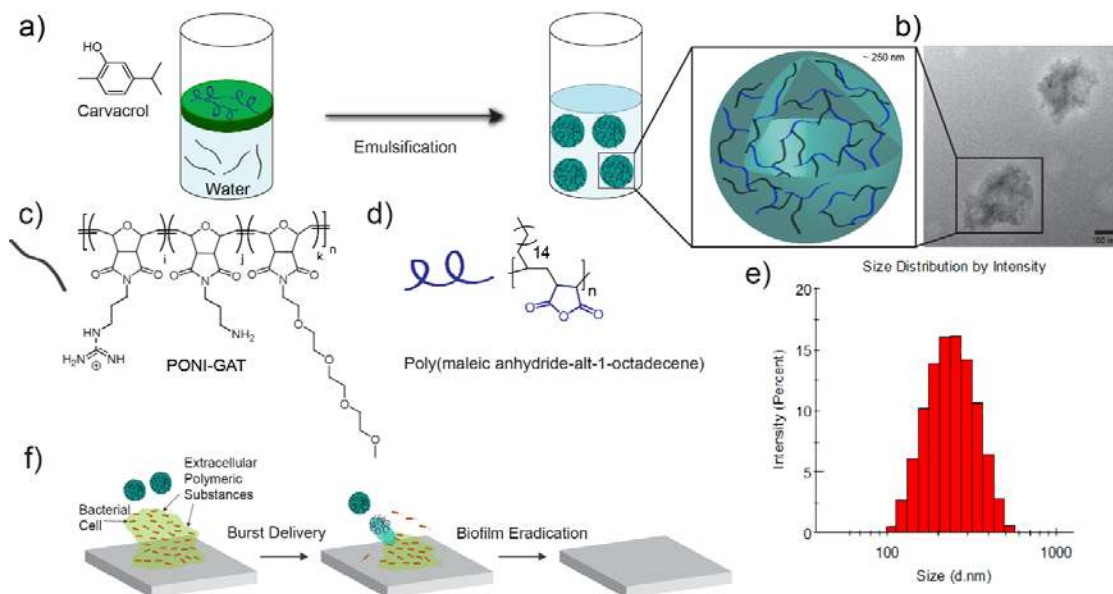


Figure 2.1. Strategy used to generate antimicrobial composites a) Carvacrol oil with dissolved **p-MA-alt-OD** is emulsified with an aqueous solution containing the **PONI-GAT** polymer. The amines on **PONI-GAT** react with the anhydride units on **p-MA-alt-OD**. This crosslinking reaction simultaneously pulls **PONI-GAT** into the oil phase as the polymer becomes more hydrophobic, generating an oil-containing nanocomposite structure. b) TEM micrograph of X-NCs. Scalebar is 100 nm. c) Chemical structure of **PONI-GAT**. d) Chemical structure of **p-MA-alt-OD**. e) DLS histogram indicating the size distribution of X-NCs in phosphate buffer saline (150mM). f) Proposed mechanism of biofilm disruption.

2.2. Results

2.2.1 Generation and Characterization of Nanocomposites

Poly(oxanorborneneimide) polymers (PONIs) were used to stabilize and crosslink the essential oil nanocomposites, providing a well-controlled,³³ easily modulated,³⁴ and scalable platform.³⁵ PONI was designed using three components. First, incorporating amines onto PONI would enable fast reactions with crosslinkable electrophiles loaded into the oil core as PONI approaches the oil interface. The commercially available poly(maleic anhydride-*alt*-octadecene (**p-MA-alt-OD**) was chosen as the electrophile to ensure effective crosslinking.³⁶ Second, guanidinium moieties were added to enable binding with

bacterial membranes³⁷ along with charge neutralization with the carboxylates released from the anhydrides,³⁸ enabling PONIs to partition further into the oil phase for further amidation reactions. Finally, tetraethylene glycol monomethyl ether (**TEG-ME**) groups can impart further amphiphilicity, ensuring PONIs are water-soluble yet can partition into the oil. Therefore, we synthesized a copolymer PONI bearing guanidine, amine, and TEG-ME units (**PONI-GAT**) at a 35-35-30 monomer ratio respectively (Supporting Figure 2.8).

PONI-GAT, carvacrol oil and **p-MA-alt-OD** were used to generate antimicrobial nanocomposites. Nanocomposites were created by emulsifying carvacrol oil loaded with **p-MA-alt-OD** or carvacrol only (non-crosslinked control) into water adjusted to a pH of 10 containing **PONI-GAT** (The pH was adjusted to ensure nucleophilicity of the amines on **PONI-GAT**). Upon emulsification, **PONI-GAT** partitions to the oil-water interface to initially stabilize the carvacrol oil droplets and with **p-MA-alt-OD** present, crosslinking further stabilizes the oil droplets in water. Multiple formulations of **PONI-GAT** and **p-MA-alt-OD** were tried to generate the smallest and most stable formulation. With a final **PONI-GAT** concentration of 6 μM and 10 wt% of **p-MA-alt-OD**, nanocomposites (10 wt% X-NCs) of $\sim 250\text{nm}$ were generated, as shown by transmission electron microscopy (TEM) and dynamic light scatter (DLS). Furthermore, the surface charge of nanocomposites was determined by zeta potential studies (Supporting Figure 2.9) showing an overall negative charge resulting from the crosslinking reaction between amines and anhydrides, generating carboxylates and imparting negative charge at the oil-water interface.

Further characterization of the generated emulsions was performed with confocal microscopy. We hypothesized that reacting **PONI-GAT** with **p-MA-alt-OD** would change

its inherent hydrophobicity and enhance its partitioning within the oil. To test this hypothesis, tetramethylrhodamine-5-isothiocyanate (TRITC, red fluorescence) was conjugated to **PONI-GAT** while 3,3-Dioctadecyloxacarbocyanine (DiO, green fluorescence) was loaded within the oil. In addition, the formulation was modulated to generate micron-sized emulsions so that confocal experiments could be performed. As shown in Figure 2.2a, both green and red fluorescence was co-localized within the oil, indicating a composite morphology.

After characterizing the physical properties of the nanocomposite, chemical properties within the composite structure were characterized using FTIR and fluorescamine assays. Attenuated total reflectance Fourier transform infrared spectroscopy (ATR-FTIR) indicated complete loss of anhydrides and formation of amides/carboxylates after nanocomposite fabrication (Supporting Figure 2.10). To further explore the crosslinking, a fluorescamine assay³⁹ (Figure 2.2b) was performed to identify the progression of the reaction between amines on **PONI-GAT** and the anhydrides on **p-MA-alt-OD**.⁴⁰ **PONI-GAT** was used to generate a calibration curve relating to the polymer concentration and the respective fluorescence generated from the assay (Supporting Figure 2.11). We expected that as the **p-MA-alt-OD** wt% increases within the oil, more amines will react, and the overall fluorescence generated from fluorescamine will decrease. The results show that a substantial reduction in amines on **PONI-GAT** occurs as **p-MA-alt-OD** wt% increases, with almost complete conversion at 10 wt%.

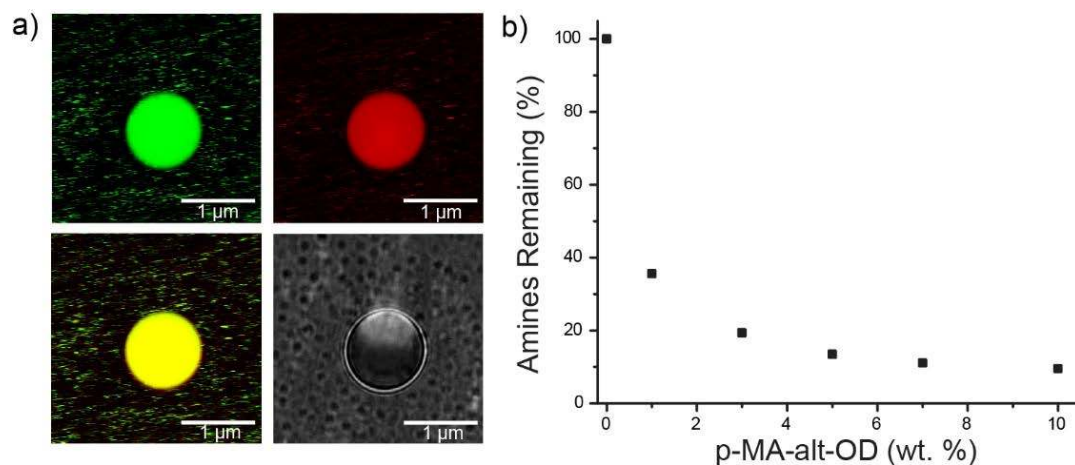


Figure 2.2. Physical and chemical characterization of X-NCs. Confocal micrograph of a) crosslinked micron-sized composites. **PONI-GAT** was partially labeled with TRITC (red fluorescence) and the oil core is loaded with DiO (green fluorescence). **PONI-GAT** labeled with TRITC can be seen co-distributed with the hydrophobic core indicating a composite (as opposed to core-shell) morphology. b) Fluorescamine assay to determine the percentage of remaining amines on **PONI-GAT** after X-NCs formation.

2.2.2 X-NCs Penetration into Biofilms

Effective treatment of biofilms requires penetration of antimicrobial agents into the film.⁴¹ We next probed the ability of X-NCs to penetrate into biofilms. X-NCs loaded with DiO within the oil were used to track their delivery into biofilms formed by red fluorescent protein (RFP) expressing *Escherichia coli*. As shown in Figure 2.3, the X-NCs diffuse into the biofilm matrix and efficiently disperse throughout the biofilm, co-localizing with the bacteria. This data supports X-NCs deliver their payload and that the oil core and nanocomposite fabrication strategy are operative for effective delivery.

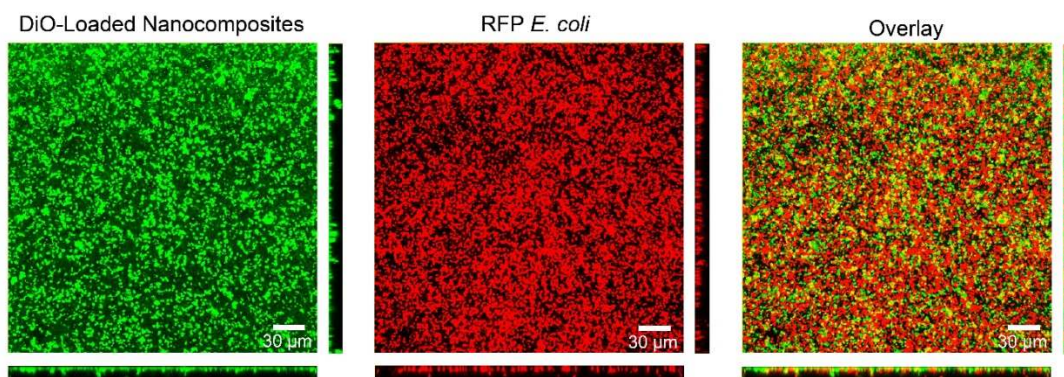


Figure 2.3. Confocal image stacks of *E. coli DH5a* biofilm after 3 h treatment with 10 wt% X-NCs. DiO was loaded into X-NCs to track them throughout the biofilm. The overlay shows X-NCs completely penetrate the biofilm, co-localizing with bacteria that expresses red fluorescent protein. Scale bars are 30 µm.

2.2.3 Antimicrobial Activity of X-NCs Against Biofilms

Next, we investigated the therapeutic efficacy of the X-NCs against multiple Gram positive and negative biofilms. Four pathogenic bacterial strains of clinical isolates, *Pseudomonas aeruginosa* (CD-1006), *Staphylococcus aureus* (CD-489, a methicillin-resistant strain), *Escherichia coli* (CD-2), and *Enterobacter cloacae* (*E. cloacae*, CD-1412) complex were chosen to test our system. As shown in Figure 2.4, X-NCs were able to effectively kill bacterial cells in all four biofilms within three hours. The individual components used to generate the nanocomposites were used as controls and they showed minimal toxicity to biofilms indicating that the combination of all components to generate X-NCs is critical for maximum therapeutic efficiency. Notably, X-NCs are able to effectively treat both Gram negative (*E. coli*, *P. aeruginosa*, and *E. cloacae* complex) and Gram positive (*S. aureus*) bacteria, demonstrating the broad-spectrum activity of X-NCs.

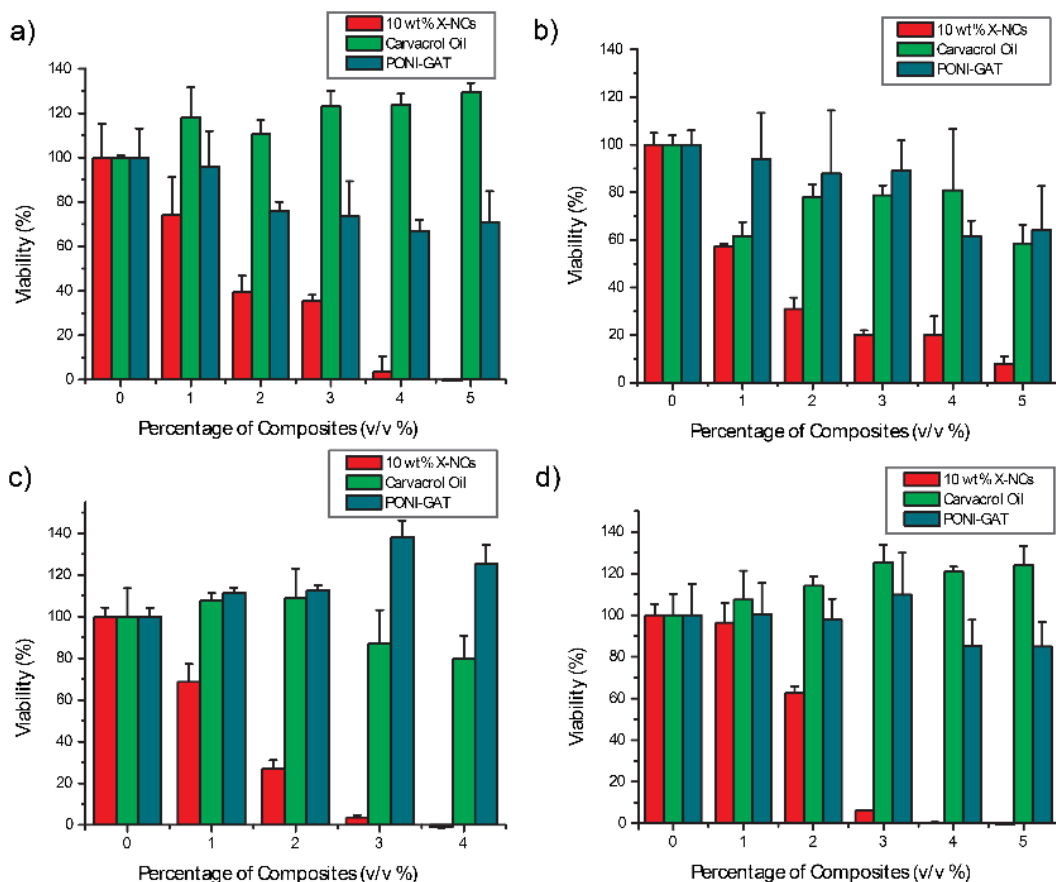


Figure 2.4. Viability of 1 day-old biofilms. (a) *E. coli* (CD-2), (b) *S. aureus* (CD-489), (c) *P. aeruginosa* (CD-1006), and (d) *E. cloacae* complex (CD-1412) biofilms after 3 h treatment with 10 wt% X-NCs, carvacrol oil, and PONI-GAT at different emulsion concentrations (v/v % of emulsion). The results are an average of triplicates, and the error bars indicate the standard deviation.

2.2.4 Eradication of Biofilms in a Co-culture Model

Treatment of bacterial infections on human tissues and organs is even more challenging and relevant for medical applications. Biofilm infections associated with wounds and indwelling implants interfere with the host's ability to regenerate damaged tissue.⁴² In particular, fibroblasts play an important role during wound healing by aiding to close the area and rebuild necessary extracellular matrix within the skin.⁴³ We used an *in vitro* co-culture model comprised of mammalian fibroblasts cells with a biofilm grown over

them. *P. aeruginosa* bacteria were seeded with a confluent NIH 3T3 fibroblast cell monolayer overnight to generate biofilms prior to X-NCs treatment. The co-cultures were treated with X-NCs for three hours, washed, and the viabilities of both bacteria and fibroblasts were determined. As shown in Figure 2.5, X-NCs effectively treated the biofilm infection while 3T3 fibroblast viability was largely unaffected. A four-fold log reduction (~99.5%) in biofilm colonies was obtained at 15 v/v% of X-NC emulsion.

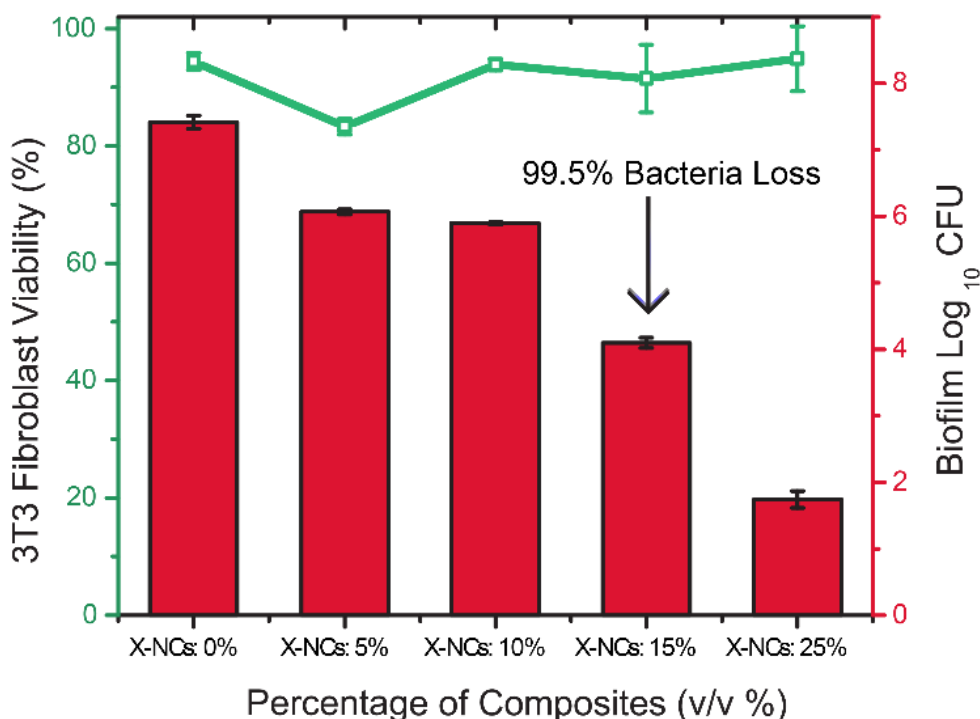


Figure 2.5. Viability of 3T3 fibroblast cells and *P. aeruginosa* biofilms in the fibroblast-biofilm co-culture model after 3 h treatment with 10 wt% X-NCs at different emulsion concentrations (v/v % of emulsion). Scatters and lines represent 3T3 fibroblast cell viability. Bars represent log₁₀ of colony forming units in biofilms. The results are an average of three runs and the error bars indicate the standard deviations.

2.2.5 Serum Stability of X-NCs

Nanoemulsion stability in serum media is critical for its application both topically and systemically.^{44,45,46,47} Negatively charged serum proteins can bind onto delivery

vehicles, forming a corona which can significantly alter their biological identity.^{48,49} Our crosslinked nanocomposite vehicle which bears a negatively charged surface should be resistant to serum protein adsorption. X-NCs were incubated with 10% serum media for two days and analyzed using DLS. As shown in Figure 2.6a, 10 wt% X-NCs showed stability with no evidence of destabilization/aggregation. As a control, non-crosslinked analogs using the same formulation minus p-MA-alt-OD showed no stability in serum (Supporting Figure 2.12). In addition, DiO was loaded into both crosslinked nanocomposites and non-crosslinked analogs and incubated in serum for one hour. Destabilization of the non-crosslinked analog would result in leakage and quenched fluorescence of the loaded dye.⁵⁰ Figure 2.6b shows that DiO maintains its fluorescence within the X-NCs while its non-crosslinked analog shows no fluorescence, further supporting the stability of X-NCs in serum conditions.

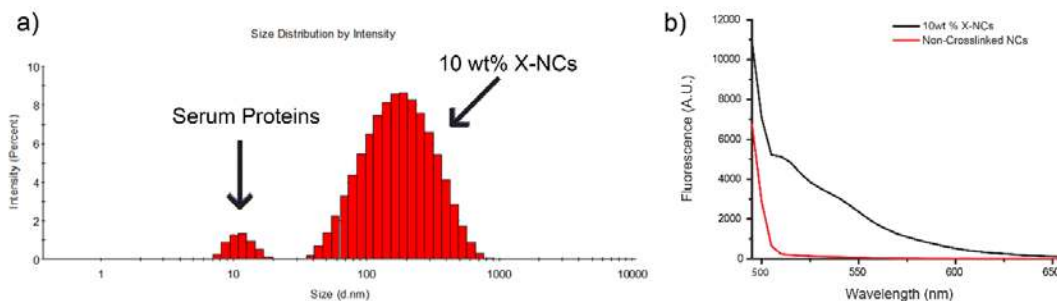


Figure 2.6. Stability of X-NCs in 10% fetal bovine serum (FBS). a) DLS histogram of 10 wt% X-NCs in 10% FBS after two days. Destabilization/aggregation of the X-NCs was not observed. b) Fluorescence spectra of loaded DiO in 10 wt% X-NCs and non-crosslinked analog. Serum proteins destabilizes the non-crosslinked analog, leaking out DiO, and quenching the fluorescence whereas X-NCs maintain fluorescence indicating stability. Excitation of DiO = 490nm.

2.3. Conclusions

In summary, we report the fabrication of a polymer-stabilized oil-in-water nanocomposite that demonstrates high therapeutic activity towards pathogenic biofilms. These nanocomposites show good stability in serum and can effectively penetrate throughout biofilms. Furthermore, specific elimination of a biofilm infection while maintaining fibroblast viability in an *in vitro* co-culture was observed. The polymer-based crosslinked essential oil-in-water nanoemulsion strategy we present is a promising antimicrobial platform, opening new applications to treat wound biofilms and other biofilm-based infections. Given the limited capabilities of current topical therapeutics, we envision these nanocomposites as powerful new tools for skin-associated infections. Going further, the efficacy and modularity of this system will enable the use of essential oil-based composites as antimicrobial additives for foods and beverages. Finally, due to their unique mechanism of action, these stabilized essential oil emulsions can provide a long-term solution to the ever-increasing danger of antibiotic resistance.

2.4. Experimental Protocol

2.4.1 Materials and Methods

All reagents and materials were purchased from Fisher Scientific and used as received. NIH-3T3 cells (ATCC CRL-1658) were purchased from ATCC. Dulbecco's Modified Eagle's Medium (DMEM) (DMEM; ATCC 30-2002) and fetal bovine serum (Fisher Scientific, SH3007103) were used in cell culture. Pierce LDH Cytotoxicity Assay Kit was purchased from Fisher Scientific.

2.4.2 Synthesis of PONI-GAT

Synthesis can be found under Supporting Figure 2.8.

2.4.3 Preparation of Nanocomposites

Stock nanocomposite solutions were prepared in 0.6 ml Eppendorf tubes. To prepare the stock X-NC emulsions, 3 μL of carvacrol oil (containing 10 wt% p-MA-alt-OD) was added to 497 μL of Milli-Q H_2O (previously adjusted to a pH of 10) containing 6 μM of PONI-GAT and emulsified in an amalgamator for 50 s. The non-crosslinked analogs were done in the same fashion however without p-MA-alt-OD dissolved in carvacrol. The emulsions were allowed to rest overnight prior to use.

2.4.4 Fluorescamine Assay

The fluorescamine calibration curve was generated by mixing various concentrations of PONI-GAT with fluorescamine (dissolved in acetonitrile – 2.5 mg/ml, 50 μL aliquots) in phosphate buffer (PB – 5mM, pH = 7.4). The solutions were sonicated in the dark for 5 min, diluted with ethanol and their emission maxima at 470 nm analyzed. The percentage of amines remaining within the X-NCs at different wt% of p-MA-alt-OD was performed by diluting the stock emulsion solution by half. Afterwards, 450 μL of PB was added along with 50 μL of fluorescamine. The solutions were sonicated in the dark for 5 min, diluted with ethanol and their emission maxima at 470 nm analyzed.

2.4.5 Biofilm Formation

Bacteria were inoculated in LB broth at 37°C until stationary phase. The cultures were then harvested by centrifugation and washed with 0.85% sodium chloride solution three times. Concentrations of resuspended bacterial solution were determined by optical density measured at 600 nm. Seeding solutions were then made in M9 to reach OD_{600} of 0.1. 100 μL of the seeding solutions were added to each well of the microplate. M9 medium

without bacteria was used as a negative control. The plates were covered and incubated at room temperature under static conditions for a desired period. Planktonic bacteria were removed by washing with PB saline three times.

Varied v/v % of X-NCs, made in M9 medium, were incubated with the biofilms for 3 h. Biofilms were washed with phosphate buffer saline (PBS) three times and viability was determined using an Alamar Blue assay. M9 medium without bacteria was used as a negative control.

2.4.6 Biofilm – 3T3 Fibroblast Cell Co-culture

Fibroblast-3T3 coculture was performed using the previously reported protocol.²⁸ A total of 20,000 NIH 3T3 (ATCC CRL-1658) cells were cultured in Dulbecco's modified Eagle medium (DMEM; ATCC 30-2002) with 10% bovine calf serum and 1% antibiotics at 37°C in a humidified atmosphere of 5% CO₂. Cells were kept for 24 hours to reach a confluent monolayer. Bacteria (*P. aeruginosa*) were inoculated and harvested as mentioned above. Afterwards, seeding solutions 10⁸ cells/ml were inoculated in buffered DMEM supplemented with glucose. Old medium was removed from 3T3 cells followed by addition of 100 µL of seeding solution. The co-cultures were then stored in a box humidified with damp paper towels at 37°C overnight without shaking.

Nanocomposites and other control solutions were diluted in DMEM media prior to use to obtain desired testing concentrations. Old media was removed from co-culture and replaced with freshly prepared testing solutions and was incubated for 3 hours at 37°C. Co-cultures were then analyzed using an LDH cytotoxicity assay to determine mammalian cell viability using manufacturer's instructions.⁵¹ To determine the bacteria viability in

biofilms, the testing solutions were removed, and co-cultures were washed with PBS. Fresh PBS was then added to disperse remaining bacteria from biofilms in co-culture by sonication for 20 min and mixing with pipet. The solutions containing dispersed bacteria were then plated onto agar plates and colony forming units were counted after incubation at 37°C overnight.

2.5. Supporting Figures

2.5.1 Shelf life of X-NC

X-NCs were prepared as stated in the main text and allowed to stand for ~1 year. Afterwards, size was determined using dynamic light scattering (DLS) on a Zetasizer Nano ZS equipped with a He-Ne laser, 633nm.

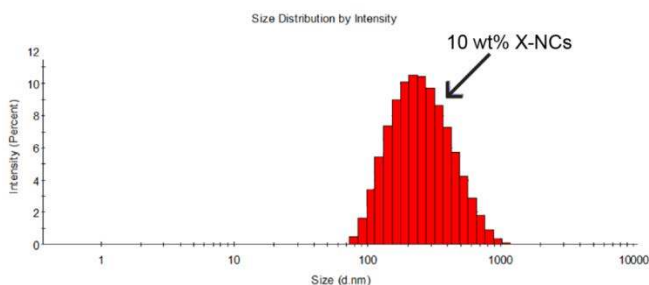
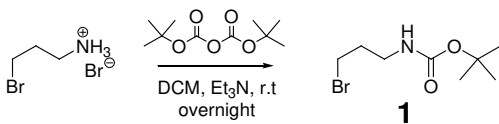


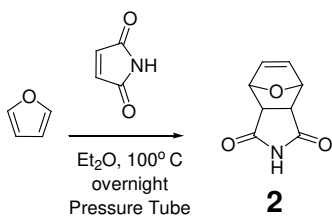
Figure 2.7. DLS size of X-NCs. The X-NCs maintained their integrity with an average diameter of 285 nm.

2.5.2 Synthesis of PONI-GAT

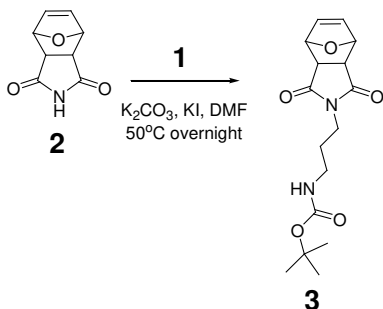


Synthesis of 1. To a 500ml round bottom flask equipped with a stirbar was added 150ml of dichloromethane (DCM). Next, 3-Bromopropylamine hydrobromide (10.0g, 45.7mmol, 1.0eq) was added to the DCM solution. Then, triethylamine (Et₃N) (25.5ml, 182.7mmol, 4.0eq) was added to the reaction mixture. Finally, Di-*tert*-butyl dicarbonate (12.6ml,

54.8mmol, 1.2eq) was added dropwise. After addition of di-*tert*-butyl dicarbonate, the reaction was stirred overnight at room temperature (r.t.). Afterwards, the DCM was rotovaped, diluted with 100ml of diethyl ether, and extracted with 1M HCL (1x 20ml), saturated sodium bicarbonate (2x 20ml), and brine (1x 20ml). The organic layer was dried with sodium sulfate, filtered, and rotovaped to yield **1** as a clear liquid. **1** was purified using column chromatography and silica gel as the stationary phase. $^1\text{H NMR}$ (400MHz, CDCl_3) 4.6 (br, 1H) 3.43 (t, 2H), 3.26 (br, 2H), 2.04 (t, 2H), 1.43 (s, 9H).

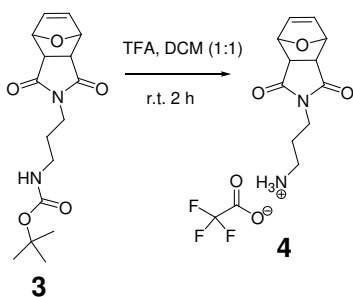


Synthesis of 2. In a pressure tube, furan (4.5ml, 61.7mmol, 1.5eq) and maleimide (4.0g, 41.1mmol, 1.0eq) were added in addition to 5ml of diethyl ether. The tube was sealed and heated at 100°C overnight. Afterwards, the pressure tube was cooled to r.t. and the formed solid was removed, filtered, and washed with copious amounts of diethyl ether to isolate **2** as a white solid and was used without further purification. $^1\text{H NMR}$ (400MHz, MeOD) 11.14 (s, 1H), 6.52 (s, 2H), 5.12 (s, 2H), 2.85 (s, 2H).

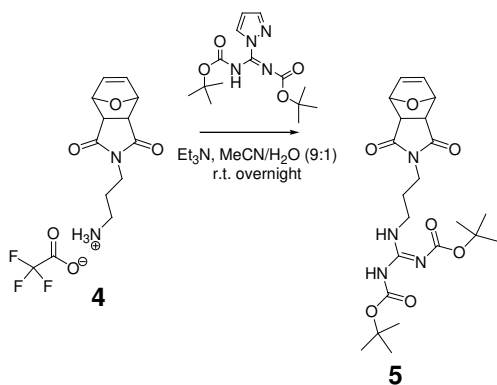


Synthesis of 3. To a 100ml round bottom flask equipped with a stirbar was added 30ml of dimethylformamide (DMF). Next, **2** (2.36g, 14.3mmol, 1.0eq) was added along with

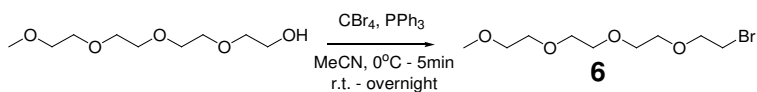
potassium carbonate (7.9g, 57.2mmol, 4.0eq). The reaction mixture was heated at 50°C for five minutes. Finally, potassium iodide (0.05g, 0.30mmol, 0.02eq) and **1** (3.47g, 14.6mmol, 1.02eq) were added and stirred at 50°C overnight. Afterwards, the reaction mixture was cooled to room temperature, diluted to 150ml with ethyl acetate and washed with water (7x, 50ml) and brine (1x, 50ml). The organic layer was dried with sodium sulfate, filtered, and rotovaped to yield **3** as a white solid. **3** was purified using column chromatography and silica gel as the stationary phase. ¹H NMR (400MHz, CDCl₃) 6.51 (s, 2H), 5.26 (s, 2H), 5.03 (br, 1H), 3.56 (t, 2H), 3.05 (q, 2H), 2.86 (s, 2H), 1.73 (quint, 2H) 1.45 (s, 9H).



Synthesis of 4. To a 50ml round bottom flask equipped with a stirbar was added **3** (2.0g, 6.2mmol, 1.0eq). Nitrogen was bubbled through DCM for five minutes and 5ml was added to the flask which was purged with nitrogen. 5ml of trifluoroacetic acid (TFA, excess) was added and the reaction was stirred for two hours. Afterwards, excess TFA was removed by rotovaping with DCM (3x) yielding **4**. **4** was isolated as a white solid by washing with diethyl ether (3x, 10ml) and used without further purification and directly used in the next reaction (Ninhydrin test confirms free primary amine).

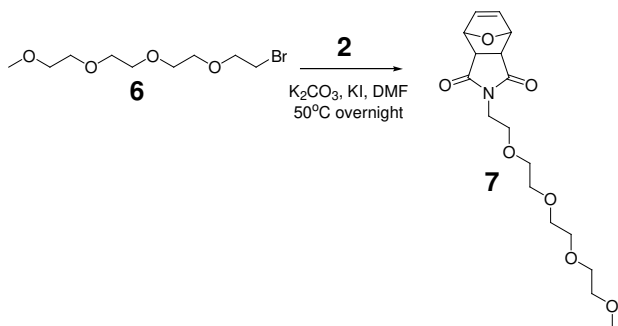


Synthesis of 5. To a 100ml round bottom flask equipped with a stirbar was added **4** (1.2g, 3.6mmol, 1.0eq), 45ml acetonitrile (MeCN), and 5ml of water. Triethylamine (4.7ml, 33.5mmol, 9.2eq) was added and finally *N,N'*-Di-Boc-1*H*-pyrazole-1-carboxamide (1.7g, 5.5mmol, 1.5eq) in portions. The reaction was allowed to stir at r.t. overnight. Afterwards, the solution was diluted with 100ml of ethyl acetate and extracted with water (2x, 50ml) and brine (2x, 50ml). The organic layer was dried with sodium sulfate, filtered, and rotovaped to yield **5**. **5** was purified using column chromatography and silica gel as the stationary phase to yield a white solid. ¹H NMR (400MHz, CDCl₃) 8.49 (t, 1H), 6.49 (s, 2H), 5.25 (s, 2H), 3.53 (t, 2H), 3.47 (q, 2H), 2.83 (s, 2H), 1.82 (quint, 2H), 1.49 (s, 18H).

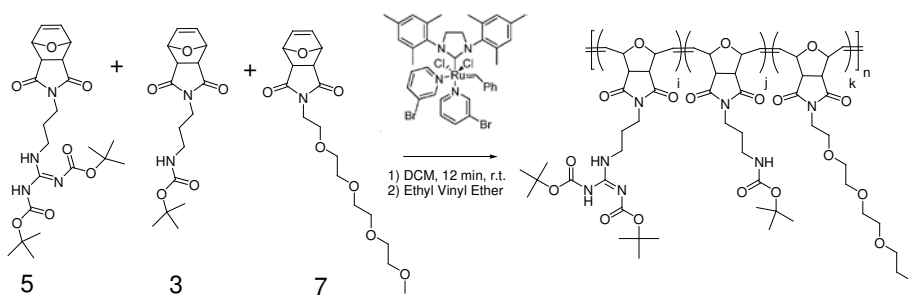


Synthesis of 6. To a 250ml round bottom flask was added Tetraethyleneglycol monomethyl ether (4.2ml, 20.9mmol, 1.0eq) and 80ml of MeCN. The reaction was cooled to 0°C and tetrabromomethane (8.4g, 25.1mmol, 1.2eq) was added. Finally, triphenylphosphine (6.6g, 25.3mmol, 1.2eq) was added in portions and allowed to stir for five minutes at 0°C. After five minutes, the reaction was warmed to room temperature and stirred overnight. Afterwards, the reaction was concentrated by rotovaping and purified

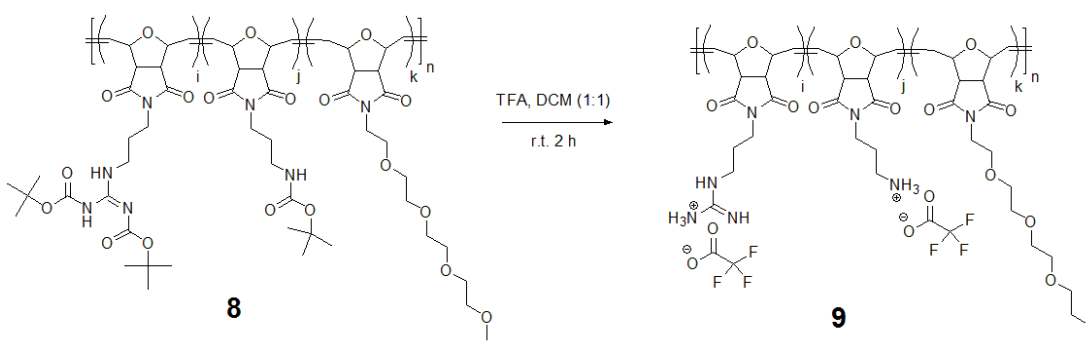
using column chromatography and silica gel as the stationary phase to yield **6** as a clear oil (Potassium permanganate was used to visualize **6**). ¹H NMR (400MHz, CDCl₃) 3.75 (t, 2H), 3.6 (br, 10H), 3.49 (t, 2H), 3.41 (t, 2H), 3.32 (s, 3H).



Synthesis of 7. To a 100ml round bottom flask equipped with a stirbar was added 30ml of DMF. Next, **2** (2.84g, 17.2mmol, 1.0eq) was added along with potassium carbonate (9.48g, 68.7mmol, 4.0eq). The reaction mixture was heated at 50°C for five minutes. Finally, potassium iodide (0.05g, 0.30mmol, 0.02eq) and **6** (4.9g, 18.0mmol, 1.05eq) were added and stirred at 50°C overnight. Afterwards, the reaction mixture was cooled to room temperature, diluted to 150ml with ethyl acetate and washed with water (7x, 50ml) and brine (1x, 50ml). The organic layer was dried with sodium sulfate, filtered, and rotovaped to yield **7**. **7** was isolated as a clear oil using column chromatography and silica gel as the stationary phase. ¹H NMR (400MHz, CDCl₃) 6.49 (s, 2H), 5.23 (s, 2H), 3.66 (t, 2H), 3.6 (br, 8H), 3.58 (br, 4H), 3.51 (t, 2H), 3.35 (s, 3H), 2.83 (s, 2H).



Synthesis of Polymer 8. To a 10ml pear-shaped flask equipped with a stirbar was added **5** (457mg, 0.98mmol, 1.0eq), **3** (317mg, 0.98mmol, 1.0eq) and **7** (300mg, 0.84mmol, 0.85eq) along with 5ml of DCM. In a separate 10ml pear-shaped flask equipped with a stirbar was added Grubbs Catalyst 3rd Generation (38.4mg, 0.043mmol, 0.04eq) along with 1ml of DCM. Both flasks underwent freeze-pump thaw three times, warmed to room temperature and the catalyst transferred to the reaction mixture. After 12 minutes, ethyl vinyl ether (200 μ l, excess) was quickly added and stirring continued for 15 minutes. The polymer was precipitated using 200ml of 1:1 hexane:ethyl ether. The polymer was collected by filtration, dissolved in a minimal amount of DCM and precipitated again in the same hexane:ethyl ether solution yielding **8** as a gray solid. MW = 31,736 (MW was determined through gel permeation chromatography (tetrahydrofuran) with a polystyrene calibration curve). ¹H NMR (400MHz, CDCl₃) 11.4 (s, 1H), 8.39 (br, 1H), 6.01 (s, 2H), 5.72 (br, 2H), 4.95 (br, 2H), 4.41 (br, 2H), 3.55 (br, 11H), 3.32 (br, 2H), 3.30 (s, 2H), 3.29 (br, 2H), 3.01 (br, 1H), 1.82 (br, 1H), 1.7 (br, 3H), 1.42 (s, 12H), 1.35 (s, 6H).



Synthesis of Polymer 9 – PONI-GAT. To a 50ml round bottom flask equipped with a stirbar was added Polymer **8** (400mg). Dichloromethane was purged with nitrogen for five minutes and 12ml was added to the flask, sealed with a septum and purged with nitrogen

for five minutes. The main nitrogen line was left in the septum and the nitrogen pressure was reduced to a steady stream. 12ml of trifluoroacetic acid (excess) was added and the reaction was allowed to stir for two hours. Afterwards, excess TFA was removed by rotovaping with DCM (3x). The reaction residue was dissolved in a minimal amount of water, filtered through a polyethersulfone (PES) syringe filter and lyophilized to yield **9** as an off-white solid which readily dissolves in water. MW ~ 23,486. ^1H NMR (400MHz, D_2O) 6.1 (br, 2H), 5.91 (br, 2H), 5.2 (br, 2H), 4.64 (br, 2H), 3.65 (br, 19H), 3.39 (s, 2H), 3.21 (br, 2H), 3.01 (br, 2H), 1.99 (br, 2H), 1.89 (br, 2H) (^1H NMR confirms complete loss of all Boc protecting groups).

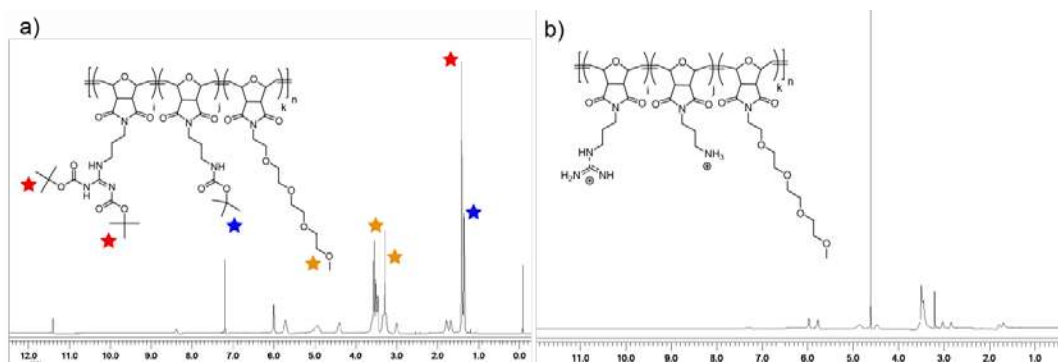


Figure 2.8. ^1H NMR spectra of a) protected and b) deprotected PONI-GAT.

2.5.3 Zeta Potential

Zeta potential of the X-NCs were performed on a Zetasizer Nano ZS equipped with a DTS1070 cuvette.

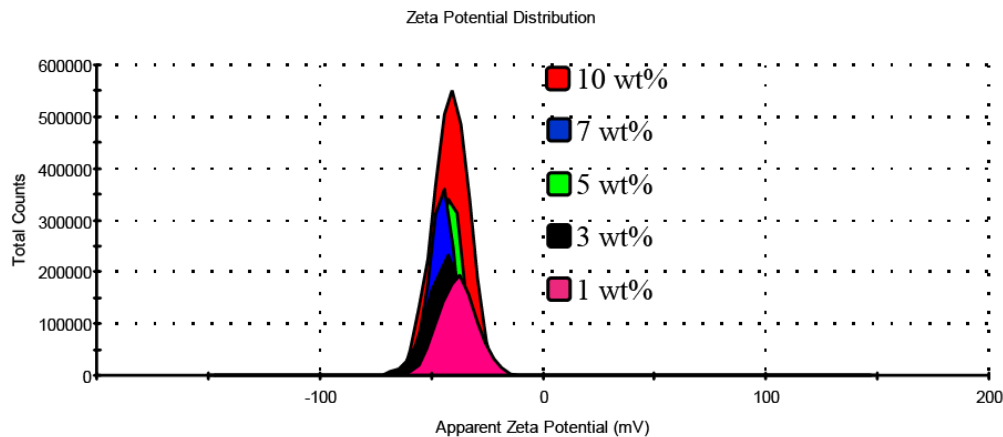


Figure 2.9. Zeta potential of X-NCs with varying wt% of p-MA-alt-OD. Results show a highly negative charged nanocomposite regardless of p-MA-alt-OD present.

2.5.4 Attenuated Total Reflectance Fourier Transform Infrared Spectroscopy (ATR-FTIR)

ATR-FTIR was performed on a Bruker Alpha FT-IR spectrophotometer fitted with a Platinum ATR QuickSnap sampling module. Freeze-dried samples of X-NCs along with p-MA-alt-OD and PONI-GAT were analyzed to determine changes in functional groups before and after emulsification.

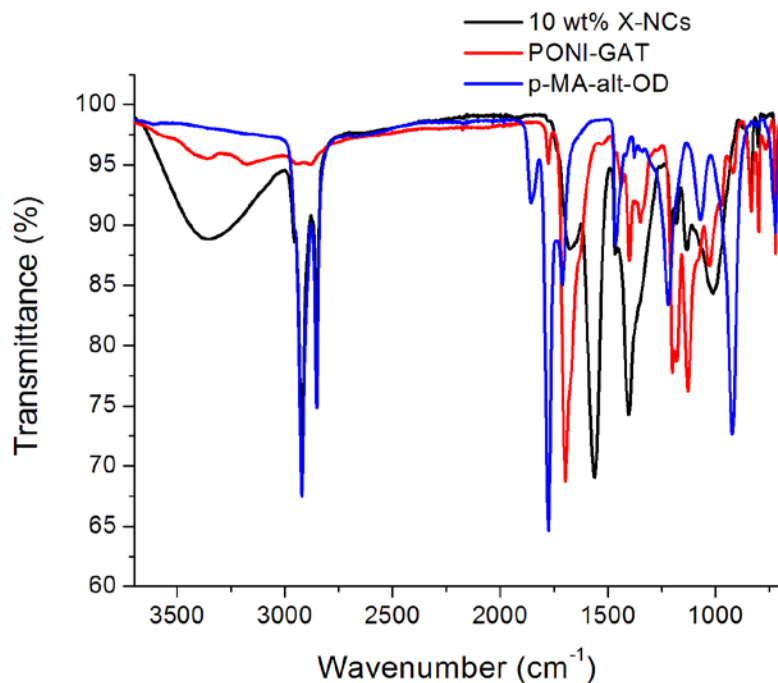


Figure 2.10. ATR-FTIR analysis before and after emulsification. Results showed complete loss of anhydrides on p-MA-alt-OD (1857 cm^{-1} , 1776 cm^{-1}) followed by the formation of carboxylate frequencies (3300 cm^{-1} , 1564 cm^{-1}) and amide frequencies (1650 cm^{-1}) supporting crosslinking between the amines of PONI-GAT and the anhydrides on p-MA-at-OD.

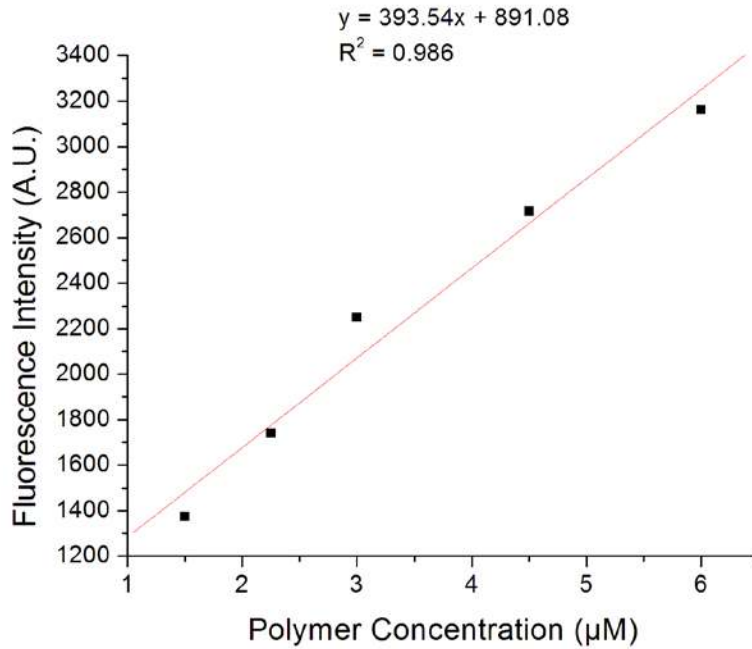


Figure 2.11. Fluorescamine calibration curve. A reaction between the amines on PONI GAT with fluorescamine generates a fluorescence signal.

2.5.5 Serum Stability of Non-Crosslinked NCs

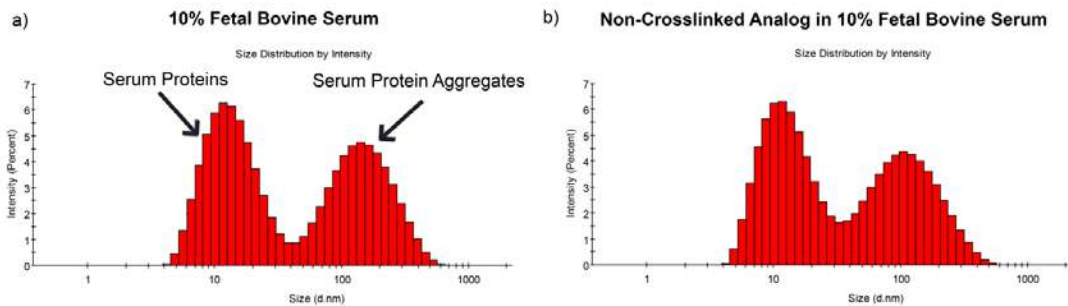


Figure 2.12. DLS size of a) 10% fetal bovine serum only and b) non-crosslinked nanocomposites. The non-crosslinked emulsion is immediately disrupted leaving only serum proteins present.

2.6. References

- (1) Gupta, A.; Landis, R. F.; Rotello, V. M. Nanoparticle-Based Antimicrobials: Surface Functionality is Critical. *F1000Res.* **2016**, *5*, F1000 Faculty Rev-364.
- (2) Tackling Drug-Resistant Infections Globally: Final Report and Recommendations. (2016, May 19). Retrieved November 05, 2016, from <https://amr-review.org/Publications>.
- (3) Bjarnsholt, T. The Role of Bacterial Biofilms in Chronic Infections. *APMIS* **2013**, *121*, 1-58.
- (4) Trautner, B. W.; Darouiche, R. O. Role of Biofilm in Catheter-Associated Urinary Tract Infection. *Am. J. Infect. Control* **2004**, *32*, 177-183.
- (5) Song, Z.; Borgwardt, L.; Hoiby, N.; Wu, H.; Sorensen, T. S.; Borgwardt, A. Prosthesis Infections After Orthopedic Joint Replacement: The Possible Role of Bacterial Biofilms. *Orthop. Rev. (Pavia)* **2013**, *5*, 65-71.
- (6) Veerachamy, S.; Yarlagadda, T.; Manivasagam, G.; Yarlagadda, P. K. Bacterial Adherence and Biofilm Formation on Medical Implants: A Review. *P. I. Mech. Eng. H* **2014**, *228*, 1083-1099.
- (7) Kostakioti, M.; Hadjifrangiskou, M.; Hultgren, S. J. Bacterial Biofilms: Development, Dispersal, and Therapeutic Strategies in the Dawn of the Postantibiotic Era. *Cold Spring Harb. Perspect. Med.* **2013**, *3*, a010306.
- (8) Boneca, I. G.; Chiosis, G. Vancomycin Resistance: Occurrence, Mechanisms and Strategies to Combat it. *Expert Opin. Ther. Targets* **2003**, *7*, 311-328.
- (9) Boger, D. L. Vancomycin, Teicoplanin, and Ramoplanin: Synthetic and Mechanistic Studies. *Med. Res. Rev.* **2001**, *21*, 356-381.
- (10) Dafopoulou, K.; Xavier, B. B.; Hotterbeekx, A.; Janssens, L.; Lammens, C.; De, E.; Goossens, H.; Tsakris, A.; Malhotra-Kumar, S.; Pournaras, S. Colistin-resistant *Acinetobacter Baumannii* Clinical Strains with Deficient Biofilm Formation. *Antimicrob. Agents Chemother.* **2016**, *60*, 1892-1895.
- (11) Kujath, P.; Kujath, C. Complicated Skin, Skin Structure and Soft Tissue Infections - Are We Threatened by Multi-resistant Pathogens? *Eur. J. Med. Res.* **2010**, *15*, 544-553.
- (12) Wu, H.; Moser, C.; Wang, H.-Z.; Hoiby, N.; Song, Z.-J. Strategies for Combating Bacterial Biofilm Infections. *In. J. Oral. Sci.* **2015**, *7*, 1-7.
- (13) Lynch, A. S.; Robertson, G. T. Bacterial and Fungal Biofilm Infections. *Annu. Rev. Med.* **2008**, *59*, 415-428.

- (14) Wang, H.; Khor, T. O.; Shu, L.; Su, Z.; Fuentes, F.; Lee, J.-H.; Kong, A.-N. T. Plants Against Cancer: A Review on Natural Phytochemicals in Preventing and Treating Cancers and Their Drugability. *Anticancer Agents Med. Chem.* **2012**, *12*, 1281-1305.
- (15) Farzaei, M. H.; Bahramsoltani, R.; Abbasabadi, Z.; Rahimi, R. A Comprehensive Review on Phytochemical and Pharmacological Aspects of *Elaeagnus Angustifolia* L. *J. Pharm. Pharmacol.* **2015**, *67*, 1467-1480.
- (16) Hintz, T.; Matthews, K. K.; Di, R. The Use of Plant Antimicrobial Compounds for Food Preservation. *Biomed. Res. Int.* **2015**, *2015*, 246264.
- (17) Kon, K. V.; Rai, M. K. Plant Essential Oils and Their Constituents in Coping with Multidrug-resistant Bacteria. *Expert Rev. Anti-Infect. Ther.* **2012**, *10*, 775-790.
- (18) Vergis, J.; Gokulakrishnan, P.; Agarwal, R. K.; Kumar, A. Essential Oils as Natural Food Antimicrobial Agents: A Review. *Crit Rev Food Sci Nutr* **2015**, *55*, 1320-1383.
- (19) Maia, M. F.; Moore, S. J. Plant-Based Insect Repellents: A Review of Their Efficacy, Development and Testing. *Malar. J.* **2011**, *10*, S11.
- (20) Freire Rocha Caldas, G.; Araujo, A. V.; Albuquerque, G. S.; Silva-Neto Jda, C.; Costa-Silva, J. H.; de Menezes, I. R.; Leite, A. C.; da Costa, J. G.; Wanderley, A. G. Repeated-doses Toxicity Study of the Essential Oil of *Hyptis Martiusii* Benth. (Lamiaceae) in Swiss Mice. *Evid. Based Complement. Alternat. Med.* **2013**, *2013*, 856168.
- (21) Johnson, S.; Boren, K. Topical and Oral Administration of Essential Oils – Safety Issues. *Aromatopia* **2013**, *22*, 43-48.
- (22) Saviuc, C.-M.; Drumea, V.; Olariu, L.; Chifiriuc, M.-C.; Bezirtzoglou, E.; Lazar, V. Essential Oils with Microbicidal and Antibiofilm Activity. *Curr. Pharm. Biotechnol.* **2015**, *16*, 137-151.
- (23) Sharifi-Rad, J.; Sharifi-Rad, M.; Hoseini-Alfatemi, S. M.; Iriti, M. Composition, Cytotoxic and Antimicrobial Activities of *Satureja Intermedia* C.A.Mey Essential Oil. *Int. J. Mol. Sci.* **2015**, *16*, 17812-17825.
- (24) Hosseinkhani, F.; Jabalameli, F.; Banar, M.; Abdellahi, N.; Taherikalani, M.; van Leeuwen, W. B.; Emaneini, M. Monoterpene Isolated from the Essential Oil of *Trachyspermum Ammi* Is Cytotoxic to Multidrug-resistant *Pseudomonas Aeruginosa* and *Staphylococcus Aureus* Strains. *Rev. Soc. Bras. Med. Trop.* **2016**, *49*, 172-176.
- (25) Samperio, C.; Boyer, R.; Eigel, W. N., 3rd; Holland, K. W.; McKinney, J. S.; O'Keefe, S. F.; Smith, R.; Marcy, J. E. Enhancement of Plant Essential Oils' Aqueous Solubility and Stability Using Alpha and Beta Cyclodextrin. *J. Agric. Food Chem.* **2010**, *58*, 12950-12956.

- (26) Turek, C.; Stintzing, F. C. Stability of Essential Oils: A Review. *Compr. Rev. Food. Sci. Food Saf.* **2013**, *12*, 40-53.
- (27) Chang, Y.; McLandsborough, L.; McClements, D. J. Fabrication, Stability and Efficacy of Dual-component Antimicrobial Nanoemulsions: Essential Oil (Thyme Oil) and Cationic Surfactant (Lauric Arginate). *Food Chem.* **2015**, *172*, 298-304.
- (28) Duncan, B.; Li, X.; Landis, R. F.; Kim, S. T.; Gupta, A.; Wang, L. S.; Ramanathan, R.; Tang, R.; Boerth, J. A.; Rotello, V. M. Nanoparticle-Stabilized Capsules for the Treatment of Bacterial Biofilms. *ACS Nano* **2015**, *9*, 7775-7782.
- (29) Amaral, D. M. F.; Bhargava, K. Essential Oil Nanoemulsions and Food Applications. *Adv. Food Technol. Nutr. Sci. Open J.* **2015**, *1*, 84-87.
- (30) Ziani, K.; Chang, Y.; McLandsborough, L.; McClements, D. J. Influence of Surfactant Charge on Antimicrobial Efficacy of Surfactant-Stabilized Thyme Oil Nanoemulsions. *J. Agric. Food Chem.* **2011**, *59*, 6247-6255.
- (31) Akhtar, J.; Siddiqui, H. H.; Fareed, S.; Badruddeen; Khalid, M.; Aqil, M. Nanoemulsion: For Improved Oral Delivery of Repaglinide. *Drug Deliv.* **2016**, *23*, 2026-2034.
- (32) Zeeb, B.; Gibis, M.; Fischer, L.; Weiss, J. Influence of Interfacial Properties on Ostwald Ripening in Crosslinked Multilayered Oil-in-water Emulsions. *J. Colloid Interface Sci.* **2012**, *387*, 65-73.
- (33) Al-Badri, Z. M.; Tew, G. N. Well-defined Acetylene-Functionalized Oxanorbornene Polymers and Block Copolymers. *Macromolecules* **2008**, *41*, 4173-4179.
- (34) Lin, C. C.; Ki, C. S.; Shih, H. Thiol-norbornene Photo-click Hydrogels for Tissue Engineering Applications. *J. Appl. Polym. Sci.* **2015**, *132*, 41563.
- (35) Cole, J. P.; Lessard, J. J.; Lyon, C. K.; Tuten, B. T.; Berda, E. B. Intra-chain Radical Chemistry as a Route to Poly(Norbornene Imide) Single-chain Nanoparticles: Structural Considerations and the Role of Adventitious Oxygen. *Polym. Chem.* **2015**, *6*, 5555-5559.
- (36) Duncan, B.; Landis, R. F.; Jerri, H. A.; Normand, V.; Benczedi, D.; Ouali, L.; Rotello, V. M. Hybrid Organic-inorganic Colloidal Composite 'sponges' via Internal Crosslinking. *Small* **2015**, *11*, 1302-1309.
- (37) Zhou, Z.; Zheng, A.; Zhong, J., Interactions of Biocidal Guanidine Hydrochloride Polymer Analogs with Model Membranes: A Comparative Biophysical Study. *Acta Biochim Biophys Sin (Shanghai)* **2011**, *43*, 729-737.

- (38) Pantos, A.; Tsogas, I.; Paleos, C. M. Guanidinium Group: A Versatile Moiety Inducing Transport and Multicompartmentalization in Complementary Membranes. *Biochim. Biophys. Acta* **2008**, *1778*, 811-823.
- (39) O'Reilly, E.; Lanza, J. Fluorescamine: A Rapid and Inexpensive Method for Measuring Total Amino Acids in Nectars. *Ecology* **1995**, *76*, 2656-2660.
- (40) Udenfriend, S.; Stein, S.; Bohlen, P.; Dairman, W.; Leimgruber, W.; Weigele, M. Fluorescamine: A Reagent for Assay of Amino Acids, Peptides, Proteins, and Primary Amines in the Picomole Range. *Science* **1972**, *178*, 871-872.
- (41) Wang, L.-S.; Gupta, A.; Rotello, V. M. Nanomaterials for the Treatment of Bacterial Biofilms. *ACS Infect. Dis.* **2015**, *2*, 3-4.
- (42) Roy, S.; Elgharably, H.; Sinha, M.; Ganesh, K.; Chaney, S.; Mann, E.; Miller, C.; Khanna, S.; Bergdall, V. K.; Powell, H. M.; Cook, C. H.; Gordillo, G. M.; Wozniak, D. J.; Sen, C. K. Mixed-species Biofilm Compromises Wound Healing by Disrupting Epidermal Barrier Function. *J. Pathol.* **2014**, *233*, 331-343.
- (43) Sun, B. K.; Sibrashvili, Z.; Khavari, P. A. Advances in Skin Grafting and Treatment of Cutaneous Wounds. *Science* **2014**, *346*, 941-945.
- (44) Sanchez-Moreno, P.; Buzon, P.; Boulaiz, H.; Peula-Garcia, J. M.; Ortega-Vinuesa, J. L.; Luque, I.; Salvati, A.; Marchal, J. A. Balancing the Effect of Corona on Therapeutic Efficacy and Macrophage Uptake of Lipid Nanocapsules. *Biomaterials* **2015**, *61*, 266-278.
- (45) Sanchez-Moreno, P.; Ortega-Vinuesa, J. L.; Martin-Rodriguez, A.; Boulaiz, H.; Marchal-Corrales, J. A.; Peula-Garcia, J. M. Characterization of Different Functionalized Lipidic Nanocapsules as Potential Drug Carriers. *Int. J. Mol. Sci.* **2012**, *13*, 2405-2424.
- (46) Baran, A.; Flisiak, I.; Jaroszewicz, J.; Swiderska, M. Serum Adiponectin and Leptin Levels in Psoriatic Patients According to Topical Treatment. *J. Dermatolog. Treat.* **2015**, *26*, 134-138.
- (47) Berthold, N.; Czihal, P.; Fritsche, S.; Sauer, U.; Schiffer, G.; Knappe, D.; Alber, G.; Hoffmann, R. Novel Apidaecin 1b Analogs with Superior Serum Stabilities for Treatment of Infections by Gram-Negative Pathogens. *Antimicrob. Agents Chemother.* **2013**, *57*, 402-409.
- (48) Wolfram, J.; Yang, Y.; Shen, J.; Moten, A.; Chen, C.; Shen, H.; Ferrari, M.; Zhao, Y. The Nano-plasma Interface: Implications of the Protein Corona. *Colloids Surf. B Biointerfaces* **2014**, *124*, 17-24.
- (49) Saha, K.; Rahimi, M.; Yazdani, M.; Kim, S. T.; Moyano, D. F.; Hou, S.; Das, R.; Mout, R.; Rezaee, F.; Mahmoudi, M.; Rotello, V. M. Regulation of Macrophage

Recognition through the Interplay of Nanoparticle Surface Functionality and Protein Corona. *ACS Nano* **2016**, *10*, 4421–4430.

(50) Haugland, R. P. *Handbook of Fluorescent Probes and Research Products*. Eugene, OR: Molecular Probes, **2002**, Print.

(51) Decker, T.; Lohmann-Matthes, M. L. A Quick and Simple Method for the Quantitation of Lactate Dehydrogenase Release in Measurements of Cellular Cytotoxicity and Tumor Necrosis Factor (TNF) Activity. *J. Immunol. Methods* **1988**, *115*, 61–69.

CHAPTER 3

DYNAMICALLY CROSSLINKED POLYMER NANOCOMPOSITES TO TREAT MULTIDRUG- RESISTANT BACTERIAL BIOFILMS

3.1. Introduction

Multidrug-resistant (MDR) bacterial biofilms are widely found in wounds, indwelling medical devices, and dead tissue fragments.¹ It is reported over 80% of all human infections are due to biofilms, such as osteomyelitis, chronic bacterial prostatitis, and chronic otitis media.²⁻⁴ Biofilms are extremely refractory to antimicrobial treatment and easily evades the hosts immune responses.^{5,6} Currently, aggressive antibiotic treatments coupled with debridement (removal of infected tissue and limbs) is the best therapeutic intervention for biofilms. However, this approach fails to fully eradicate biofilms,⁷ and has considerable drawbacks including increased patient suffering, health care costs, and accumulative drug resistance.^{8,9} Hence, it is urgent to develop alternative therapeutic platforms that can eliminate these dangerous infections.

Phytochemical extracts, components isolated from trees and plants, have been previously used as natural antimicrobial agents.^{10,11} However, their lack of solubility and stability in physiological environments limit their practical use.^{12,13} Stabilizing these oils with surfactants or nanoparticles to generate emulsions can improve their solubility in aqueous environments and antimicrobial activity against bacteria.^{14,15} However, long-term mechanical stability and potentially adverse mammalian cell toxicity limit their therapeutic

practicality.¹⁶ Covalently crosslinking the emulsions can dramatically improve their stability in serum-containing conditions while maintaining high antimicrobial efficacy.¹⁷ However, this crosslinking strategy does not incorporate degradable linkage sites and may cause accumulation of the antimicrobial system in the body if used long-term.¹⁸

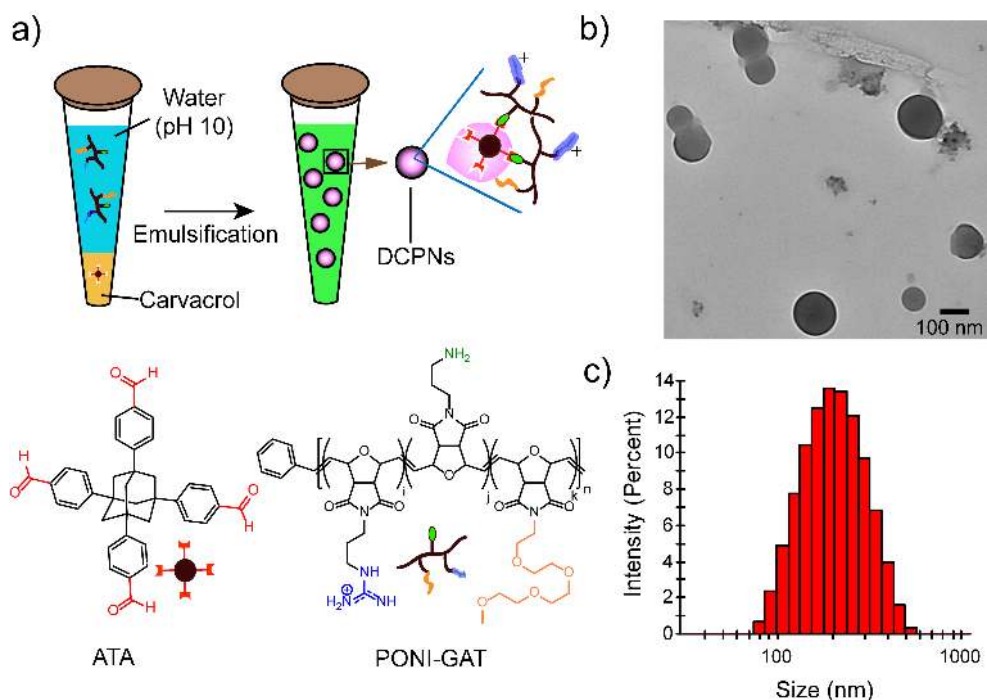


Figure 3.1. a) Schematic depiction of the strategy used to generate DCPNs along with the chemical structures of ATA crosslinker and PONI-GAT; b) TEM micrograph of DCPNs. Scale bar is 100 nm; c) DLS histogram indicating the size distribution of DCPNs in phosphate buffer saline (PBS, 150 mM).

Taking advantage of the acidic microenvironments within biofilms we set out to develop degradable analogues of our previously reported composites. Herein, we describe the design and therapeutic applicability of dynamically crosslinked polymer nanocomposites (DCPNs). DCPNs fabrication is based on spatial-directed crosslinking derived from in situ Schiff-base reactions (Figure 3.1). An adamantyl-core tetrakisaldehyde (ATA) was used as the crosslinker. The adamantyl core has excellent solubility in hydrophobic solvents and contains reactive aldehyde groups to bridge amino-

functionalized polymers used to stabilize the oil composite.^{19,20} We hypothesized ATAs would make a suitable polymer crosslinker and produce pH responsive imine bonds throughout and at the oil-water interface of the emulsion. Furthermore, these composites are envisioned to degrade over-time after the antimicrobial payload has been released. We demonstrate DCPNs have good serum stability and shelf-life and easily penetrates the extracellular polymeric substance (EPS) matrix, eliminating enclosed MDR bacteria. Taken together, the therapeutic properties of DCPNs make them promising candidates to treat wound biofilm infections.

3.2. Results

3.2.1 Generation and Characterization of DCPNs

As shown in **Figure 3.1.**, a poly(oxanorborneneimide) scaffold bearing guanidine, amino, and tetraethylene glycol monomethyl ether groups (PONI-GAT), an adamantyl-based crosslinker ATA, and carvacrol oil are used to generate the antimicrobial nanocomposites. The synthesis and characterization of PONI-GAT has been described previously.¹⁷ The synthesis of ATA was carried out following the modified procedures,^{23,24} and it was characterized using ¹HNMR and ATR-FTIR (Supporting Figure 3.7, Supporting Figure 3.8). The nanocomposites were prepared by emulsifying ATA-containing carvacrol oil (DCPN) or carvacrol oil only (Non-crosslinked control, PN) in a water solution which contains PONI-GAT. The pH of the aqueous solution was pre-adjusted to around 10, so that the amines on PONI-GAT are nucleophilic towards ATA aldehydes. Upon emulsification, PONI-GAT acts as a stabilizer and assembles at the oil-water interface of

the oil droplets. In the presence of ATA, PONI-GAT amines crosslink with ATA aldehydes, generating DCPNs. The morphology and size of DCPNs were characterized with transmission electron microscopy (TEM) and dynamic light scattering (DLS), indicating they are spherical-shaped particles with an average size of ~220nm. ATR-FTIR spectrum of freeze dried DCPNs indicated a complete loss of aldehydes from ATA and formation of imines (Supporting Figure 3.9), demonstrating successful Schiff-base crosslinking. To provide more insight into the Schiff base crosslinking, hydroxylamine (HA, possessing much higher equilibrium constant with benzaldehyde group than that of alkyl amine) was used as a competitive molecule to despoil the benzaldehyde groups reacted with amino groups in DCPNs. DLS results show that the DCPNs becomes unstable after incubating with hydroxylamine for 1h, with obvious aggregation after 3h (Supporting Figure 3.10). However, the control samples with only PBS do not show a size change. These results further support that Schiff base crosslinking is responsible for DCPN stability.

We next probed the morphological structure of DCPNs using CSLM. The formulation was modulated to generate micron-sized analogues that are easily seen under CSLM. PONI-GAT was partially labelled with TRITC (red fluorescence) and emulsified with the ATA-containing oil loaded with 3,3-Dioctadecyloxycarbocyanine (DiO, green fluorescence). As shown in Figure 3.2, the confocal images demonstrate a co-localization of red and green fluorescence, indicating DCPNs adopt a composite morphology as opposed to a core-shell structure. A composite morphology is plausible given PONI-GATs amphiphilic properties and its loss of hydrophilicity as it reacts with hydrophobic ATAs.

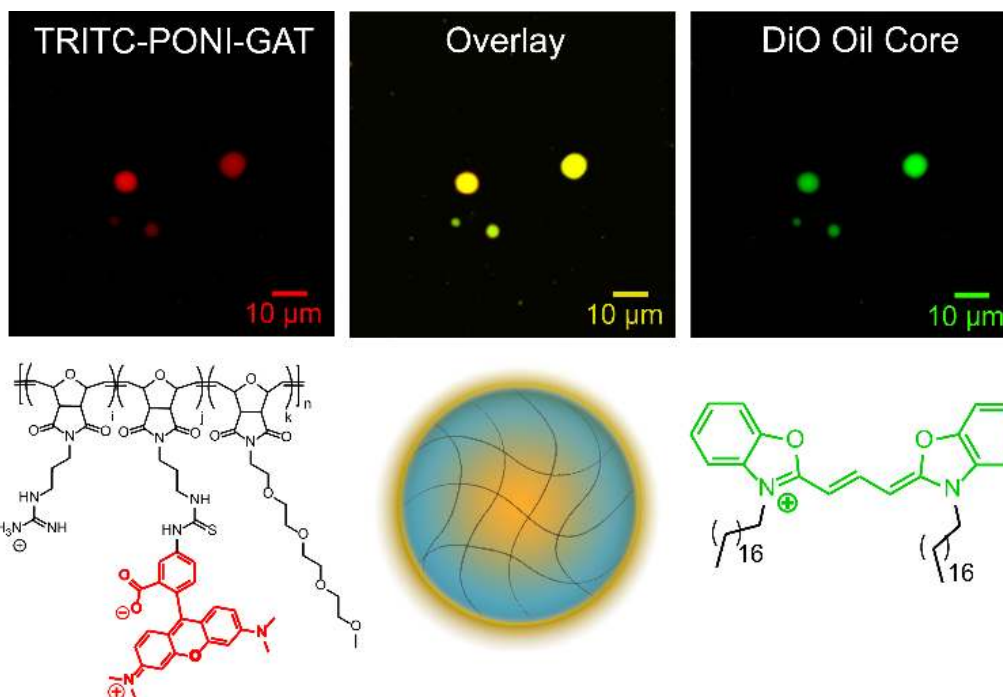


Figure 3.2. Confocal micrographs of the corresponding micron-sized counterparts of DCPNs. PONI-GAT was partially labelled with TRITC (red fluorescence), and the oil core is loaded with DiO (green fluorescence). The results show that red fluorescent PONI-GAT can be seen colocalized with the green fluorescent oil core, indicating a composite (as opposed to core-shell) morphology.

3.2.2 Stability and pH Responsiveness of DCPNs

Nanoemulsion stability in serum media is vital for biomedical applications.^{25,26} An ideal antimicrobial therapeutic platform should be stable enough to maintain its antimicrobial payload both during storage and delivery, while readily dissociating and releasing its payload at the infection site. We further characterized DCPNs and determined its structural integrity in aqueous environments. We hypothesized that DCPNs with imine crosslinking would have suitable stability in the presence of high ionic strength and serum environments, while losing stability in the presence of acidic environments.²⁷ Therefore, we monitored the stability and dissociation of DCPNs using DLS. A series of DCPN samples with increasing amounts of ATA were fabricated and their size monitored after

incubation with 10% fetal bovine serum (FBS) for 6h (Supporting Figure 3.11). It is observed that the stability of DCPN increases with increasing concentrations of ATA, with a 5wt% ATA loading showing no evidence of destabilization/aggregation. In stark contrast to non-crosslinked PNs which had no stability in serum (Figure 3.3a), DCPNs maintained stability in serum within the time duration of our studies. A 5wt% loading of ATA within the oil core was chosen as the optimized formulation. Afterwards, we monitored the size of optimized DCPNs in PBS media at different pH conditions. As shown in Figure 3.3b, we observed DCPNs displayed high stability under physiological conditions (pH=7.4). Furthermore, DCPN samples demonstrated long-term stability in these conditions even after 6 months of storage. (Supporting Figure 3.12). However, the size of DCPN was compromised at pH=6.5, with further instability observed when the pH was decreased to 5. The DLS results indicate that DCPNs are sufficiently stable in physiological conditions yet become unstable in acidic conditions. According to previous literature, the average biofilm infection pH has been observed to be ~ 5.5 .²⁸ At these conditions, DCPNs within biofilms would theoretically dissociate, simultaneously addressing vehicle degrading and payload release (Figure 3.3c).

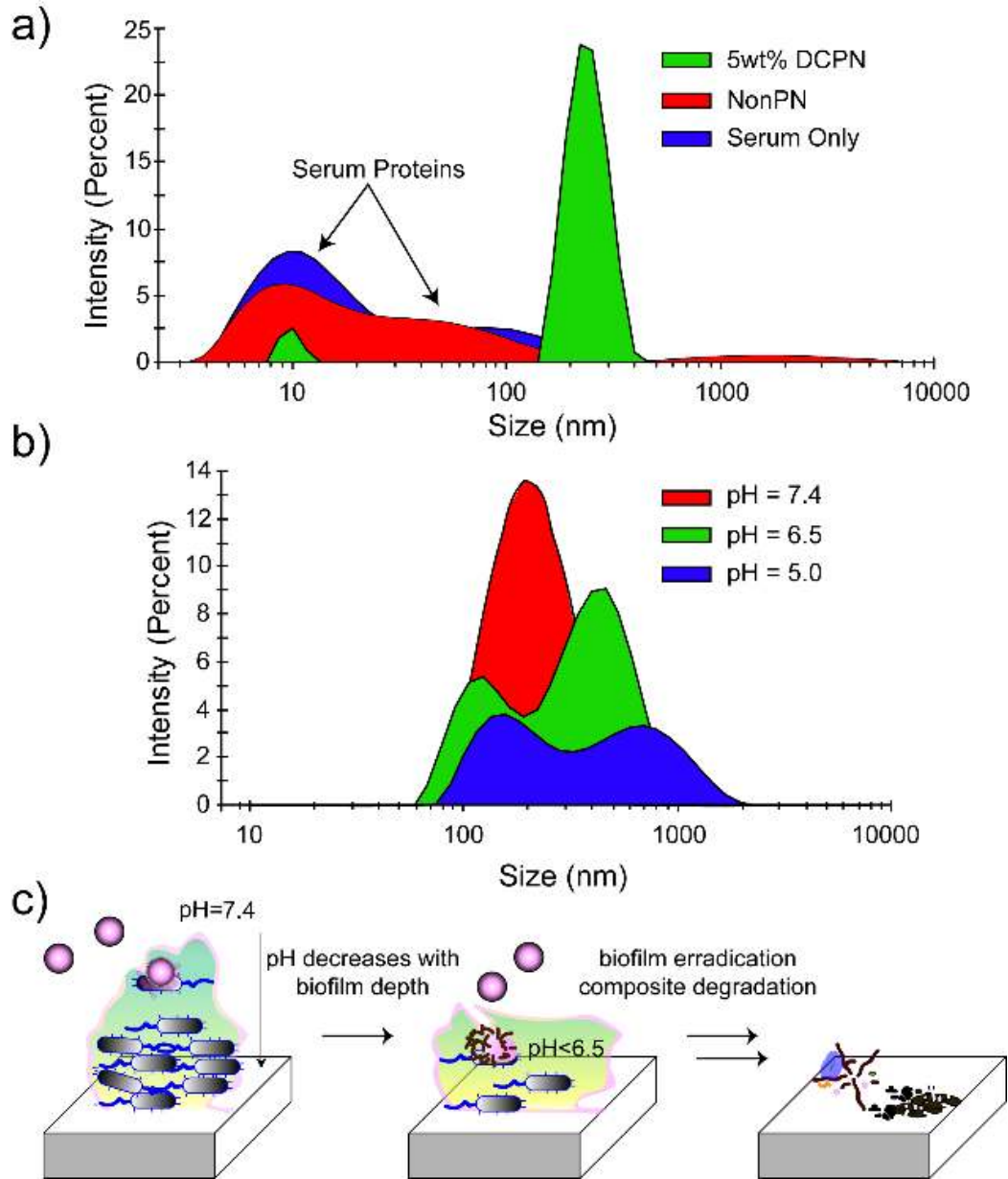


Figure 3.3. a) DLS curves of DCPNs. NonPNs and serum media are only in 10% fetal bovine serum (FBS); b) DLS curves of DCPN with different pH in PBS; c) Proposed antibiofilm mechanism.

3.2.3 DCPNs Penetration into Biofilm

Antimicrobial penetration into biofilms is essential for biofilm eradication.²⁹ With DCPNs size, morphology, and stability characterized, we next probed DCPNs ability to

penetrate biofilms using confocal microscopy. DiO was again loaded into DCPNs oil core and used to track their delivery into biofilms formed by red fluorescent protein (RFP) expressing *Escherichia coli*. DCPNs were incubated with biofilms for 1 h, washed, and their penetration analysed using ImageJ software. As illustrated in Figure 3.4, the fluorescence overlay shows DCPNs are distributed throughout the entire biofilm, colocalizing with the enclosed bacteria. The results indicate DCPNs are suitable carriers for antimicrobial payloads that can be delivered efficiently to biofilms.

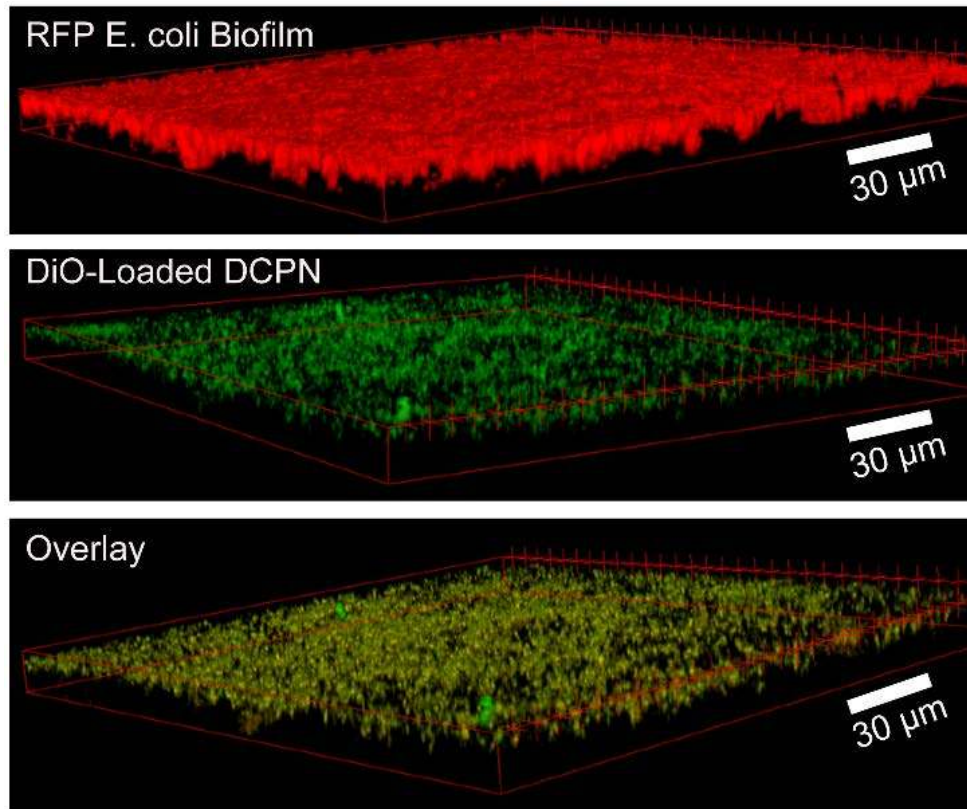


Figure 3.4. Representative 3D views of confocal image stacks of RFP-expressing DH5- α *E. coli* biofilms. DiO-loaded DCPN and their overlay after treating the biofilm for 1 h with 5wt% DiO-Loaded DCPN at 5% (v/v%) concentration in M9 media.

3.2.4 DCPNs Antibiofilm Activity

Having validated DCPNs ability to penetrate a biofilm matrix, we next evaluated their antimicrobial activity against multiple Gram-negative and positive bacteria in their plankton or biofilm state. First, we determined the minimum inhibition concentrations (MIC) against a library of bacteria. DCPNs demonstrate MIC values ranging from 0.74-1.50 mM (Supporting Table 3.1). In addition to MIC, we investigated the structural integrity of Gram-negative and positive planktonic species using scanning electron microscopy (SEM) after 3 h incubation with DCPNs (Figure 3.13). In contrast to untreated bacteria, bacteria treated with DCPNs showed obvious cell wall/membrane damage along with a reduction in bacteria populations. Afterwards, four pathogenic bacterial strains of clinical isolates, *Pseudomonas aeruginosa* (*P. aeruginosa*, CD-1006), *Enterobacter cloacae* (*E. cloacae*, CD-1412) complex, *Escherichia coli* (*E. coli*, CD-2), and a methicillin-resistant strain *Staphylococcus aureus* (*S. aureus*, CD-489, MRSA) were chosen to test DCPNs antibiofilm properties. As shown in Figure 3.5, biofilms treated with DCPNs for three hours were effectively eliminated at a concentration of 4 v/v% (1.50 mM carvacrol oil). Notably, Gram-negative (CD-1006, CD-2, CD-1412) and positive (CD-489) bacterial biofilms can be treated, demonstrating DCPNs have broad-spectrum activity. Compared to the individual components of DCPN as control samples, DCPN exhibited significantly higher antibiofilm activity than that of pure carvacrol oil or PONI-GAT, supporting our antibiofilm mechanism proposed in Figure 3.3c.

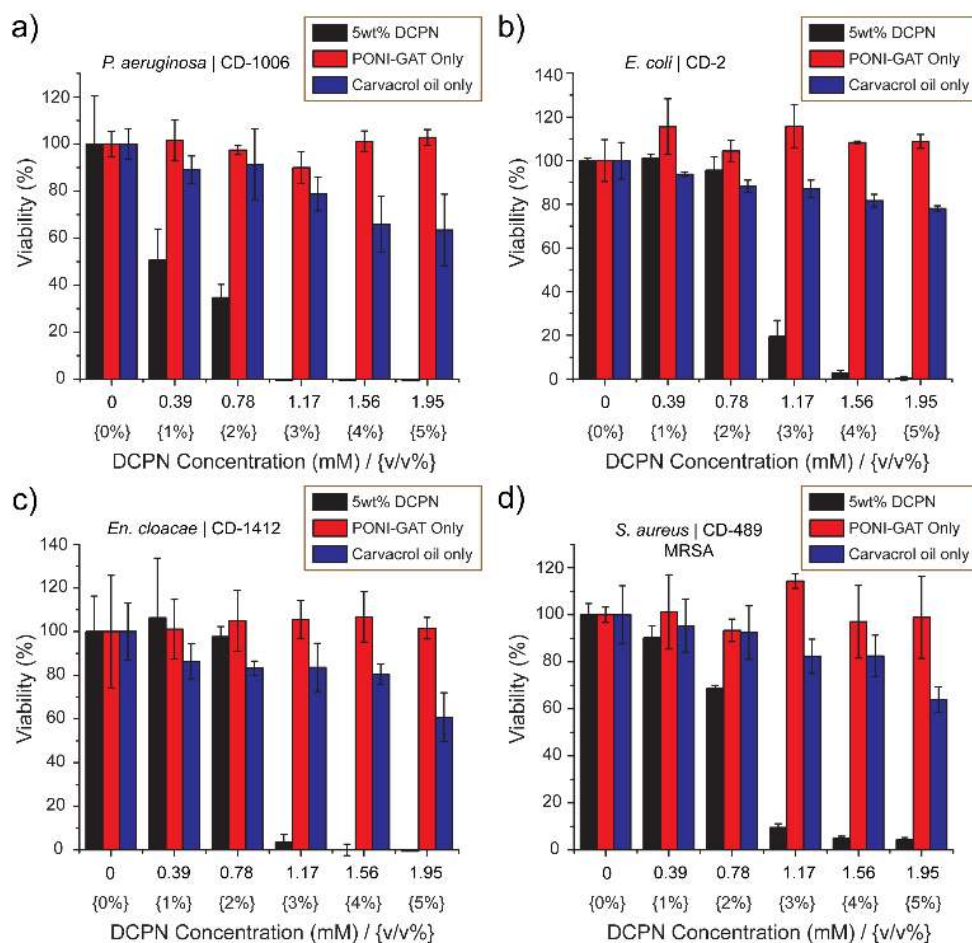


Figure 3.5. Viability of 1-day-old biofilms. (a) *P. aeruginosa* (CD-1006), (b) *E. coli* (CD-2), (c) *En. cloacae* complex (CD-1412) and (d) *S. aureus* (CD-489) biofilms after 3-hour treatment with 5wt% DCPN, PONI-GAT only, and Carvacrol oil only at different antimicrobial concentrations (mM)/ (v/v %). The data are average of triplicates, and the error bars indicate the standard deviations.

3.2.5 Cytotoxicity Assessment of DCPNs Against Fibroblast Cells

Finally, we investigated the cytotoxicity of DCPN to mammalian NIH 3T3 (ATCC CRL-1658) Fibroblast cells. Fibroblasts are critical in rebuilding the structural framework in animal tissues during wound healing processes.³⁰ We incubated fibroblast cells with DCPNs using the same experimental conditions as used for biofilms. As shown in Figure 3.6, no observable cytotoxicity to Fibroblast cells at 4 v/v % of DCPN was observed. Given

that DCPNs successfully eliminate both Gram-negative and positive biofilms below this concentration, the results suggest that DCPNs are promising candidates to eliminate pathogenic biofilms in the presence of mammalian cells, a critical need in wound therapy.

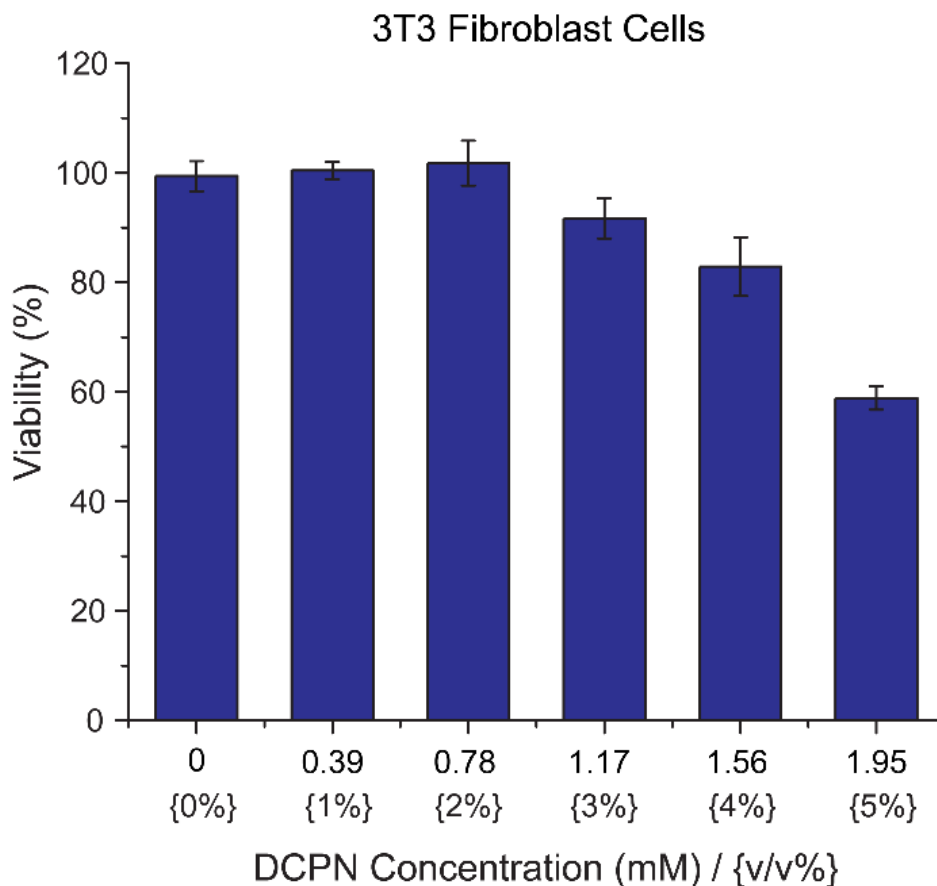


Figure 3.6. Viability of 3T3 fibroblast cells after treated with 5wt% DCPN at different emulsion concentrations for three hours. Each result is an average of five experiments, and the error bars designate the standard deviations.

3.3. Conclusions

In conclusion, we have developed a dynamically crosslinked polymeric nanocomposite that demonstrates promise as an MDR biofilm therapeutic. Taking advantage of the dynamic scaffold presented within DCPNs, the nanoemulsions

demonstrated good stability in physiological conditions while readily degrading in acidic conditions found commonly in biofilm infections. Furthermore, DCPNs are broad-spectrum antimicrobials that effectively penetrate and eliminate enclosed pathogens within biofilms at concentrations that do not compromise fibroblast cell viability. Given the oil core is a suitable environment to encapsulate a range of other hydrophobic antimicrobials and drugs, we envision future degradable antimicrobial emulsions can build off this strategy, potentially providing potent therapeutic platforms to fight against the rising number of MDR biofilm infections in biomedical settings.

3.4. Experimental Protocols

3.4.1 Chemicals and Reagents

Titanium tetrachloride (99.9%), Dichloromethyl methylether, Hydroxylamine (50wt% in water) were purchased from Sigma Aldrich, all the other reagents and materials were purchased from Fisher Scientific and used as received. NIH-3T3 cells (ATCC CRL-1658) were purchased from ATCC. Dulbecco's modified Eagle's medium (DMEM; ATCC 30-2002) and fetal bovine serum (Fisher Scientific, SH3007103) were used in cell culture. The Pierce LDH cytotoxicity assay kit was purchased from Fisher Scientific.

3.4.2 Fabrication of DCPNs

Stock nanocomposite emulsions were prepared in 0.6 mL Eppendorf tubes. To prepare the stock DCPN emulsions, 3 μL of carvacrol oil (containing 5 wt% ATA) was first added to a 0.6 mL Eppendorf tube, then a 20 μL (150 μM) PONI-GAT solution was added into the tube, followed by 477 μL of Milli-Q H₂O (previously adjusted to a pH of

10) and emulsified in an amalgamator for 50s. The non-crosslinked analogue (Non-PN) was generated in the same fashion, however without ATA dissolved in carvacrol. The emulsions were allowed to rest overnight prior to use.

3.4.3 MIC Measurements

Bacteria were inoculated in LB broth in a shaker at 275 rpm and 37 °C until they reached stationary phase. The cultures were then harvested by centrifugation and washed with 0.85% sodium chloride solution three times. The concentrations of resuspended bacterial solution were determined by optical density measured at 600 nm. MICs of DCPNs against all bacteria were determined by the microdilution method reported previously with slight modifications.²¹ Briefly, the DCPNs emulsions were serially diluted with M9 to various concentrations (64-0.5) v/v%. The bacterial suspension was diluted in M9 broth to a final concentration of 10^6 CFU mL⁻¹. Equal volumes (50 µL) of microbial suspension and DCPNs solution with varied concentrations were mixed in each well of a 96-well plate. Thus, the final concentration of bacteria in each well was 5×10^5 CFU mL⁻¹ and those of DCPN emulsions were 32-0.25 v/v %, respectively. M9 broth containing only microbial cells was used as the negative control, and M9 broth only as the growth control. Each test was performed in three replicates. The plates were then incubated in a shaker at 275 rpm and 37 °C overnight and their optical density was measured at 600 nm. The MIC values were reported as the lowest concentration of the antimicrobial to inhibit the visible growth of bacteria.

3.4.4 Antibiofilm Activity Measurements

Bacteria seeding solutions were made in M9 to reach 0.1 OD (10^8 CFU mL⁻¹). 100 µL portions of the seeding solutions were added to each well of the microplate. M9 medium

without bacteria was used as a negative control. The plates were covered and incubated at room temperature under static conditions. The biofilms were used after 1 day. Biofilms were washed with PBS (three times) to remove the planktonic bacteria. Next, varied concentration of DCPNs, made in M9 medium, were added to each well of the microplate. The microplate was then incubated at 37°C under static conditions. After 3 h, biofilms were washed with PBS three times, and the viabilities were determined using Alamar Blue assay according to the manufacturer's protocol.

3.4.5 Cytotoxicity Evaluation of DCPNs Against Fibroblast Cells

NIH 3T3 cells (ATCC, Manassas, VA, U.S.A) were cultured in Dulbecco's modified Eagle's medium supplemented with 4.5g/L glucose, 10% FBS and 1% antibiotics (100 U/mL penicillin and 100 µg/mL streptomycin). Cells were maintained at 37°C in a humidified atmosphere containing 5% CO₂. Cells were regularly passaged by trypsinization with 0.25% trypsin with EDTA, (Invitrogen) in PBS (pH 7.4). At ~80% confluence, cells were trypsinized and seeded in a 96-well plate at a density of 20,000 cells/well. After allowed to attach overnight, cells were washed by PBS and treated with desired concentration of DCPNs for 3 h. At the end of treatment, the cell viability was measured using a Pierce LDH Cytotoxicity Assay Kit (Thermo Fisher Scientific). Procedures were performed according to manufacturer's instruction.

3.4.6 TEM, Dynamic Light Scattering (DLS), Confocal Scanning Laser Microscopy (CSLM), and SEM Methods

The samples for TEM were prepared by dropping 5 µL of the DCPNs emulsion onto Formvar Film on 300 Square Mesh, Nickel Grids (EMS FF300-Ni). The TEM images were taken on a JOEL 2000FX TEM instrument at an acceleration voltage of 200 kV. DLS

measurements were performed on a Malvern NanoZS apparatus operating at a 173-degree scattering angle. The CSLM experiments both for the DCPNs morphology and their penetration into biofilms were performed on a Nikon A1 Resonant scanning confocal microscope. SEM was carried out according to modified procedure.^[22] 2 ml 0.1 OD (10^8 CFU mL⁻¹) bacterial suspension in M9 media was incubated with 4v/v% DCPNs at 37°C for 3h. The bacteria were collected by centrifugation at 1,200 rpm for 10 min and washed twice using PBS (pH=7.4), and then made a thin smear on a silica wafer. Glutaraldehyde solution (2.5% in PBS) was used to fix the bacteria cells at 4°C overnight. After rinsing three times using PBS, the samples were dehydrated by ethanol in a gradient alcohol concentration (25%, 50%, 75%, 90%, and 100%). Finally, after sputter coating with gold for 1 min, the samples were observed in FEI Magellan 400 field emission scanning electron microscope operated at 1 kV with 13 μ A of beam current. Control samples without treatment were also prepared and tested in the same way as mentioned above.

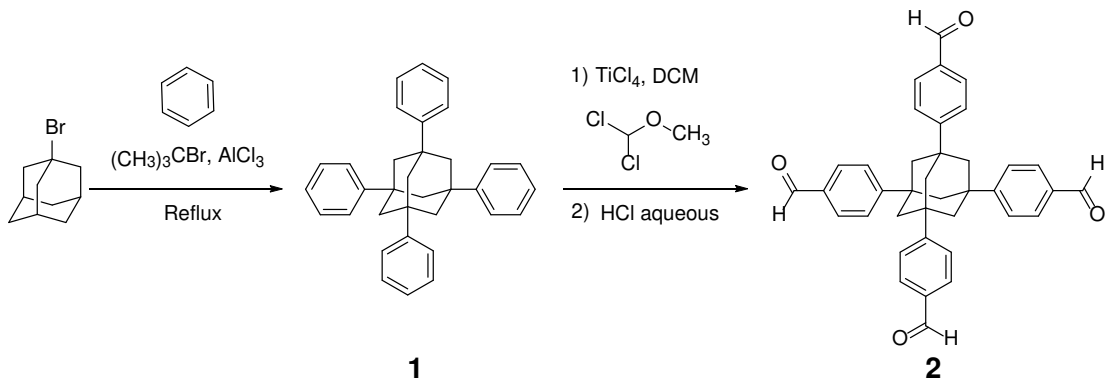
3.4.7 Evaluate DCPNs Imine Bond Displacement

The crosslinking of DCPNs through imine bonds was further observed using an imine-oxime displacement reaction. 10 μ L hydroxylamine solution was added to 50 μ L DCPNs stock and mixed. Then the bottles were placed on an orbital shaker (1200 rpm) at room temperature for 1h and 3h, respectively. The control samples were also prepared in the same method except using PBS instead of hydroxylamine. The size of both control and treated samples were measured by DLS.

3.5. Supporting Figures

3.5.1 Synthesis and Characterization of Crosslinker 1,3,5,7-Tetrakis(4-formylphenyl)

) adamantane (ATA)



Synthesis of 1. To a 150 mL three-neck flask equipped with a reflux condenser, a calcium chloride drying tube, and magnetic stir-bar, 1-bromoadamantane (5.0 g, 23.0 mmol, 1.0 eq), tert-butyl bromide (6.3 g, 46.0 mmol, 2 eq), and benzene (50 ml, 560 mmol, 560.0 eq) was added and allowed to stir at 55°C for 10 min. Then, aluminum chloride (0.6 g, 4.60 mmol, 0.2 eq) was added slowly and the reaction solution was heated and stirred under vigorous reflux for 1 hour. Afterwards, the system was then poured into ice water and ether was then added into the mixture while stirring. The resulting undissolved substance was filtered and vacuum dried followed by Soxhelt purification in chloroform for 48 hours. After vacuuming dry, **1** was obtained as white powder and carried directly to the next step.

Synthesis of 2. Following a modified literature procedure, to a 250 mL three-neck round-bottom flask equipped with a magnetic stir-bar, **1** (3.8 g, 8.6 mmol, 1.0 eq) and 150 mL dichloromethane was added. Under a continuous flow of nitrogen, the mixture was stirred rapidly and cooled to -10°C with an ice/salt bath. Afterwards, titanium tetrachloride (19.0 mL, 172.4 mmol, 20.0 eq) was added slowly to the mixture and stirred at -10°C for 30 min. Then, dichloromethyl methylether (12.5 mL, 137.9 mmol, 16.0 eq) was subsequently added dropwise to the mixture. The reaction was held at -10°C for 3 hours and then allowed to warm to room temperature and stirred overnight. The mixture was poured into 300 mL ice-water, and 100 mL of 1 M HCl was added and allowed to stir for 30 minutes. The two-phase mixture was separated, and the aqueous phase was washed twice with 100 mL DCM. The combined organic phases were successively washed with saturated aqueous NaHCO_3

and saturated NaCl and then dried with Na₂SO₄. The solution was filtered, and the solvent removed with a rotavapor. The resultant yellow solid was purified by column chromatography and then recrystallized from dioxane to give ATA as white crystals.

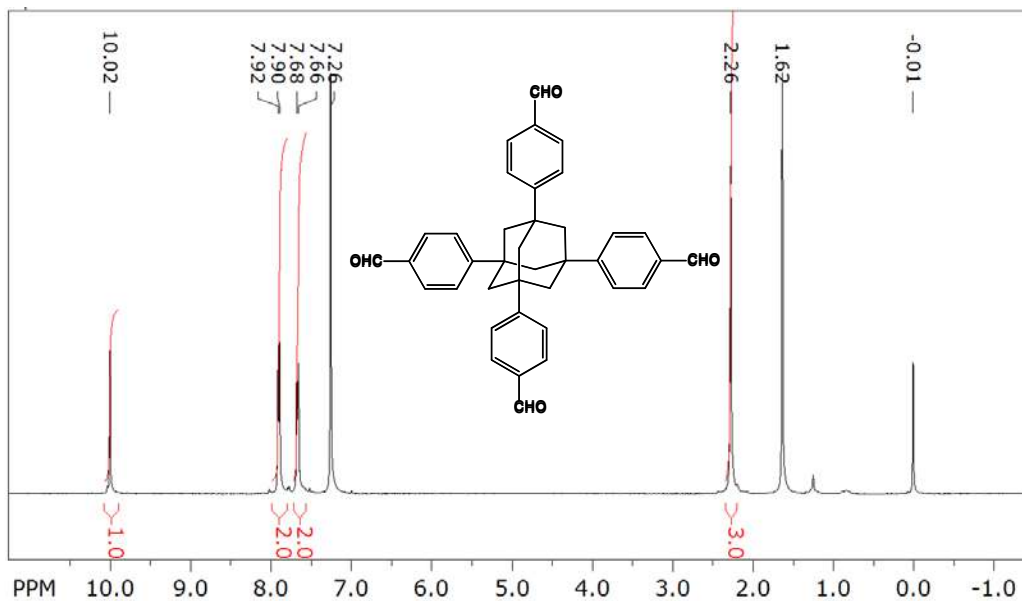


Figure 3.7. ¹H NMR spectrum of ATA with CDCl₃ as the solvent. ¹H NMR (400 MHz, CDCl₃): δ (ppm) 10.02 (s, 4H), 7.91 (d, 8H), 7.67 (d, 8H), 2.26 (s, 12H).

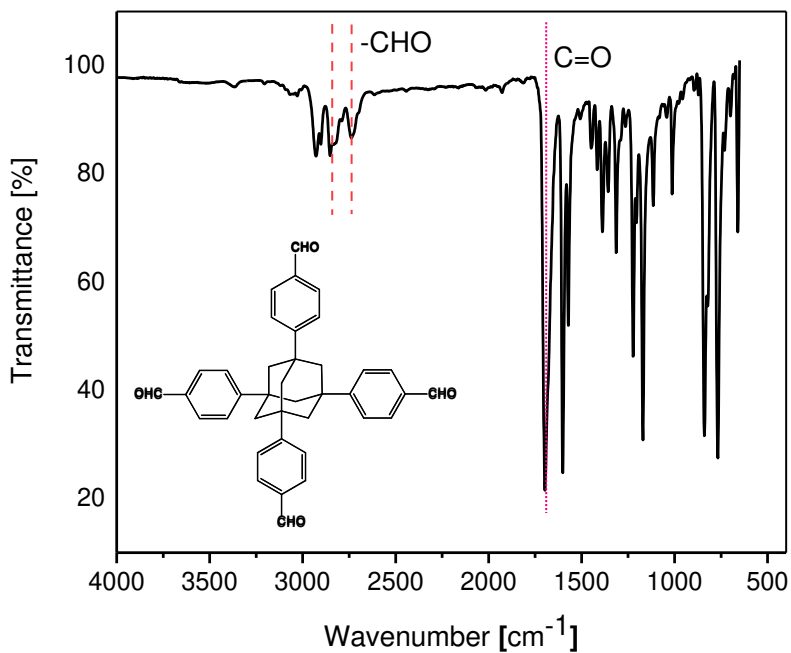


Figure 3.8. Attenuated Total Reflectance Fourier Transform Infrared Spectroscopy (ATR-FTIR) spectrum of ATA. ATR-FTIR(cm^{-1}): 3029 (Phenyl, C-H); 2928 (Adamantyl, CH_2); 2852, 2738 (CHO, CH); 1697 (C=O); 1601, 1571 (Phenyl ring).

3.5.2 Synthesis and Characterization of DCPNs

Freeze-dried samples of DCPN along with the non-crosslinked counterparts (NonPN) as the control samples were analyzed using ATR-FTIR.

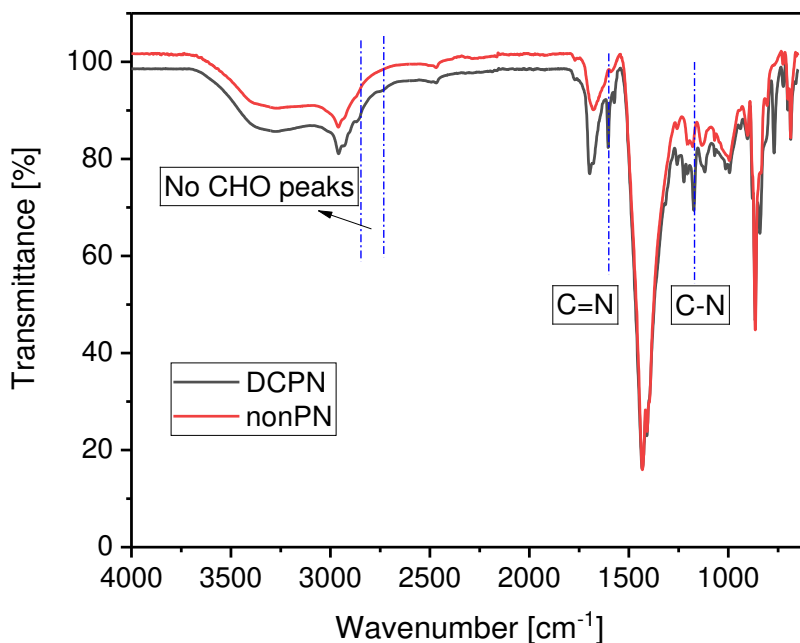


Figure 3.9. ATR-FTIR spectra of DCPN and NonPN. The results show that the aldehyde groups ($2852, 2738 \text{ cm}^{-1}$) from crosslinker ATA are lost, and imine bonds (C=N, 1605 cm^{-1} ; C-N, 1173 cm^{-1}) formed within DCPN.

3.5.3 Dynamic Light Scattering (DLS) of DCPNs

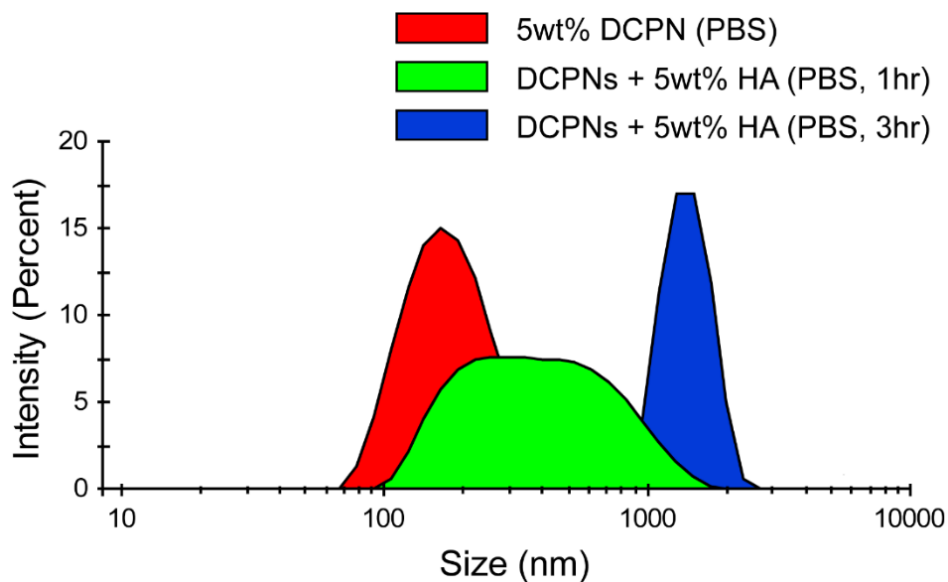


Figure 3.10. DLS curves monitoring imine – oxime displacement in PBS. DCPNs were incubated with the imine-displacing reagent hydroxylamine (HA) for the indicated durations. DCPNs size is compromised in the presence of HA, indicating PONI-GAT no longer provides stability and results in composite aggregation.

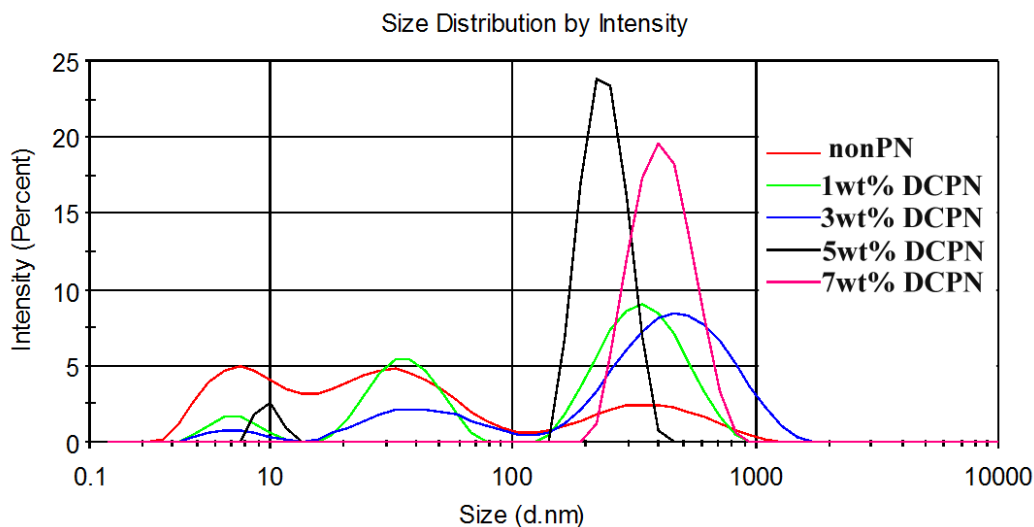


Figure 3.11. Variation of DLS curves detected after incubated half an hour in serum media for DCPN. The results show that the DCPN stability increases with the crosslinker content until 5wt%, so the 5wt% was chosen as the optimal crosslinker content in this study.

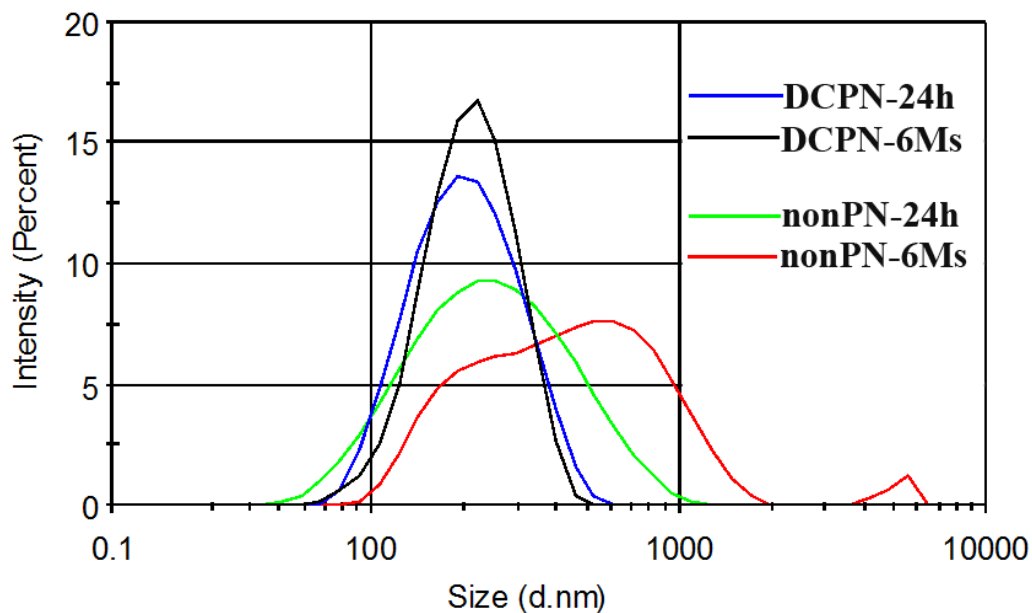
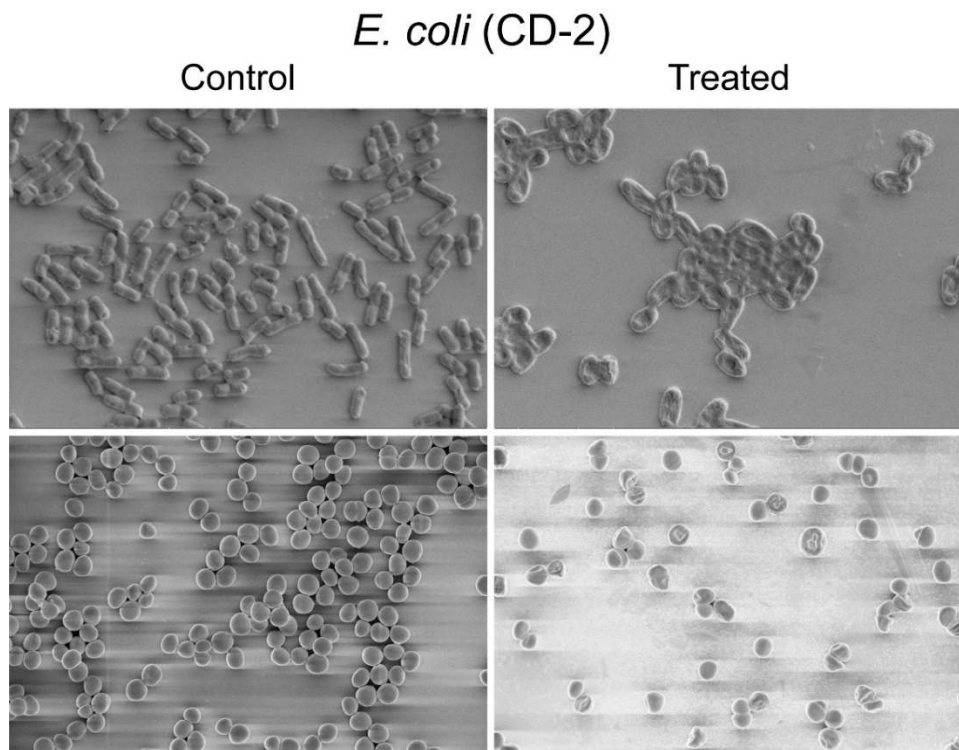


Figure 3.12. DLS curves monitoring the shelf life of DCPN and the NonPN control. Both the DCPN and NonPN were prepared as stated in main text and allowed to stand for 6months within our studied range, The DLS curves were obtained by detecting the same sample after 24h and 6 months, respectively. The results illustrate that DCPN has significantly improved storage stability than the non-crosslinked analog.



S. aureus (CD-489, MRSA)

Figure 3.13. SEM micrographs of pathogenic planktonic bacteria. *E. coli* and *S. aureus* were incubated either with M9 only (control) or 4 v/v% DCPNs (treated) for 3 h. Treated samples show a reduction in bacteria population and compromised bacterial cell walls/membranes.

Bacterial strain	DCPN MICs	
	(v/v%)	(mM)
CD-1006	4.0	1.5
CD-575	4.0	1.5
CD-2	2.0	0.74
CD-1412	2.0	0.74
ATCC	2.0	0.74
CD-489	4.0	1.5

Table 3.1. MICs of the 5wt%DCPN against different strains of bacteria

3.6. References

- (1) Tackling Drug-Resistant Infections Globally: Final Report and Recommendations, May 19, 2016, <https://amr-review.org/Publications>.
- (2) Costerton, J. W.; Stewart, P. S.; Greenberg, E. P. Bacterial Biofilms: A Common Cause of Persistent Infections. *Science* **1999**, *284*, 1318-1322.
- (3) Fux, C. A.; Costerton, J. W.; Stewart, P. S.; Stoodley, P. Survival Strategies of Infectious Biofilms. *Trends Microbiol.* **2005**, *13*, 34-40.
- (4) Drenkard, E.; Ausubel, F. M. Pseudomonas Biofilm Formation and Antibiotic Resistance are Linked to Phenotypic Variation. *Nature* **2002**, *416*, 740.
- (5) Høiby, N.; Ciofu, O.; Johansen, H. K.; Song, Z. J.; Moser, C.; Jensen, P. Ø.; Molin, S.; Givskov, M.; Tolker-Nielsen, T.; Bjarsholt, T. The Clinical Impact of Bacterial Biofilms. *Int. J. Oral. Sci.* **2011**, *3*, 55-65.
- (6) Wang, H.; Wu, H.; Ciofu, O.; Song, Z.; Høiby, N. In Vivo Pharmacokinetics/Pharmacodynamics of Colistin and Imipenem in *Pseudomonas aeruginosa* Biofilm Infection. *Antimicrob. Agents Chemother.* **2012**, *56*, 2683-2690.
- (7) Høiby, N. Recent Advances in the Treatment of Pseudomonas aeruginosa Infections in Cystic Fibrosis. *BMC Med.* **2011**, *9*, 32.
- (8) Lynch, A. S.; Robertson, G. T. Bacterial and Fungal Biofilm Infections. *Annu. Rev. Med.* **2008**, *59*, 415-428.
- (9) Olsen, I. Biofilm-Specific Antibiotic Tolerance and Resistance. *Eur. J. Clin. Microbiol. Infect. Dis.* **2015**, *34*, 877-886.
- (10) Vergis, J.; Gokulakrishnan, P.; Agarwal, R. K.; Kumar, A. Essential Oils as Natural Food Antimicrobial Agents: A Review. *Crit. Rev. Food Sci. Nutr.* **2015**, *55*, 1320-1323.
- (11) Espina, L.; Berdejo, D.; Alfonso, P.; García-Gonzalo, D.; Pagan, R. Potential Use of Carvacrol and Citral to Inactivate Biofilm Cells and Eliminate Biofouling. *Food Control* **2017**, *82*, 256-265.
- (12) Samperio, C.; Boyer, R.; Eigel III, W. N.; Holland, K. W.; McKinney, J. S.; O'Keefe, S. F.; Smith, R.; Marcy, J. E. Enhancement of Plant Essential Oils' Aqueous Solubility and Stability Using Alpha and Beta Cyclodextrin. *J. Agric. Food Chem.* **2010**, *58*, 12950-12956.
- (13) Turek, C.; Stintzing, F. C. Stability of Essential Oils: A Review. *Compr. Rev. Food Sci. Food Saf.* **2013**, *12*, 40.
- (14) Anwer, M. K.; Jamil, S.; Ibnouf, E. O.; Shakeel, F. Enhanced Antibacterial Effects of Clove Essential Oil by Nanoemulsion. *J. Oleo. Sci.* **2014**, *63*, 347-354.

- (15) Duncan, B.; Li, X.; Landis, R. F.; Kim, S. T.; Gupta, A.; Wang, L.-S. Ramanathan, R.; Tang, R.; Boerth, J. A.; Rotello, V. M. Nanoparticle-Stabilized Capsules for the Treatment of Bacterial Biofilms. *ACS Nano* **2015**, *9*, 7775-7782.
- (16) Ziani, K.; Chang, Y.; McLandsborough, L.; McClements, D. J. Influence of Surfactant Charge on Antimicrobial Efficacy of Surfactant-Stabilized Thyme Oil Nanoemulsions. *J. Agric. Food Chem.*, **2011**, *59*, 6247-6255.
- (17) Landis, R. F.; Gupta, A.; Lee, Y.-W.; Wang, L.-S.; Golba, B.; Couillaud, B.; Ridolfo, R.; Das, R.; Rotello, V. M. Cross-Linked Polymer-Stabilized Nanocomposites for the Treatment of Bacterial Biofilms. *ACS Nano*, 2017, *11*, 946-952.
- (18) Kataoka, K.; Harada, A.; Nagasaki, Y. Block Copolymer Micelles for Drug Delivery: Design, Characterization and Biological Significance. *Adv. Drug. Deliv. Rev.*, **2001**, *47*, 113-131.
- (19) Grillaud, M.; Russier, J.; Bianco, A. Polycationic Adamantane-Based Dendrons of Different Generations Display High Cellular Uptake Without Triggering Cytotoxicity. *J. Am. Chem. Soc.* **2014**, *136*, 810-819.
- (20) Štimac, A.; Šekutor, M.; Mlinarić-Majerski, K.; Frkanec, L.; Frkanec, R. Adamantane in Drug Delivery Systems and Surface Recognition. *Molecules*, **2017**, *22*, 297.
- (21) Cheng, J.; Chin, W.; Dong, H.; Xu, L.; Zhong, G.; Huang, Y.; Li, L.; Xu, K.; Wu, M.; Hedrick, J. L.; Yang, Y. Y.; Fan, W. Biodegradable Antimicrobial Polycarbonates with In Vivo Efficacy Against Multidrug-Resistant MRSA Systemic Infection. *Adv. Health c. Mater.* **2015**, *4*, 2128-2136.
- (22) Xu, C.; Li, J.; Yang, L.; Shi, F.; Yang, L.; Ye, M. Antibacterial Activity and a Membrane Damage Mechanism of *Lachnum* YM30 Melanin Against *Vibrio parahaemolyticus* and *Staphylococcus aureus*. *Food Control* **2017**, *73*, 1445-1451.
- (23) Zhu, D. Y.; Guo, J. W.; Xian, J. X.; Fu, S. Q. Novel Sulfonate-Containing Halogen-Free Flame-Retardants: Effect of Ternary and Quaternary Sulfonates Centered on Adamantane on the Propewrties of Polycarbonate Composites. *RSC Adv.* **2017**, *7*, 39270-39278.
- (24) Duncan, N. C.; Hay, B. P.; Hagan, E. W.; Custelcean, R. Thermodynamic, Kinetic, and Structural Factors in the Synthesis of Imine-Linked Dynamic Covalent Frameworks. *Tetrahedron* **2012**, *68*, 53-64.
- (25) Baran, A.; Flisiak, I.; Jaroszewicz, J.; Swiderska, J. Serum Adiponectin and Leptin Levels in Psoriatic Patients According to Topical Treatment. *J. Dermatol. Treat.* **2015**, *26*, 134-138.
- (26) Berthold, N.; Czihal, P.; Fritsche, S.; Sauer, U.; Schiffer, G.; Knappe, D.; Alber, G.; Hoffmann, R. Novel Apidaecin 1b Analogs with Superior Serum Stabilities for Treatment

of Infections by Gram-Negative Pathogens. *Antimicrob. Agents Chemother.* **2013**, *57*, 402-409.

(27) Vroom, J. M.; De Grauw, K. J.; Gerritsen, H. C.; Bradshaw, D. J.; Marsh, P. D.; Watson, G. K.; Birmingham, J. J.; Allison, C. Depth Penetration and Detection of pH Gradients in Biofilms by Two-Photon Excitation Microscopy. *Appl. Environ. Microbiol.* **1999**, *65*, 3502-3511.

(28) Wang, L.-S.; Rotello, V. M. Nanomaterials for the Treatment of Bacterial Biofilms. *ACS Infect. Dis.*, **2016**, *2*, 3-4.

(29) Sun, B. K.; Siprashvili, Z.; Khavari, P. A. Advances in Skin Grafting and Treatment of Cutaneous Wounds. *Science* **2014**, *346*, 941-945.

(30) Nathwani, D.; Raman, G.; Sulham, K.; Gavaghan, M.; Menon, V. Clinical and Economic Consequences of Hospital-Acquired Resistant and Multidrug-Resistant *Pseudomonas aeruginosa* Infections: A Systematic Review and Meta-Analysis. *Antimicrob. Resist. Infect. Control* **2014**, *3*, 32-47.

CHAPTER 4

BIODEGRADABLE NANOCOMPOSITE ANTIMICROBIALS FOR THE ERADICATION OF MULTIDRUG-RESISTANT BACTERIAL BIOFILMS WITHOUT ACCUMULATED RESISTANCE

4.1. Introduction

Multidrug-resistant (MDR) bacteria infect more than two million people annually in the U.S., resulting in significant loss of life and limb, with treatment requiring prolonged and costly therapeutic regimens.^{1,2,3} These dangerous pathogens, including *P. aeruginosa* and *S. aureus*, further frustrate treatment due to their innate ability to micro-colonize into biofilms.^{4,5,6} Bacterial biofilm infections are challenging to treat on wounds and indwelling medical devices, as the extracellular polymeric substances (EPS) in these biofilms both inhibit antibiotic penetration and aid bacteria to evade host immune responses.^{7,8,9} Furthermore, the slow growth rate of bacteria and the biofilm microenvironment act together to facilitate the development of antibiotic resistance.^{10,11,12} The emerging threat of antibiotic resistant biofilm infections has triggered an international push to develop alternative therapeutic platforms capable of eliminating these infections.^{13,14}

Plant-derived phytochemicals have emerged as an alternative to traditional antibiotic paradigms to combat MDR bacteria,^{15,16,17,18,19} providing a potential strategy for avoiding antibiotic tolerance and horizontal gene transfer that dramatically accelerate acquisition of drug resistance.^{20,21} Phytochemicals feature low cost,²² biocompatibility,²³

and can be effective towards bacterial infections.²⁴ However, the poor solubility of these hydrophobic oils in aqueous media limit their practical application as antimicrobial agents.²⁵ Surfactant, nanoparticle, and polymer additives aid in phytochemical delivery by forming oil-in-water emulsions.^{26,27,28,29} Furthermore, crosslinking of these emulsions have demonstrated phytochemical stability in even complex media such as serum.³⁰ However, such crosslinking strategies are non-biodegradable and may persist and accumulate within the body, causing unwanted side effects, such as inflammation and carcinogenesis.^{31,32,33}

Here, we report crosslinked poly(oxanorborneneimide)-stabilized oil-in-water nanocomposites (**X-BNCs**) engineered to be biodegradable in the presence of endogenous biomolecules such as glutathione and esterase enzymes (Figure 4.1). These ‘nanosponges’ incorporate disulfide³⁴ and ester^{35,36} crosslinkers that provide long-term stability in aqueous environments while facilitating nanocomposite degradation in biological milieus. We demonstrate the loading of these **X-BNCs** with carvacrol to provide therapeutics that eradicate Gram negative/positive bacteria including MDR strains. These nanocomposites are stable in serum-containing media, however degrade rapidly in the presence of glutathione or esterase proteins. The potential of **X-BNCs** as a wound healing therapeutic was demonstrated in an *in vitro* coculture with biofilms grown on top of mammalian 3T3 fibroblast cells. A 4-log reduction in bacterial colonies was observed with no change in fibroblast cells viability. In stark contrast to antibiotics, **X-BNCs** do not evoke resistance in bacteria, maintaining their potency against pathogenic *E. coli* (CD-2) in a 20-cycle serial passage study. Taken together, the efficacy, biodegradability, and stability of these anti-biofilm agents coupled with their lack of resistance accumulation make them a promising therapeutic platform to combat the rising dangers of MDR bacterial infections.

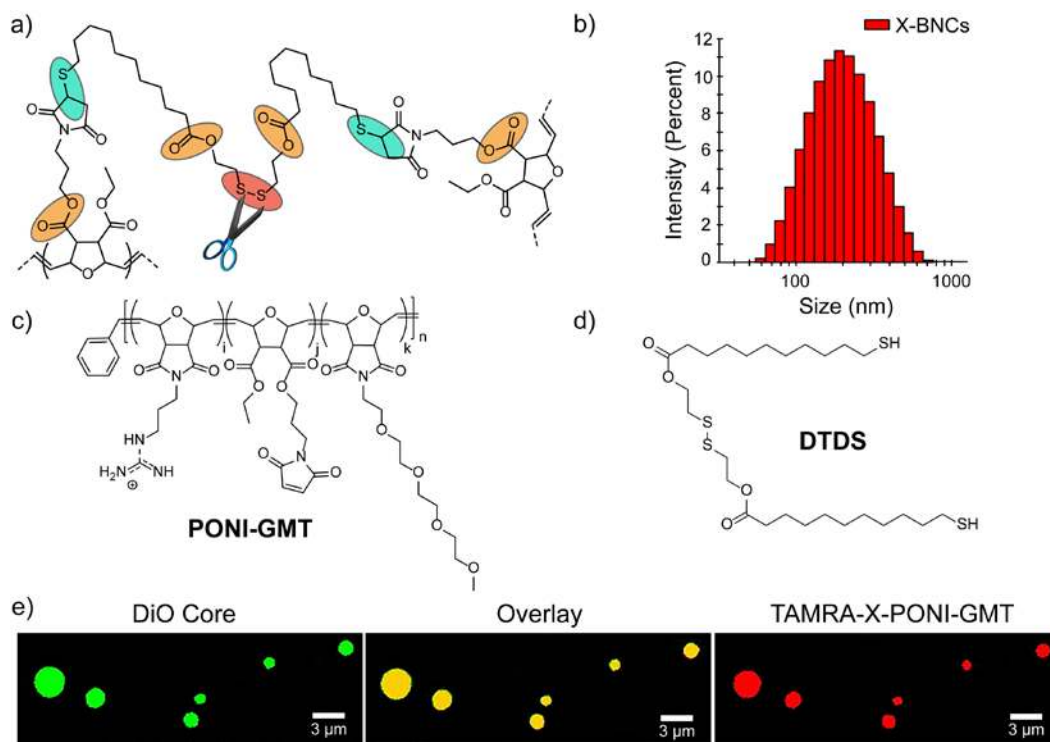


Figure 4.1. (a) Crosslinked **PONI-GMT-DTDS** structure showing linkage points reactive to endogenous biomolecules. (b) DLS histogram of crosslinked **PONI-GMT-DTDS** nanosponges loaded with carvacrol, in phosphate buffer saline (150 mM). (c) Chemical structures of **PONI-GMT** and (d) **DTDS**. (e) Confocal micrograph of crosslinked micron-sized biodegradable composites. **PONI-GMT** labeled with TAMRA-X (red fluorescence), and the oil core is loaded with DiO (green fluorescence). A composite morphology is indicated by co-distribution of **PONI-GMT** with the hydrophobic oil core. Scale bar is 3 μ m.

4.2. Results

4.2.1 Generation and Characterization of Nanocomposites

The **X-BNC** platform uses a poly(oxanorborneneimide) scaffold bearing guanidine, maleimide, and tetraethyleneglycol monomethyl ether groups (**PONI-GMT**) and provides a well-controlled and scalable platform. Biodegradability was imparted through use of a dithiol-disulfide (**DTDS**) crosslinker that is stable > 2 years in storage (Supporting Figure 4.7). An additional degradation modality was provided using ester-linked maleimide groups to enable thiols of **DTDS** to crosslink rapidly once the polymers assemble at the

oil-water interface.³⁷ Copolymerization of monomers bearing guanidine, maleimido, and tetraethylene glycol monomethyl ether units at a 40:10:50 monomer ratio respectively provided the precursor polymer **PONI-GMT**. The maleimido monomer ratio was kept low to ensure adequate solubility of **PONI-GMT** in aqueous conditions, necessary for efficient nanocomposite formation.

Nanocomposites were fabricated by emulsifying carvacrol oil loaded with **DTDS** or carvacrol only (non-crosslinked control, **NX-NC**) into water. Upon emulsification, **PONI-GMT** assembles and initially stabilizes the oil-water interface. In the presence of **DTDS**, crosslinking further stabilizing the oil droplets in water. **PONI-GMT** and **DTDS** generated nanocomposites (**X-BNCs**) with a diameter of ~220nm as shown by dynamic light scattering (DLS). We hypothesized the overall charge of **X-BNCs** would be reversed yielding a positively charged surface. The measured zeta (ζ) potential (Supporting Figure 4.8) supported this prediction, reporting a cationic nanocomposite, attributed to guanidine units at or beyond the oil-water interface. Significantly, DLS experiments on stock solutions of **X-BNCs** that were stored on the bench for one year indicated the composites maintained stability with a minimal change in size (Supporting Figure 4.9).

Next, the morphology (core-shell versus nanocomposites) of **X-BNCs** was established through confocal microscopy of larger micron-sized analogs of the **X-BNC** nanoemulsions. TAMRA-X (red fluorescence) was conjugated to **PONI-GMT**, while 3,3-dioctadecyloxycarbocyanine (DiO, green fluorescence) was loaded within the oil. As shown in Figure 4.1e, both green and red fluorescence were co-distributed across the microparticle, indicating the morphology adopts a composite “sponge” architecture. Given that previous reports have observed norbornene-based polymers (M_n 's ~ 100,000 g/mol)

adopt length scales of ~ 40 nanometers,³⁸ it is reasonable to suggest that **PONI-GMT** would exist in a composite morphology in the **X-BNCs** nanoemulsions. This notion is further supported in literature as carvacrol and other phytochemicals are miscible with glycols,³⁹ such as the high density of tetraethylene glycol units found on **PONI-GMT**.

4.2.2 Stability and Degradability of X-BNCs

Macromolecular vehicles need to be stable to deliver therapeutic payloads yet degrade to avoid vehicle accumulation over time.⁴⁰ After characterizing the morphology of **X-BNCs**, we next probed the colloidal stability of the composites via monitoring particle size by dynamic light scattering (DLS).⁴¹ As shown in Figure 4.2a, when **X-BNCs** were incubated with 10% serum media for 2 hours, an increase in **X-BNCs** size (~25 nm) was observed, suggesting negatively charged serum proteins adsorb onto the positively charged **X-BNCs** surface. Notably, no evidence of **X-BNC** destabilization/aggregation was observed even at longer incubation times (e.g. 6 hours). However, as a control, non-crosslinked analogues using the same formulation minus **DTDS** showed essentially no stability in serum (Supporting Figure 4.10).

We next explored the degradability of **X-BNCs** in the presence of glutathione (**GSH**) and the ester-hydrolyzing enzyme porcine liver esterase (**PLE**). Using physiologically relevant concentrations of both biomolecules, **X-BNCs** were incubated for 24 hours with either 10mM **GSH** or 35 μ M **PLE** (1 U/ μ L) with PBS as a control. Figure 4.2b shows the size of **X-BNCs** remained the same after 24 hours in PBS, however the size increased significantly in **GSH/PLE** solutions, indicating degradation of the nanocomposites structure with concomitant generation of agglomerated structures through an Ostwald ripening-like process. Taken together, the results indicate the crosslinked

composite framework within **X-BNCs** are robust in serum yet biodegrade in the presence of chosen biological environments.

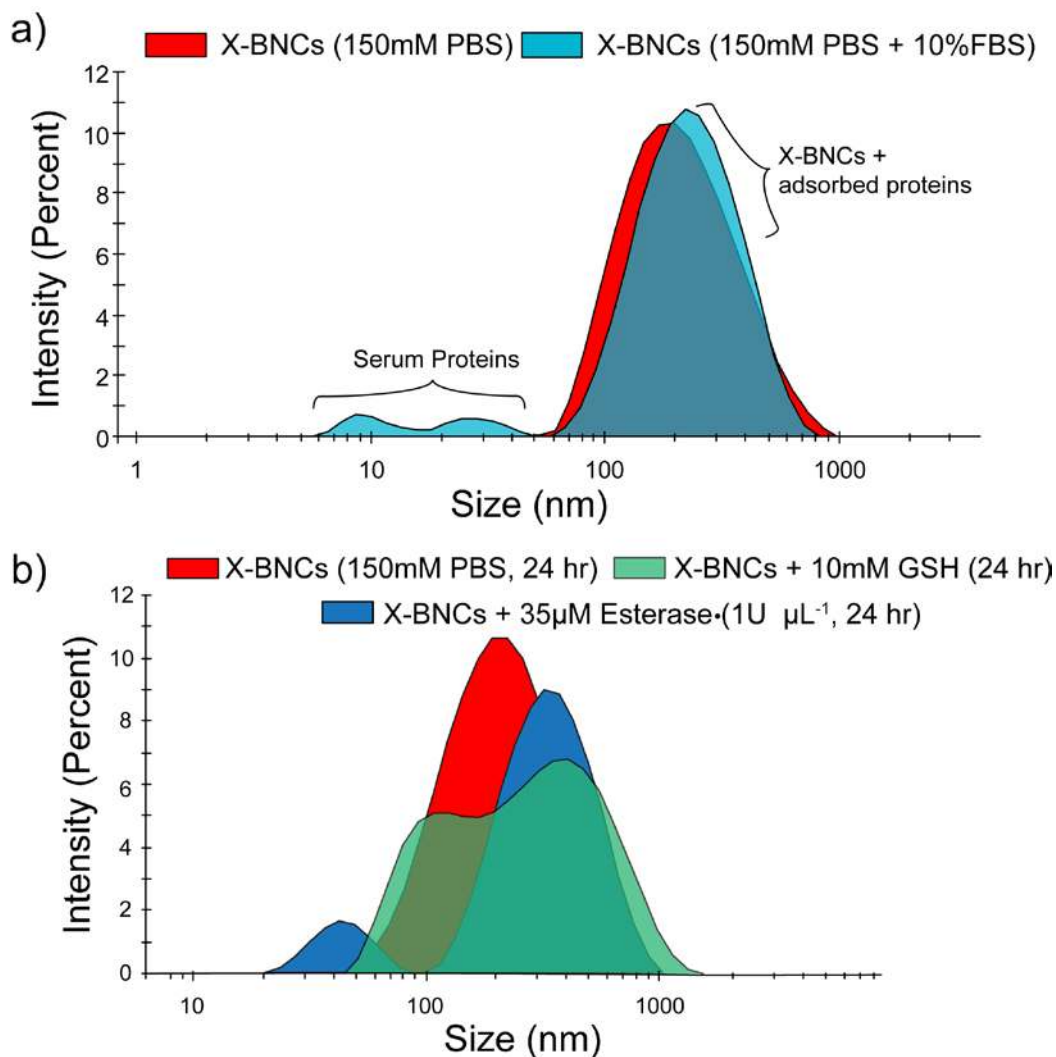


Figure 4.2. Stability and degradability of **X-BNCs**. DLS size distribution changes of **X-BNCs** when incubated with (a) 10% FBS media for two hours or (b) physiologically relevant biomolecules (glutathione and lipase) in PBS, showing degradation from disulfide cleavage and hydrolysis.

4.2.3 Antimicrobial Activity of **X-BNCs** Against Biofilms

We focused our antimicrobial efforts on highly refractory biofilms, where the efficacy of traditional antibiotic therapy is significantly compromised relative to planktonic

pathogens.⁴² We investigated the ability of **X-BNCs** to penetrate EPS followed by quantitative analysis of their therapeutic efficacy towards enclosed pathogenic bacteria. **X-BNC** penetration into biofilms formed by red fluorescent protein (RFP)-expressing *E. coli* was tracked by loading 3,3-dioctadecyloxacarbocyanine (DiO, green fluorescence) within the oil core. As shown in Figure 4.3, **X-BNCs** readily penetrate and diffuse throughout the biofilm, with fluorescence colocalizing with enclosed bacteria. The data demonstrates **X-BNCs** deliver their payload efficiently, reaching enclosed pathogens deep within the films matrix.

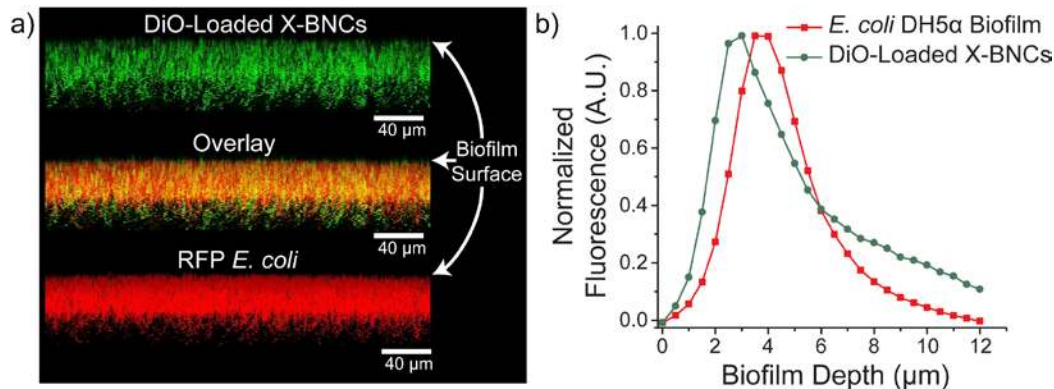


Figure 4.3. Confocal image stacks and penetration profile of *E. coli* DH5α biofilm after 1-hour treatment with X-BNCs loaded with DiO. Scale bars are 40μm and are not representative of the biofilm depth. Each projected z-stack image (a) is spaced by 1.3 μm at a 5° angle from the biofilms x-plane. Both the overlay and biofilm depth fluorescence graph (b) indicates X-BNCs completely penetrates the biofilm, colocalizing with bacteria that expresses red fluorescent protein.

Next, the antimicrobial activity of **X-BNCs** against multiple pathogenic Gram-negative and Gram-positive biofilms were evaluated. Four pathogenic bacterial strains of clinical isolates, *Staphylococcus aureus* (CD-489, a methicillin-resistant strain), *Pseudomonas aeruginosa* (CD-1006), *Escherichia coli* (CD-2), and *Enterobacter cloacae* (*E. cloacae*, CD-1412) complex were chosen to be tested as their associated infections are

typically common in hospital-related settings.^{43,44} As shown in Figure 4.4, **X-BNCs** effectively eliminated bacterial cells in all four-biofilm species within 3 hours. Notably, both Gram positive (*S. aureus*) and Gram negative (*P. aeruginosa*, *E. coli*, and *E. cloacae* complex) bacteria can be treated with **X-BNCs**, highlighting their broad-spectrum activity even in a biofilm matrix setting.

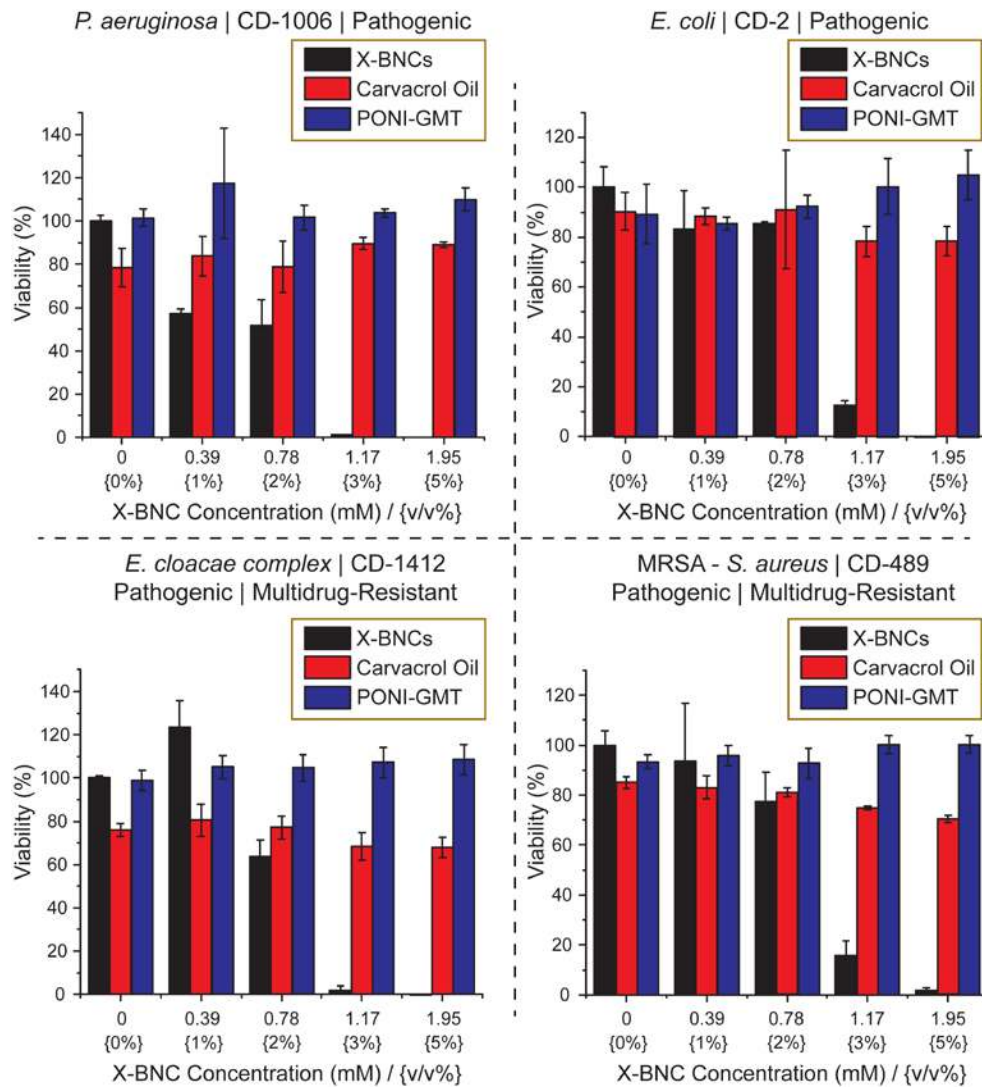


Figure 4.4. Viability of one-day-old Gram-negative/positive biofilms after a three-hour treatment with X-BNCs. The individual components are controls at different emulsion concentrations (Displayed as mM and v/v % of emulsion). The results shown are averaged triplicates, and the error bars indicate the standard deviation.

4.2.4 Selective Killing of Biofilms in a Coculture Model

Beyond treating biofilms on surfaces, eliminating these bacterial infections on human tissue and organs is a greater challenge and more relevant to patients who suffer from skin ulcers, burn injuries, or wound trauma. A fundamental issue associated with these infections is their ability to interfere with the host's tissue regeneration process. We evaluated the efficacy of X-BNCs as a topical treatment by using an *in vitro* co-culture model comprised of a biofilm grown on top of mammalian fibroblasts. *P. aeruginosa* and NIH 3T3 fibroblast cells were selected to build this co-culture model, since *P. aeruginosa* is widely associated with skin infections and fibroblast cells are critical during wound healing.^{45,46,47} The co-cultures were treated with X-BNCs for 3 hours, washed, and the viabilities of bacteria and fibroblast cells were determined. As shown in Figure 4.5, a 4-fold log reduction (~99.5%) in biofilm colonies was observed at a X-BNCs concentration of 16 v/v %, while 3T3 fibroblast viability remained uncompromised. Significantly, little change in fibroblast viability was observed at 32 v/v %, where a 6-log unit reduction in bacteria was observed. This selective toxicity to biofilm bacteria makes the X-BNC platform promising for addressing wound biofilms.

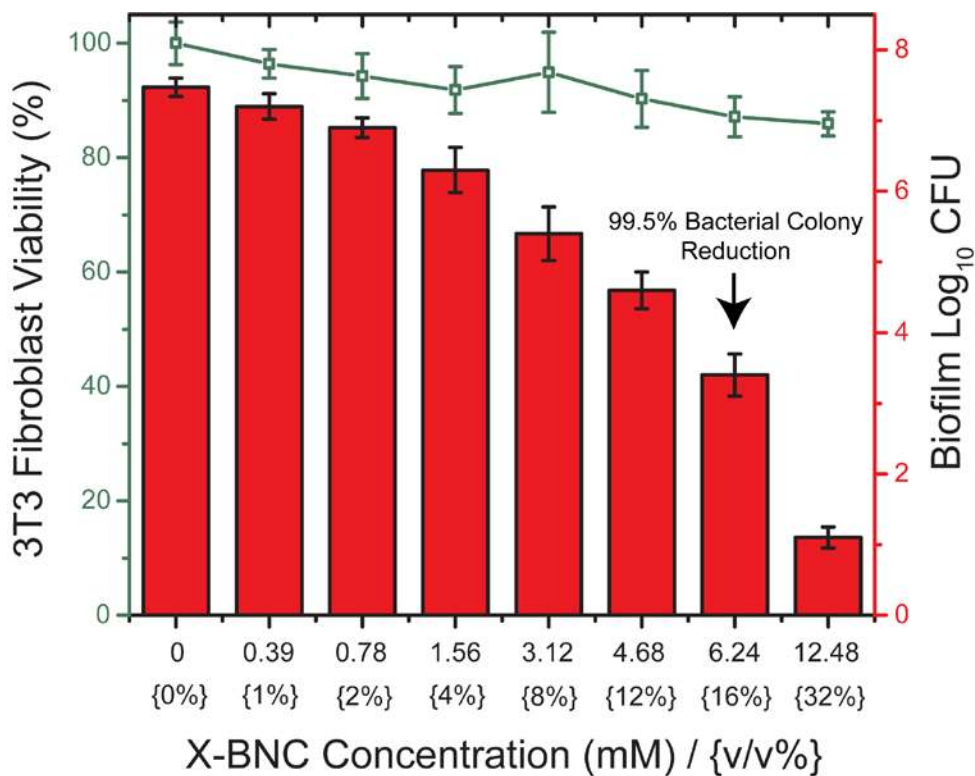


Figure 4.5. Viability of 3T3 fibroblast cells and *P. aeruginosa* biofilms in the coculture model after treating X-BNCs at different emulsion concentrations for three hours. 3T3 fibroblast cell viabilities are shown as a line. Bar plots represent log₁₀ of colony-forming bacteria units in biofilms. Each result is an average of three experiments, and the error bars designate the standard deviations.

4.2.5 Bacterial Resistance Towards Antibiotics Vs. X-BNCs

The number of antibiotic-resistant bacteria and their associated infections is increasing globally, leading to cases where infections have become untreatable. Although efforts to discover novel antibiotic classes to slow the progression of antibiotic resistance is ongoing,⁴⁸ developing alternative therapeutic platforms where bacteria cannot develop resistance towards must take precedence. We hypothesized that the membrane disruption induced by the antimicrobial phytochemical payload of X-BNCs would sidestep normal bacterial defense adaptations, preventing accumulated resistance. We tested this hypothesis

by subjecting planktonic bacteria to **X-BNCs** and a negative control antibiotic (ciprofloxacin, enzyme inhibitor) in the presence of propidium iodide (PI, Supporting Figure 4.11). PI is not permeant to live bacterial cells, however easily diffuses through membrane-compromised cells, generating fluorescence upon intercalating with DNA. **X-BNC** treatment quickly generated PI fluorescence, indicating their action mechanism compromises bacterial membrane integrity. Ciprofloxacin is an enzyme inhibitor antibiotic and therefore does not act on bacterial membranes, generating no observed fluorescence. Next, pathogenic *E. coli* (CD-2) was passaged in the presence of **X-BNCs**, or three commercially available antibiotics, ciprofloxacin (quinolone class), ceftazidime (β -lactam class), and tetracycline (tetracycline class). Briefly, we subjected the bacteria to the sub-minimum inhibitory concentrations (66% of MIC) of the antimicrobial agent. The resulting bacterial populations for each individual therapeutic was defined as the first passage, harvested, and their respective MICs evaluated. The subsequent passage was derived by exposing the previous passage with the 66% MIC of each respective therapeutic dosage. As shown in Figure 4.6a, no resistance was generated towards **X-BNCs** even after 20 serial passages (~1,300 bacterial generations). Meanwhile, *E. coli* rapidly developed resistance towards each of the antibiotics, with respective MIC increases of 33,000, 4,200, and 256-fold where the drugs reached their solubility limit in media. Going further, biofilms were grown with the 20th serial passage and subjected to **X-BNCs** for 3 hours, where CD-2 *E. coli* was still susceptible to nanoemulsion treatment (Figure 4.6b). These results indicate the mechanism of **X-BNCs** mitigates the onset of resistance in both planktonic and biofilm settings.

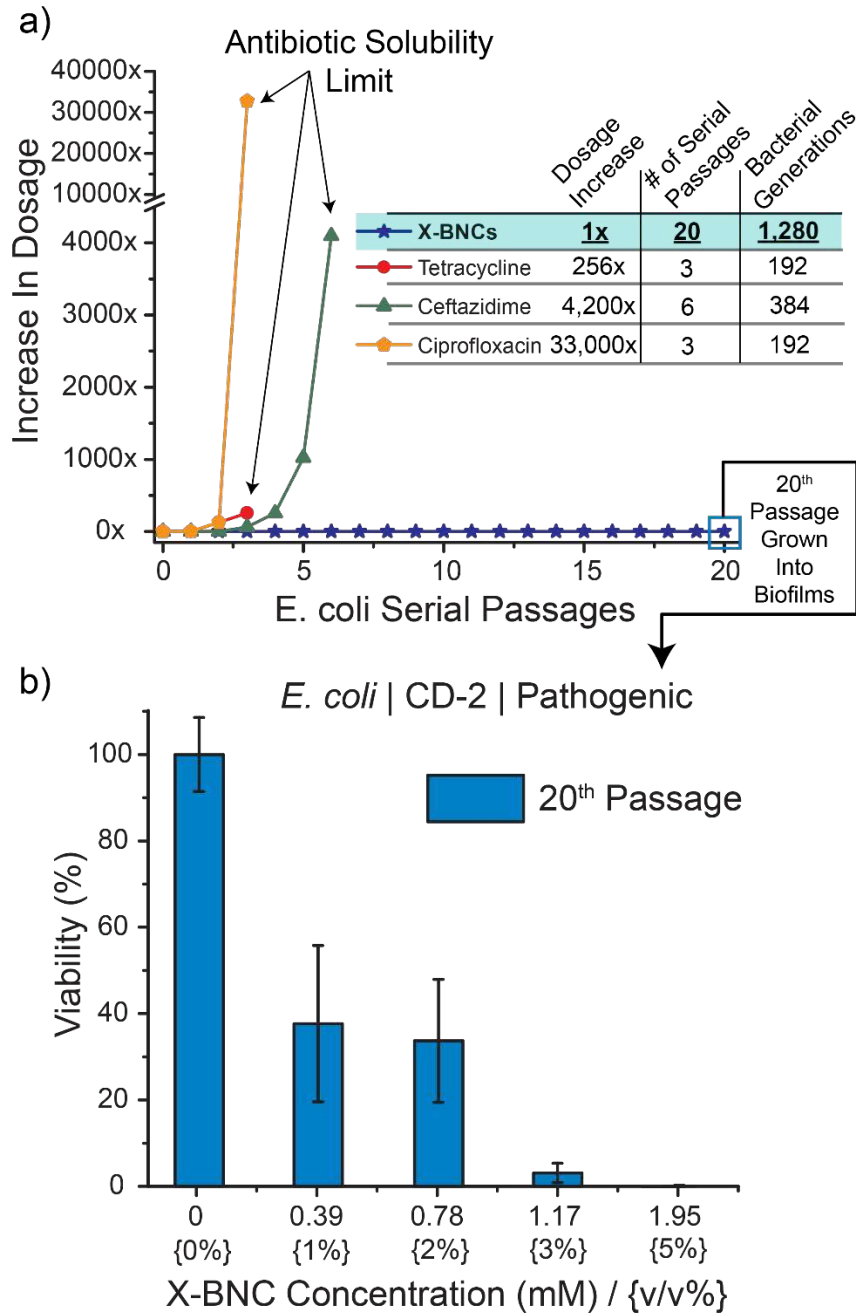


Figure 4.6. Accumulated resistance of pathogenic *E. coli* (CD-2) in both plankton and biofilm settings. (a) Resistance development of planktonic species during serial passaging in the presence of sub-MIC dosing's of antimicrobials. The y-axis indicates the increase in dosage as compared to the initial bacterial cells (0th passage) and the figure is representative of three independent experiments. (b) Derived *E. coli* cells from 20 serial passages of sub-MIC X-BNCs dosing was grown into a biofilm and subjected to a three-hour treatment of X-BNCs at different emulsion concentrations. The results indicate that evolved pathogenic *E. coli* remain susceptible to X-BNCs.

4.3. Conclusions

In summary, we report the construction, characterization, and antimicrobial potential of a biodegradable crosslinked polymer-stabilized oil-in-water nanocomposite. These nanoemulsions maintain stability in serum yet degrade in the presence of selected biomolecules, a necessary attribute to avoid vehicle accumulation over time. Furthermore, the nanocomposites are highly effective against both Gram negative and positive bacteria biofilms, with no observed toxicity to mammalian fibroblast cells. In stark contrast to traditional antibiotics, bacteria were unable to accumulate resistance towards our nanoemulsions whether the bacteria were planktonic or in biofilms. The therapeutic polymer-based phytochemical nanoemulsion we present is a highly promising antimicrobial platform with the potential to impact treatment of wound biofilms and other difficult bacterial infections.

4.4. Experimental Protocols

4.4.1 Materials and Methods

All reagents and materials were purchased from Fisher Scientific and used as received. NIH-3T3 cells (ATCC CRL-1658) were purchased from ATCC. Dulbecco's Modified Eagle's Medium (DMEM) (DMEM; ATCC 30-2002) and fetal bovine serum (Fisher Scientific, SH3007103) were used in cell culture. Pierce LDH Cytotoxicity Assay Kit was purchased from Fisher Scientific.

4.4.2 Preparation of Nanocomposites

Stock nanocomposite solutions were prepared in 0.6 ml Eppendorf tubes. To prepare the stock **X-BNC** emulsions, 3 μL of carvacrol oil (containing 3 wt% **DTDS**) was added to 497 μL of Milli-Q H_2O containing 6 μM of **PONI-GMT** and emulsified in an amalgamator for 50 s. The non-crosslinked analogs were done in the same fashion however without **DTDS** dissolved in carvacrol. The emulsions were allowed to rest overnight prior to use.

4.4.3 Biofilm Formation

Bacteria were inoculated in LB broth at 37°C until stationary phase. The cultures were then harvested by centrifugation and washed with 0.85% sodium chloride solution three times. Concentrations of resuspended bacterial solution were determined by optical density measured at 600 nm. Seeding solutions were then made in M9 to reach OD_{600} of 0.1. 100 μL of the seeding solutions were added to each well of the microplate. M9 medium without bacteria was used as a negative control. The plates were covered and incubated at room temperature under static conditions for a desired period. Planktonic bacteria were removed by washing with PB saline three times.

Varied v/v % of X-NCs, made in M9 medium, were incubated with the biofilms for 3 h. Biofilms were washed with phosphate buffer saline (PBS) three times and viability was determined using an Alamar Blue assay. M9 medium without bacteria was used as a negative control.

4.4.4 Biofilm – 3T3 Fibroblast Cell Co-culture

A total of 20,000 NIH 3T3 (ATCC CRL-1658) cells were cultured in Dulbecco's modified Eagle medium (DMEM; ATCC 30-2002) with 10% bovine calf serum and 1%

antibiotics at 37°C in a humidified atmosphere of 5% CO₂. Cells were kept for 24 hours to reach a confluent monolayer. Bacteria (*P. aeruginosa*) were inoculated and harvested. Afterwards, seeding solutions were made in buffered DMEM supplemented with glucose to reach an OD₆₀₀ of 0.1. Old medium was removed from 3T3 cells followed by addition of 100 µL of seeding solution. The co-cultures were then stored in a box with damp paper towels at 37°C overnight without shaking. Testing solutions at different concentrations were made by diluting nanocomposites into DMEM prior to use. Media was removed from co-culture, replaced with testing solutions, and incubated for 3 hours at 37°C. Co-cultures were then analyzed using a LDH cytotoxicity assay to determine mammalian cell viability. To determine the bacteria viability in biofilms, the testing solutions were removed, and co-cultures were washed with PBS. Fresh PBS was then added to disperse remaining bacteria from biofilms in co-culture by sonication for 20 min and mixing with pipet. The solutions containing dispersed bacteria were then plated onto agar plates and colony forming units were counted after incubation at 37°C overnight.

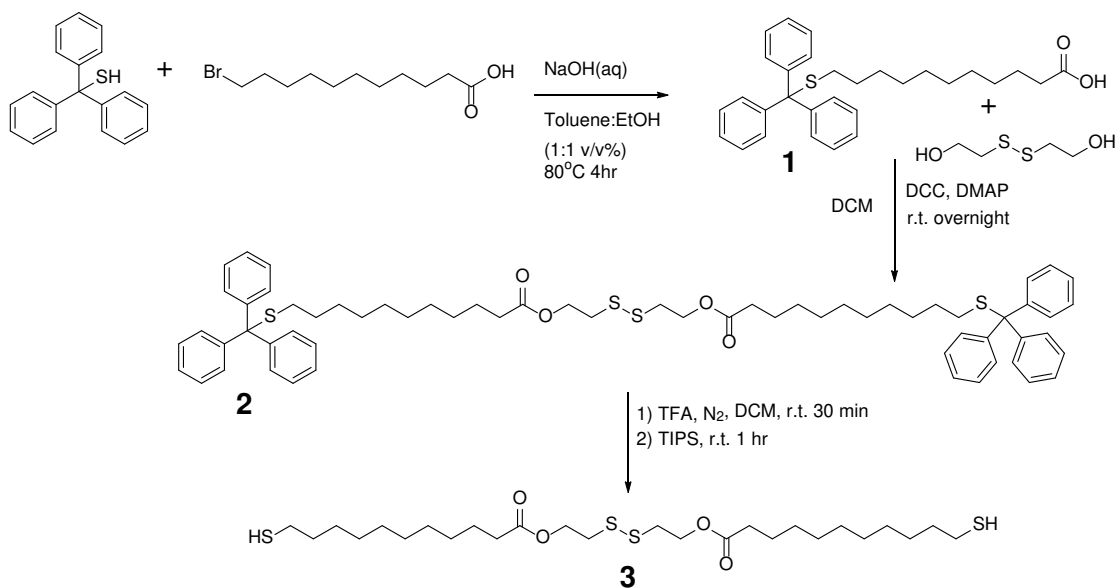
4.4.5 Membrane Disruption Study *via* PI Staining

P. aeruginosa was cultured in LB medium at 37°C and 275 rpm until reaching the stationary phase. The cultures were centrifuged then resuspended in 70% isopropyl alcohol for obtaining dead bacteria or resuspended in 0.85% sodium chloride solution for live bacteria. Both bacteria were incubated for 1 hour at room temperature and then washed with 0.85% sodium chloride solution again. The O.D. of these solutions were determined and adjusted to 1.

100 µL of live bacteria were added to the wells of a black 96-well plate. 5 uL of 1 mg/L propidium iodide (PI) was then added. Fluorescence intensities were measured

immediately after adding 100 μ L of PBS containing 10X MIC of X-BNCs (Excitation/Emission: 535 nm/ 617 nm). Live bacteria were also treated with PI and ciprofloxacin as negative control. Dead bacteria were treated with PI as positive control.

4.4.6 Synthesis of DTDS (3)



Synthesis of 1. To a 250ml round bottom flask equipped with a stir-bar was added triphenylmethylmercaptan (5.0g, 18.09mmol, 1.0eq), 11-bromoundecanoic acid (4.80g, 18.09mmol, 1.0eq), and 75ml of both toluene and ethanol. The mixture was allowed to stir to completely dissolve the reagents. Meanwhile, sodium hydroxide (1.60g, 39.80mmol, 2.2 eq) was dissolved in a minimal amount of water and then added to the reaction flask. The flask was heated to 80°C for 4 hours, cooled to room temperature, and the solvents rotovaped. Water was then added, and the mixture acidified with 1M HCL. The aqueous mixture was extracted with ethyl acetate three times. The combined organic layers were washed with brine, dried with sodium sulfate, filtered, and rotovaped to yield an off-white solid that was purified through column chromatography to yield **1** (White solid, yield =

92%). (¹H NMR, CDCL₃, 400 MHz) 11.2 (br, 1H), 7.45 (d, 6H), 7.3 (t, 6H), 7.21 (t, 3H), 2.35 (t, 2H), 2.15 (t, 2H), 1.65 (m, 2H), 1.4 (m, 2H), 1.25 (m, 12H).

Synthesis of 2. To a 250ml round bottom flask equipped with a stir-bar was added **1** (4.71g, 10.22mmol, 2.0eq), 2-hydroxyethyl disulfide (0.63ml, 5.11mmol, 1.0eq), 4-dimethylaminopyridine (0.31g, 2.55mmol, 0.5eq), and 100ml of dichloromethane. The reaction flask was stirred and finally N,N'-dicyclohexylcarbodiimide (2.22g, 10.74mmol, 2.1eq) was added and allowed to stir at room temperature overnight. Afterwards, the solvent was evaporated and diethyl ether (150ml) was added to the reaction residue, sonicated, and placed in a freezer for 1 hour to precipitate most of the DCU biproduct. The reaction mixture was filtered and washed with cold diethyl ether. The filtrate was rotovaped and the product was purified with column chromatography to yield **2** (light yellow, yield = 90%). (¹H NMR, CDCL₃, 400 Mhz) 7.41 (d, 12H), 7.28 (t, 12H), 7.21 (t, 6H), 4.35 (t, 4H), 2.92 (t, 4H), 2.32 (t, 4H), 2.15 (t, 4H), 1.63 (m, 4H), 1.4 (m, 4H), 1.25 (m, 24).

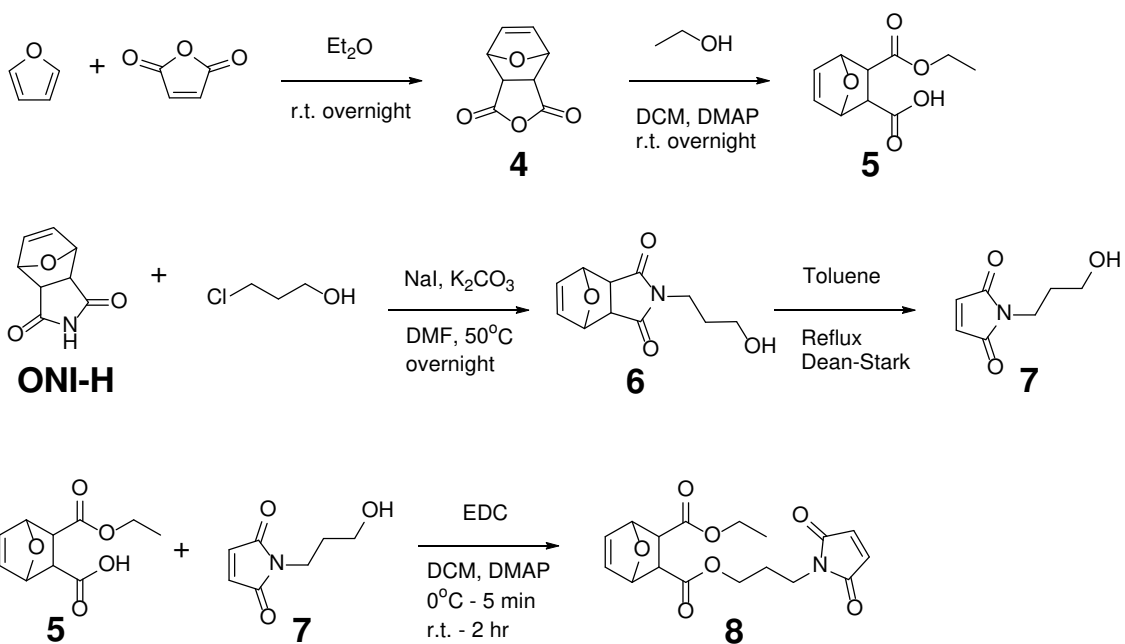
Synthesis of 3 (DTDS). To a 250ml round bottom flask equipped with a stir-bar, was added **2** (2.6g, 2.50mmol, 1.0eq). Next, nitrogen was bubbled through 100ml of dichloromethane for 5 minutes and added to the reaction flask. The flask was sealed with a septum and a continuous flow of nitrogen was introduced to the reaction flask until after trifluoroacetic acid (7.66ml, 100.04mmol, 40.0eq) was added. The reaction mixture color immediately changed to yellow and was allowed to stir for 30 minutes to completely form the triphenylmethyl carbocation. After 30 minutes, triisopropylsilane (1.1ml, 5.25mmol, 2.1eq) was added to the reaction flask and allowed to stir for 1 hour. During this time the color changed back to nearly colorless. Afterwards, excess trifluoroacetic acid was

removed by rotovaping the reaction 4 times with 100ml of dichloromethane. The obtained residue was easily purified and isolated using column chromatography with no degradation or rearrangement of **3** (**DTDS**, off-white solid, yield = 85%). (¹H NMR, CDCl₃, 400 MHz) 4.31 (t, 4H), 2.91 (t, 4H), 2.5 (q, 4H), 2.31 (t, 4H), 1.61 (m, 8H), 1.31 (m, 24H).

4.4.7 Synthesis of PONI-GMT

Maleimide Monomer Synthesis (**8**)

Note: Synthesis of **ONI-H**, **9**, and **10** has been reported previously.³⁰



Synthesis of 4. To a 250ml round bottom flask equipped with a stir-bar, was added furan (18.5ml, 255.0mmol, 5.0eq) and 100ml of diethyl ether. Maleic anhydride (5.0g, 51.0mmol, 1.0eq) was added to the flask and the reaction was stirred at room temperature overnight. Afterwards, the formed precipitate in the reaction flask was filtered and washed with copious amounts of diethyl ether to afford **4** (white solid, yield = 88%). (¹H NMR, DMSO-D₆, 400 MHz) 6.55 (s, 2H), 5.31 (s, 2H), 3.3 (s, 2H).

Synthesis of 5. To a 250ml round bottom flask equipped with a stir-bar, was added **4** (7.5g, 45.22mmol, 1.0eq), 4-dimethylaminopyridine (0.55g, 4.52mmol, 0.1eq), and 100ml of dichloromethane. Anhydrous ethanol (3.17ml, 54.26mmol, 1.2eq) was added and the reaction was stirred at room temperature overnight. Afterwards the solvent was evaporated, and the product was purified with column chromatography to yield **5** (White solid, yield = 82%). (¹H NMR, CDCL₃, 400 MHz) 10.2 (br, 1H), 6.45 (q, 2H), 5.28 (s, 1H), 5.21 (s, 1H), 4.15 (q, 2H), 2.81 (q, 2H), 1.21 (t, 3H).

Synthesis of 6. To a 250ml round bottom flask equipped with a stir-bar, was added **ONI-H** (7.0g, 42.40mmol, 1.0eq) and 50ml of n,n-dimethylformamide. Then, potassium carbonate (23.40g, 169.55mmol, 4.0eq) was added and the reaction flask was stirred at 50°C for 5 minutes. Afterwards, sodium iodide (1.27g, 8.48mmol, 0.2eq) was added followed by 3-chloropropanol (3.72ml, 44.51mmol, 1.05eq) and the reaction flask was stirred overnight at 50°C. Afterwards, the reaction flask was cooled to room temperature and water was added. The reaction mixture was transferred to a separatory funnel and extracted with ethyl acetate three times. The organic layers were combined and washed with saturated sodium bicarbonate, 1M HCL, and brine. The organic layer was dried with sodium sulfate, filtered and rotovaped to yield a solid residue that was purified using column chromatography to afford **6** (White solid, yield = 86%). (¹H NMR, CDCL₃, 400 MHz) 6.49 (s, 2H), 5.21 (s, 2H), 3.58 (t, 2H), 3.49 (q, 2H), 2.81 (s, 2H), 2.65 (br, 1H), 1.73 (m, 2H).

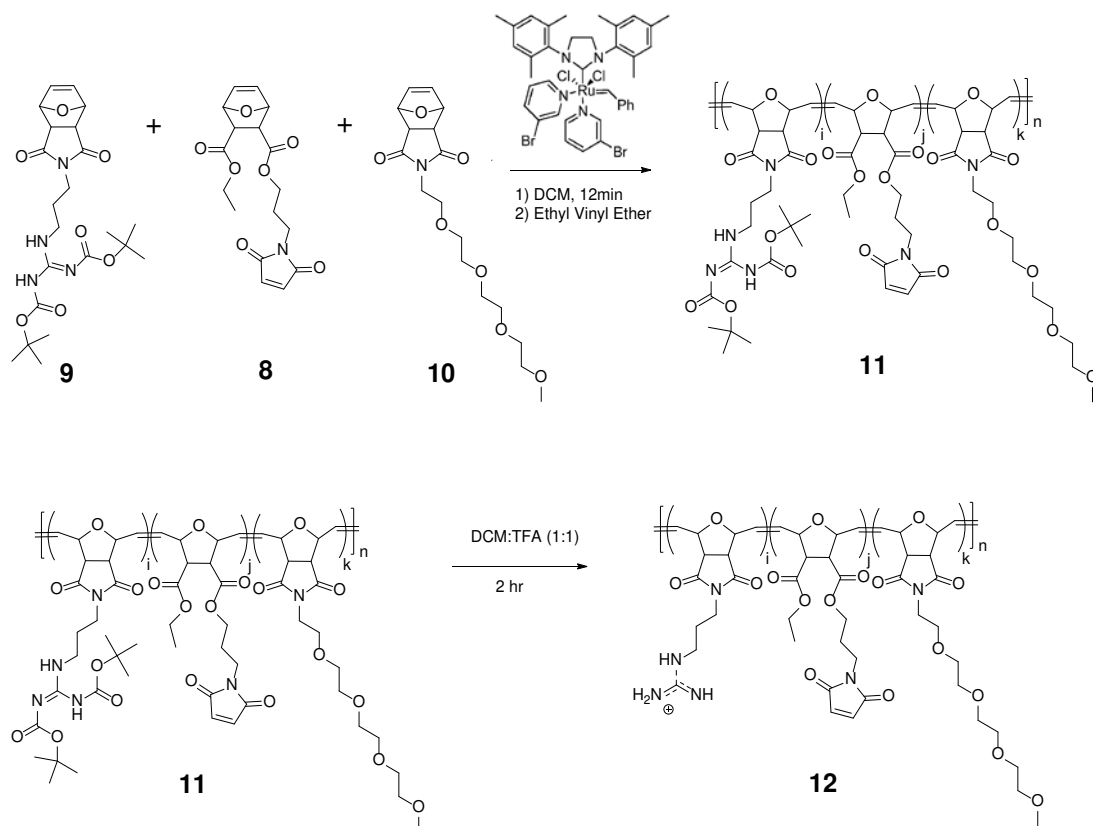
Synthesis of 7. To a 250ml round bottom flask equipped with a stir-bar, was added **6** (7.0g, 31.36mmol, 1.0eq) and 150ml of toluene. A dean-stark trap was added to the reaction flask and the reaction was stirred under reflux overnight. Afterwards, the solvent was rotovaped

and purified using column chromatography to afford **7** (White solid, yield = 88%). (¹H NMR, CDCL₃, 400 MHz) 6.65 (s, 2H), 3.6 (t, 2H), 3.51 (t, 2H), 2.65 (br, 1H), 1.73 (m, 2H).

Synthesis of 8. To a 250ml round bottom flask equipped with a stir-bar, was added **7** (1.6g, 10.31mmol, 1.0eq), **5** (2.20g, 10.31mmol, 1.0eq), 4-dimethylaminopyridine (0.13g, 1.03mmol, 0.1eq), and 100ml of dichloromethane. The reaction flask was cooled to 0°C and 1-Ethyl-3-(3-dimethylaminopropyl)carbodiimide (2.17g, 11.34mmol, 1.1eq) was added and stirred at 0°C for 10 minutes, followed by at room temperature for 2 hours.

Note: It is critical to only allow the reaction to proceed for 2 hours and not overnight. Leaving the reaction overnight will result in complete degradation of the product.

Afterwards, the solvent was rotovaped and the residue was purified using column chromatography to afford **8** (Light yellow oil, yield = 75%). (¹H NMR, CDCL₃, 400 MHz) 6.69 (s, 2H), 6.45 (s, 2H), 5.29 (s, 1H), 5.23 (s, 1H), 4.13 (t, 2h), 4.1 (m, 2H), 3.61 (t, 2H), 2.8 (s, 2H), 1.92 (m, 2H), 1.25 (t, 3H).

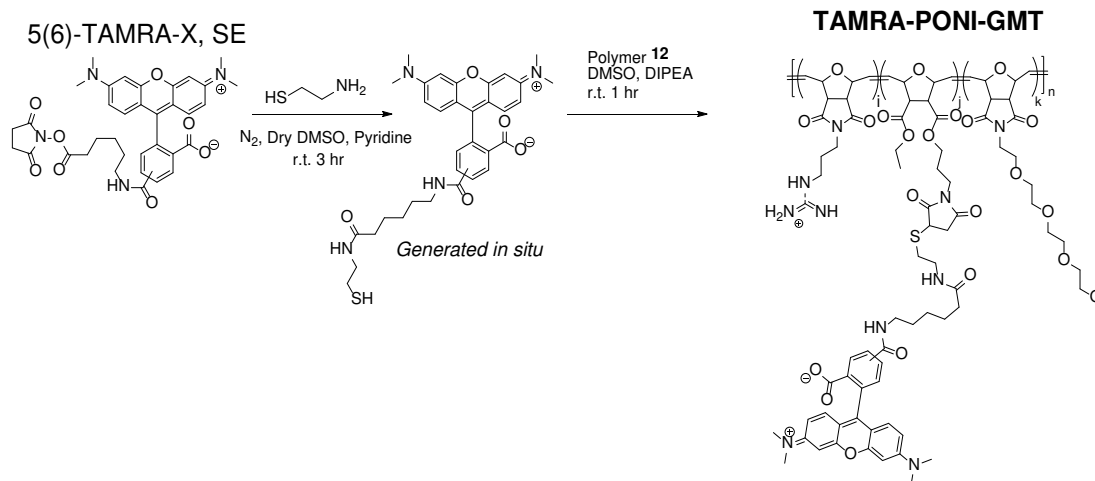


Synthesis of Polymer 11. To a 10ml pear-shaped air-free flask equipped with a stir-bar was added **9** (0.27g, 0.57mmol, 0.4eq), **10** (0.25g, 0.72mmol, 0.5eq), **8** (0.05g, 0.14mmol, 0.1eq), and 4ml of dichloromethane. In a separate 10ml pear-shaped air-free flask was added Grubbs 3rd generation catalyst (0.015g, 0.017mmol, 0.012eq) and 1ml of dichloromethane. Both flasks were sealed with septa and attached to a schlenk nitrogen/vacuum line. Both flasks were freeze-pump-thawed three times. After thawing, Grubbs 3rd generation catalyst solution was syringed out and quickly added to the flask containing the monomers and allowed to react for 12 minutes. After the allotted time, ethyl vinyl ether (200 μ L) was added and allowed to stir for 15 minutes. The reaction mixture was then diluted to two times the volume and precipitated into a heavily stirred solution of ether:hexane (150ml, 1:1 volume ratio) to yield Polymer **11**. MW = 46,157, PDI = 1.45, as determined by THF GPC using a polystyrene calibration curve). ^1H NMR (500MHz,

CDCl₃) 11.49 (s, 2H), 8.45 (br, 2H), 6.71 (br, 0.8H), 6.09 (br, 4H), 5.8 (br, 6H), 5.05 (br, 6H), 4.5 (br, 4H), 3.65 (br, 52H), 3.45 (br, 2H), 3.35 (s, 7H), 3.33 (br, 2H), 1.89 (br, 4H), 1.8 (br, 4H), 1.49 (s, 20H), 1.2 (br, 2H).

Synthesis of Polymer 12. To a 50ml round bottom flask equipped with a stir-bar was added Polymer **11** (400 milligrams). Dichloromethane was purged with nitrogen for five minutes and 12ml was added to the flask, sealed with a septum and purged with nitrogen for five minutes. The main nitrogen line was left in the septum and the nitrogen pressure was reduced to a steady stream. 12ml of trifluoroacetic acid (excess) was added and the reaction was stirred for two hours. Afterwards, excess TFA was removed by rotovaping with dichloromethane, three times. The reaction residue was dissolved in a minimal amount of water, filtered through a polyethersulfone (PES) syringe filter and lyophilized to yield polymer **12** as a white solid which readily dissolves in water. MW ~ 33,157, as determined using GPC. ¹H NMR (400MHz, D₂O) 6.7 (br, 0.4H), 5.94 (br, 4H), 5.74 (br, 4H), 4.82 (br, 4H), 4.45 (br, 4H), 3.5 (br, 40H), 3.2 (s, 6H), 3.02 (br, 4H), 1.7 (br, 4H), 1.05 (br, 2H).

Synthesis of TAMRA-PONI-GMT



4.4.8 Synthesis of TAMRA-PONI-GMT

To a 7ml scintillation vial equipped with a stir-bar, was added 5(6)-TAMRA-X, SE (0.001g, 0.0016mmol, 1.0eq), pyridine (0.14ml, 0.0017mmol, 1.1eq), and 1ml of anhydrous DMSO (previously purged with nitrogen). A blanket of nitrogen was introduced to the vial, cysteamine (0.00012g, 0.0016mmol, 1.0eq) was added, the vial was sealed, covered with aluminum foil, and was stirred at room temperature for 3 hours. Meanwhile, in a 20ml scintillation vial equipped with a stir-bar, was added Polymer **12** (0.08g), N,N-diisopropylethylamine (0.1ml), and 2ml of anhydrous DMSO. After three hours, the terminal thiol-TAMRA that was generated in situ was added to the stirred vial containing Polymer **12**, covered with aluminum foil, sealed with a blanket of nitrogen, and stirred at room temperature overnight. Afterwards, the reaction vial was diluted with water and acidified using 1M HCL as to avoid a turbid solution. The reaction solution was completely homogenous at this time and was transferred to a 10,000 MWCO dialysis snake skin tubing. The dialysis tube was stirred in a 5L bucket for three days, changing the water every two hours the first day, and periodically for the remaining two days. Afterwards, the reaction solution was filtered through a PES syringe filter and lyophilized to afford **TAMRA-PONI-GMT** (Red-crystalline solid). TLC analysis (Mobile phase = ethyl acetate) of **TAMRA-PONI-GMT** against the in situ generated terminal thiol indicated that TAMRA was successfully conjugated to **12** in addition to any free TAMRA dye being removed during dialysis.

4.5. Supporting Figures

4.5.1 DTDS Storage Stability

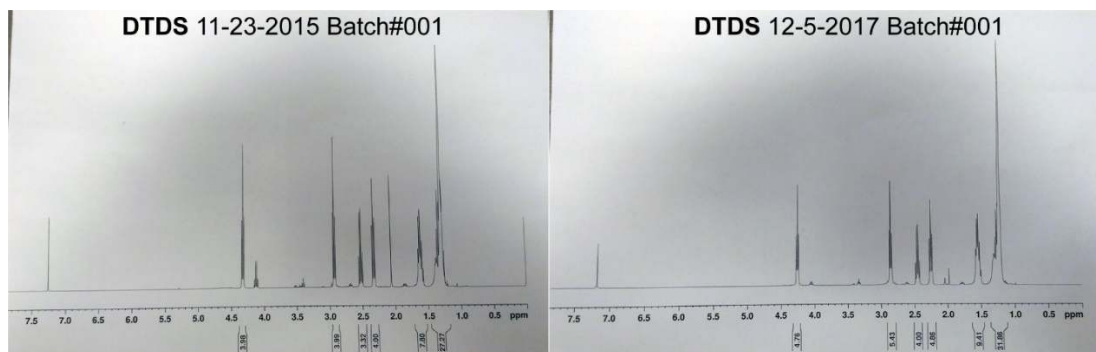


Figure 4.7. Storage of **DTDS**. **DTDS** was stored in a nitrogen purged 20ml scintillation vial, covered with aluminum foil and kept in a -4°C freezer for over two years. ¹H NMR analysis of **DTDS** two years later revealed no degradation or rearrangement of its initial structure. It is hypothesized that **DTDS**'s stability is attributed to its solid physical properties.

4.5.2 Zeta Potential of X-BNCs

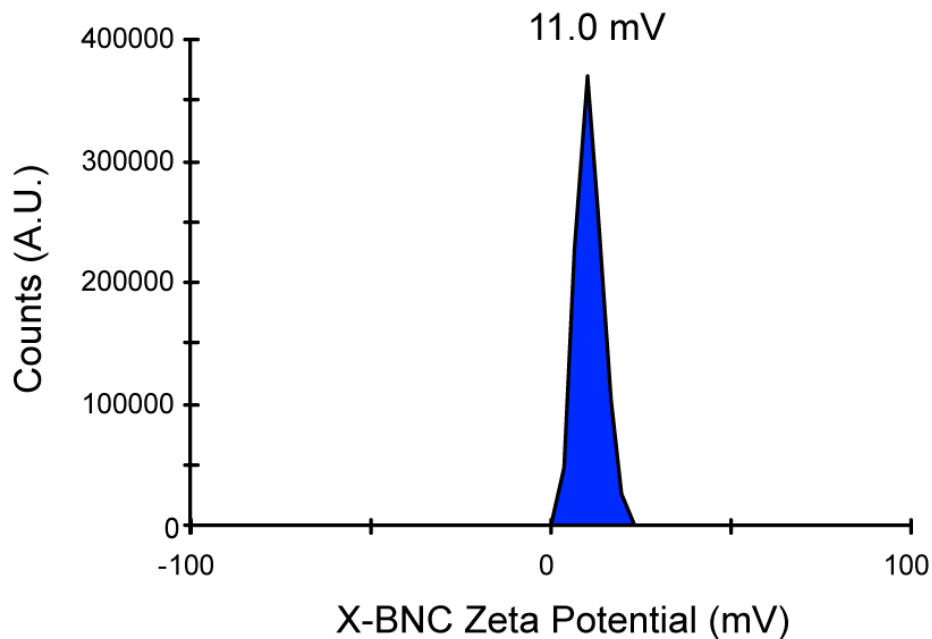


Figure 4.8. Zeta potential of **X-BNCs**. The cationic charge is derived from guanidine moieties found on **PONI-GMT** and is expected to be located at the oil-water interface and throughout the emulsion, given the architecture is a composite morphology.

4.5.3 Long-Term Storage of X-BNCs

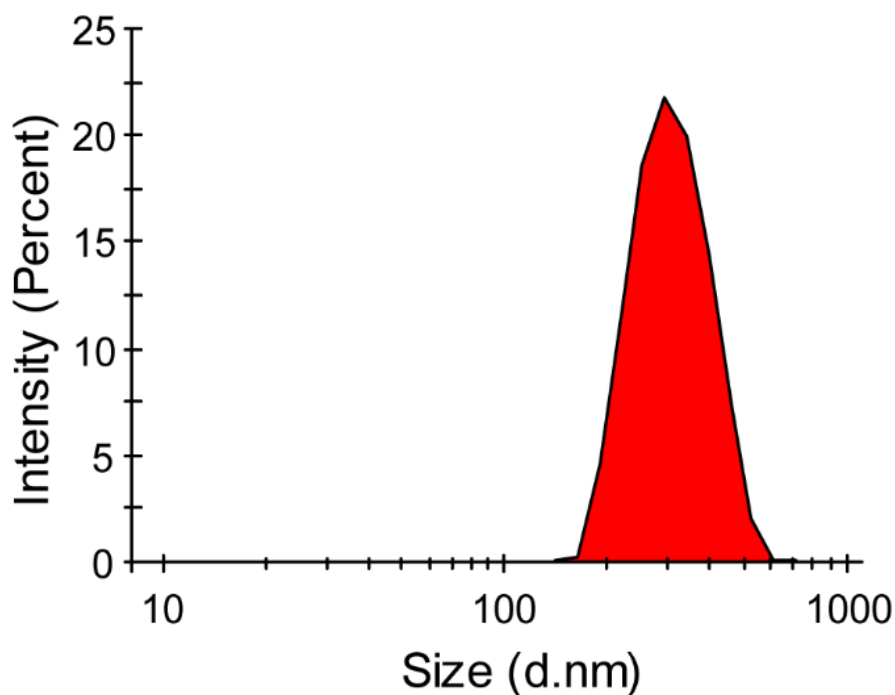


Figure 4.9. Size distribution of X-BNCs stock solution in PBS after 1 year of storage. The average size of X-BNCs increased to ~ 310nm indicating that the crosslinking scaffold of X-BNCs slows the onset of flocculation.

4.5.4 Serum Stability of NX-NCs

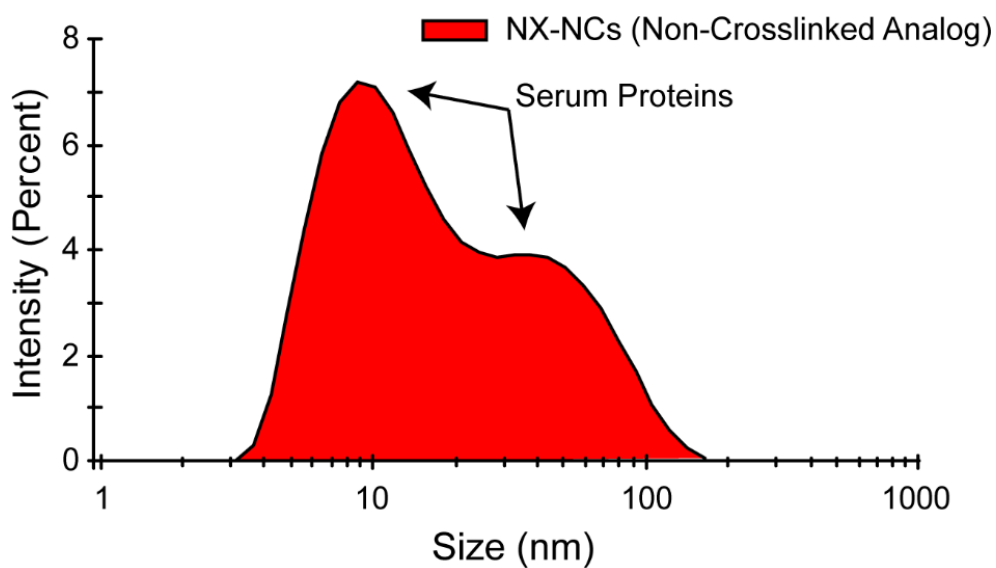


Figure 4.10. DLS size distribution. Size distribution of non-crosslinked analogs of X-BNCs (NX-NCs) after two hours in 10% fetal bovine serum using dynamic light scattering

(DLS) measurements. **NX-NCs** show no stability in serum-containing conditions with the DLS results indicating only serum proteins present.

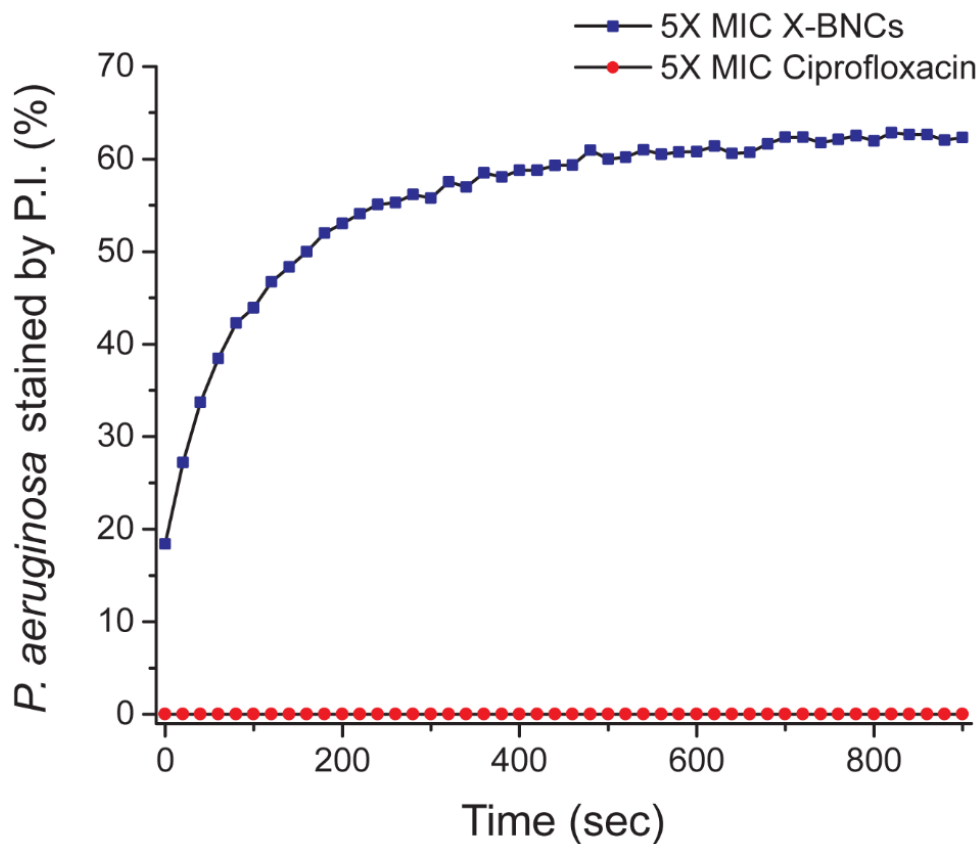


Figure 4.11. Percentage of *P. aeruginosa* stained by propidium iodide (PI) following treatment with **X-BNCs** or ciprofloxacin. **X-BNCs** quickly disrupted cell membrane, therefore PI could bind to nucleic acids and generate red fluorescence. However, no fluorescence was observed with ciprofloxacin as its action mechanism towards bacteria involves enzyme inhibition and not membrane disruption. The remaining percent of *P. aeruginosa* that were not stained is likely due to the large concentration of bacteria used (OD = 0.5) along with a complete consumption of **X-BNC** composites during the study.

4.6. References

- (1) Nathwani, D.; Raman, G.; Sulham, K.; Gavaghan, M.; Menon, V. Clinical and Economic Consequences of Hospital-Acquired Resistant and Multidrug-Resistant *Pseudomonas aeruginosa* Infections: A Systematic Review and Meta-Analysis. *Antimicrob. Resist. Infect. Control* **2014**, *3*, 32–47.
- (2) Morales, E.; Cots, F.; Sala, M.; Comas, M.; Belvis, F.; Riu, M.; Salvadó, M.; Grau, S.; Horcajada, J. P.; Montero, M. M.; Castells, X. Hospital Costs of Nosocomial Multidrug-Resistant *Pseudomonas aeruginosa* Acquisition. *BMC Health Serv. Res.* **2012**, *12*, 122–129.
- (3) Tam, V. H.; Rogers, C. A.; Chang, K.-T.; Weston, J. S.; Caeiro, J.-P.; Garey, K. W. Impact of Multidrug-Resistant *Pseudomonas aeruginosa* Bacteremia on Patient Outcomes. *Antimicrob. Agents Chemother.* **2010**, *54*, 3717–3722.
- (4) Drenkard, E.; Ausubel, F. M. *Pseudomonas* Biofilm Formation and Antibiotic Resistance are Linked to Phenotypic Variation. *Nature* **2002**, *416*, 740–743.
- (5) Schierle, C. F.; De la Garza, M.; Mustoe, T. A.; Galiano, R. D. *Staphylococcal* Biofilms Impair Wound Healing by Delaying Reepithelialization in a Murine Cutaneous Wound Model. *Wound Repair Regen.* **2009**, *17*, 354–359.
- (6) Sanchez, C. J.; Mende, K.; Beckius, M. L.; Akers, K. S.; Romano, D. R.; Wenke, J. C.; Murray, C. K. Biofilm Formation by Clinical Isolates and the Implications in Chronic Infections. *BMC Infect. Dis.* **2013**, *13*, 47–58.
- (7) Wu, H.; Moser, C.; Wang, H.; Høiby, N.; Song, Z.-J.; Hoiby, N.; Song, Z.-J. Strategies for Combating Bacterial Biofilm Infections. *Int. J. Oral Sci.* **2014**, *7*, 1–7.
- (8) Anderl, J. N.; Franklin, M. J.; Stewart, P. S. Role of Antibiotic Penetration Limitation in *Klebsiella pneumoniae* Biofilm Resistance to Ampicillin and Ciprofloxacin. *Antimicrob. Agents Chemother.* **2000**, *44*, 1818–1824.
- (9) Tseng, B. S.; Zhang, W.; Harrison, J. J.; Quach, T. P.; Song, J. L.; Penterman, J.; Singh, P. K.; Chopp, D. L.; Packman, A. I.; Parsek, M. R. The Extracellular Matrix Protects *Pseudomonas aeruginosa* Biofilms by Limiting the Penetration of Tobramycin. *Environ. Microbiol.* **2013**, *15*, 2865–2878.
- (10) Szomolay, B.; Klapper, I.; Dockery, J.; Stewart, P. S. Adaptive Responses to Antimicrobial Agents in Biofilms. *Environ. Microbiol.* **2005**, *7*, 1186–1191.
- (11) Walters, M. C.; Roe, F.; Bugnicourt, A.; Franklin, M. J.; Stewart, P. S. Contributions of Antibiotic Penetration, Oxygen Limitation, and Low Metabolic Activity to Tolerance of *Pseudomonas aeruginosa* Biofilms to Ciprofloxacin and Tobramycin. *Antimicrob. Agents Chemother.* **2003**, *47*, 317–323.

- (12) Olsen, I. Biofilm-Specific Antibiotic Tolerance and Resistance. *Eur. J. Clin. Microbiol. Infect. Dis.* **2015**, *34*, 877–886.
- (13) Stewart, P. S.; William Costerton, J. Antibiotic Resistance of Bacteria in Biofilms. *Lancet* **2001**, *358*, 135–138.
- (14) del Pozo, J. L.; Patel, R. The Challenge of Treating Biofilm-Associated Bacterial Infections. *Clin. Pharmacol. Ther.* **2007**, *82*, 204–209.
- (15) Cowan, M. M. Plant Products as Antimicrobial Agents. *Clin. Microbiol. Rev.* **1999**, *12*, 564–582.
- (16) Djeussi, D. E.; Noumedem, J. A. K.; Seukep, J. A.; Fankam, A. G.; Voukeng, I. K.; Tankeo, S. B.; Nkuete, A. H. L.; Kuete, V. Antibacterial Activities of Selected Edible Plants Extracts Against Multidrug-Resistant Gram-Negative Bacteria. *BMC Complement. Altern. Med.* **2013**, *13*, 164–171
- (17) Monte, J.; Abreu, C. A.; Borges, A.; Simões, C. L.; Simões, M. Antimicrobial Activity of Selected Phytochemicals Against *Escherichia coli* and *Staphylococcus aureus* and Their Biofilms. *Pathogens* **2014**, *3*, 473–498.
- (18) Ahmad, I.; Beg, A. Z. Antimicrobial and Phytochemical Studies of 45 Indian Medicinal Plants Against Multi-Drug Resistant Pathogens. *J. Ethnopharmacol.* **2001**, *74*, 113–123.
- (19) Simoes, M.; Bennett, R. N.; Rosa, E. A. S. Understanding Antimicrobial Activities of Phytochemicals Against Multidrug-Resistant Bacteria and Biofilms. *Nat. Prod. Rep.* **2009**, *26*, 746–757.
- (20) O’Connell, K. M. G.; Hodgkinson, J. T.; Sore, H. F.; Welch, M.; Salmond, G. P. C.; Spring, D. R. Combating Multidrug-Resistant Bacteria: Current Strategies for the Discovery of Novel Antibacterials. *Angew. Chemie Int. Ed.* **2013**, *52*, 10706–10733.
- (21) Madsen, J. S.; Burmølle, M.; Hansen, L. H.; Sørensen, S. J. The Interconnection Between Biofilm Formation and Horizontal Gene Transfer. *FEMS Immunol. Med. Microbiol.* **2012**, *65*, 183–195.
- (22) Maia, M. F.; Moore, S. J. Plant-Based Insect Repellents: A Review of Their Efficacy, Development, and Testing. *Malar. J.* **2011**, *10*, S11–S11.
- (23) Freire Rocha Caldas, G.; Araújo, A. V.; Albuquerque, G. S.; Silva-Neto, J. da C.; Costa-Silva, J. H.; de Menezes, I. R. A.; Leite, A. C. L.; da Costa, J. G. M.; Wanderley, A. G. Curcumin and Diabetes: A Systematic Review. *Evidence-Based Complement. Altern. Med.* **2013**, *2013*, 1–11.
- (24) Nazzaro, F.; Fratianni, F.; De Martino, L.; Coppola, R.; De Feo, V. Effect of Essential Oils on Pathogenic Bacteria. *Pharmaceuticals* **2013**, *6*, 1451–1474.

- (25) Chen, H.; Davidson, P. M.; Zhong, Q. Impacts of Sample Preparation Methods on Solubility and Antilisterial Characteristics of Essential Oil Components in Milk. *Appl. Environ. Microbiol.* **2013**, *80*, 907–916.
- (26) Chang, Y.; McLandsborough, L.; McClements, D. J. Physicochemical Properties and Antimicrobial Efficacy of Carvacrol Nanoemulsions Formed by Spontaneous Emulsification. *J. Agric. Food Chem.* **2013**, *61*, 8906–8913.
- (27) Anwer, M. K.; Jamil, S.; Ibnouf, E. O.; Shakeel, F. Enhanced Antibacterial Effects of Clove Essential Oil by Nanoemulsion. *J. Oleo Sci.* **2014**, *63*, 347–354.
- (28) Duncan, B.; Li, X.; Landis, R. F.; Kim, S. T.; Gupta, A.; Wang, L.-S. S.; Ramanathan, R.; Tang, R.; Boerth, J. A.; Rotello, V. M. Nanoparticle-Stabilized Capsules for the Treatment of Bacterial Biofilms. *ACS Nano* **2015**, *9*, 7775–7782.
- (29) Donsì, F.; Annunziata, M.; Vincenzi, M.; Ferrari, G. Design of Nanoemulsion-Based Delivery Systems of Natural Antimicrobials: Effect of the Emulsifier. *J. Biotechnol.* **2012**, *159*, 342–350.
- (30) Landis, R. F.; Gupta, A.; Lee, Y.-W.; Wang, L.-S.; Golba, B.; Couillaud, B.; Ridolfo, R.; Das, R.; Rotello, V. M. Cross-Linked Polymer-Stabilized Nanocomposites for the Treatment of Bacterial Biofilms. *ACS Nano* **2017**, *11*, 946–952.
- (31) Chandra Sekhara Rao, G.; Satish Kumar, M.; Mathivanan, N.; Bhanoji Rao, M. E. The Use of Polymer-Based Electrospun Nanofibers Containing Amorphous Drug Dispersions for the Delivery of Poorly Water-Soluble Pharmaceuticals. *Pharmazie* **2004**, *59*, 5–9.
- (32) Kamaly, N.; Yameen, B.; Wu, J.; Farokhzad, O. C. Degradable Controlled-Release Polymers and Polymeric Nanoparticles: Mechanisms of Controlling Drug Release. *Chem. Rev.* **2016**, *116*, 2602–2663.
- (33) Simone, E. A.; Dziubla, T. D.; Muzykantov, V. R.; Eric A Simone, Thomas D Dziubla, V. R. M. Polymeric Carriers: Role of Geometry in Drug Delivery. *Expert Opin. Drug Deliv.* **2008**, *5*, 1283–1300.
- (34) Cheng, R.; Feng, F.; Meng, F.; Deng, C.; Feijen, J.; Zhong, Z. Glutathione-Responsive Nano-Vehicles as a Promising Platform for Targeted Intracellular Drug and Gene Delivery. *J. Control. Release* **2011**, *152*, 2–12.
- (35) Sanson, C.; Schatz, C.; Le Meins, J.-F.; Brûlet, A.; Soum, A.; Lecommandoux, S. Biocompatible and Biodegradable Poly(trimethylene carbonate)-b-Poly(L-glutamic acid) Polymersomes: Size Control and Stability. *Langmuir* **2010**, *26*, 2751–2760.
- (36) Yang, J.; Liu, F.; Yang, L.; Li, S. Hydrolytic and Enzymatic Degradation of Poly(trimethylene carbonate-co-D,L-lactide) Random Copolymers With Shape Memory Behavior. *Eur. Polym. J.* **2010**, *46*, 783–791.

- (37) Pounder, R. J.; Stanford, M. J.; Brooks, P.; Richards, S. P.; Dove, A. P. Metal Free Thiol-Maleimide 'Click' Reaction as a Mild Functionalisation Strategy for Degradable Polymers. *Chem. Commun.* **2008**, *0*, 5158–5160.
- (38) Sukegawa, T.; Masuko, I.; Oyaizu, K.; Nishide, H. Expanding the Dimensionality of Polymers Populated with Organic Robust Radicals Toward Flow Cell Application: Synthesis of TEMPO-Crowded Bottlebrush Polymers using Anionic Polymerization and ROMP. *Macromolecules* **2014**, *47*, 8611–8617.
- (39) Jovanka, L.; Ivana, Č.; Goran, T.; Sava, P.; Slavica, S.; Tamara, C.-G.; Ljiljana, K. In Vitro Antibacterial Activity of Essential Oils from Plant Family Lamiaceae. *Rom. Biotechnol. Lett.* **2011**, *16*, 6034–6041.
- (40) Kataoka, K.; Harada, A.; Nagasaki, Y. Block Copolymer Micelles for Drug Delivery: Design, Characterization and Biological Significance. *Adv. Drug Deliv. Rev.* **2001**, *47*, 113–131.
- (41) Gèze, A.; Putaux, J.-L.; Choisnard, L.; Jehan, P.; Wouessidjewe, D. Long Term Shelf Stability of Amphiphilic B-Cyclodextrin Nanospheres Suspensions Monitored by Dynamic Light Scattering and Cyro-Transmission Electron Microscopy. *J. Microencapsul.* **2004**, *21*, 607–613.
- (42) Flemming, H.-C.; Wingender, J.; Szewzyk, U.; Steinberg, P.; Rice, S. A.; Kjelleberg, S. Biofilms: An Emergent Form of Bacterial Life. *Nat. Rev. Microbiol.* **2016**, *14*, 563–575.
- (43) Richards, M. J.; Edwards, J. R.; Culver, D. H.; Gaynes, R. P. Nosocomial Infections in Combined Medical-Surgical Intensive Care Units in the United States. *Infect. Control Hosp. Epidemiol.* **2000**, *21*, 510–515.
- (44) Jarvis, W. R.; Martone, W. J. Predominant Pathogens in Hospital Infections. *J. Antimicrob. Chemother.* **1992**, *29*, 19–24.
- (45) Serra, R.; Grande, R.; Butrico, L.; Rossi, A.; Settimio, U. F.; Caroleo, B.; Amato, B.; Gallelli, L.; de Franciscis, S. Chronic Wound Infections: The Role of *Pseudomonas aeruginosa* and *Staphylococcus aureus*. *Expert Rev. Anti. Infect. Ther.* **2015**, *13*, 605–613.
- (46) Fazli, M.; Bjarnsholt, T.; Kirketerp-Møller, K.; Jørgensen, B.; Andersen, A. S.; Krogfelt, K. A.; Givskov, M.; Tolker-Nielsen, T. Nonrandom Distribution of *Pseudomonas aeruginosa* and *Staphylococcus aureus* in Chronic Wounds. *J. Clin. Microbiol.* **2009**, *47*, 4084–4089.
- (47) Sun, B. K.; Siprashvili, Z.; Khavari, P. A. Advances in Skin Grafting and Treatment of Cutaneous Wounds. *Science* **2014**, *346*, 941–945.
- (48) Ling, L. L.; Schneider, T.; Peoples, A. J.; Spoering, A. L.; Engels, I.; Conlon, B. P.; Mueller, A.; Schaberle, T. F.; Hughes, D. E.; Epstein, S.; Jones, M.; Lazarides, L.; Steadman, V. A.; Cohen, D. R.; Felix, C. R.; Fetterman, K. A.; Millett, W. P.; Nitti, A. G.;

(49) Zullo, A. M.; Chen, C.; Lewis, K. A New Antibiotic Kills Pathogens Without Detectable Resistance. *Nature* **2015**, *517*, 455–459.

CHAPTER 5

NATURE-DERIVED CROSSLINKED NANOCOMPOSITES FOR A SUSTAINABLY-RELEVANT TREATMENT OF MULTIDRUG-RESISTANT BIOFILMS

5.1. Introduction

Overuse of antibiotic regimens in biomedical and agriculture industries has directly contributed to the exponential growth of multidrug-resistant (MDR) pathogenic bacteria and their associated infections found in hospitals or on farms.¹ Current death toll predictions indicate that by 2050, 10 million lives will be lost each year, along with incurring costs exceeding \$100 trillion.² This issue is only further exacerbated by serious chronic infections caused by bacterial biofilms, nearly untreatable by long-term antibiotic therapies coupled with dead tissue debridement tactics.³ As the clinical antibiotic pipelines continue to ‘dry-up’, an international push to discover sustainable methods to combat MDR infections has taken priority.⁴

A variety of antibiotic alternatives have emerged or are being reinvestigated for their therapeutic relevance towards MDR. Notably, host-guest peptides,⁵ bacteriophages,⁶ and antibodies⁷ are three main therapeutic avenues that have shown promise either *in vitro* or in a clinical setting. These methods offer key advantages over antibiotic counterparts, including mammalian toxicity reduction,⁸ high specificity,⁹ and can be potentially administered where accumulated resistance is less likely to happen.¹⁰ Furthermore, host-

guest peptides and antibodies are already in clinical trials and have shown good promise, delivering the possibility of antibiotic alternatives for upcoming decades.¹¹ However, the benefits of these therapeutic methods are still out-weighted by their drawbacks. In the case of host-guest peptides, the adverse effects of red blood cell lysis (hemolysis) remain with almost all peptide analogs.¹² Regarding bacteriophages, disease models in animals and humans are low compared to the other two methods and more experimental insight is required to better understand their mechanism and long-term effects.¹³ While antibodies offer a low toxicity avenue, their effectiveness has been better demonstrated in high-risk patients and has had less success as a therapeutic intervention.¹⁴ Finally, all three of these methods suffer from poor scale-up logistics, a process most critical if global adoption is to be considered. It is clear that whichever strategy is chosen to replace antibiotics, their ability to be produced and administered must be sustainable and environmentally conscience.

Another promising alternative that has emerged in recent decades is the encapsulation of essential oils in nano-carrier delivery vehicles.¹⁵ Essential oils offer high biocompatibility,¹⁶ significantly lower cost than other antimicrobials, and has been demonstrated *in vitro* to eliminate MDR pathogens, even in a biofilm setting or coculture wound models.¹⁷ Furthermore, a variety of crosslinkable nano-carriers have been developed to stabilize essential oils in water, dramatically enhancing their bioactive properties and stability.¹⁸ Although great efforts have been made to translate these research materials into commercially viable products, the carrier's stabilizers are made from poly(oxanorbornene) synthetic polymers using 'heavy-metal' ruthenium catalysts. Residual ruthenium leftover from polymerization may raise concerns about their long-term

genotoxicity to mammalian hosts.¹⁹ Therefore, if low-cost natural stabilizers could be biocompatibly crosslinked at an essential oil-water interface, in theory, highly robust and sustainable essential oil carriers could be developed to address the rising dangers of MDR on a global scale consideration.

Inspired by a recently developed Corneal Collagen Crosslinking (CXL)²⁰ technique using riboflavin and UV-A light, we hypothesized that hydrolyzed collagen fragments (Gelatin) could also be intermolecularly crosslinked in a similar fashion demonstrated in CXL, but at an oil-water interface. Herein, we report the generation, characterization, and biological activities of crosslinked gelatin-stabilized nanocomposites containing the highly antimicrobial oil carvacrol (GEL-XC). We demonstrate through dynamic light scattering (DLS), GEL-XCs could retain an average size of 300 nm regardless of their production on a microliter or liter-scale, with slight modifications to the emulsification procedure. Additionally, GEL-XCs were shown to adopt a composite morphology under confocal microscopy and retained their size and stability during a two-year shelf-life test. Furthermore, GEL-XCs were as equally capable of eliminating Gram-Negative and Gram-Positive MDR pathogens, even in a biofilm setting when compared to previous synthetic essential oil composites. *Finally, future work continues to determine GEL-XCs effectiveness in vivo as a wound healing agent in mice and will be reported in due course.* Taken together, the bio-inspired oil-in-water crosslinking presented here may address the needs for a sustainably-relevant antibiotic alternative with hopes future platforms will be further developed around this crosslinking strategy with applications in biomedical, agriculture, food, surface, and textile industries.

5.2. Results

5.2.1 Generation of GEL-XCs

Generation of gelatin-stabilized nanocomposites was accomplished through emulsifying carvacrol oil containing partially dissolved and suspended riboflavin and an aqueous solution containing 3 mg/ml of gelatin type B (MW ~20,000 g/mol), followed by irradiation with 365 nm light (Figure 5.1a). Briefly, 3 μ L of carvacrol loaded with 0.1 wt% of riboflavin was amalgamated for 60 seconds with a 497 μ L solution of gelatin type B (pre-warmed to 37°C) in a 600 μ L Eppendorf tube. Afterwards, Eppendorf tubes containing the oil-templated gelatin emulsion was subjected to a handheld 365nm UV lamp for 20 minutes. After irradiation, the emulsion solution became more apparently viscous and opaque. Notably, emulsion controls including the absence of either gelatin, riboflavin, or UV light did not generate stable emulsions and fell apart one day after emulsification (in the case of no gelatin present, no emulsion was observed). The size of GEL-XCs was characterized through dynamic light scattering (DLS). The DLS results obtained showed narrow PDI as gelatin type B's refractive index is well understood and agreeance in Intensity, Number, and Volume size was observed with an average size of 300 nm (Figure 5.1b). Figure 5.1c shows the proposed mechanism of crosslinking and will be discussed later.²¹ Notably, GEL-XCs demonstrated high shelf-life, maintaining its inherent size even after on the benchtop for 2 years.

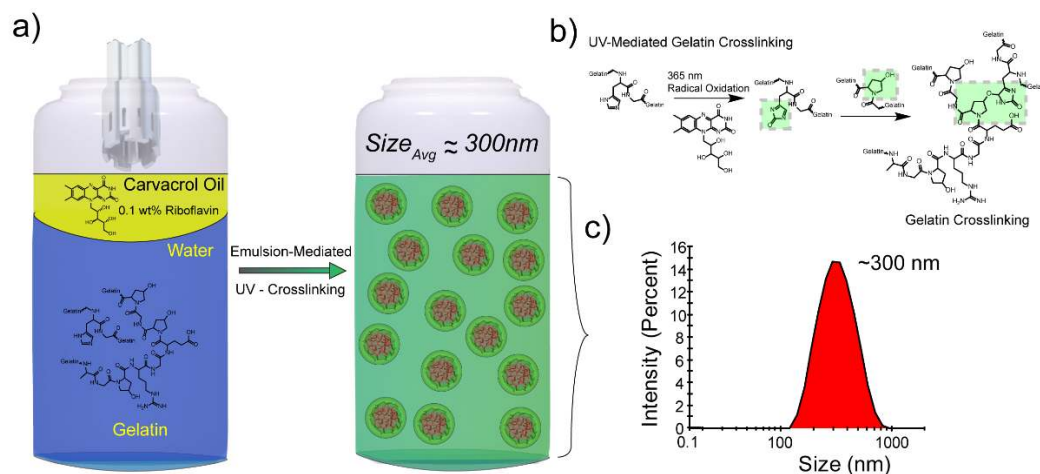


Figure 5.1. a) Schematic depiction of GEL-XCs generation. b) Proposed mechanism of inter-gelatin crosslinking mediated by photooxidation. c) Dynamic light Scattering of GEL-XCs in 150mM PBS.

5.2.2 Morphology of GEL-XCs

After GEL-XCs formulation was optimized, its morphology was observed under confocal microscopy by generating micron-sized emulsion analogs. Given that gelatin fits similar size domains as compared to previously generated synthetic norbornene polymer stabilizers, it is hypothesized that the morphology for micron or nano-sized emulsions will be largely the same. First, gelatin was labelled with a blue fluorescent coumarin dye through its residual lysine residues that take no part in the crosslinking process. Next, green fluorescent DiO dye was loaded within the oil to clearly juxtapose the oil core from the gelatin stabilizer. Micron-sized emulsions were viewed under confocal and analyzed with Image J software (Figure 5.2). The results indicate that gelatin can be observed to co-localized with the oil core in addition to localizing at the oil-water interface and beyond. The reason for this observation can be hypothesized as the following. Gelatin's native structure contains a large number of proline and hydroxyproline residues, imparting β -sheet structures.²² Additionally, gelatin contains numerous hydrophobic residues that carvacrol oil can embed within. Crosslinked gelatin would in theory be a

more hydrophobic material given the number of hydrophobic residues outweigh its polar residue domains. Explanation of gelatin present beyond the oil can be explained during its formulation process. Although riboflavin has some solubility in carvacrol, it is not completely soluble. Therefore, during UV irradiation, riboflavin leaks into the water and enables crosslinking units beyond the oil. Residual gelatin still floating outside of the emulsions may attach later on. This is further supported in the confocal as entire emulsions may attach later on. This is further supported in the confocal as entire emulsions can be crosslinked and are linked through these exterior gelatin appendages. No evidence of inter-emulsion crosslinking can be observed under DLS when nano-sized emulsions are formed, suggesting that this type of crosslinking occurs during emulsification of a larger volume oil. Taken together, GEL-XCs largely adopt a composite morphology with hydrogel-like appendages, a particularly interesting result. Future studies to generate additional nano and micron-sized structures are underway.

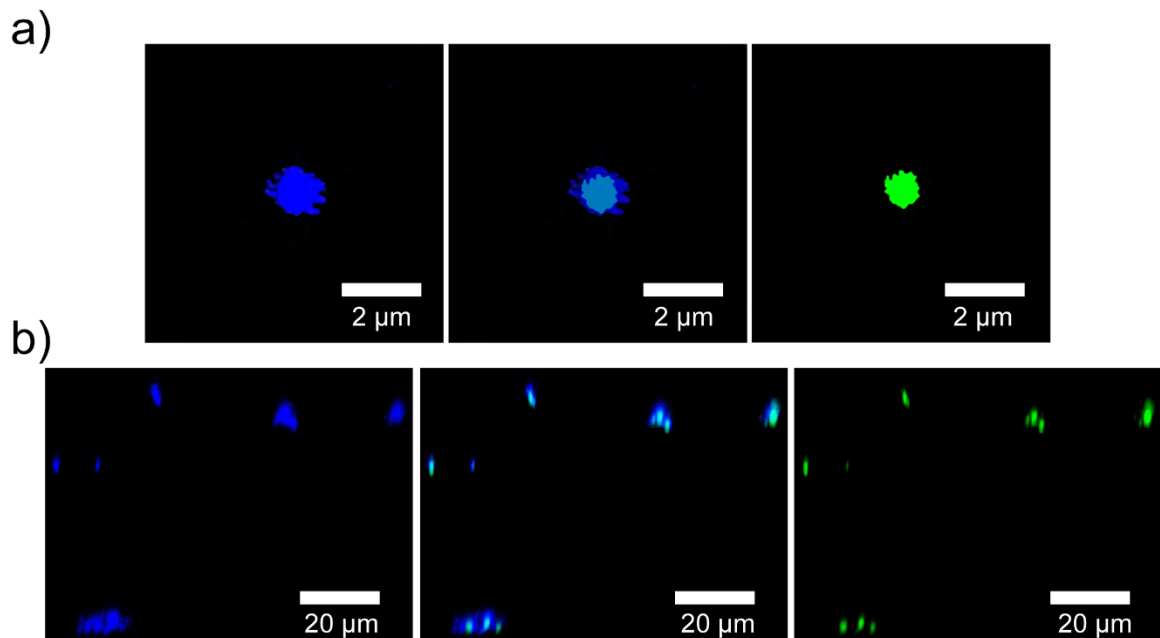


Figure 5.2. a) Confocal of isolated GEL-XCs emulsion indicating a composite morphology, in addition to hydrogel-like appendages found external to the oil-water

interface. b) Confocal z-stack images at a 15° from x-axis vector demonstrating inter-Gel-XC crosslinking via hydrogel-like appendages. Scale bars are 2 and 20 μm, respectively.

5.2.3 Chemical Identification of GEL-XCs

After characterization of GEL-XCs physical and morphological attributes, its chemical properties were explored, particularly its crosslinking mechanism route. As shown in Figure 5.1, prior literature indicates that UVA irradiation of riboflavin generates singlet oxygen, oxidizing imidazole units on histidine residues on collagen (Or in this case, gelatin) to imidazolones.²³ Imidazolones are susceptible to nucleophilic attack from hydroxy moieties found within gelatin (e.g, hydroxyproline, tyrosine, and serine). We hypothesize that gelatin's crosslinking occurs through this mechanism with an additional step. Given the relatively high concentration of carvacrol at the sites of crosslinking, its phenol unit may also participate in the reaction in a similar fashion as gelatin's tyrosine residues. Furthermore, this result would give additional support to GEL-XCs morphology as conjugated carvacrol onto gelatin would impart further hydrophobic domains and interact more with the oil core. We used attenuated total reflectance Fourier transform infrared spectroscopy to monitor both inter-gelatin crosslinking and carvacrol-gelatin conjugation (Figure 5.3). Figure 5.3a shows the ATR spectra for carvacrol with its indicative peaks, including a phenol stretch at 3337 cm⁻¹, aliphatic C-H stretches at 2959, 2927, and 2860 cm⁻¹, alkane bending at 1457 and 1419 cm⁻¹, and C-O stretch at 1250 cm⁻¹. Next, three individual reactions were setup to monitor changes in gelatin's IR frequencies. The first reaction (Figure 5.3b, positive control) mixes riboflavin and gelatin in the presence of UVA light for 30 minutes, the second (Figure 5.3c, negative control) performs the same reaction however in the presence of sodium azide, a well-known quencher of singlet oxygen. The final experiment (Figure 5.3d) is generation of GEL-

XCs. All three reactions underwent dialysis and were lyophilized to remove by-product noise (riboflavin, residual carvacrol oil, sodium azide, and water). The results indicate that inter-gelatin crosslinking occurs (aliphatic ether formation: 1118 cm^{-1} , aliphatic-aromatic ether formation: 1033 cm^{-1}) in the positive control, however these signatures are completely absent in the negative control.²⁴ Interestingly, GEL-XCs IR spectra not only shows inter-gelatin crosslinking signatures (Stronger in frequency due to gelatin concentration at the oil-water interface), but signatures from gelatin-carvacrol conjugation can also be seen (broadening of 1033 cm^{-1} and additional aromatic ether signature at 1242 cm^{-1}). Furthermore, obvious carvacrol conjugation can be seen due to appearance of sp^3 C-H stretches at 2957 cm^{-1} and is nearly identical to the carvacrol oil IR. Taken together with the observations from confocal microscopy, carvacrol serves to not only enable inter-gelatin crosslinking through oil-templating, but conjugates onto gelatin imparting more hydrophobicity and allow gelatin to better transverse the oil core.

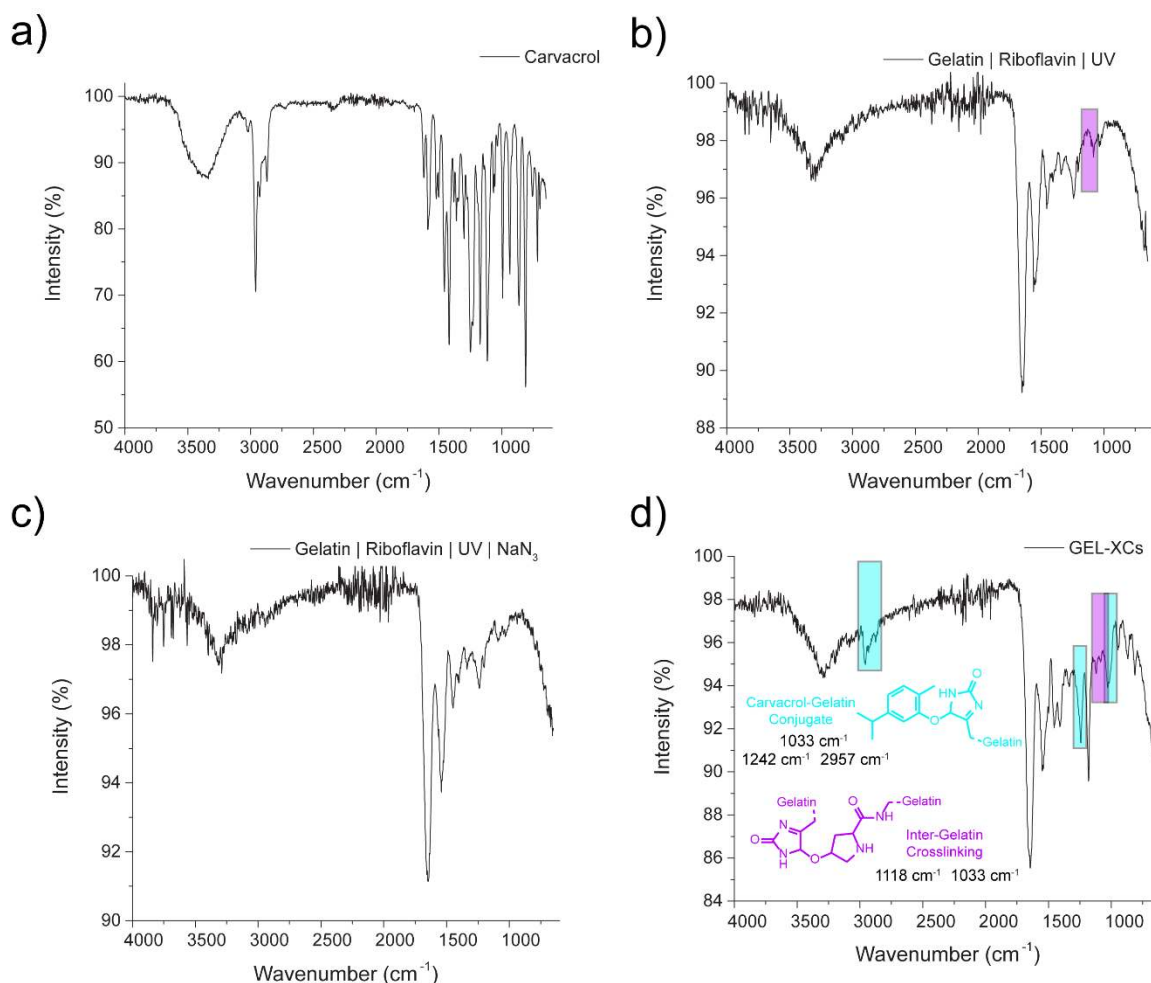


Figure 5.3. ATR-FTIR spectra. a) carvacrol oil, b) inter-gelatin crosslinking, c) negative control, d) GEL-XCs. Observed crosslinking/conjugation signatures and their proposed structures are highlighted in purple and teal respectively.

5.2.4 Stability of GEL-XCs

After determining GEL-XCs physical and chemical composition, we next explored their stability in a complex biological environment. A successful therapeutic must maintain their activities when translating from *in vitro* to *in vivo*.²⁵ One challenge with nano-assemblies is loss of their activity *in vivo* due to protein adsorption, causing aggregation or precipitation.²⁶ We explored GEL-XCs stability in 10% fetal bovine serum (FBS) (Figure 5.4) using DLS and compared its size to the standard size found in 150

mM phosphate buffer saline (PBS). After incubating GEL-XCs in 10% FBS for one hour, a size increase of ~30 nm was observed, likely due to serum protein adsorption. Prior literature indicates that carvacrol can induce protein unfolding of BSA and it is this process that may occur on the surface of GEL-XCs.²⁷ Compared to our previous synthetic analogs, GEL-XCs are less stable, however gelatin is a better suited stabilizer for its high biocompatibility and may even become sequestered during wound healing processes.²⁸ Future experiments are needed to better ascertain this hypothesis.

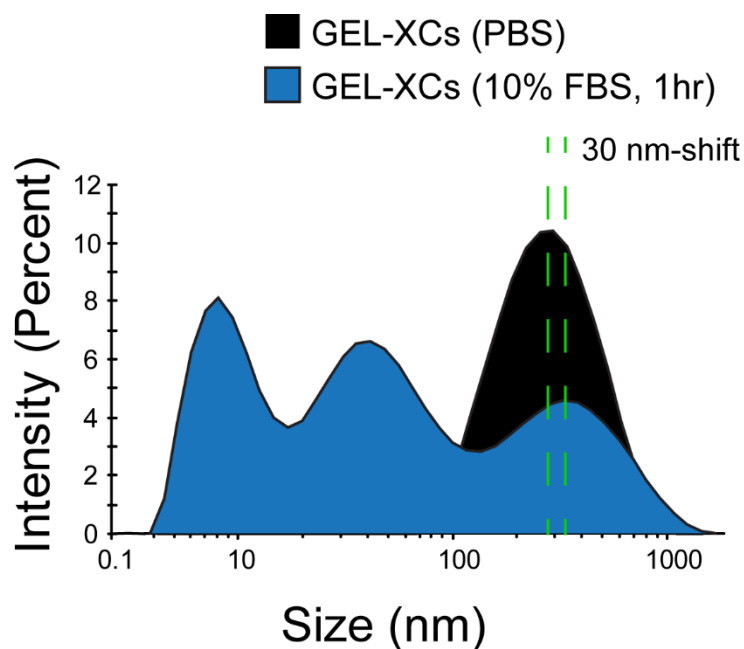


Figure 5.4. GEL-XC Stability. Stability of GEL-XCs in high ionic strength (black) for 24 hours or similarly with a 10% addition of fetal bovine serum (blue) for one hour.

5.2.5 Biological Activity of GEL-XCs

Next, we monitored GEL-XCs activity towards pathogenic biofilms, generated from Gram-Negative and Gram-Positive bacteria (Figure 5.5). Four bacterial strains of clinical isolates, *Staphylococcus aureus* (CD-489, a methicillin-resistant strain), *Pseudomonas aeruginosa* (CD-1006), *Escherichia coli* (CD-2), and *Enterobacter cloacae*

(*E. cloacae*, CD-1412) complex were chosen to be tested as their associated infections are becoming more challenging to eliminate with traditional antibiotic therapy. GEL-XCs, along with its individual components at similar concentrations as controls were incubated with 1-day-old biofilms for three hours, washed, and their viabilities analyzed. Individual components, gelatin and carvacrol, showed almost no antimicrobial effect. However, when combined into the GEL-XCs nano-assembly, impressive killing effect was observed, performing similarly to previous synthetic phytochemical assemblies. Taken together, natural components that previously showed no antimicrobial activity can be assembled through nanotechnology insights to generate potent broad-spectrum antimicrobials and eliminate difficult to treat infections found in hospital settings.

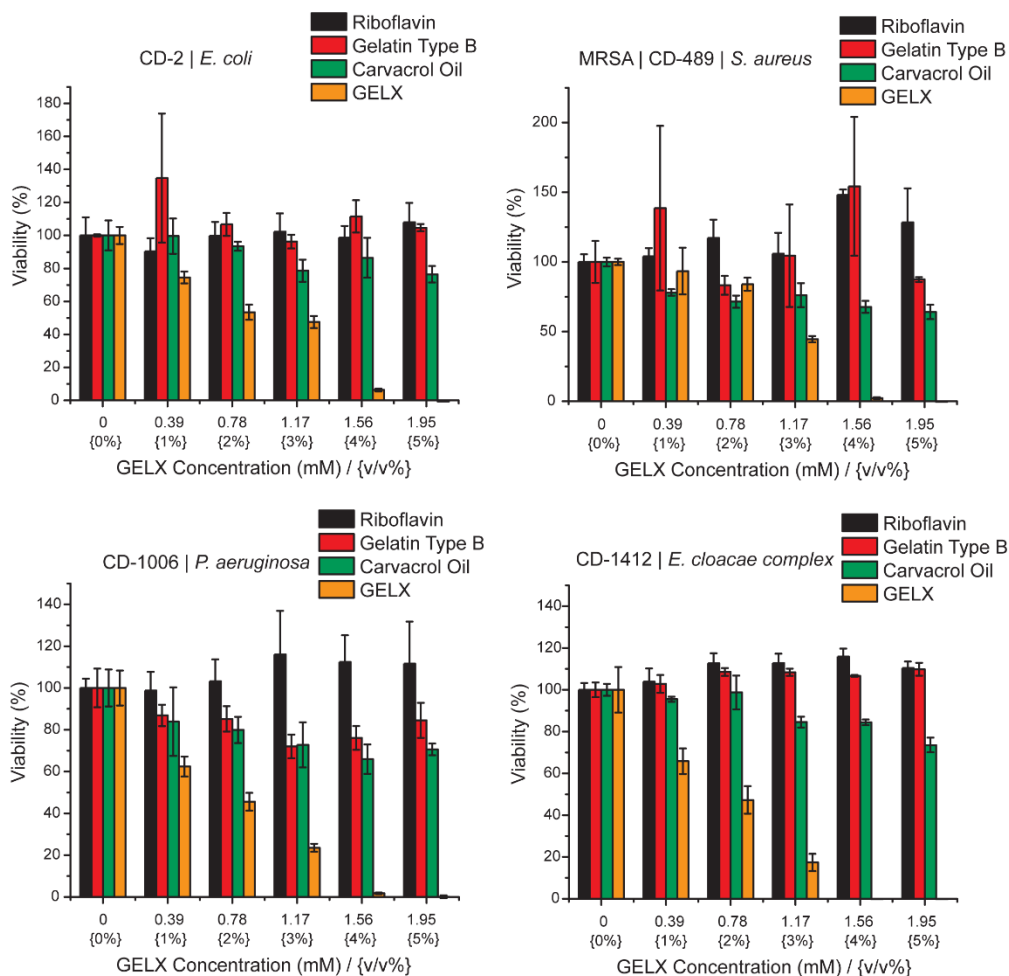


Figure 5.5. Activity of GEL-XCs against pathogenic biofilms. Individual components of GEL-XCs show marginal or no antimicrobial effect. Combination of these components into GEL-XCs incubated at various concentrations penetrate and eliminate pathogenic bacterium enclosed within. Results are an average of three experiments. Error bars are representative of their standard deviation.

5.2.6 Scalability of GEL-XCs

Fighting MDR pathogens, from a therapeutic standpoint, must take into consideration sustainability. Given the dangers of MDR, not only should future therapies eliminate these pathogens without accumulating resistance but be manufactured from easily accessible materials. Furthermore, these materials should not be a large burden from a financial and economic view. GEL-XCs shows great promise to satisfy the

conditions of sustainability as gelatin, riboflavin, and carvacrol oil are some of the most easily accessed materials and are well-documented as food-grade ingredients. Therefore, GEL-XCs can be considered a nutraceutical platform that could be implemented beyond biomedical and integrated into agriculture, food, and textile industries. However, these industries require a significantly greater amounts of material than biomedical and GEL-XCs may easily satisfy this need. Emulsification processes are well-documented to scale linearly, even under large-scale manufacturing practices. Therefore, we hypothesized that as long as each parameter during the emulsification/crosslinking process is scaled appropriately, GEL-XCs could be produced in large amounts. Using a two-liter scale homogenizer and a proprietary UVA apparatus, Figure 5.6 shows the successful result of scaling over 4,000 times our original 500 μ L formulation. Current testing is ongoing, however the stability of large-scale GEL-XCs is remarkably the same to our research scale (currently, one year). GEL-XCs has been preliminary shown to satisfy the needs of scalability for industries that have greater material requirements.



Figure 5.6. Image of 2 L scale GEL-XC production. Emulsification process was found to scale linearly between 500 μ L – 2 L.

5.3. Conclusions

In conclusion, we demonstrate here nature inspired/derived crosslinked gelatin-stabilized nanocomposites demonstrating similar physical, morphological, and bioactivities to previous synthetic phytochemical emulsions. These natural composites were found to have great shelf-life and could be easily scaled to industrial standards at a fraction of the cost of prior synthetic stabilizers. Furthermore, these phytochemical vehicles were found to have similar antimicrobial capabilities of previous analogs and were found to have broad-spectrum potency towards pre-formed biofilms, even biofilms formed from MDR species. Interestingly, the use of gelatin as a stabilizer generates unique hydrogel-like appendages external to the oil core, enabling the possibility of inter-particle crosslinking, potentially opening new antimicrobial applications beyond a 3D aqueous matrix. Most critically, the work presented within is, to the best of our knowledge, the first demonstration at generating sustainably relevant phytochemical antimicrobials to combat the impending dangers of MDR in biomedical, agriculture, food, and textile industries. *This PhD candidate looks forward to continuing the translation of these nano-assemblies from the research setting into the hands of commercial end-users.*

5.4. Experimental Protocols

5.4.1 Materials and Methods

All reagents and materials were purchased from Fisher Scientific and used as received. Dulbecco's Modified Eagle's Medium (DMEM) (DMEM; ATCC 30-2002) and fetal bovine serum (Fisher Scientific, SH3007103) were used in cell culture.

5.4.2 Preparation of GEL-XCs

Stock nanocomposite solutions were prepared in 0.6 ml Eppendorf tubes. To prepare the stock GEL-XC emulsions, 3 μ L of carvacrol oil (containing 0.1 wt% riboflavin) was added to 497 μ L of Milli-Q H₂O containing 3mg/ml of gelatin and emulsified in an amalgamator for 50 s. Afterwards, tubes were subjected to 365 nm light from a handheld UV lamp for 20 minutes. The emulsions were allowed to rest overnight prior to use.

5.4.3 Biofilm Formation

Bacteria were inoculated in LB broth at 37°C until stationary phase. The cultures were then harvested by centrifugation and washed with 0.85% sodium chloride solution three times. Concentrations of resuspended bacterial solution were determined by optical density measured at 600 nm. Seeding solutions were then made in M9 to reach OD₆₀₀ of 0.1. 100 μ L of the seeding solutions were added to each well of the microplate. M9 medium without bacteria was used as a negative control. The plates were covered and incubated at room temperature under static conditions for a desired period. Planktonic bacteria were removed by washing with PB saline three times.

Varied v/v % of GEL-XCs, made in M9 medium, were incubated with the biofilms for 3 h. Biofilms were washed with phosphate buffer saline (PBS) three times and viability was determined using an Alamar Blue assay. M9 medium without bacteria was used as a negative control.

5.5. References

- (1) Tam, V. H.; Rogers, C. A.; Chang, K.-T.; Weston, J. S.; Caeiro, J.-P.; Garey, K. W. Impact of Multidrug-Resistant *Pseudomonas aeruginosa* Bacteremia on Patient Outcomes. *Antimicrob. Agents Chemother.* **2010**, *54*, 3717–3722.
- (2) Tackling Drug-Resistant Infections Globally: Final Report and Recommendations. (2016, May 19). Retrieved November 05, 2016, from <https://amr-review.org/Publications>.
- (3) Wu, H.; Moser, C.; Wang, H.; Høiby, N.; Song, Z.-J.; Hoiby, N.; Song, Z.-J. Strategies for Combating Bacterial Biofilm Infections. *Int. J. Oral Sci.* **2014**, *7*, 1–7.
- (4) Lynch, A. S.; Robertson, G. T. Bacterial and Fungal Biofilm Infections. *Annu. Rev. Med.* **2008**, *59*, 415-428.
- (5) Dennison, S. R.; Harris, F.; Mura, M.; Morton, L. H. G.; Zvelindovsky, A.; Phoenix, D. A. A Novel Form of Bacterial Resistance to the Action of Eukaryotic Host Defense Peptides, the Use of a Lipid Receptor. *Biochemistry*, **2013**, *52*, 6021-6029.
- (6) Wittebole, X.; De Roock, S.; Opal, S. M. A Historical Overview of Bacteriophage Therapy as an Alternative to Antibiotics for the Treatment of Bacterial Pathogens. *Virulence* **2014**, *5*, 226-235.
- (7) Babb, R.; Pirofski, L. -A. Help is on the Way: Monoclonal Antibody Therapy for Multi-Drug Resistant Bacteria. *Virulence* **2017**, *8*, 1055-1058.
- (8) DiGiandomenico, A.; Sellman, B. R. Antibacterial Monoclonal Antibodies: The Next Generation? *Curr. Opin. Microbiol.* **2015**, *27*, 78-85.
- (9) Reichert, J. M. Antibodies to Watch in 2015. *MAbs* **2015**, *7*, 1-8.
- (10) Mishra, C.; Reiling, S.; Zarena, D.; Wang, G. Host Defense Antimicrobial Peptides as Antibiotics: Design and Application Strategies. *Curr. Opin. Chem. Biol.* **2017**, *38*, 87-96.
- (11) Seo, M. -D.; Won, H. -S.; Kim, J. -H.; Mishig-Ochir, T.; Lee, B. -J. Antimicrobial Peptides for Therapeutic Applications: A Review. *Molecules* **2012**, *17*, 12276-12286.
- (12) Furci, L.; Baldan, R.; Bianchini, V.; et al. New Role for Human Alpha-Defensin 5 in the Fight Against Hypervirulent *Clostridium difficile* Strains. *Infect. Immun.* **2015**, *83*, 986-995.
- (13) Hodyra-Stefaniak, K.; Miernikiewicz, P.; Drapala, J.; et al. Mammalian Host-Versus-Phage Immune Response Determines Phage Fate *in vivo*. *Sci. Rep.* **2015**, *5*, 14802.

- (14) Buchwald, U. K.; Pirofski, L. Immune Therapy for Infectious Diseases at the Dawn of the 21st Century: The Past, Present, and Future Role of Antibody Therapy, Therapeutic Vaccination, and Biological Response Modifiers. *Curr. Pharm. Des.* **2003**, *9*, 945-968.
- (15) Chang, Y.; McLandsborough, L.; McClements, D. J. Physicochemical Properties and Antimicrobial Efficacy of Carvacrol Nanoemulsions Formed by Spontaneous Emulsification. *J. Agric. Food Chem.* **2013**, *61*, 8906–8913.
- (16) Freire Rocha Caldas, G.; Araujo, A. V.; Albuquerque, G. S.; Silva-Neto Jda, C.; Costa-Silva, J. H.; de Menezes, I. R.; Leite, A. C.; da Costa, J. G.; Wanderley, A. G. Repeated-doses Toxicity Study of the Essential Oil of *Hyptis Martiusii* Benth. (Lamiaceae) in Swiss Mice. *Evid. Based Complement. Alternat. Med.* **2013**, *2013*, 856168.
- (17) Landis, R. F.; Gupta, A.; Lee, Y. -W.; et al. Cross-Linked Polymer-Stabilized Nanocomposites for the Treatment of Bacterial Biofilms. *ACS Nano* **2017**, *11*, 946-952.
- (18) Landis, R. F.; Li, C.-H.; Gupta, A.; Lee, Y. -W.; Yazdani, M.; et al. Biodegradable Nanocomposite Antimicrobials for the Eradication of Multidrug-Resistant Bacterial Biofilms Without Accumulated Resistance. *J. Am. Chem. Soc.* **2018**, *140*, 6176-6182.
- (19) De Grandis, R. A.; Resende, F. A.; da Silva, M. M.; Pavan, F. R.; Batista, A. A.; Varanda, E. A. In Vitro Evaluation of the Cyto-Genotoxic Potential of Ruthenium(II) SCAR Complexes: A Promising Class of Antituberculosis Agents. *Mutat. Res. Genet. Toxicol. Environ. Mutagen.* **2016**, *11*, 798-799.
- (20) Ashwin, P. T.; McDonnel, P. J.; Collagen Cross-Linkage: a Comprehensive Review And Directions For Future Research. *Br. J. Ophthalmol.* **2010**, *94*, 965e970.
- (21) McCall, A. S.; Kraft, S.; Edelbauser, H. F.; et al. Mechanisms of Corneal Tissue Cross-Linking In Response To Treatment With Topical Riboflavin and Long-Wavelength Ultraviolet Radiation (UVA). *Invest. Ophthalmol. Vis. Sci.* **2010**, *51*, 129-138.
- (22) Liu, D.; Nikoo, M.; Boran, G.; Zhou, P.; Regenstein, J. M. Collagen and Gelatin. *Annu. Rev. Food Sci. Technol.* **2015**, *6*, 527-557.
- (23) Au, V.; Madison, A. Effects Of Singlet Oxygen On The Extracellular Matrix Protein Collagen: Oxidation Of The Collagen Crosslink Histidinohydroxylysinonorleucine And Histidine. *Arch Biochem Biophys.* **2000**, *384*, 133-142.
- (24) Kato, Y.; Uchida, K.; Kawakishi, S. Aggregation Of Collagen Exposed To UVA In The Presence Of Riboflavin: A Plausible Role Of Tyrosine Modification. *Photochem Photobiol.* **1994**, *59*, 343-349.
- (25) Blanco, E.; Shen, H.; Ferrari, M. Principles of Nanoparticle Design for Overcoming Biological Barriers to Drug Delivery. *Nat. Biotechnol.* **2015**, *33*, 941-951.

(26) Wolfram, J.; Yang, Y.; Shen, J.; Moten, A.; Chen, C.; Shen, H.; Ferrari, M.; Zhao, Y. The Nano-plasma Interface: Implications of the Protein Corona. *Colloids Surf. B Biointerfaces* **2014**, *124*, 17-24.

(27) Veldhuizen, E. J. A.; Creutzberg, T. O.; Burt, S. A.; Haagsman, H. P. Low Temperature And Binding To Food Components Inhibit The Antibacterial Activity Of Carvacrol Against *Listeria Monocytogenes* In Steak Tartare. *J. Food. Prot.* **2007**, *70*, 2127-2132.

(28) Jang, H. J.; Kim, Y. M.; Yoo, B. Y.; Seo, Y. K. Wound-Healing Effects Of Human Dermal Components With Gelatin Dressing. *J. Biomater. Appl.* **2018**, *32*, 716-724.

CHAPTER 6

ENGINEERED POLYMER NANOPARTICLES WITH UNPRECEDENTED ANTIMICROBIAL PROPERTIES FOR THE TREATMENT OF MULTIDRUG-RESISTANT BACTERIAL AND BIOFILMS INFECTIONS

6.1. Introduction

Overusing antibiotics have created “superbugs” such as methicillin-resistant *Staphylococcus aureus* (MRSA) and particularly hard to treat Gram-negative species that pose a serious threat to global health due to treatment failure and high mortality rates.¹ While planktonic bacteria can frequently cause acute infections resulting in a threatening situation such as sepsis, the threat is further aggravated by chronic infections from biofilms.^{2,3} Biofilm-associated infections frequently occur on medical implants and indwelling devices such as catheters, prosthesis and dental implants. Biofilm infections can also occur on or around dead tissues leading to endocarditis and chronic wound infections.^{4,5} These resilient infections are challenging to treat as biofilms exhibit high resistance towards a host’s immune response and traditional antimicrobial therapies.^{6,7} Current biofilm treatment techniques require aggressive antibiotic therapy coupled with debridement of infected tissue. However, this standard treatment incurs high treatment costs and low patient compliance due to the invasive nature of the treatment.⁸ The issue is exacerbated by the increasing number of antibiotic-resistant bacterial strains, further impairing their therapeutic effectiveness.⁹

Antimicrobial peptides (AMPs) have recently emerged as an alternative to conventional antibiotic therapy, exhibiting broad spectrum activity against antibiotic-resistant bacteria.^{10,11} While some AMPs have demonstrated high therapeutic indices (selectivity towards bacterial cells) of ~900 and ~3,300¹² against planktonic bacteria, these α -helical peptides are susceptible to proteolytic degradation within the patient, greatly reducing their efficacy.^{13,14} Additionally, the cost and labor intensive requirements of sequence-specific peptides further limits their clinical practicality. As an alternative to AMPs, host-defense peptide mimicking synthetic polymers have been designed to demonstrate broad spectrum activity against microbes.^{15,16,17,18,19,20} However, high toxicity towards mammalian cells resulting in low therapeutic indices (ranging from ~1-150¹⁵⁻¹⁹) have impaired their practical applications in clinical settings. Limited studies have demonstrated synthetic polymers with promising therapeutic selectivity,^{21,22,23,24} however they have primarily focused on the treatment of planktonic microbes, overlooking their more drug-resistant biofilm counterparts. To the best of our knowledge, synthetic polymers exhibiting high biofilm efficacy while maintaining low toxicity towards mammalian cells have not been reported. Therefore, designing polymers possessing these properties will be invaluable towards developing highly effective therapeutics for bacterial-based infections.

Here, we report engineered polymers that can effectively eradicate pre-formed biofilms while maintaining a high therapeutic index against red blood cells (RBCs). We hypothesized that the therapeutic window of cationic polymers can be regulated by varying their hydrophobic properties, similar to hydrophobic residues present in the active sites of antimicrobial peptides. We synthesized a library of quaternary ammonium poly(oxanorborneneimides) possessing different degrees of hydrophobicity and screened

their antimicrobial and hemolytic activities. These polymers form 10-15 nm nanoparticles in aqueous solution, increasing their overall cationic charge and molecular mass. We observed that longer hydrophobic alkyl chains that bridge the cationic head group and polymer backbone greatly enhances toxicity against planktonic bacteria while maintaining excellent hemolytic activities towards RBCs (Therapeutic Index ~ 5000). These nanoparticles readily penetrate biofilms and eradicate pre-formed biofilms while still maintaining high therapeutic indices (~120). Polymeric NPs (PNPs) demonstrated a 6-fold log reduction in bacterial colonies, when tested in a biofilm-mammalian cell coculture model. Most notably, we observed that bacteria did not develop any resistance against PNPs even after 20 serial passages. Overall, our engineered polymeric nanoparticle platform shows strong potential as an infectious disease therapeutic and simultaneously provides a rational approach to design novel antimicrobials for sustainably combating bacterial infections.

6.2. Results

Norbornene-based amphiphilic polymers with varying quaternary nitrogen side chains have been previously demonstrated to have excellent antimicrobial properties.^{25,26,27} Additionally, well-controlled living chain-growth polymerization kinetics, ease of modulation, and scalability further highlights their value as a promising therapeutic platform.^{28,29,30} Hence, we adopted this backbone to design our cationic amphiphilic antimicrobial polymers. Distribution of hydrophobic moieties on antimicrobial macromolecules plays a pivotal role in determining their bactericidal activity.^{31,32} We generated a library of oxanorbornene polymers (Figure 6.1) with varying unbranched alkyl

chains both bridging the cationic head group and the polymer backbone itself to systematically determine the most effective antimicrobial polymer formulation. Notably, polymers containing a bridged undecyl alkyl chain spontaneously self-assemble into cationic PNPs (~13 nm) in aqueous solutions as confirmed by transmission electron microscopy (TEM, Figure 6.1d, Supporting Figure 6.7), dynamic light scattering (DLS, Figure 6.1e) and Förster resonance energy transfer (FRET) experiments (Figure 6.1.f, Structural details of dye-tagged polymer is in Supporting Figure 6.6). Dilution experiments of encapsulated Nile Red within P5 NPs indicated a critical micelle concentration of < 2.5 μM (Supporting Figure 6.11).³³

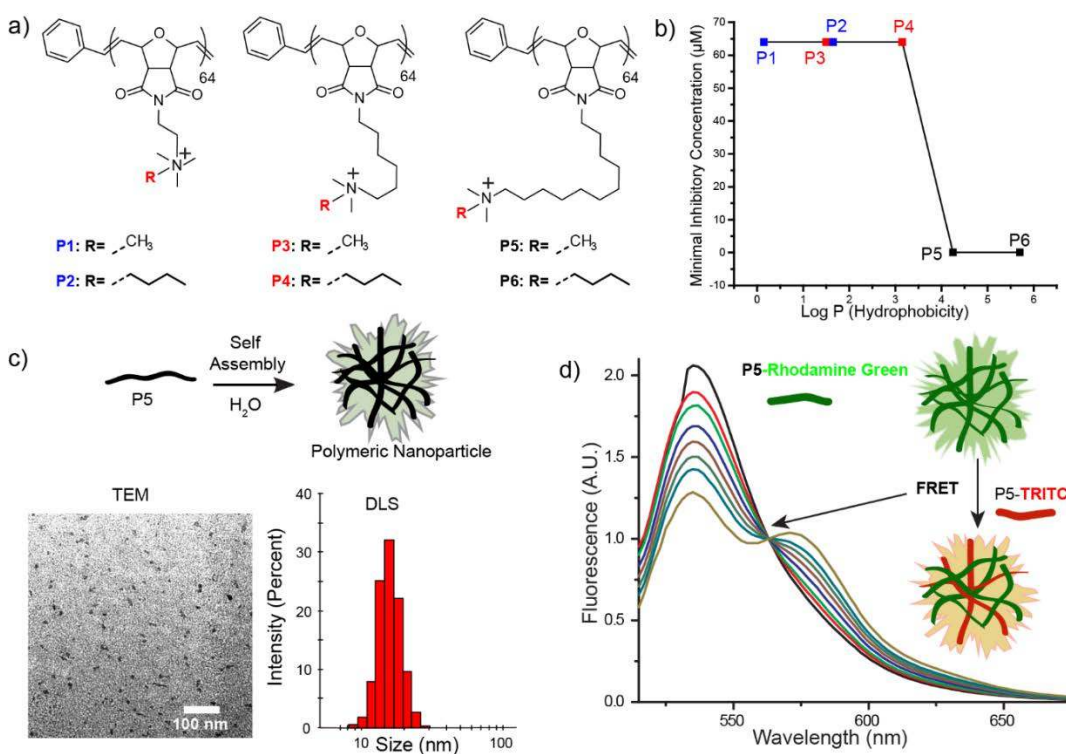


Figure 6.1. Molecular structures of a) oxanorbornene polymer derivatives. b) MIC values of polymer derivatives with different hydrophobic chain lengths. Log P represents the calculated hydrophobic values of each monomer c) Schematic representation depicting self-assembly of P5-homopolymers. Characterization of P5 NPs using TEM imaging and DLS measurement. d) Graph for FRET experiments between P5-Rhodamine Green and P5-TRITC indicating formation of polymeric NPs.

Cationic PNPs were screened for their antimicrobial activity against an uropathogenic strain of *Escherichia coli* (CD-2), using broth dilution methods to evaluate their minimal inhibitory concentrations (MICs).³⁴ We observed a 1000-fold increase in the antimicrobial activity of polymeric nanoparticles upon increasing the hydrophobicity of the alkyl chain bridging the backbone and cationic headgroup (Figure 6.1b). P1-P4 with smaller internal alkyl chain displayed MICs of 64 μM , while P5 and P6 with more hydrophobic (11 C-chain) inhibited bacteria growth at 0.064 μM . We further extended the hydrophobicity on the cationic headgroup of the polymers and monitored the change in antimicrobial activity. We determined that the MICs of PNPs did not change significantly upon increasing the hydrophobicity at the cationic headgroup (Figure 6.2a). Similar behavior has also been reported in AMPs where the location of hydrophobic residues along with overall hydrophobicity determines their antimicrobial activity.^{35,36} Subsequently, we performed hemolysis assays on human RBCs with our most potent polymer P5 and P6 and calculated their HC_{50} (concentration that causes 50% lysis of RBCs) to determine their biocompatibility.³⁷ MIC and HC_{50} values were used to calculate a therapeutic index ($\text{T.I} = \text{HC}_{50}/\text{MIC}$) of PNPs against planktonic bacteria. PNPs (P5- P6) with undecyl-bridging alkyl chains showed minimal hemolytic character (Figure 6.2.b). The highest antimicrobial efficiency was observed with P5 NPs, with an MIC of 64 nM ($0.9 \mu\text{g}\cdot\text{ml}^{-1}$) against *E. coli*. P5 NPs showed little hemolytic character (HC_{50} , $>150 \mu\text{M}$, $4700 \mu\text{g}\cdot\text{ml}^{-1}$) providing an unprecedented therapeutic index of more than 5000, 10-fold higher than previous polymer-based antimicrobials. Having established P5 NPs are acutely non-toxic, we next investigated their chronic toxicity in relation to inflammatory cytokine responses from macrophage RAW 264.7 cells (Figure 6.2c). NP concentrations up to $2\mu\text{M}$ showed no

significant toxicity or tumor necrosis factor alpha (TNF- α) cytokine expression (Figure 6.2d), suggesting *in vitro* immunocompatibility with mammalian immune cells.³⁸

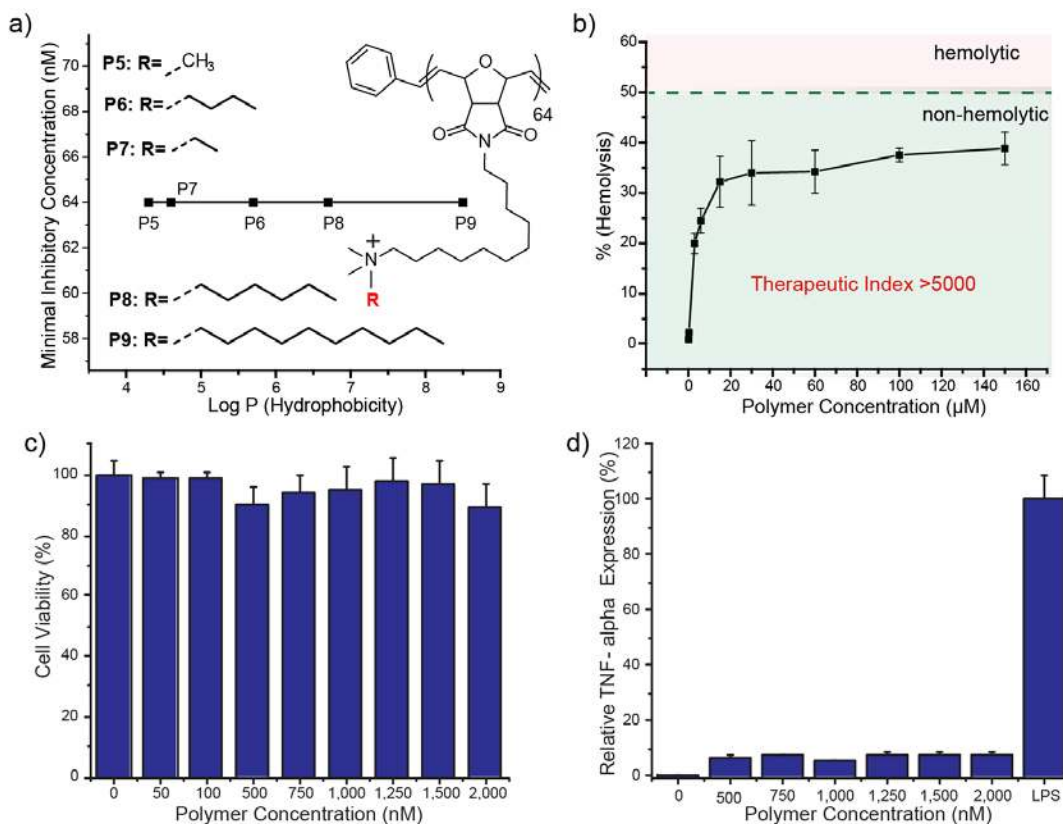


Figure 6.2. a) Graph showing minimum inhibitory concentrations (MIC) and structure details of oxanorbornene derivatives with different hydrophobicity of the cationic headgroups. Log *P* represents the calculated hydrophobic values of each monomer. b) Hemolytic activity of PNPs at different concentrations indicate their non-hemolytic behavior at relevant therapeutic concentrations. c) Cytotoxicity of P5- PNPs against Raw 264.7 macrophage cells. d) TNF- α secretion of Raw 264.7 cells in the presence of PNPs. Lipopolysaccharide (LPS) was used as a positive control.

We next tested our most potent P5 NPs against multiple uropathogenic clinical isolates (Table 6.1) to establish its broad-spectrum activity. P5 NPs suppressed bacterial proliferation at concentrations ranging from 64-128 nM ($0.9 \mu\text{g}.\text{ml}^{-1}$ – $1.8 \mu\text{g}.\text{ml}^{-1}$), similar or lower to previously reported antimicrobial polymers. These polymers showed similar antimicrobial activity against 5 clinical isolates of *E. coli* with different susceptibilities to

clinical antibiotics (resistant to 1-17 drugs), indicating their ability to evade common mechanisms of bacterial resistance. Additionally, engineered polymers were effective against clinical isolates of Gram-negative *P. aeruginosa* and *E. cloacae* complex. Similarly, Gram-positive strains of *S. aureus* were susceptible to P5 NPs including the highly virulent strain of methicillin-resistant *S. aureus* (MRSA).

Strain	Species	MIC (nM)	TI (HC ₅₀ /MIC)
CD-23	<i>P. aeruginosa</i>	64	~2,300
CD-1006	<i>P. aeruginosa</i>	128	~1,200
CD-489	<i>S. aureus</i> - MRSA	64	~2,300
CD-2	<i>E. coli</i>	64	~2,300
CD-3	<i>E. coli</i>	64	~2,300
CD-19	<i>E. coli</i>	64	~2,300
CD-549	<i>E. coli</i>	128	~1,200
CD-496	<i>E. coli</i>	128	~1,200
CD-866	<i>E. cloacae</i> complex	128	~1,200
CD-1412	<i>E. cloacae</i> complex	128	~1,200
CD-1545	<i>E. cloacae</i> complex	128	~1,200

Table 6.1. Minimum inhibitory concentrations and therapeutic indices of P5 NPs against multiple uropathogenic clinical isolate bacterial strains. Therapeutic indices are calculated with respect to red blood cells.

Due to the highly cationic and hydrophobic nature of our PNPs, we hypothesized they can be particularly effective in disrupting bacterial cell membranes.^{39,40} We used a propidium iodide (PI) staining assay to support our hypothesis. PI can only stain cells which have compromised membranes, allowing them to bind with nucleic acids and generate red fluorescence.^{41,42} Pathogenic *E. coli* (CD-2), *S. aureus* (CD-489) and non-pathogenic *P. aeruginosa* (ATCC 19660) were treated with 1 μ M of P5 NPs for 3 hours at 37 °C and subsequently stained with PI before imaging. The confocal images (Figure 6.3b)

clearly show that PNPs mechanism of action leads to bacterial membrane disruption in all three species, regardless of membrane composition or pathogenicity.

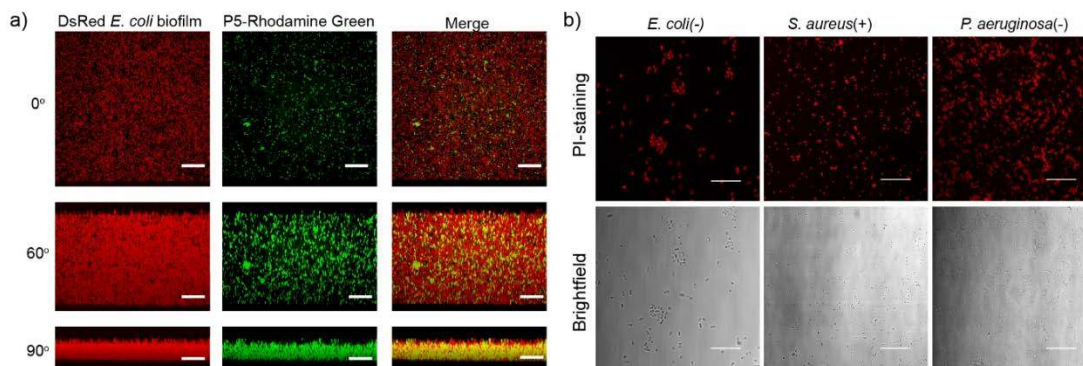


Figure 6.3. Confocal micrographs. a) Representative 3D projection of confocal image stacks of E2-Crimson (Red Fluorescent Protein) expressing *E. coli* DH5 α biofilm after 1 h treatment with P5-Rhodamine Green at 1 μ M concentration. The panels are projection at 0°, 60° and 90° angle turning along X axis. Scale bars are 30 μ m. b) Confocal images of *E. coli* (CD-2), *S. aureus* (MRSA, CD-489) and *P. aeruginosa* (ATCC 19660) stained with Propidium Iodide (PI) after treatment with PNPs. Scale bars are 30 μ m.

After establishing the efficacy of our NPs against bacterial “superbugs”, we tested their efficacy against more resilient bacterial infections- “biofilms”. Biofilms produce extracellular polymeric substance, acting as a barrier against therapeutics. Penetration and accumulation of therapeutics inside biofilms is crucial for effective therapy of these infections.^{43,44} Hence, we used confocal microscopy to examine the ability of PNPs to penetrate biofilms. We treated biofilms formed by *E. coli* expressing DS Red (a red fluorescent protein) with P5 NPs functionalized with Rhodamine Green fluorescent dyes. As shown in Figure 6.3a, fluorescently labeled nanoparticles could readily penetrate and disperse throughout the biofilms (Supporting Figure 6.8), indicating their ability to be an effective anti-biofilm agent.

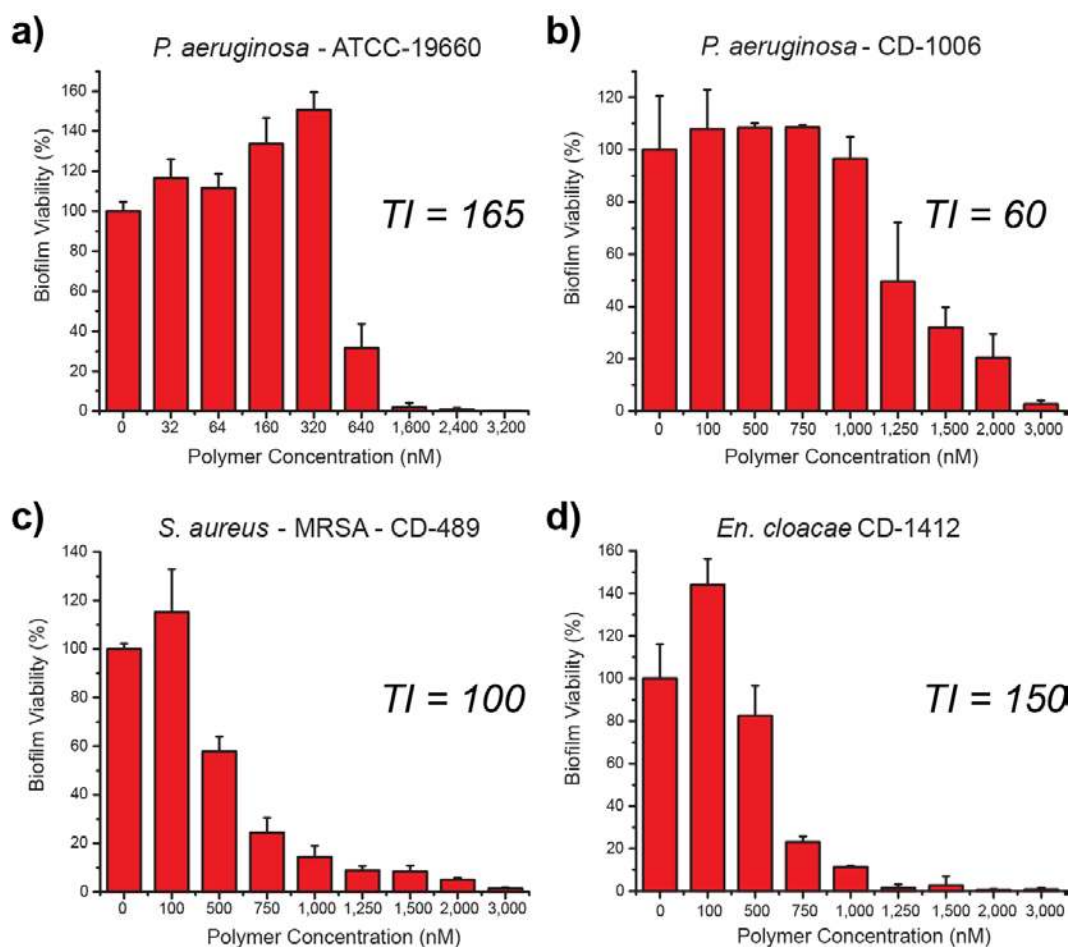


Figure 6.4. Biofilm viability towards P5 NPs. Viability of 1-day-old (a) *P. aeruginosa* (ATCC-19660), (b) *P. aeruginosa* (CD-1006), (c) *S. aureus*(CD-489), and (d) *En. cloacae* complex (CD-1412) biofilms after 3 h treatment with P5 NPs. The data are average of triplicates, and the error bars indicate the standard deviations. TI is the therapeutic index relative to MBEC₉₀ and hemolysis.

Next, we investigated the therapeutic ability of P5 NPs against pre-formed bacterial biofilms. We chose a laboratory strain of *P. aeruginosa* (ATCC 19660) and 3 uropathogenic clinical isolates, *P. aeruginosa* (CD-1006), *En. cloacae* complex (CD-1412) and *S. aureus* (CD-489, a methicillin-resistant strain). As shown in Figure 6.4, P5 NPs demonstrate minimum concentrations to eradicate 90% of biofilms (MBEC₉₀) ranging from 1-3 μ M, providing unprecedented therapeutic indices ranging from 60-165 for

biofilms (TI = HC₅₀/MBEC₉₀). Nanoparticles could treat both Gram-negative (*P. aeruginosa*, and *En. cloacae* complex) and Gram-positive (*S. aureus*) bacterial strains, further highlighting their broad-spectrum activity against biofilms. Notably, P5 NPs demonstrated similar efficacy in treating MDR (CD-489, CD-1412) and non-resistant strains (CD-1006, ATCC 19660), suggesting their value as a promising therapeutic alternative to traditional antibiotics.

The ability to eradicate biofilms on biomedical surfaces such medical implants and indwelling devices is a critical capability. However, treating biofilm infections on human tissues or organs is more challenging and relevant to medical settings. Biofilm infections on wounds significantly impair the healing process regulated by fibroblast skin cells.⁴⁵ We used an *in-vitro* coculture model comprised of mammalian fibroblast cells with biofilms grown over them.^{46,47,48} First, we investigated P5 NPs compatibility with mammalian NIH 3T3 fibroblast cells at similar concentrations used to eradicate pre-formed biofilms and observed no significant toxicity (Supporting Figure 6.9). Next, *P. aeruginosa* bacteria were seeded on a confluent monolayer of NIH 3T3-fibroblast cells overnight to generate biofilms prior to treatment. The cocultures were treated with P5 NPs for 3 hours, washed, and the viabilities of both bacteria and fibroblasts determined. As shown in Figure 6.5a, a 4-6-fold log reduction (99.5%-99.99%) in bacterial colonies was observed at concentrations ranging from 7.5-15 μ M, while the fibroblast viability was still maintained.

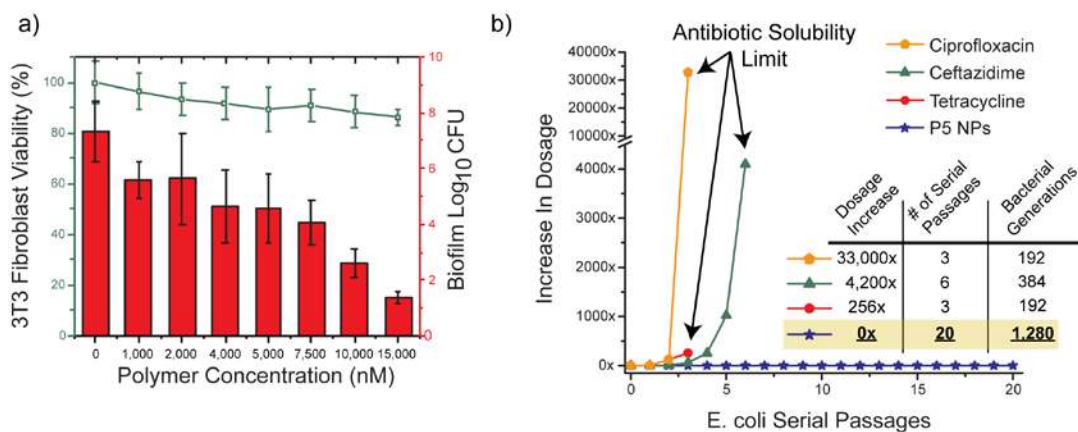


Figure 6.5. a) Viability of 3T3 fibroblast cells and *E. coli* biofilms in the coculture model after 3 h treatment with P5 NPs. Scatters and lines represent 3T3 fibroblast cell viability. Bars represent log₁₀ of colony forming units in biofilms. The data are average of triplicates and the error bars indicate the standard deviations. b) Resistance development during serial passaging in the presence of sub-MIC levels of antimicrobials. The y axis is the highest concentration the cells grew in during passaging. The figure is representative of 3 independent experiments.

Bacteria can acquire resistance quickly towards antibiotics and other antimicrobials, minimizing their therapeutic prospects in clinical settings. We subjected uropathogenic *E. coli* (CD-2) to multiple serial passages of sub-MIC (66% of MIC) concentrations of P5 NPs to investigate if resistance towards our polymer nanoparticles would occur.²⁷ The resulting bacterial population was defined as the first generation, harvested, and its MIC was evaluated. Subsequently, a second generation was produced by exposing first generation with 66% MIC dosage of polymers. As shown in Figure 6.5b, it was observed that even at the 20th serial passage (~1,300 bacterial generations) of CD-2, *E. coli* was still susceptible to 128 nM of P5 NPs, as compared to the zeroth generation. Similar experiments were conducted on ciprofloxacin (quinolone), ceftazidime (β -lactam) and tetracycline, clinically relevant antibiotics. Respectively, there was a 33,000, 4,200 and 256-fold increase in the MICs of antibiotics against CD-2 *E. coli*. This significant result

indicates the killing mechanism of our engineered nanoparticles significantly undermine the onset of resistance development in bacteria. Notably, we have demonstrated our polymeric nanoparticles remain un-resistant towards bacteria longer than previously reported polymer-based nanomaterials⁴⁹ (~600 generations – *A. baumannii* FADDI-AB156) and comparable to a recently discovered and novel antibiotic, teixobactin (~1,300 generations – *S. aureus* ATCC 29213).⁵⁰

6.3. Conclusions

We have reported here a novel therapeutic platform to combat MDR bacterial and biofilm infections using engineered polymeric nanoparticles. Our study demonstrates the ability to modulate antimicrobial activity and therapeutic efficacy of polymeric NPs by incorporating hydrophobic alkyl groups in polymer side-chains. Cationic hydrophobic polymers can self-assemble to form polymeric NPs and demonstrate excellent efficiency in combating planktonic superbugs as well as their more drug-resistant biofilm counterparts. Their ability to penetrate and eradicate biofilms can foster a therapeutic advancement that can fundamentally alter the treatment strategy of these dangerous infections. Notably, bacteria do not develop resistance against polymeric NPs for 20 serial passages, an elusive feat for clinical antibiotics. Taken together, polymer NP-based antimicrobial therapy has the potential to provide an effective platform to combat bacterial infections while circumventing standard antibiotic resistance pathways. Moreover, our study provides a crucial insight for designing next-generation antimicrobials with implications in a wide-range of planktonic and biofilm-related infections.

6.4. Experimental Protocols

6.4.1 Synthesis of Grubbs 3rd Generation Catalyst

Grubbs 3rd generation catalyst was synthesized as described in previously published reports.⁵¹ Detailed synthesis can be found in the Supporting Information.

6.4.2 Determination of Antimicrobial Activities of Cationic Polymers

Bacteria were cultured in LB medium at 37 °C and 275 rpm until stationary phase. The cultures were then harvested by centrifugation and washed with 0.85% sodium chloride solution for three times.²⁷ Concentrations of resuspended bacterial solution were determined by optical density measured at 600 nm. M9 medium was used to make dilutions of bacterial solution to a concentration of 1×10^6 cfu/mL. A volume of 50 μ L of these solutions was added into a 96-well plate and mixed with 50 μ L of polymer solutions in M9, giving a final bacterial concentration of 5×10^5 cfu/mL. Polymer concentration varied in half fold per a standard protocol, ranging from 1024 to 4 nM. A growth control group without polymers and a sterile control group with only growth medium were carried out at the same time. Incubation of the polymers with bacteria was performed for 16 hours. Cultures were performed in triplicates, and at least two independent experiments were repeated on different days. The MIC is defined as the lowest concentration of polymer that inhibits visible growth as observed with the unaided eye.⁵²

6.4.3 Determination of Hemolysis of Cationic Polymers

We used the previously established protocol to conduct hemolysis assays on Red Blood Cells.²⁸ Citrate-stabilized human whole blood (pooled, mixed gender) was

purchased from Bioreclamation LLC, NY and processed as soon as received. 10 mL of phosphate buffered saline (PBS) was added to the blood and centrifuged at 5000 r.p.m. for 5 minutes. The supernatant was carefully discarded and the red blood cells (RBCs) were dispersed in 10 mL of PBS. This step was repeated at least five times. The purified RBCs were diluted in 10 mL of PBS and kept on ice during the sample preparation. 0.1 mL of RBC solution was added to 0.4 mL of polymer solution in PBS in a 1.5 mL centrifuge tube (Fisher) and mixed gently by pipetting. RBCs incubated with PBS and water was used as negative and positive controls, respectively. All polymer samples as well as controls were prepared in triplicate. The mixture was incubated at 37 °C for 30 minutes while shaking at 150 r.p.m. After incubation period, the solution was centrifuged at 4000 r.p.m. for 5 minutes and 100 µL of supernatant was transferred to a 96-well plate. The absorbance value of the supernatant was measured at 570 nm using a microplate reader (SpectraMax M2, Molecular devices) with absorbance at 655 nm as a reference. The percent hemolysis was calculated using the following formula:

$$\% \text{ Hemolysis} = \frac{(\text{Sample Absorbance} - \text{Negative Control Absorbance})}{(\text{Positive Control Absorbance} - \text{Negative Control Absorbance})} * 100$$

6.4.4 Macrophage Cell Studies and TNF-alpha Secretion

RAW 264.7 macrophage cell line was purchased from American Type Culture Collection (ATCC, Manassas, VA). Roswell Park Memorial Institute media (RPMI 1640) supplemented with 10% fetal bovine serum, 1% antibiotics (100 µg/ml penicillin and 100 µg/ml streptomycin) and sodium pyruvate, was used for cell culture. The cells were

incubated at 37 °C under a humidified atmosphere of 5% CO₂. The cells were cultured once every four days under the above-mentioned conditions.

6.4.5 Polymer Nanoparticles and LPS Treatment

These studies were conducted as per the previously reported protocols.⁵³ Briefly, to evaluate the effect of polymer on the immune system, 1.0×10^5 of RAW 264.7 cells were cultured in a 24-well plate for 24 h. Then, cells were washed once with cold PBS and treated with different concentration of polymer for 3 h or 24h. The macrophage with 100ng/ml of lipopolysaccharide were the positive control. At the end of incubation, culture media was collected for TNF- α level measurement by ELISA (R&D Systems, MN, USA). Experiments were performed in triplicate.

6.4.6 Propidium Iodide Staining Assay

E. coli CD-2, *P. Aeruginosa* ATCC19660 and MRSA CD-489 (1×10^8 cfu/mL) were incubated with 1 μ M P5 NPs in M9 media at 37 °C and 275 rpm for 3 h. The bacteria solutions were then mixed with PI (2 μ M) and incubated for 30 min in dark. Five microliters of the samples were placed on a glass slide with a glass coverslip and observed with a confocal laser scanning microscopy, Zeiss 510 (Carl Zeiss, Jena, Germany) using a 543-nm excitation wavelength.

6.4.7 Biofilm Formation and Treatment

Bacteria were inoculated in lysogeny broth (LB) medium at 37 °C until stationary phase. The cultures were then harvested by centrifugation and washed with 0.85% sodium chloride solution three times. Concentrations of resuspended bacterial solution were determined by optical density measured at 600 nm. Seeding solutions were then made in

M9 medium to reach an OD₆₀₀ of 0.1. A 100 µL amount of the seeding solutions was added to each well of the 96-well microplate. The plates were covered and incubated at room temperature under static conditions for 1 day. The stock solution of polymers was then diluted to the desired level and incubated with the biofilms for 3 hours at 37°C. Biofilms were washed with phosphate buffer saline (PBS) three times and viability was determined using an Alamar Blue assay. Minimal M9 medium without bacteria was used as a negative control.³⁷

6.4.8 Biofilm-3T3 Fibroblast Cell Co-culture

Co-culture was performed using the previously reported protocol.⁵⁴ A total of 20000 NIH 3T3 (ATCC CRL-1658) cells were cultured in Dulbecco's modified Eagle medium (DMEM; ATCC 30-2002) with 10% bovine calf serum and 1% antibiotics at 37 °C in a humidified atmosphere of 5% CO₂. Cells were kept for 24 h to reach a confluent monolayer. Bacteria (*P. aeruginosa*) were inoculated and harvested as mentioned above. Afterward, seeding solutions 10⁸ cells/mL were inoculated in buffered DMEM supplemented with glucose. Old medium was removed from 3T3 cells followed by addition of 100 µL of seeding solution. The cocultures were then stored in a box humidified with damp paper towels at 37 °C overnight without shaking. Polymer NPs and other control solutions were diluted in DMEM media prior to use to obtain the desired testing concentrations. Old media was removed from coculture, replaced with freshly prepared testing solutions, and incubated for 3 h at 37 °C. Cocultures were then analyzed using an LDH cytotoxicity assay to determine mammalian cell viability using manufacturer's instructions.⁵⁵ To determine the bacteria viability in biofilms, the testing solutions were removed and cocultures were washed with PBS. Fresh PBS was then added to disperse

remaining bacteria from biofilms in coculture by sonication for 20 min and mixing with pipet. The solutions containing dispersed bacteria were then plated onto agar plates, and colony forming units were counted after incubation at 37 °C overnight.

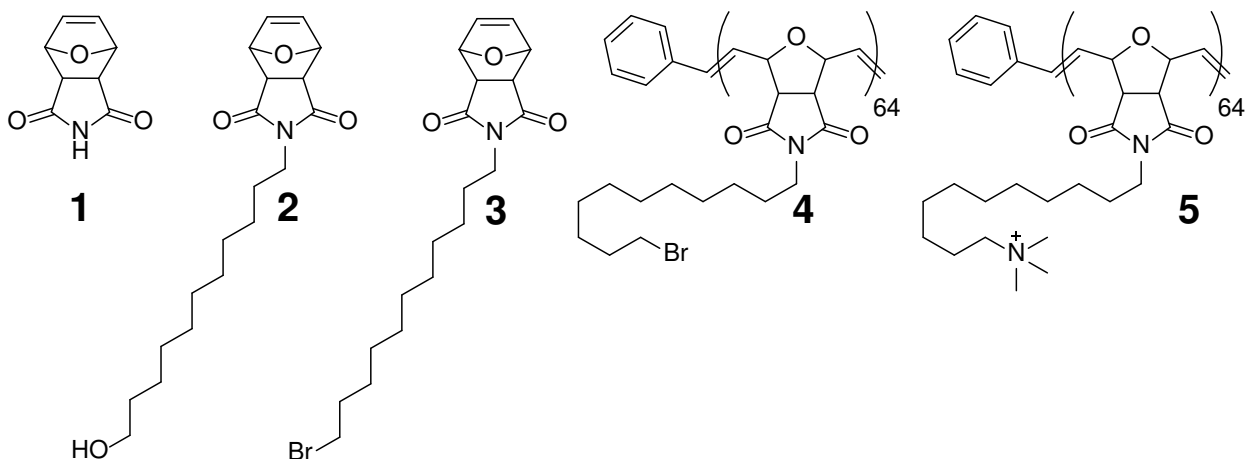
6.4.9 Resistance Development

E. coli CD-2 was inoculated in M9 medium with 85 nM (2/3 of 128 nM, MIC) of P5 NPs at 37 °C and 275 rpm for 16 h (~ 64 bacterial generations for 1 serial passage). The culture was then harvested and tested for MIC as describe above. *E. coli* CD-2 was cultured without polymer as well every time as a control for comparison of MICs. In the case of P5 NPs, 20 serial passages were performed giving ~ 1,300 generations.

6.5. Supporting Figures

6.5.1 Oxanorbornene Monomer Synthesis

Note: Generation of C2 and C6-bridged polyoxanorbornene polymers can be successfully made using the same procedures used to generate C11-bridged polymers however replacing 11-bromoundecanol with bromoethanol or 6-bromohexanol, respectively.



Synthesis of 1. In a pressure tube, furan (4.5ml, 61.7mmol, 1.5eq) and maleimide (4.0g, 41.1mmol, 1.0eq) were added in addition to 5ml of diethyl ether. The tube was sealed and

heated at 100°C overnight. Afterwards, the pressure tube was cooled to r.t. and the formed solid was removed, filtered, and washed with copious amounts of diethyl ether to isolate **1** as a white solid (95% yield) and was used without further purification. ¹H NMR (400MHz, MeOD) 11.14 (s, 1H), 6.52 (s, 2H), 5.12 (s, 2H), 2.85 (s, 2H).

Synthesis of 2. To a 250ml round bottom flask equipped with a stir bar was added 60ml of DMF. Next, **1** (3.76g, 22.7mmol, 1.0eq) was added along with potassium carbonate (12.59g, 91.1mmol, 4.0eq). The reaction mixture was heated at 50°C for five minutes. Finally, potassium iodide (0.68g, 4.5mmol, 0.2eq) and 11-bromoundecanol (6.00g, 23.90mmol, 1.05eq) were added and stirred at 50°C overnight. Afterwards, the reaction mixture was cooled to room temperature, diluted to 150ml with ethyl acetate and washed with water (7x, 50ml) and brine (1x, 50ml). The organic layer was dried with sodium sulfate, filtered, and rotovaped to yield **2**. **2** was purified by sonication of the rotovaped solid in hexanes and filtered (82% yield). ¹H NMR (400MHz, CDCl₃) 6.44 (s, 2H), 5.19 (s, 2H), 3.55 (t, 2H), 3.49 (t, 2H), 2.79 (s, 2H), 1.9 (s, 1H), 1.39 (m, 4H), 1.2 (m, 14H).

Synthesis of 3. To a 250ml round bottom flask equipped with a stir bar was added **2** (2.64g, 7.87mmol, 1.0eq). Next, DCM (100ml) was added along with tetrabromomethane (3.13g, 9.44mmol, 1.2eq). The reaction was cooled to 0°C using an ice bath. Finally, triphenylphosphine was added in portions (2.47g, 9.44mmol, 1.2eq) and allowed to stir for three hours. Afterwards, the reaction mixture was rotovaped and ethyl ether was added (200ml) and placed in the freezer for 2 hours to precipitate out triphenylphosphine oxide. The reaction mixture was filtered, and the filtrate was rotovaped. Column chromatography was performed to yield **3**, a white solid (79% yield). ¹H NMR (400MHz, CDCl₃) 6.51 (s,

2H), 5.27 (s, 2H), 3.45 (t, 2H), 3.41 (t, 2H), 2.83 (s, 2H), 1.85 (q, 2H), 1.55 (q, 2H), 1.41 (q, 2H), 1.29 (m, 12H).

6.5.2 Oxanorbornene Polymer Synthesis

Synthesis of 4. To a 10ml pear-shaped air-free flask equipped with a stir bar was added **3** (800mg, 2.0mmol, 1.0eq) and 4ml of DCM. In a separate 10ml pear-shaped air-free flask was added Grubbs 3rd generation catalyst⁵⁶ (35.4mg, 0.04mmol, 0.02eq) and 1ml DCM. Both flasks were sealed with septa and attached to a schlenk nitrogen/vacuum line. Both flasks were freeze-pump-thawed three times. After thawing, Grubbs 3rd generation catalyst was syringed out and quickly added to the flask containing **3** and allowed to react for 10min. After the allotted time, ethyl vinyl ether (200 μ L) was added and allowed to stir for 15 minutes. Afterwards, the reaction was diluted to two times the volume and precipitated into a heavily stirred solution of hexane (300ml). The precipitated polymer was filtered and dissolved into tetrahydrofuran (THF). The polymer was precipitated again into hexane and filtered to yield **4**. MW = 25,698, PDI = 1.04 (determined by THF-GPC using a Polystyrene calibration curve) ¹H NMR (400MHz, CDCl₃) 6.0 (br, 1H), 5.7 (br, 1H), 4.95 (br, 1H), 4.4 (br, 1H), 3.4 (br, 2H), 3.25 (br, 2H), 1.79 (q, 2H), 1.5 (br, 2H), 1.34 (br, 2H), 1.2 (br, 14H).

6.5.3 Synthesis of 5 Quaternary Ammonium Polymers

To generate the library of quaternary ammonium poly(oxanorborneneimides), **4** (50mg) was added to 20ml vials equipped with a stir bar. Next, excess of the necessary tertiary amines was added (10ml of a 1M trimethylamine solution in THF, all other amines were 200mg) to the vial and purged with nitrogen. First stage of the reactions involved stirring for 30 minutes at 80°C. The polymers precipitated during this time. Half of the THF was

evaporated and replaced with methanol which re-dissolved the polymers. The reaction was allowed to proceed overnight at 50°C. Afterwards, the solvent was completely evaporated, washed with hexane 2 times, and dissolved into a minimal amount of water. The polymers were added to 10,000 MWCO dialysis membranes and allowed to stir for 3 days, changing the water periodically. The polymers were filtered through PES syringe filters and freeze-dried to yield all the respective quaternary ammonium polymers **5**. NMR indicated conversion into the desired quaternary ammonium salts.

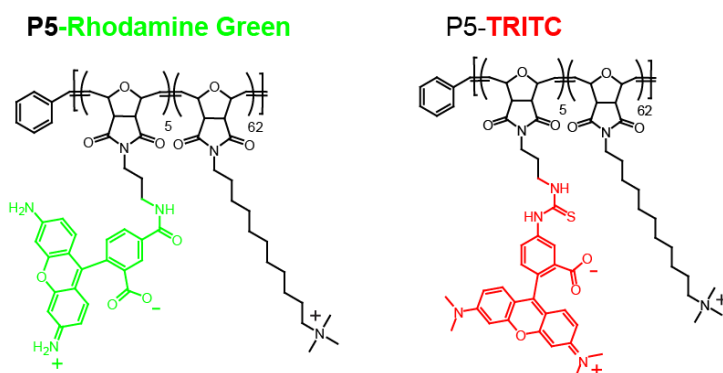


Figure 6.6. Molecular structures of P5 polymer derivatives used for FRET NP studies.

6.5.4 FRET NP Formation

FRET NPs were generated using the **P5** polymer scaffold, labelled either with donor Rhodamine Green or acceptor TRITC (Functionalized by incorporating a boc-protected amino monomer during the polymerization, followed by purification using a 10,000 MWCO dialysis bag). Keeping **P5-Rhodamine Green**'s concentration constant at ~ 1.6µM in 2ml Eppendorf tubes, increasing concentrations of **P5-TRITC** in MQ water was added and the tubes were sonicated for one minute and allowed to stand for one hour. The solutions were then transferred to a 96-well microplate and the total emission spectrum

of both **P5** derivatives were recorded on a SpectroMax M5 microplate reader (Molecular Device) using 480nm as the excitation wavelength (480nm was selected so that only **P5-Rhodamine Green** would be excited).

6.5.5 TEM Characterization of Polymeric Nanoparticles (NPs)

TEM samples of polymers were prepared by placing one drop of the desired solution (10 μ M) on to a 300-mesh Cu grid-coated with carbon film. These samples were analyzed and photographed using JEOL CX-100 electron microscopy. The average diameter of P5 nanoparticles is 12.7 ± 2.7 nm.

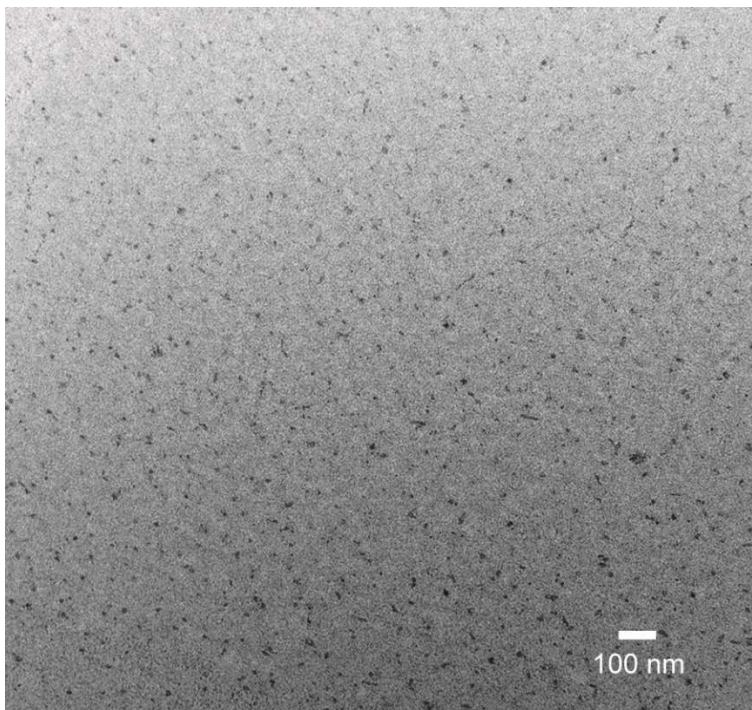


Figure 6.7. TEM image of polymer nanoparticles.

6.5.6 Biofilm Penetration Studies Using Confocal Laser Scanning Microscopy

10^8 bacterial cells/ml of DS Red (Red Fluorescent Protein) expressing *E. coli*, supplemented with 1mM of IPTG ((isopropyl β -D-1-thiogalactopyranoside), were seeded (2 ml in M9 media) in a confocal dish and were allowed to grow. After 3 days media was replaced by 1000 nM of PONI-C11-TMA-NPs and biofilms were incubated for 1 hour, biofilm samples incubated with only M9 media were used as control. After 1 h, biofilms were washed with PBS three times and were incubated with 100 μ M of the substrates for 1 h. The cells were then washed with PBS three times. Confocal microscopy images were obtained on a Zeiss LSM 510 Meta microscope by using a 63 \times objective. The settings of the confocal microscope were as follows: green channel: λ_{ex} =488 nm and λ_{em} =BP 505-530 nm; red channel: λ_{ex} =543 nm and λ_{em} =LP 650 nm. Emission filters: BP=band pass, LP=high pass.

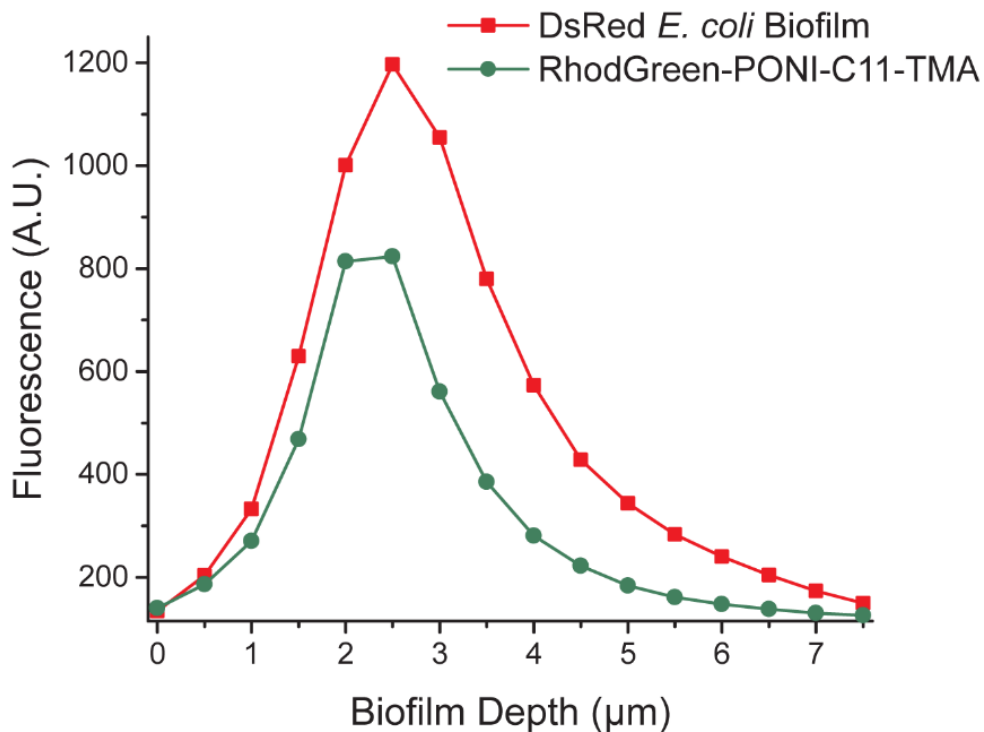


Figure 6.8. Penetration of Rhodamine Green labelled PONI-C11-TMA nanoparticles into DsRed expressing *E. coli* biofilms. The mean fluorescence of each confocal z-stack image was calculated using ImageJ software.

6.5.7 Mammalian Cell Viability Assay⁵⁷

A total of 20,000 NIH 3T3 (ATCC CRL-1658) cells were cultured in Dulbecco's modified Eagle medium (DMEM; ATCC 30-2002) with 10% bovine calf serum and 1% antibiotics at 37 °C in a humidified atmosphere of 5% CO₂ for 48 h. Old media was removed and cells were washed one time with phosphate-buffered saline (PBS) before addition of NPs in the prewarmed 10% serum containing media. Cells were incubated for 24 h at 37 °C under a humidified atmosphere of 5% CO₂. Cell viability was determined using Alamar blue assay according to the manufacturer's protocol (Invitrogen Biosource). After a wash step with PBS three times, cells were treated with 220 µL of 10% alamar blue in serum containing media and incubated at 37 °C under a humidified atmosphere of 5% CO₂ for 3 h. After incubation, 200 µL of solution from each well was transferred in a 96-well black microplate. Red fluorescence, resulting from the reduction of Alamar blue solution, was quantified (excitation/emission: 560 nm/590 nm) on a SpectroMax M5 microplate reader (Molecular Device) to determine the cellular viability. Cells without any NPs were considered as 100% viable. Each experiment was performed in triplicate.

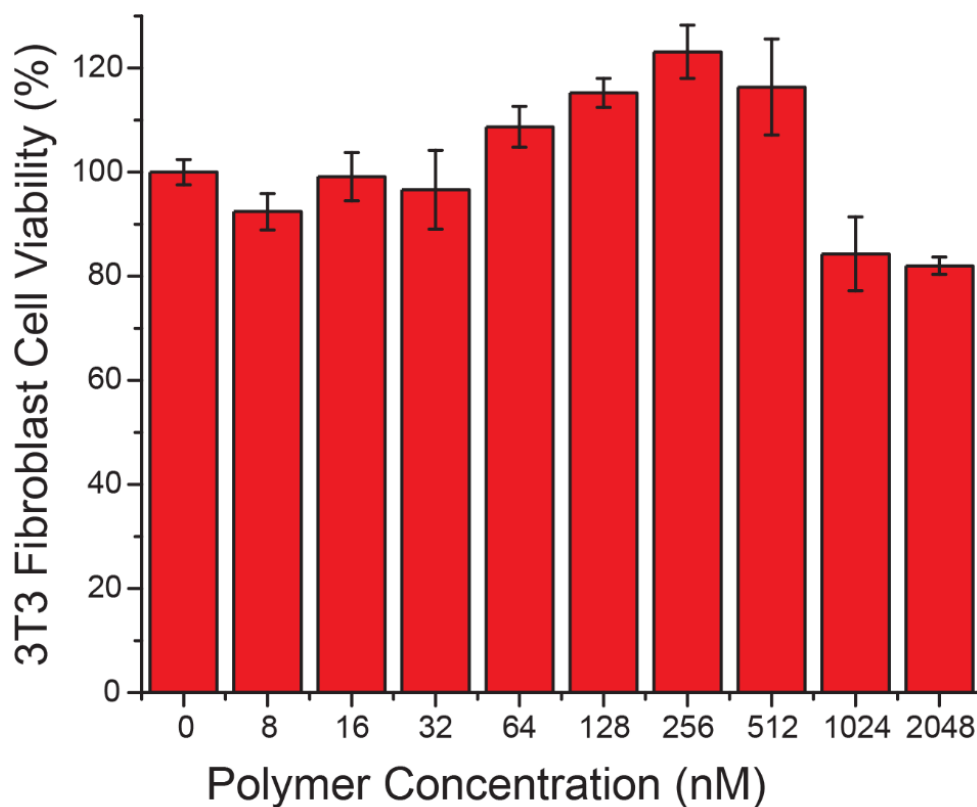


Figure 6.9. Cytotoxicity of PNPs against NIH-3T3 Fibroblast cells.

6.5.8 Therapeutic Indices Against Biofilms⁵⁸

Bacteria were inoculated in lysogeny broth (LB) medium at 37 °C until stationary phase. The cultures were then harvested by centrifugation and washed with 0.85% sodium chloride solution three times. Concentrations of resuspended bacterial solution were determined by optical density measured at 600 nm. Seeding solutions were then made in M9 medium to reach an OD₆₀₀ of 0.1. A 100 µL amount of the seeding solutions was added to each well of the 96-well microplate. The plates were covered and incubated at room temperature under static conditions for 1 day. The stock solution of PONI-C11-TMA-NPs was then diluted to the desired level and incubated with the biofilms for 3 hours at 37°C.

Biofilms were washed with phosphate buffer saline (PBS) three times and viability was determined using an Alamar Blue assay. Minimal M9 medium without bacteria was used as a negative control. Concentrations were converted to Log, plotted with bacteria viability, and fitted to a curve to determine the minimum biofilm eradication concentration at 90% (MBEC₉₀).⁵⁹ The therapeutic index with respect to red blood cells was calculated by the concentration of PONI-C11-TMA at MBEC₉₀ divided by the hemolysis at 50%.

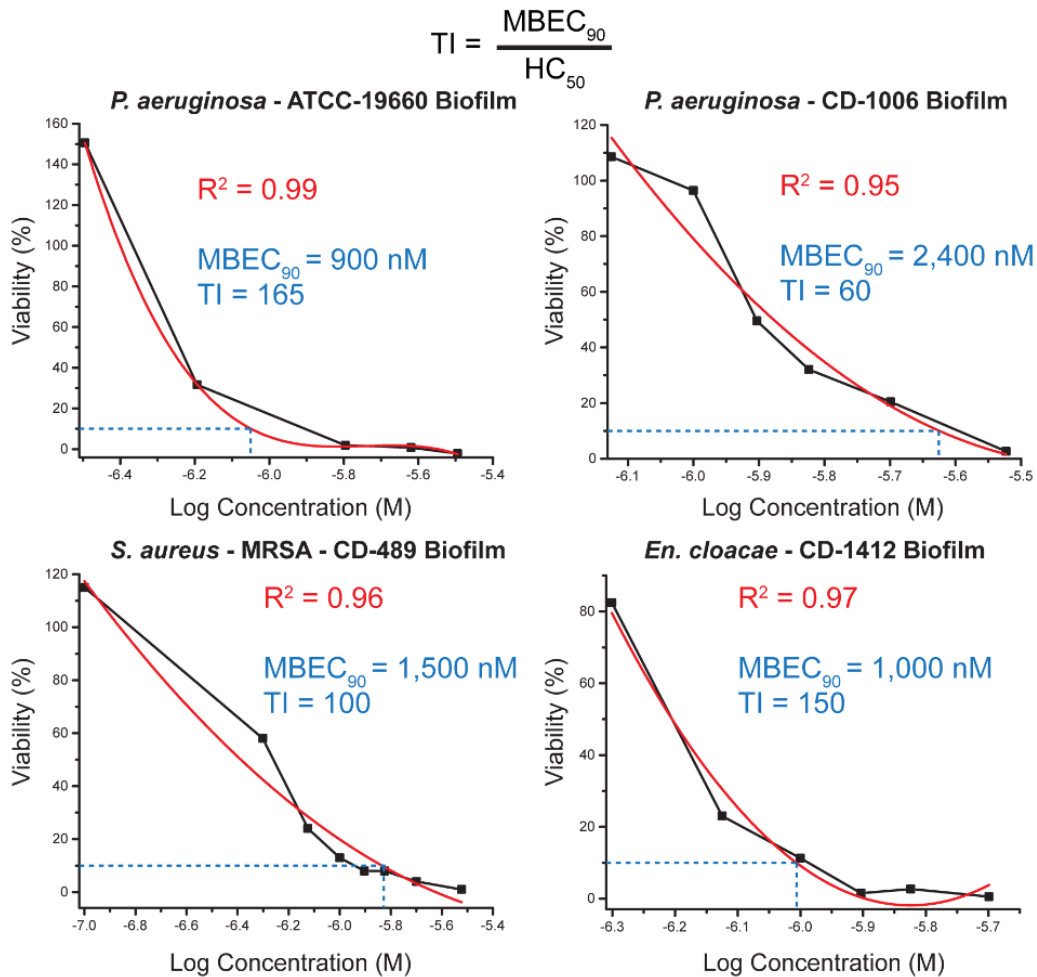


Figure 6.10. Therapeutic indices of PNPs against four bacterial biofilms.

6.5.9 Critical Micelle Concentration Study

Critical Micelle Concentration of P5 NP was determined through dilution of Nile Red encapsulated NPs. Briefly, 16.0 mg of Polymer P5 and 2.0 mg of Nile Red was dissolved in 2 ml of dimethylsulfoxide in a 7ml scintillation vial. While under vigorous stirring, 3 ml of water was slowly added over the course of 1 hour and allowed to stir overnight. Afterwards, the vial was centrifuged, and the solution decanted to remove precipitated Nile Red that was not encapsulated. Followed by filtration through a PES syringe filter, the solution was transferred to a 3,500 MWCO dialysis bag and allowed to stir in 5L of water for two days, changing the water twice each day. Afterwards, the solution was filtered again through a PES syringe filter yielding Nile Red encapsulated P5 NPs. Nile Red's fluorescence spectrum was monitored (Excitation = 550nm) as a function of decreasing polymer concentration. it was observed that at 2.5 μM , fluorescence decrease became non-linear. Further dilution was not possible due to limitations in the amount of Nile Red encapsulated. Therefore, the critical micelle concentration was determined to be $\sim 2.5 \mu\text{M}$ and is well within the range of previously reported diblock polymer carriers.

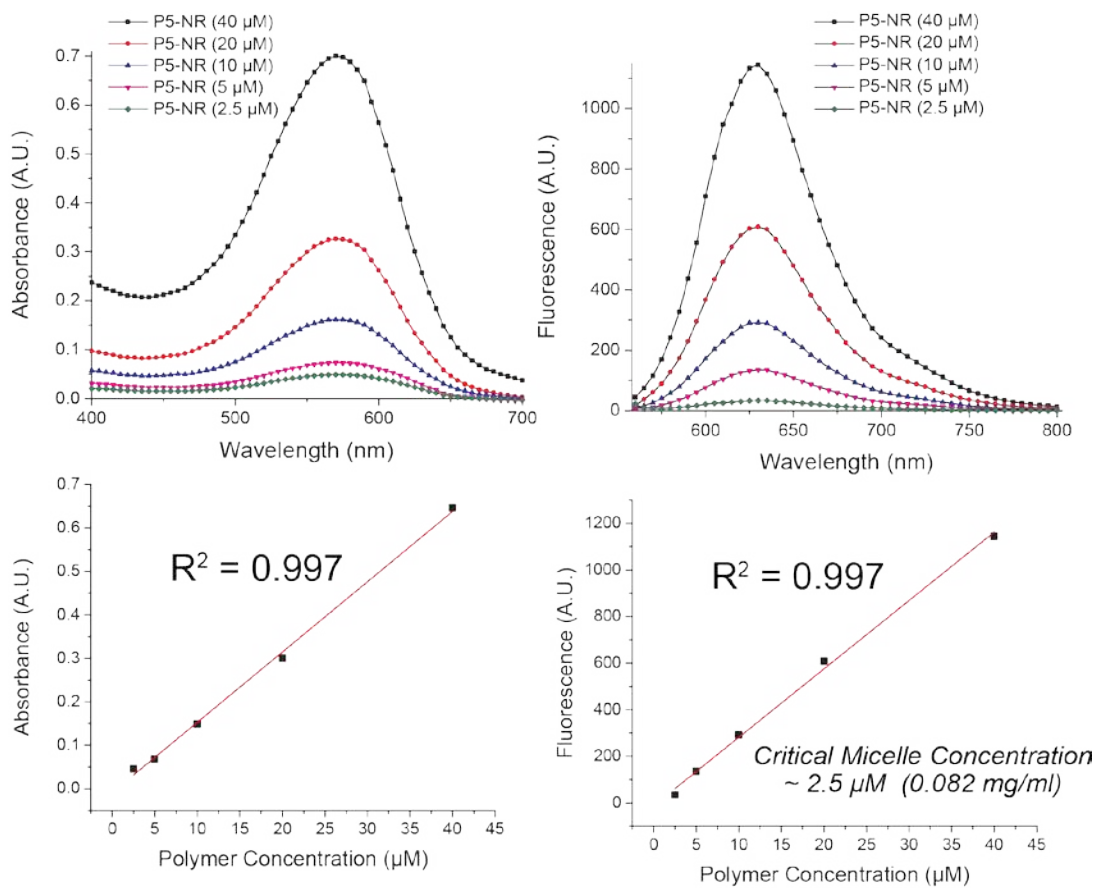


Figure 6.11. Critical micelle concentration of P5 NPs.

6.6. References

- (1) Harris, S. R. *et al.* Evolution of MRSA During Hospital Transmission and Intercontinental Spread. *Science* **2010**, 327, 469–474.
- (2) Van Amersfoort, E. S., Van Berkel, T. J. C. & Kuiper, J. Receptors, mediators, and mechanisms involved in bacterial sepsis and septic shock. *Clin. Microbiol. Rev.* **2003**, 16, 379–414.
- (3) RD, W. & GD, E. Biofilms and chronic infections. *JAMA* **2008**, 299, 2682–2684.
- (4) Donlan, R. M. Biofilms and device-associated infections. *Emerg. Infect. Dis.* **2001**, 7, 277–281.
- (5) Costerton, J. W., Stewart, P. S. & Greenberg, E. P. Bacterial biofilms: a common cause of persistent infections. *Science* **1999**, 284, 1318–1322.
- (6) Lewis, K. Riddle of biofilm resistance. *Antimicrob. Agents Chemother.* **2001**, 45, 999–1007.
- (7) Fux, C. A *et al.* Survival strategies of infectious biofilms. *Trends Microbiol.* **2005**, 13, 34–40.
- (8) Del Pozo, J. L. & Patel, R. Infection Associated with Prosthetic Joints. *N. Engl. J. Med.* **2009**, 361, 787–794.
- (9) Laxminarayan, R. *et al.* Antibiotic resistance—the need for global solutions. *Lancet Infect. Dis.* **2013**, 13, 1057–1098.
- (10) Baltzer, S. a. & Brown, M. H. Antimicrobial Peptides – Promising Alternatives to Conventional Antibiotics. *J. Mol. Microbiol. Biotechnol.* **2011**, 20, 228–235.
- (11) Hancock, R. E. W. & Sahl, H.-G. Antimicrobial and host-defense peptides as new anti-infective therapeutic strategies. *Nat. Biotech.* **2006**, 24, 1551–1557.
- (12) Jiang, Z. *et al.* Rational design of α -helical antimicrobial peptides to target Gram-negative pathogens, *Acinetobacter baumannii* and *Pseudomonas aeruginosa*: Utilization of charge, ‘specificity determinants,’ total hydrophobicity, hydrophobe type and location as design parameters to improve the therapeutic ratio. *Chem. Biol. Drug. Des.* **2011**, 77, 225–240.
- (13) Marr, A. K., Gooderham, W. J. & R.E.W., H. Antibacterial peptides for therapeutic use: obstacles and realistic outlook. *Curr. Opin. Pharmacol.* **2006**, 6, 468–472.
- (14) Sieprawska-Lupa, M. *et al.* Degradation of human antimicrobial peptide LL-37 by *Staphylococcus aureus*-derived proteinases. *Antimicrob. Agents Chemother.* **2004**, 48, 4673–4679.

- (15) Palermo, E. F. & Kuroda, K. Structural determinants of antimicrobial activity in polymers which mimic host defense peptides. *Appl. Microbiol. Biotechnol.* **2010**, *87*, 1605–1615.
- (16) Mowery, B. P. *et al.* Mimicry of antimicrobial host-defense peptides by random copolymers. *J. Am. Chem. Soc.* **2007**, *129*, 15474–15476.
- (17) Patch, J. A. & Barron, A. E. Helical peptoid mimics of magainin-2 amide. *J. Am. Chem. Soc.* **2003**, *125*, 12092–12093.
- (18) Kuroda, K. & Caputo, G. A. Antimicrobial polymers as synthetic mimics of host-defense peptides. *Wiley Interdiscip. Rev. Nanomedicine Nanobiotechnology* **2013**, *5*, 49–66.
- (19) Arnt, L., Nüsslein, K. & Tew, G. N. Nonhemolytic abiogenic polymers as antimicrobial peptide mimics. *J. Polym. Sci. Part A Polym. Chem.* **2004**, *42*, 3860–3864.
- (20) Kuroda, K. & DeGrado, W. F. Amphiphilic polymethacrylate derivatives as antimicrobial agents. *J. Am. Chem. Soc.* **2005**, *127*, 4128–4129.
- (21) Muñoz-Bonilla, A. & Fernández-García, M. Polymeric materials with antimicrobial activity. *Prog. Polym. Sci.* **2012**, *37*, 281–339.
- (22) Tashiro, T. Antibacterial and Bacterium Adsorbing Macromolecules. *Macromol. Mater. Eng.* **2001**, *286*, 63–87.
- (23) Choi, S. *et al.* De novo design and in vivo activity of conformationally restrained antimicrobial arylamide foldamers. *Proc. Natl. Acad. Sci.* **2009**, *106*, 6968–6973.
- (24) Melo, M. N., Dugourd, D. & Castanho, M. A. R. B. Omiganan pentahydrochloride in the front line of clinical applications of antimicrobial peptides. *Recent Pat. Antiinfect. Drug Discov.* **2006**, *1*, 201–207.
- (25) Ilker, M. F., Nüsslein, K., Tew, G. N. & Coughlin, E. B. Tuning the Hemolytic and Antibacterial Activities of Amphiphilic Polynorbornene Derivatives. *J. Am. Chem. Soc.* **2004**, *126*, 15870–15875.
- (26) Gabriel, G. J. *et al.* Synthetic Mimic of Antimicrobial Peptide with Nonmembrane-Disrupting Antibacterial Properties. *Biomacromolecules* **2008**, *9*, 2980–2983.
- (27) Lienkamp, K. *et al.* Antimicrobial Polymers Prepared by ROMP with Unprecedented Selectivity: A Molecular Construction Kit Approach. *J. Am. Chem. Soc.* **2008**, *130*, 9836–9843.
- (28) Al-Badri, Z. M.; Tew, G. N. Well-defined Acetylene-Functionalized Oxanorbornene Polymers and Block Copolymers. *Macromolecules* **2008**, *41*, 4173–4179.
- (29) Lin, C. C.; Ki, C. S.; Shih, H. Thiol-Norbornene Photo-Click Hydrogels for Tissue Engineering Applications. *J. Appl. Polym. Sci.* **2015**, *132*, 41563.

- (30) Cole, J. P.; Lessard, J. J.; Lyon, C. K.; Tuten, B. T.; Berda, E. B. Intra-Chain Radical Chemistry as a Route to Poly(Norbornene Imide) Single-Chain Nanoparticles: Structural Considerations and the Role of Adventitious Oxygen. *Polym. Chem.* **2015**, *6*, 5555-5559.
- (31) Yin, L. M., Edwards, M. A., Li, J., Yip, C. M. & Deber, C. M. Roles of hydrophobicity and charge distribution of cationic antimicrobial peptides in peptide-membrane interactions. *J. Biol. Chem.* **2012**, *287*, 7738–7745.
- (32) Kuroda, K., Caputo, G. A. & DeGrado, W. F. The role of hydrophobicity in the antimicrobial and hemolytic activities of polymethacrylate derivatives. *Chem. - A Eur. J.* **2009**, *15*, 1123–1133.
- (33) Chen, C. *et al.* Photo-responsive, biocompatible polymeric micelles self-assembled from hyperbranched polyphosphate-based polymers. *Polym. Chem.* **2011**, *2*, 1389–1397.
- (34) Li, X. *et al.* Functional gold nanoparticles as potent antimicrobial agents against multi-drug-resistant bacteria. *ACS Nano* **2014**, *8*, 10682–10686.
- (35) Dathe, M. *et al.* Hydrophobicity, hydrophobic moment and angle subtended by charged residues modulate antibacterial and haemolytic activity of amphipathic helical peptides. *FEBS Lett.* **1997**, *403*, 208–212.
- (36) Huang, Y., Huang, J. & Chen, Y. Alpha-helical cationic antimicrobial peptides: Relationships of structure and function. *Protein Cell* **2010**, *1*, 143–152.
- (37) Huo, S. *et al.* Fully Zwitterionic Nanoparticle Antimicrobial Agents through Tuning of Core Size and Ligand Structure. *ACS Nano* **2016**, *10*, 8732–8737.
- (38) Parameswaran, N., & Patial S. necrosis factor- α signaling in macrophages. *Crit. Rev. Eukaryot. Gene Expr.* **2010**, *20*, 87-103.
- (39) Nederberg, F. *et al.* Biodegradable nanostructures with selective lysis of microbial membranes. *Nat. Chem.* **2011**, *3*, 409–414.
- (40) Hayden, S. C. *et al.* Aggregation and interaction of cationic nanoparticles on bacterial surfaces. *J. Am. Chem. Soc.* **2012**, *134*, 6920–6923 (2012)
- (41) Desjardins, R., Boulos, L. & Barbeau, B. Methods LIVE / DEAD \oplus Bac Light E: application of a new rapid staining method for direct enumeration of viable and total bacteria in drinking water. *J. Microbiol. Methods* **1999**, *37*, 77–86.
- (42) Cox, S. D. *et al.* The mode of antimicrobial action of the essential oil of *Melaleuca alternifolia* (tea tree oil). *J. Appl. Microbiol.* **2000**, *88*, 170–175.
- (43) Gupta, A., Landis, R. F. & Rotello, V. M. Nanoparticle-Based Antimicrobials: Surface Functionality is Critical. *F1000Research* **2016**, *5*, 1–10.
- (44) Anderl, J. N., Franklin, M. J. & Stewart, P. S. Role of Antibiotic Penetration Limitation in *Klebsiella pneumoniae* Biofilm Resistance to Ampicillin and Ciprofloxacin. *Antimicrob. Agents Chemother.* **2000**, *44*, 1818–1824.

- (45) Roy, S. *et al.* Mixed-species biofilm compromises wound healing by disrupting epidermal barrier function. *J. Pathol.* **2014**, *233*, 331–343.
- (46) Anderson, G. G., Moreau-Marquis, S., Stanton, B. A. & O'Toole, G. A. In vitro analysis of tobramycin-treated *Pseudomonas aeruginosa* biofilms on cystic fibrosis-derived airway epithelial cells. *Infect. Immun.* **2008**, *76*, 1423–1433.
- (47) Landis, R. F. *et al.* Cross-Linked Polymer-Stabilized Nanocomposites for the Treatment of Bacterial Biofilms. *ACS Nano* **2017**, *11*, 946–952.
- (48) Gupta, A., Das, R., Yesilbag Tonga, G., Mizuhara, T. & Rotello, V. M. Charge-Switchable Nanozymes for Bioorthogonal Imaging of Biofilm-Associated Infections. *ACS Nano* **2017**, *12*, acsnano.7b07496.
- (49) Lam, S. J. *et al.* Combating multidrug-resistant Gram-negative bacteria with structurally nanoengineered antimicrobial peptide polymers. *Nat. Microbiol.* **2016**, *1*, 16162.
- (50) Ling, L. L. *et al.* A new antibiotic kills pathogen without detectable resistance. *Nature* **2015**, *517*, 455–459.
- (51) Love, J. A., Morgan, J. P., Trnka, T. M. & Grubbs, R. H. A practical and highly active ruthenium-based catalyst that effects the cross metathesis of acrylonitrile. *Angew. Chem., Int. Ed.* **2002**, *41*, 4035–4037.
- (52) Wiegand, I., Hilpert, K. & Hancock, R. E. W. Agar and broth dilution methods to determine the minimal inhibitory concentration (MIC) of antimicrobial substances. *Nat. Protoc.* **2008**, *3*, 163–75.
- (53) Moyano, D. F. *et al.* Immunomodulatory Effects of Coated Gold Nanoparticles in LPS-Stimulated In Vitro and In Vivo Murine Model Systems. *Chem.* **2016**, *1*, 320–327.
- (54) Duncan, B. *et al.* Nanoparticle Stabilized Capsules for the Treatment of Bacterial Biofilms. *ACS Nano* **2015**, *9*, 7775–7782.
- (55) Decker, T. & Lohmann-Matthes, M. L. A quick and simple method for the quantitation of lactate dehydrogenase release in measurements of cellular cytotoxicity and tumor necrosis factor (TNF) activity. *J. Immunol. Methods* **1988**, *115*, 61–69.
- (56) Madkour, A. E., Koch, A. H. R., Lienkamp, K. & Tew, G. N. End-functionalized ROMP polymers for biomedical applications. *Macromolecules* **2010**, *43*, 4557–4561.
- (57) Li, X. *et al.* Rapid Identification of Bacterial Biofilms and Biofilm Wound Models Using a Multichannel Nanosensor. *ACS Nano* **2014**, *8*, 12014–12019.
- (58) Cafiso, V., Bertuccio, T., Spina, D., Purrello, S. & Stefani, S. Tigecycline inhibition of a mature biofilm in clinical isolates of *Staphylococcus aureus*: comparison with other drugs. *FEMS. Immunol. Med. Microbiol.* **2010**, *59*, 466–469.

(59) CLSI. *Methods for Dilution Antimicrobial Susceptibility Tests for Bacteria That Grow Aerobically; Approved Standard—Tenth Edition*. CLSI document M07-A10. Wayne, PA: Clinical and Laboratory Standards Institute; **2015**.

CHAPTER 7

HYBRIDIZED NANO-ASSEMBLIES: A PARADOX IN BIOFILM PENETRATION

“Opinions from The PhD Candidate”

7.1. Antimicrobial Nanocomposites

A wide range of carvacrol-containing polymeric nanocomposites have been presented in Chapters 2 through 5, each containing the ability to penetrate bacterial biofilms and eliminate enclosed pathogens. While each composite scaffold contains the highly antimicrobial phytochemical carvacrol, the scaffold's composite morphology throughout the oil phase and at the oil-water interface is largely different. Furthermore, the surface charge is vastly different between each composite. For instance, Chapter 2's composite is crosslinked between a polymeric amine and polymeric anhydride, generating a large negative charge at the oil-water interface. Meanwhile Chapter 4's composite is crosslinked between a polymeric maleimide and small-molecule disulfide-dithiols, retaining an overall positive charge at the interface and would empirically adopt a largely different composite morphology throughout the nano-assembly. Given the notion in literature that cationic charge is critical for bacterial membrane binding and subsequent antimicrobial activity, why is that a highly negative charged composite can additionally penetrate and contribute nearly equal antimicrobial potency as compared to its cationic counterparts? To the best of my knowledge, other than literature publications highlighted in this thesis, there are no other literature examples discussing crosslinked

polymeric nanocomposites with antimicrobial phytochemicals. Therefore, future studies on these nano-assemblies will be fundamental to not only understand their physical and biochemical mechanisms, but to also further engineer improved nano-assemblies to fight against the dangers of MDR infections. *The following are research considerations that should be investigated to further ascertain these undefined mechanisms and are merely opinions of this PhD candidate.*

7.1.1 Electrostatic Argument Doesn't Hold with Biofilms

While it is true that pathogens in their planktonic state will preferentially bind to cationic materials and subsequently lead to their demise, this argument does not hold ground when pathogens are colonized into complex 3-dimensional architectures such as biofilms. This argument holds even less merit when compounds containing true molecularity are constructed further into nanoarchitecture scaffolds or assemblies that have undefined morphologies due to characterization technique limitations. Previous reports have indicated that reactive oxidants and cationic molecules have slower penetration rates in biofilms and retard the materials through reaction, sorption, and diffusion processes. For instance, research performed by Li et al. showed that quantum dots bearing cationic charge ligands show little penetration, however adding localized hydrophobicity beyond the charged head group improved biofilm penetration.¹ Although in this instance, negatively charge quantum dots did not penetrate, it is plausible the reason for this is derived from the quantum dots poor stability in a biofilm interface where a variety of biomass containing coordinating units like amines or thiols may result in ligand dissociation and nanomaterial aggregation, although the authors (myself included) showed no reports of this and was out of the scope of the study. A more defined example has been observed with liposomes.

Previous work has demonstrated that cationic liposomes could kill biofilm pathogens at a lower concentration than neutral or anionic counterparts, however anionic liposomes penetrated just as efficiently as their cationic counterparts. This result supports the notion described in Chapter 1 that penetration does not equal activity in addition to my suggestion that charge on complex nano-assemblies is a less critical parameter when determining activity, as demonstrated in Chapters 2 and 5. I will extend an olive branch however that if the antimicrobial component has inherent electrostatic attachments, then indeed charge matters. However, in the case of these phytochemical nano-assemblies, the antimicrobial component is largely hydrophobic and contains no bias charge. Therefore, I argue that electrostatics will never give us an answer into these phytochemical nano-assemblies mechanism(s) of action. I believe efforts into understanding mechanical changes to the biofilms EPS matrix upon interacting with phytochemical nano-assemblies will provide better insights to improve these antimicrobial designs.

7.1.2 Consider Mechanical Dynamics

The EPS matrix is responsible for nearly 90% of all the dry biomass within biofilms.² Therefore, it is reasonable to suggest that EPS is fundamental for bacteria to survive in their static biofilm state by essentially being their life-line for nutrition, protection, and ultimately their release into the environment for further colonization.³ In many biofilm cases of *P. aeruginosa* the EPS is largely made of polysaccharides, Pel and Psl.⁴ Psl is fundamental for biofilms heterogenous, yet semi-ordered structure frame for the EPS matrix. Furthermore, Pel is surprisingly a cationic polysaccharide that crosslinks with eDNA additionally critical for biofilm morphology.

Each phytochemical nano-assembly had been subjected to biofilm penetration experiments using confocal microscopy. In every case, not only are the assemblies co-localized with bacteria, but can also be found throughout the entire biofilm matrix. Therefore, I became very curious to observe what happens when phytochemical nano-assemblies are added to extremely mature biofilms on a large Petri dish surface (Grown to a film thickness of a few millimeters). Within 10 seconds of incubation and very little agitation with my hand, I immediately noticed the biofilm became significantly less viscous and in fact the biofilm was completely removed from the plastic petri dish it was originally attached to. Therefore, I have reason to believe that the overall structural dynamic framework of EPS becomes severely compromised in the presence of these phytochemical nano-assemblies. I believe this hypothesis can be determined by generating Förster resonance energy transfer (FRET) labeled Pel and Psl polysaccharides and monitor the FRET signal prior to and after assembly incubation. Additionally, if Pel and Psl films could be generated on a surface and if these surfaces were incubated for a defined period, contact angle experiments may indicate differences in surface wettability prior to and after phytochemical nano-assembly incubation. Success of these experiments would garner support for my hypothesis and indicate mechanically compromised EPS is fundamental for antimicrobial activity of these assemblies enabling them to further penetrate and reach enclosed pathogens where the main antimicrobial component carvacrol can induce membrane disruption. However, I believe carvacrol does much more than disrupt pathogen membranes and can play an even greater role as a biochemical-mediated mechanical dynamic disruptor of the EPS matrix via Quorum Sensing Inhibition (QSI).⁵

7.1.3 Consider Biochemical-Mediated Mechanical Dynamics

In addition to mechanical dynamics, Quorum Sensing (QS) can be considered a biochemical-mediated mechanical dynamic with biofilms. QS ultimately leads to biofilm growth and enzyme production necessary to provide biofilm homeostasis in the form of EPS breakdown or build-up through enzymes like chitinases, collagenases, elastases.⁶ Therefore, inhibition of QS, QSI, would have dramatic effects not only on initial biofilm growth, but severely impair biofilm integrity, making it more susceptible to antimicrobial intervention. For instance, carvacrol has been known for some time to directly act as a QSI agent.⁷ Although the direct impact carvacrol has on biofilm growth is not well understood, there are literature precedence indicating its inhibition effects on *ExpI*, a homoserine lactone synthase enzyme and *ExpR*, its respective regulatory protein.⁸ Furthermore, carvacrol has been demonstrated to inhibit certain enzymes critical in extracellular matrix decomposition such as chitinases, collagenases, and elastases. However, it should be noted that carvacrol works more effectively as a biofilm inhibitor and in some cases demonstrate no effect on pre-formed biofilms.⁹ I personally find this, scientifically-speaking, a huge opportunity to reinvestigate carvacrol's activity now that carrier vehicles have been developed to enable complete phytochemical penetration into a biofilm matrix. If the scientific community were to explore QSI in the context of biofilm-penetrating nano-assemblies, I believe additional insights into carvacrol's or any other QSI agents activity on QS will become more apparent. Therefore, I suggest a repeat of prior experiments involving QSI agents loaded within these nano-assemblies. It may be possible to extract Pel/Psl from biofilms and appropriately label the polysaccharides with a carefully selected fluorophore that could be used as feed stock during biofilm growth. After these biofilms are grown with incorporated Pel/Psl feed-stock, morphological discrepancies could be

observed through confocal microscopy before and after the incubation of the phytochemical nano-assembly. Of course, careful selection of controls will be necessary, such as the use of a well known non-antimicrobial oil that previously showed no QSI activity. Although with that said, it is possible that prior non-active QSI agents may show activity upon encapsulation. If observed, this will open the possibility of discovering new QSI agents.

7.2. Antimicrobial Polymeric Nanoparticles

Chapter 6 discusses a synthetic engineering strategy to produce polymeric nanoparticles containing highly potent antimicrobial activities, even penetrating biofilms and eliminating enclosed pathogens. Prior to this research, literature insight over the past couple of decades has made it clear that careful consideration to the balance of hydrophobicity and cationic charge, or “Amphiphilic Balance”, must be made to ensure some level of antimicrobial selectivity to bacteria over mammalian cells.¹⁰ However, I was and still am not convinced “Amphiphilic Balance” is the only key parameter for antimicrobial selectivity towards bacteria.

7.2.1 Looking Beyond Amphiphilic Balance and Membrane Disruption

Work published by Sambhy et al. back in 2008, suggests that further consideration to the placement of local hydrophobic domains is equally critical, where it was observed that co-localization of the charge and hydrophobic domains reduces the antibacterial effect, however dramatically reduces the chance of red blood cell hemolysis.¹¹ Without question, there needs to be more attention in the scientific community towards reducing hemolysis effects of their natural, synthetic, and engineered antimicrobial polymers. Inspired by this discovery, I wanted to monitor this effect using semi-rigid Poly(Oxanorbornene) polymers

and instead of having the hydrophobic domain exterior to the charge head group, we embedded the domain as a bridge between the polymer backbone and charged head group. My reasoning for this selection was partially based on a previous work reported by Li et al. where they observed that increasing the hydrophobic domain exterior to the charge group increased the chance for red blood cell hemolysis and in fact, we see this same effect on these polymer scaffolds.¹² Combined with the notion that mammalian cell membranes are vastly more zwitterionic than their bacteria counterparts (negatively charged), we hypothesize these polymers are not capable of interacting with mammalian membranes as the hydrophobic domains are buried within the scaffold. Furthermore, we believe that once these polymers interact with bacterial membranes, their polymeric particle structure “unfolds” allowing the polymers to imbed, compromising membrane integrity, leading to its antimicrobial activity. Therefore, future work could reside in determining this proposed mechanism using a fluorescence recovery after photobleaching (FRAP) experiment, described in the following work which successfully applied this technique to the mammalian antimicrobial peptide LL-37.¹³

While the following proposed experiment can be used to monitor these polymeric nanoparticles effect on bacterial membranes, I am reluctant to believe that membrane disruption is the only activity these polymers have. Even though propidium iodide experiments indicate bacteria undergo membrane disruption, the disruption may arise from the polymers binding to extracellular DNA. This can result in DNA aggregation or inhibition of protein transcription that ultimately leads to a compromised membrane. Work published recently by Gupta et al. identified that the activity of their antimicrobial gold nanoparticles goes beyond membrane disruption and through proteomic analysis, indicated

a significant down-regulation of efflux pump membrane proteins.¹⁴ I believe a similar study should be applied to these polymeric nanoparticle systems to better ascertain less obvious action mechanisms that can attribute to the observed membrane disruption experiments.

7.2.2 Further Analysis into Polymeric Nanoparticle-Biofilm Dynamics

Furthermore, understanding how these polymeric nanoparticles can penetrate biofilms and eliminating enclosed pathogens is an equally important next step. Previous studies on antimicrobial peptides indicate they are capable of penetrating biofilms, however are less effective against mature biofilms.¹⁵ This empirically makes sense as any oligomeric or polymeric cationic material possesses strong binding affinities to respective anionic materials enclosed within the biofilm matrix such as eDNA. In fact, previous studies have indicated that mature biofilms incubated with antimicrobial peptides are unable to reach enclosed pathogens and become either sequestered via electrostatic interactions with eDNA.¹⁶ Alternatively, cationic polymeric materials within the biofilm matrix prevent penetration through electrostatic repulsion. I believe the polymeric nanoparticles presented in Chapter 6 falls victim to the same outcome and evidence of this observation can be seen in the confocal microscopy experiments monitoring penetration depth. While fluorescence signatures from the polymer is shown co-localized with bacteria, polymers can be seen adhered throughout the film, most likely binding to anionic biomaterials enclosed within the matrix. I hypothesize that quantitative proof of this interaction can be performed in a similar fashion as proposed in the antimicrobial nanocomposite section. If eDNA can be isolated, carefully labelled with a FRET dye, and reintroduced back as a feed stock for biofilm growth, a respective FRET dye can be added within the polymeric nanoparticle and monitor any observed FRET signatures. Success of

this experiment would heavily support the notion of polymeric entanglement with the biofilm matrix as it was observed the amount of polymer necessary to kill biofilms increases from low nanomolar to low micromolar concentrations.

7.2.3 Optimization to Prevent Protein Fouling

While the polymer nanoparticles presented in Chapter 6 demonstrate low MICs, great hemolytic activities, and biofilm penetration, these valuable characteristics nearly disappear *in vitro* when incubated in a media that contains negatively charged serum proteins. Preliminary dynamic light scattering (DLS) experiments indicate that when these polymer nanoparticles are in the presence of serum proteins, a single protein will adhere, changing the nanomaterials composition and overall charge. This is not surprising as numerous nanomaterials fail *in vivo* due to protein corona formation.¹⁷ Therefore, additional optimization of the polymeric nanoparticles will need to be performed, followed by testing their MICs with planktonic bacteria in non-serum and serum containing media. One plausible strategy that demonstrated success in Chapter 2 is to generate polymeric nanoparticles that bear an overall negative charge. This would, in theory, reduce protein corona formation due to electrostatic repulsion. Careful selection into what anionic group to use will be critical as to not compromise membrane adhesion onto bacterium. I hypothesize that given the nature of these polymeric nanoparticles, initial adherence may result in morphological changes of the particles, allowing them to embed within the membranes resulting in a killing effect. However, reinvestigation into bacterium proteomics will need to be performed as an anionic polymeric nanoparticle may show discrepancies in its activity compared to its cationic analogs. If successful, I am confident

anionic analogs will be capable of penetrating biofilms, although penetration kinetics will change accordingly.

7.3. References

- (1) Li, X.; Yeh, Y.-C.; Giri, K.; Mout, R.; Landis, R. F.; Prakash, Y. S.; Rotello, V. M. Control of Nanoparticle Penetration into Biofilms Through Surface Design. *Chem. Comm.* **2015**, *51*, 282-285.
- (2) Shi, Y.; Huang, J.; Zeng, G.; Gu, Y.; et al. Exploiting Extracellular Polymer Substances (EPS) Controlling Strategies for Performance Enhancement of Biological Wastewater Treatments: An Overview. *Chemosphere* **2017**, *180*, 396-411.
- (3) Hall, C. W.; Mah, T.-F. Molecular Mechanisms of Biofilm-Based Antibiotic Resistance and Tolerance in Pathogenic Bacteria. *FEMS Microbiol. Rev.* **2017**, *41*, 276-301.
- (4) Franklin, M. J.; Nivens, D. E.; Weadge, J. T. et al. Biosynthesis of the *Pseudomonas aeruginosa* Extracellular Polysaccharides, Alginate, Pel, and Psl. *Front Microbiol.* **2011**, *2*, 167-170.
- (5) Burt, S. A.; Ojo-Fakunle, V. T. A.; Woertman, J.; Veldhuizen, E. J. A. The Natural Antimicrobial Carvacrol Inhibits Quorum Sensing in *Chromobacterium violaceum* and Reduces Bacterial Biofilm Formation at Sub-Lethal Concentrations. *PLoS One* **2014**, *9*, e93414.
- (6) Joshi, J. R.; Khazanov, N.; Senderowitz, H.; Burdman, S.; Lipsky, A.; Yedidia, I. Plant Phenolic Volatiles Inhibit Quorum Sensing in Pectobacteria and Reduce Their Virulence by Potential Binding to ExpI and ExpR Proteins. *Sci. Rep.* **2016**, *6*, 38126.
- (7) Espina, L.; Pagan, R.; Lopez, D.; Garcia-Gonzalo, D. Individual constituents from Essential Oils Inhibit Biofilm Mass Production by Multi-Drug Resistant *Staphylococcus aureus*. *Molecules* **2015**, *20*, 11357–11372.
- (8) Cui, Y. et al. ExpR, a LuxR Homolog of *Erwinia carotovora* subsp. *Carotovora*, Activates Transcription of rsmA, Which Specifies a Global Regulatory RNA-Binding Protein. *J. Bacteriol.* **2005**, *187*, 4792–4803.
- (9) Gray K. M.; Garey J. R. (2001) The evolution of bacterial LuxI and LuxR quorum sensing regulators. *Microbiology* **2001**, *147*, 2379–2387.
- (10) Findlay, B.; Zhanel, G. G.; Schweizer, F. Cationic Amphiphiles, a New Generation of Antimicrobials Inspired by the Natural Antimicrobial Peptide Scaffold. *Antimicrob. Agents Chemother.* **2010**, *54*, 4049-4058.
- (11) Sambhy, V.; Peterson, B. R.; Sen, A. Antibacterial and Hemolytic Activities of Pyridinium Polymers as a Function of the Spatial Relationship Between the Positive Charge and the Pendant Alkyl Tail. *Angew. Chem. Int. Ed.* **2008**, *47*, 1250-1254.
- (12) Li, X.; Robinson, S. M.; Gupta, A.; Saha, K.; et al. Functional Gold Nanoparticles as Potent Antimicrobial Agents Against Multi-Drug-Resistant Bacteria. *ACS Nano* **2014**, *8*, 10682-10686.

- (13) Sun, Y.; Sun, T.-L.; Huang, H. W. Mode of Action of Antimicrobial Peptides on *E. coli* Spheroplasts. *Biophys. J.* **2016**, *111*, 132-139.
- (14) Gupta, A.; Saleh, N. M.; Das, R.; Landis, R. F.; et al. Synergistic Antimicrobial Therapy Using Nanoparticles and Antibiotics for the Treatment of Multidrug-Resistant Bacterial Infection. *Nano Futures* **2017**, *1*, 015004.
- (15) Luca, M. D.; Maccari, G.; Nifosi, R. Treatment of Microbial Biofilms in the Post-Antibiotic Era: Prophylactic and Therapeutic Use of Antimicrobial Peptides and Their Design by Bioinformatics Tools. *Pathogens and Disease* **2014**, *70*, 257-270.
- (16) Jones, E. A.; McGillivray, G.; Bakaletz, L. O. Extracellular DNA Within a Nontypeable *Haemophilus Influenzae*-Induced Biofilm Binds Human Beta Defensin-3 and Reduces its Antimicrobial Activity. *J. Innate. Immun.* **2013**, *5*, 24–38.
- (17) Blanco, E.; Shen, H.; Ferrari, M. Principles of Nanoparticle Design for Overcoming Biological Barriers to Drug Delivery. *Nat. Biotechnol.* **2015**, *33*, 941-951.

BIBLIOGRAPHY

- Abedon, S. T. Ecology of Anti-Biofilm Agents I: Antibiotics Versus Bacteriophages. *Pharmaceuticals* **2015**, *8*, 525-558.
- Abreu, F. O. M. S.; Oliveira, E. F.; Paula, H. C. B.; de Paula, R. C. M. Chitosan/Cashew Gum Nanogels for Essential Oil Encapsulation. *Carbohydr. Polym.* **2012**, *89*, 1277-1282.
- Ahmad, I.; Beg, A. Z. Antimicrobial and Phytochemical Studies of 45 Indian Medicinal Plants Against Multi-Drug Resistant Pathogens. *J. Ethnopharmacol.* **2001**, *74*, 113–123.
- Akhtar, J.; Siddiqui, H. H.; Fareed, S.; Badruddeen; Khalid, M.; Aqil, M. Nanoemulsion: For Improved Oral Delivery of Repaglinide. *Drug Deliv.* **2016**, *23*, 2026-2034.
- Al-Badri, Z. M.; Tew, G. N. Well-defined Acetylene-Functionalized Oxanorbornene Polymers and Block Copolymers. *Macromolecules* **2008**, *41*, 4173-4179.
- Amaral, D. M. F.; Bhargava, K. Essential Oil Nanoemulsions and Food Applications. *Adv. Food Technol. Nutr. Sci. Open J.* **2015**, *1*, 84-87.
- Anderl, J. N.; Franklin, M. J.; Stewart, P. S. Role of Antibiotic Penetration Limitation in *Klebsiella pneumoniae* Biofilm Resistance to Ampicillin and Ciproflaxacin. *Antimicrob. Agents Chemother.* **2000**, *44*, 1818–1824.
- Anderson, G. G., Moreau-Marquis, S., Stanton, B. A. & O'Toole, G. A. In vitro analysis of tobramycin-treated *Pseudomonas aeruginosa* biofilms on cystic fibrosis-derived airway epithelial cells. *Infect. Immun.* **2008**, *76*, 1423–1433.
- Antibiotic / Antimicrobial Resistance. (2018, March 05). Retrieved from <https://www.cdc.gov/drugresistance/about.html>
- Anwer, M. K.; Jamil, S.; Ibnouf, E. O.; Shakeel, F. Enhanced Antibacterial Effects of Clove Essential Oil by Nanoemulsion. *J. Oleo. Sci.* **2014**, *63*, 347-354.
- Arnt, L., Nüsslein, K. & Tew, G. N. Nonhemolytic abiogenic polymers as antimicrobial peptide mimics. *J. Polym. Sci. Part A Polym. Chem.* **2004**, *42*, 3860–3864.
- Ashwin, P. T.; McDonnel, P. J.; Collagen Cross-Linkage: a Comprehensive Review And Directions For Future Research. *Br. J. Ophthalmol.* **2010**, *94*, 965e970.
- Au, V.; Madison, A. Effects Of Singlet Oxygen On The Extracellular Matrix Protein Collagen: Oxidation Of The Collagen Crosslink Histidinohydroxylysinonorleucine And Histidine. *Arch Biochem Biophys.* **2000**, *384*, 133-142.
- Babb, R.; Pirofski, L. -A. Help is on the Way: Monoclonal Antibody Therapy for Multi-Drug Resistant Bacteria. *Virulence* **2017**, *8*, 1055-1058.

- Baltzer, S. a. & Brown, M. H. Antimicrobial Peptides – Promising Alternatives to Conventional Antibiotics. *J. Mol. Microbiol. Biotechnol.* **2011**, *20*, 228–235.
- Baran, A.; Flisiak, I.; Jaroszewicz, J.; Swiderska, J. Serum Adiponectin and Leptin Levels in Psoriatic Patients According to Topical Treatment. *J. Dermatol. Treat.* **2015**, *26*, 134-138.
- Berthold, N.; Czihal, P.; Fritsche, S.; Sauer, U.; Schiffer, G.; Knappe, D.; Alber, G.; Hoffmann, R. Novel Apidaecin 1b Analogs with Superior Serum Stabilities for Treatment of Infections by Gram-Negative Pathogens. *Antimicrob. Agents Chemother.* **2013**, *57*, 402-409.
- Bjarnsholt, T. The Role of Bacterial Biofilms in Chronic Infections. *APMIS* **2013**, *121*, 1-58.
- Blanco, E.; Shen, H.; Ferrari, M. Principles of Nanoparticle Design for Overcoming Biological Barriers to Drug Delivery. *Nat. Biotechnol.* **2015**, *33*, 941-951.
- Boeckel, T. P. V.; Glennon, E. E.; Chen, D.; Gilbert, M.; Robinson, T. P.; Grenfell, B. T.; Levin, S. A.; Bonhoeffer, S.; Laxminarayan, R. Reducing Antimicrobial Use in Food Animals. *Science* **2017**, *357*, 1350-1352.
- Boger, D. L. Vancomycin, Teicoplanin, and Ramoplanin: Synthetic and Mechanistic Studies. *Med. Res. Rev.* **2001**, *21*, 356-381.
- Boneca, I. G.; Chiosis, G. Vancomycin Resistance: Occurrence, Mechanisms and Strategies to Combat it. *Expert Opin. Ther. Targets* **2003**, *7*, 311-328.
- Bowler, L. L.; Zhanel, G. G.; Ball, T. B.; et al. Mature *Pseudomonas aeruginosa* Biofilm Preval Compared to Young Biofilms in the Presence of Ceftazidime. *Antimicrob. Agents Ch.* **2012**, *56*, 4976-4979.
- Bryskier, A. (ed.) **2005**, Antimicrobial Agents: Antibacterials and Antifungals. *ASM Press*, Washington, DC.
- Buchwald, U. K.; Pirofski, L. Immune Therapy for Infectious Diseases at the Dawn of the 21st Century: The Past, Present, and Future Role of Antibody Therapy, Therapeutic Vaccination, and Biological Response Modifiers. *Curr. Pharm. Des.* **2003**, *9*, 945-968.
- Burt, S. A.; Ojo-Fakunle, V. T. A.; Woertman, J.; Veldhuizen, E. J. A. The Natural Antimicrobial Carvacrol Inhibits Quorum Sensing in *Chromobacterium violaceum* and Reduces Bacterial Biofilm Formation at Sub-Lethal Concentrations. *PLoS One* **2014**, *9*, e93414.
- Burt, S. Essential Oils: Their Antibacterial Properties and Potential Applications in Foods – A Review. *Int. J. Food Microbiol.* **2004**, *94*, 223-253.

- Bush, K.; Fisher, J. F. Epidemiological Expansion, Structural Studies, and Clinical Challenges of New Beta-Lactamases from Gram-Negative Bacteria. *Annu. Rev. Microbiol.* **2011**, *65*, 455-478.
- Bush, K.; Jacoby, G. A. Updated Functional Classification of β -Lactamases. *Antimicrob. Agents Chemother.* **2010**, *54*, 969-976.
- Byrd, M. S.; Sadovskaya, I.; Vinogradov, E.; et al. Genetic and Biochemical Analyses of the *Pseudomonas aeruginosa* Psl Exopolysaccharide Reveal Overlapping Roles for Polysaccharide Synthesis Enzymes in Psl and LPS Production. *Mol. Microbiol.* **2009**, *73*, 622-638.
- Cafiso, V., Bertuccio, T., Spina, D., Purrello, S. & Stefani, S. Tigecycline inhibition of a mature biofilm in clinical isolates of *Staphylococcus aureus*: comparison with other drugs. *FEMS. Immunol. Med. Microbiol.* **2010**, *59*, 466–469.
- Castanon, J. I. R. History of the use of Antibiotic as Growth Promoters in European Poultry Feeds. *Poult. Sci.* **2007**, *86*, 2466-2471.
- Chandra Sekhara Rao, G.; Satish Kumar, M.; Mathivanan, N.; Bhanoji Rao, M. E. The Use of Polymer-Based Electrospun Nanofibers Containing Amorphous Drug Dispersions for the Delivery of Poorly Water-Soluble Pharmaceuticals. *Pharmazie* **2004**, *59*, 5–9.
- Chang, Y.; McLandsborough, L.; McClements, D. J. Fabrication, Stability and Efficacy of Dual-component Antimicrobial Nanoemulsions: Essential Oil (Thyme Oil) and Cationic Surfactant (Lauric Arginate). *Food Chem.* **2015**, *172*, 298-304.
- Chang, Y.; McLandsborough, L.; McClements, D. J. Physicochemical Properties and Antimicrobial Efficacy of Carvacrol Nanoemulsions Formed by Spontaneous Emulsification. *J. Agric. Food Chem.* **2013**, *61*, 8906–8913.
- Chen, C. *et al.* Photo-responsive, biocompatible polymeric micelles self-assembled from hyperbranched polyphosphate-based polymers. *Polym. Chem.* **2011**, *2*, 1389–1397.
- Chen, H.; Davidson, P. M.; Zhong, Q. Impacts of Sample Preparation Methods on Solubility and Antilisterial Characteristics of Essential Oil Components in Milk. *Appl. Environ. Microbiol.* **2013**, *80*, 907–916.
- Cheng, J.; Chin, W.; Dong, H.; Xu, L.; Zhong, G.; Huang, Y.; Li, L.; Xu, K.; Wu, M.; Hedrick, J. L.; Yang, Y. Y.; Fan, W. Biodegradable Antimicrobial Polycarbonates with In Vivo Efficacy Against Multidrug-Resistant MRSA Systemic Infection. *Adv. Health c. Mater.* **2015**, *4*, 2128-2136.
- Cheng, R.; Feng, F.; Meng, F.; Deng, C.; Feijen, J.; Zhong, Z. Glutathione-Responsive Nano-Vehicles as a Promising Platform for Targeted Intracellular Drug and Gene Delivery. *J. Control. Release* **2011**, *152*, 2–12.

- Chiang, W.- C.; Pamp, S. J.; Nilsson, M.; et al. The Metabolically Active Subpopulation in *Pseudomonas aeruginosa* Biofilms Survives Exposure to Membrane-Targeting Antimicrobials via Distinct Molecular Mechanisms. *FEMS Immunol. Med. Mic.* **2012**, *65*, 245-256.
- Chiang, W.-C.; Nilsson, M.; Jensen, P. O.; et al. Extracellular DNA Shields Against Aminoglycosides in *Pseudomonas aeruginosa* Biofilms. *Antimicrob. Agents Ch.* **2013**, *57*, 2352-2361.
- Choi, S. *et al.* De novo design and in vivo activity of conformationally restrained antimicrobial arylamide foldamers. *Proc. Natl. Acad. Sci.* **2009**, *106*, 6968–6973.
- CLSI. *Methods for Dilution Antimicrobial Susceptibility Tests for Bacteria That Grow Aerobically; Approved Standard—Tenth Edition*. CLSI document M07-A10. Wayne, PA: Clinical and Laboratory Standards Institute; **2015**.
- Cole, J. P.; Lessard, J. J.; Lyon, C. K.; Tuten, B. T.; Berda, E. B. Intra-chain Radical Chemistry as a Route to Poly(Norbornene Imide) Single-chain Nanoparticles: Structural Considerations and the Role of Adventitious Oxygen. *Polym. Chem.* **2015**, *6*, 5555-5559.
- Costerton, J. W., Stewart, P. S. & Greenberg, E. P. Bacterial biofilms: a common cause of persistent infections. *Science* **1999**, *284*, 1318–1322.
- Costerton, J. W.; Stewart, P. S.; Greenberg, E. P. Bacterial Biofilms in Nature and Disease. *Annu. Rev. Microbiol.* **1987**, *41*, 435-464.
- Costerton, J. W.; Stewart, P. S.; Greenberg, E. P. Bacterial Biofilms: A Common Cause of Persistent Infections. *Science* **1999**, *284*, 1318-1322.
- Cowan, M. M. Plant Products as Antimicrobial Agents. *Clin. Microbiol. Rev.* **1999**, *12*, 564–582.
- Cox, S. D. *et al.* The mode of antimicrobial action of the essential oil of *Melaleuca alternifolia* (tea tree oil). *J. Appl. Microbiol.* **2000**, *88*, 170–175.
- Cui, Y. *et al.* ExpR, a LuxR Homolog of *Erwinia carotovora* subsp. *Carotovora*, Activates Transcription of rsmA, Which Specifies a Global Regulatory RNA-Binding Protein. *J. Bacteriol.* **2005**, *187*, 4792–4803.
- D’Costa, V. M.; King, C. E.; Kalan, L.; Morar, M.; Sung, W. W.; Schwarz, C.; et al. Antibiotic resistance is ancient. *Nature* **2011**, *477*, 457-461.
- Dafopoulou, K.; Xavier, B. B.; Hotterbeekx, A.; Janssens, L.; Lammens, C.; De, E.; Goossens, H.; Tsakris, A.; Malhotra-Kumar, S.; Pournaras, S. Colistin-resistant *Acinetobacter Baumannii* Clinical Strains with Deficient Biofilm Formation. *Antimicrob. Agents Chemother.* **2016**, *60*, 1892-1895.

- Dathe, M. *et al.* Hydrophobicity, hydrophobic moment and angle subtended by charged residues modulate antibacterial and haemolytic activity of amphipathic helical peptides. *FEBS Lett.* **1997**, *403*, 208–212.
- Datta, N.; Hughes, V. M. Plasmids of the Same Inc Groups in Enterobacteria Before and After the Medical Use of Antibiotics. *Nature* **1983**, *306*, 616-617.
- Davies, J. Vicious Circles: Looking Back on Resistance Plasmids. *Genetics* **1995**, *139*, 1465-1468.
- Davies, J.; Davies, D. Origins and Evolution of Antibiotic Resistance. *Microbiol. Mol. Biol. Rev.* **2010**, *74*, 417-433.
- De Grandis, R. A.; Resende, F. A.; da Silva, M. M.; Pavan, F. R.; Batista, A. A.; Varanda, E. A. In Vitro Evaluation of the Cyto-Genotoxic Potential of Ruthenium(II) SCAR Complexes: A Promising Class of Antituberculosis Agents. *Mutat. Res. Genet. Toxicol. Environ. Mutagen.* **2016**, *11*, 798-799.
- Decker, T.; Lohmann-Matthes, M. L. A Quick and Simple Method for the Quantitation of Lactate Dehydrogenase Release in Measurements of Cellular Cytotoxicity and Tumor Necrosis Factor (TNF) Activity. *J. Immunol. Methods* **1988**, *115*, 61–69.
- Del Pozo, J. L. & Patel, R. Infection Associated with Prosthetic Joints. *N. Engl. J. Med.* **2009**, *361*, 787–794.
- Del Pozo, J. L.; Patel, R. The Challenge of Treating Biofilm-Associated Bacterial Infections. *Clin. Pharmacol. Ther.* **2007**, *82*, 204–209.
- Delbrück, M. The Growth of Bacteriophage and Lysis of the Host. *J. Gen. Physiol.* **1940**, *23*, 643-660.
- Demain, A. L.; Sanchez, S. Microbial Drug Discovery: 80 Years of Progress. *J. Antibiot.* **2009**, *62*, 5-16.
- Dennison, S. R.; Harris, F.; Mura, M.; Morton, L. H. G.; Zvelindovsky, A.; Phoenix, D. A. A Novel Form of Bacterial Resistance to the Action of Eukaryotic Host Defense Peptides, the Use of a Lipid Receptor. *Biochemistry*, **2013**, *52*, 6021-6029.
- Desjardins, R., Boulos, L. & Barbeau, B. Methods LIVE / DEAD ® Bac Light E: application of a new rapid staining method for direct enumeration of viable and total bacteria in drinking water. *J. Microbiol. Methods* **1999**, *37*, 77–86.
- DiGiandomenico, A.; Sellman, B. R. Antibacterial Monoclonal Antibodies: The Next Generation? *Curr. Opin. Microbiol.* **2015**, *27*, 78-85.
- Djeussi, D. E.; Noumedem, J. A. K.; Seukep, J. A.; Fankam, A. G.; Voukeng, I. K.; Tankeo, S. B.; Nkuete, A. H. L.; Kuete, V. Antibacterial Activities of Selected Edible Plants

Extracts Against Multidrug-Resistant Gram-Negative Bacteria. *BMC Complement. Altern. Med.* **2013**, *13*, 164–171

Domenech, M.; Ramos-Sevillano, E.; Garcia, E.; Moscoso, M.; Yuste, J. Biofilm Formation Avoids Complement Immunity and Phagocytosis of *Streptococcus pneumoniae*. *Infect. Immun.* **2013**, *81*, 2606-2615.

Donlan, R. M. Biofilms and device-associated infections. *Emerg. Infect. Dis.* **2001**, *7*, 277–281.

Donsì, F.; Annunziata, M.; Vincenzi, M.; Ferrari, G. Design of Nanoemulsion-Based Delivery Systems of Natural Antimicrobials: Effect of the Emulsifier. *J. Biotechnol.* **2012**, *159*, 342–350.

Drenkard, E.; Ausubel, F. M. *Pseudomonas* Biofilm Formation and Antibiotic Resistance are Linked to Phenotypic Variation. *Nature* **2002**, *416*, 740–743.

Duncan, B.; Landis, R. F.; Jerri, H. A.; Normand, V.; Benczedi, D.; Ouali, L.; Rotello, V. M. Hybrid Organic-inorganic Colloidal Composite 'sponges' via Internal Crosslinking. *Small* **2015**, *11*, 1302-1309.

Duncan, B.; Landis, R. F.; Jerri, H. A.; Normand, V.; et al. Hybrid Organic-Inorganic Colloidal Composite 'Sponges' via Internal Crosslinking. *Small* **2015**, *11*, 1302-1309.

Duncan, B.; Li, X.; Landis, R. F.; Kim, S. T.; Gupta, A.; Wang, L. S.; Ramanathan, R.; Tang, R.; Boerth, J. A.; Rotello, V. M. Nanoparticle-Stabilized Capsules for the Treatment of Bacterial Biofilms. *ACS Nano* **2015**, *9*, 7775-7782.

Duncan, N. C.; Hay, B. P.; Hagaman, E. W.; Custelcean, R. Thermodynamic, Kinetic, and Structural Factors in the Synthesis of Imine-Linked Dynamic Covalent Frameworks. *Tetrahedron* **2012**, *68*, 53-64.

Eberhard, A.; Burlingame, A. L.; Eberhard, C.; et al. Structural Identification of Autoinducer of *Photobacterium Fischeri* Luciferase. *Biochemistry* **1981**, *20*, 2444-2449.

El Asbahani, A.; Miladi, K.; Badri, W.; Sala, M.; et al. Essential Oils: From Extraction to Encapsulation. *Int. J. Pharm.* **2015**, *483*, 220-243.

Elraiyah, T.; Domecq, J. P.; Prutsky, G.; Tsapas, A.; et al. A Systematic Review and Meta-Analysis of Debridement Methods For Chronic Diabetic Foot Ulcers. *J. Vasc. Surg.* **2016**, *63*, 37S-45S.

Espina, L.; Berdejo, D.; Alfonso, P.; García-Gonzalo, D.; Pagan, R. Potential Use of Carvacrol and Citral to Inactivate Biofilm Cells and Eliminate Biofouling. *Food Control* **2017**, *82*, 256-265.

- Espina, L.; Pagan, R.; Lopez, D.; Garcia-Gonzalo, D. Individual constituents from Essential Oils Inhibit Biofilm Mass Production by Multi-Drug Resistant *Staphylococcus aureus*. *Molecules* **2015**, *20*, 11357–11372.
- Farzaei, M. H.; Bahramsoltani, R.; Abbasabadi, Z.; Rahimi, R. A Comprehensive Review on Phytochemical and Pharmacological Aspects of *Elaeagnus Angustifolia* L. *J. Pharm. Pharmacol.* **2015**, *67*, 1467-1480.
- Fazli, M.; Bjarnsholt, T.; Kirketerp-Møller, K.; Jørgensen, B.; Andersen, A. S.; Krogfelt, K. A.; Givskov, M.; Tolker-Nielsen, T. Nonrandom Distribution of *Pseudomonas aeruginosa* and *Staphylococcus aureus* in Chronic Wounds. *J. Clin. Microbiol.* **2009**, *47*, 4084–4089.
- Fernandes, R. V.; Borges, S. V.; Botrel, D. A. Gum Arabic Starch, Maltodextrin, and Inulin as Wall Materials on the Microencapsulation of Rosemary Essential Oil. *Carbohydr. Polym.* **2014**, *101*, 524-532.
- Findlay, B.; Zhanel, G. G.; Schweizer, F. Cationic Amphiphiles, a New Generation of Antimicrobials Inspired by the Natural Antimicrobial Peptide Scaffold. *Antimicrob. Agents Chemother.* **2010**, *54*, 4049-4058.
- Flemming, H.-C.; Wingender, J.; Szewzyk, U.; Steinberg, P.; Rice, S. A.; Kjelleberg, S. Biofilms: An Emergent Form of Bacterial Life. *Nat. Rev. Microbiol.* **2016**, *14*, 563–575.
- Franklin, M. J.; Nivens, D. E.; Weadge, J. T. et al. Biosynthesis of the *Pseudomonas aeruginosa* Extracellular Polysaccharides, Alginate, Pel, and Psl. *Front Microbiol.* **2011**, *2*, 167-170.
- Freire Rocha Caldas, G.; Araujo, A. V.; Albuquerque, G. S.; Silva-Neto Jda, C.; Costa-Silva, J. H.; de Menezes, I. R.; Leite, A. C.; da Costa, J. G.; Wanderley, A. G. Repeated-doses Toxicity Study of the Essential Oil of *Hyptis Martiusii* Benth. (Lamiaceae) in Swiss Mice. *Evid. Based Complement. Alternat. Med.* **2013**, *2013*, 856168.
- Freire Rocha Caldas, G.; Araújo, A. V.; Albuquerque, G. S.; Silva-Neto, J. da C.; Costa-Silva, J. H.; de Menezes, I. R. A.; Leite, A. C. L.; da Costa, J. G. M.; Wanderley, A. G. Curcumin and Diabetes: A Systematic Review. *Evidence-Based Complement. Altern. Med.* **2013**, *2013*, 1–11.
- Furci, L.; Baldan, R.; Bianchini, V.; et al. New Role for Human Alpha-Defensin 5 in the Fight Against Hypervirulent *Clostridium difficile* Stains. *Infect. Immun.* **2015**, *83*, 986-995.
- Fux, C. A.; Costerton, J. W.; Stewart, P. S.; Stoodley, P. Survival Strategies of Infectious Biofilms. *Trends Microbiol.* **2005**, *13*, 34-40.
- Gabriel, G. J. et al. Synthetic Mimic of Antimicrobial Peptide with Nonmembrane-Disrupting Antibacterial Properties. *Biomacromolecules* **2008**, *9*, 2980–2983.

- Gèze, A.; Putaux, J.-L.; Choisnard, L.; Jéhan, P.; Wouessidjewe, D. Long Term Shelf Stability of Amphiphilic B-Cyclodextrin Nanospheres Suspensions Monitored by Dynamic Light Scattering and Cyro-Transmission Electron Microscopy. *J. Microencapsul.* **2004**, *21*, 607–613.
- Gray K. M.; Garey J. R. (2001) The evolution of bacterial LuxI and LuxR quorum sensing regulators. *Microbiology* **2001**, *147*, 2379–2387.
- Grillaud, M.; Russier, J.; Bianco, A. Polycationic Adamantane-Based Dendrons of Different Generations Display High Cellular Uptake Without Triggering Cytotoxicity. *J. Am. Chem. Soc.* **2014**, *136*, 810-819.
- Gullberg, E.; Cao, S.; Berg, O.; Ilback, C.; et al. Selection of Resistant Bacteria at Very Low Antibiotic Concentrations. *PLoS Pathog.* **2011**, *7*, e1002158.
- Gupta, A., Das, R., Yesilbag Tonga, G., Mizuhara, T. & Rotello, V. M. Charge-Switchable Nanozymes for Bioorthogonal Imaging of Biofilm-Associated Infections. *ACS Nano* **2017**, *12*, acsnano.7b07496.
- Gupta, A., Landis, R. F. & Rotello, V. M. Nanoparticle-Based Antimicrobials: Surface Functionality is Critical. *F1000Research* **2016**, *5*, 1–10.
- Gupta, A.; Saleh, N. M.; Das, R.; Landis, R. F.; et al. Synergistic Antimicrobial Therapy Using Nanoparticles and Antibiotics for the Treatment of Multidrug-Resistant Bacterial Infection. *Nano Futures* **2017**, *1*, 015004.
- Hall, C. W.; Mah, T.-F. Molecular Mechanisms of Biofilm-Based Antibiotic Resistance and Tolerance in Pathogenic Bacteria. *FEMS Microbiol. Rev.* **2017**, *41*, 276-301.
- Hancock, R. E. W. & Sahl, H.-G. Antimicrobial and host-defense peptides as new anti-infective therapeutic strategies. *Nat. Biotech.* **2006**, *24*, 1551–1557.
- Handbook of Biologically Active Peptides*, Kastin, A. J. (Ed.) Academic Press: San Diego, CA, USA, **2006**.
- Harris, S. R. *et al.* Evolution of MRSA During Hospital Transmission and Intercontinental Spread. *Science* **2010**, *327*, 469–474.
- Hatfull, G. F.; Hendrix, R. W. Bacteriophages and their Genomes. *Curr. Opin. Virol.* **2011**, *1*, 298-303.
- Haugland, R. P. *Handbook of Fluorescent Probes and Research Products*. Eugene, OR: Molecular Probes, **2002**, Print.
- Hayden, S. C. *et al.* Aggregation and interaction of cationic nanoparticles on bacterial surfaces. *J. Am. Chem. Soc.* **2012**, *134*, 6920–6923 (2012)
- Hintz, T.; Matthews, K. K.; Di, R. The Use of Plant Antimicrobial Compounds for Food Preservation. *Biomed. Res. Int.* **2015**, *2015*, 246264.

- Hodyra-Stefaniak, K.; Miernikiewicz, P.; Drapala, J.; et al. Mammalian Host-Versus-Phage Immune Response Determines Phage Fate *in vivo*. *Sci. Rep.* **2015**, *5*, 14802.
- Høiby, N. Recent Advances in the Treatment of *Pseudomonas aeruginosa* Infections in Cystic Fibrosis. *BMC Med.* **2011**, *9*, 32.
- Høiby, N.; Ciofu, O.; Johansen, H. K.; Song, Z. J.; Moser, C.; Jensen, P. Ø.; Molin, S.; Givskov, M.; Tolker-Nielsen, T.; Bjarnsholt, T. The Clinical Impact of Bacterial Biofilms. *Int. J. Oral. Sci.* **2011**, *3*, 55-65.
- Hong, K.; Park, S. Melamine Resin Microcapsules Containing Fragrant Oil: Synthesis and Characterization. *Mater. Chem. Phys.* **1999**, *58*, 128-131.
- Horrevorts, A. M.; Borst, J.; Puyk, J. T.; Ridder, R. D.; Dzoljic-Danilovic, J. E.; et al. Ecology of *Pseudomonas aeruginosa* in Patients With Cystic Fibrosis. *J. Med. Microbiol.* **1990**, *31*, 119-124.
- Hosseinkhani, F.; Jabalameli, F.; Banar, M.; Abdellahi, N.; Taherikalani, M.; van Leeuwen, W. B.; Emaneini, M. Monoterpene Isolated from the Essential Oil of *Trachyspermum Ammi* Is Cytotoxic to Multidrug-Resistant *Pseudomonas Aeruginosa* and *Staphylococcus Aureus* Strains. *Rev. Soc. Bras. Med. Trop.* **2016**, *49*, 172-176.
- Hrvatín, V. Combating Antibiotic Resistance: New Drugs or Alternative Therapies? *CMAJ* **2017**, *189*, E1199.
- Hu, A. L.; Zheng, M. C.; Li, W. J. Modern Clinical Nursing Practice of Wound and Stoma. *Peking Union Medical College Press* **2010**, *11*.
- Huang, Y., Huang, J. & Chen, Y. Alpha-helical cationic antimicrobial peptides: Relationships of structure and function. *Protein Cell* **2010**, *1*, 143–152.
- Huo, S. *et al.* Fully Zwitterionic Nanoparticle Antimicrobial Agents through Tuning of Core Size and Ligand Structure. *ACS Nano* **2016**, *10*, 8732–8737.
- Hwang, J. S.; Kim, J. N.; Wee Y. J.; Yun, J. S.; Jang, H. G.; Kim S. H.; Ryu, H. W. Preparation and Characterization of Melamine-Formaldehyde Resin Microcapsules Containing Fragrant Oil. *Biotechnol. Bioproc. E* **2006**, *11*, 332-336.
- Iannitelli, A.; Grande, R.; Di Stefano, A.; Di Giulio, M.; et al. Potential Antibacterial Activity of Carvacrol-Loaded Poly(DL-Lactide-co-Glycolide) (PLGA) Nanoparticles Against Microbial Biofilm. *Int. J. Mol. Sci.* **2011**, *12*, 5039-5051.
- Ilker, M. F., Nüsslein, K., Tew, G. N. & Coughlin, E. B. Tuning the Hemolytic and Antibacterial Activities of Amphiphilic Polynorbornene Derivatives. *J. Am. Chem. Soc.* **2004**, *126*, 15870–15875.
- Ito, A.; Taniuchi, A.; May, T.; Kawata, K.; Okabe, S. Increased Antibiotic Resistance of *Escherichia coli* in Mature Biofilms. *Appl. Environ. Microbiol.* **2009**, *75*, 4093-4100.

Jacoby, G. A.; Griggin, C. M.; Hooper, D. C. *Citrobacter* spp. As a Source of *qnrB* Alleles. *Antimicrob. Agents Chemother.* **2011**, *55*, 4979-4984.

Jang, H. J.; Kim, Y. M.; Yoo, B. Y.; Seo, Y. K. Wound-Healing Effects Of Human Dermal Components With Gelatin Dressing. *J. Biomater. Appl.* **2018**, *32*, 716-724.

Jarvis, W. R.; Martone, W. J. Predominant Pathogens in Hospital Infections. *J. Antimicrob. Chemother.* **1992**, *29*, 19-24.

Jiang, Z. *et al.* Rational design of α -helical antimicrobial peptides to target Gram-negative pathogens, *Acinetobacter baumannii* and *Pseudomonas aeruginosa*: Utilization of charge, 'specificity determinants,' total hydrophobicity, hydrophobe type and location as design parameters to improve the therapeutic ratio. *Chem. Biol. Drug. Des.* **2011**, *77*, 225-240.

Johnson, S.; Boren, K. Topical and Oral Administration of Essential Oils – Safety Issues. *Aromatopia* **2013**, *22*, 43-48.

Jones, E. A.; McGillivray, G.; Bakaletz, L. O. Extracellular DNA Within a Nontypeable Haemophilus Influenzae-Induced Biofilm Binds Human Beta Defensin-3 and Reduces its Antimicrobial Activity. *J. Innate. Immun.* **2013**, *5*, 24-38.

Joshi, J. R.; Khazanov, N.; Senderowitz, H.; Burdman, S.; Lipsky, A.; Yedidia, I. Plant Phenolic Volatiles Inhibit Quorum Sensing in Pectobacteria and Reduce Their Virulence by Potential Binding to Exl and Exr Proteins. *Sci. Rep.* **2016**, *6*, 38126.

Jovanka, L.; Ivana, Č.; Goran, T.; Sava, P.; Slavica, S.; Tamara, C.-G.; Ljiljana, K. In Vitro Antibacterial Activity of Essential Oils from Plant Family Lamiaceae. *Rom. Biotechnol. Lett.* **2011**, *16*, 6034-6041.

Kalia, V. C. ed. *Quorum Sensing vs Quorum Quenching: A Battle with No End in Sight*. Springer, New Delhi, India; **2014**.

Kamaly, N.; Yameen, B.; Wu, J.; Farokhzad, O. C. Degradable Controlled-Release Polymers and Polymeric Nanoparticles: Mechanisms of Controlling Drug Release. *Chem. Rev.* **2016**, *116*, 2602-2663.

Kataoka, K.; Harada, A.; Nagasaki, Y. Block Copolymer Micelles for Drug Delivery: Design, Characterization and Biological Significance. *Adv. Drug. Deliv. Rev.*, **2001**, *47*, 113-131.

Kato, Y.; Uchida, K.; Kawakishi, S. Aggregation Of Collagen Exposed To UVA In The Presence Of Riboflavin: A Plausible Role Of Tyrosine Modification. *Photochem Photobiol.* **1994**, *59*, 343-349.

Kon, K. V.; Rai, M. K. Plant Essential Oils and Their Constituents in Coping with Multidrug-resistant Bacteria. *Expert Rev. Anti-Infect. Ther.* **2012**, *10*, 775-790.

Kostakioti, M.; Hadjifrangiskou, M.; Hultgren, S. J. Bacterial Biofilms: Development, Dispersal, and Therapeutic Strategies in the Dawn of the Postantibiotic Era. *Cold Spring Harb. Perspect. Med.* **2013**, *3*, a010306.

Kujath, P.; Kujath, C. Complicated Skin, Skin Structure and Soft Tissue Infections - Are We Threatened by Multi-Resistant Pathogens? *Eur. J. Med. Res.* **2010**, *15*, 544-553.

Kuroda, K. & Caputo, G. A. Antimicrobial polymers as synthetic mimics of host-defense peptides. *Wiley Interdiscip. Rev. Nanomedicine Nanobiotechnology* **2013**, *5*, 49–66.

Kuroda, K. & DeGrado, W. F. Amphiphilic polymethacrylate derivatives as antimicrobial agents. *J. Am. Chem. Soc.* **2005**, *127*, 4128–4129.

Kuroda, K., Caputo, G. A. & DeGrado, W. F. The role of hydrophobicity in the antimicrobial and hemolytic activities of polymethacrylate derivatives. *Chem. - A Eur. J.* **2009**, *15*, 1123–1133.

Lam, S. J. *et al.* Combating Multidrug-Resistant Gram-Negative Bacteria With Structurally Nanoengineered Antimicrobial Peptide Polymers. *Nat. Microbiol.* **2016**, *1*, 16162.

Landis, R. F.; Gupta, A.; Lee, Y.-W.; Wang, L.-S.; Golba, B.; Couillaud, B.; Ridolfo, R.; Das, R.; Rotello, V. M. Cross-Linked Polymer-Stabilized Nanocomposites for the Treatment of Bacterial Biofilms. *ACS Nano*, **2017**, *11*, 946-952.

Landis, R. F.; Li, C.-H.; Gupta, A.; Lee, Y. -W.; Yazdani, M.; *et al.* Biodegradable Nanocomposite Antimicrobials for the Eradication of Multidrug-Resistant Bacterial Biofilms Without Accumulated Resistance. *J. Am. Chem. Soc.* **2018**, *140*, 6176-6182.

Laxminarayan, R. *et al.* Antibiotic Resistance—The Need For Global Solutions. *Lancet Infect. Dis.* **2013**, *13*, 1057–1098.

Levy, S. B.; Marshall, B. Antibacterial Resistance Worldwide: Causes, Challenges and Responses. *Nat. Med.* **2004**, *10*, S122-S129.

Lewis, K. Riddle of biofilm resistance. *Antimicrob. Agents Chemother.* **2001**, *45*, 999–1007.

Li, X. *et al.* Rapid Identification of Bacterial Biofilms and Biofilm Wound Models Using a Multichannel Nanosensor. *ACS Nano* **2014**, *8*, 12014 –12019.

Li, X.; Robinson, S. M.; Gupta, A.; Saha, K.; *et al.* Functional Gold Nanoparticles as Potent Antimicrobial Agents Against Multi-Drug-Resistant Bacteria. *ACS Nano* **2014**, *8*, 10682-10686.

Li, X.; Yeh, Y.-C.; Giri, K.; Mout, R.; Landis, R. F.; Prakash, Y. S.; Rotello, V. M. Control of Nanoparticle Penetration into Biofilms Through Surface Design. *Chem. Comm.* **2015**, *51*, 282-285.

Lienkamp, K. *et al.* Antimicrobial Polymers Prepared by ROMP with Unprecedented Selectivity: A Molecular Construction Kit Approach. *J. Am. Chem. Soc.* **2008**, *130*, 9836–9843.

Lin, C. C.; Ki, C. S.; Shih, H. Thiol-norbornene Photo-click Hydrogels for Tissue Engineering Applications. *J. Appl. Polym. Sci.* **2015**, *132*, 41563.

Ling, L. L.; Schneider, T.; Peoples, A. J.; Spoering, A. L.; Engels, I.; Conlon, B. P.; Mueller, A.; Schaberle, T. F.; Hughes, D. E.; Epstein, S.; Jones, M.; Lazarides, L.; Steadman, V. A.; Cohen, D. R.; Felix, C. R.; Fetterman, K. A.; Millett, W. P.; Nitti, A. G.; Zullo, A. M.; Chen, C.; Lewis, K. A New Antibiotic Kills Pathogens Without Detectable Resistance. *Nature* **2015**, *517*, 455–459.

Link-Gelles, R.; Thomas, A.; Lynfield, F.; Petit, S.; Schaffner, W.; Harrison, L.; Farley, M. M.; Aragon, D.; Nicols, M.; et al. Geographic and Temporal Trends in Antimicrobial Nonsusceptibility in *Streptococcus Pneumoniae* in the Post-Vaccine Era in the United States. *J. Infect. Dis.* **2013**, *208*, 1266-1273.

Liu, B.; Pop, M. **2009**, ARDB – Antibiotic Resistance Genes Database. *Nucleic Acids Res.* *37*, D443-D447.

Love, J. A., Morgan, J. P., Trnka, T. M. & Grubbs, R. H. A practical and highly active ruthenium-based catalyst that effects the cross metathesis of acrylonitrile. *Angew. Chem., Int. Ed.* **2002**, *41*, 4035-4037.

Luca, M. D.; Maccari, G.; Nifosi, R. Treatment of Microbial Biofilms in the Post-Antibiotic Era: Prophylactic and Therapeutic Use of Antimicrobial Peptides and Their Design by Bioinformatics Tools. *Pathogens and Disease* **2014**, *70*, 257-270.

Lupp, C.; Ruby, E. G. *Vibrio fischeri* uses Two Quorum-Sensing Systems for the Regulation of Early and Late Colonization Factors. *J. Bacteriol.* **2005**, *187*, 3620-3629.

Lynch, A. S.; Robertson, G. T. Bacterial and Fungal Biofilm Infections. *Annu. Rev. Med.* **2008**, *59*, 415-428.

Madhok, B. M.; Vowden, K.; Vowden, P. New Techniques for Wound Debridement. *Int. Wound J.* **2013**, *10*, 247-251.

Madkour, A. E., Koch, A. H. R., Lienkamp, K. & Tew, G. N. End-functionalized ROMP polymers for biomedical applications. *Macromolecules* **2010**, *43*, 4557–4561.

Madsen, J. S.; Burmølle, M.; Hansen, L. H.; Sørensen, S. J. The Interconnection Between Biofilm Formation and Horizontal Gene Transfer. *FEMS Immunol. Med. Microbiol.* **2012**, *65*, 183–195.

Maia, M. F.; Moore, S. J. Plant-Based Insect Repellents: A Review of Their Efficacy, Development and Testing. *Malar. J.* **2011**, *10*, S11.

Marks, L. R.; Reddinger, R. M.; Hakansson, A. P. High Levels of Genetic Recombination During Nasopharyngeal Carriage and Biofilm Formation in *Streptococcus pneumoniae*. *mBio*. **2012**, *3*, e00200-e00212.

Marr, A. K., Gooderham, W. J. & R.E.W., H. Antibacterial peptides for therapeutic use: obstacles and realistic outlook. *Curr. Opin. Pharmacol.* **2006**, *6*, 468–472.

Marrie, T. J.; Nelligan, J.; Costerton, J. W. A Scanning and Transmission Electron Microscopic Study of an Infected Endocardial Pacemaker Lead. *Circulation* **1982**, *66*, 1339-1341.

Mataseje, L. F.; Neumann, N.; Crago, B.; Baudry, P.; Zhanel, G. G.; Louie, M; Mulvey, M. R. Characterization of Cefoxitin-resistant *Escherichia coli* isolates from Recreational Beaches and Private Drinking Water in Canada Between 2004 and 2006. *Antimicrob. Agents Chemother.* **2009**, *53*, 3126-3130.

McCall, A. S.; Kraft, S.; Edelbauser, H. F.; et al. Mechanisms of Corneal Tissue Cross-Linking In Response To Treatment With Topical Riboflavin and Long-Wavelength Ultraviolet Radiation (UVA). *Invest. Ophthalmol. Vis. Sci.* **2010**, *51*, 129-138.

Melo, M. N., Dugourd, D. & Castanho, M. A. R. B. Omiganan pentahydrochloride in the front line of clinical applications of antimicrobial peptides. *Recent Pat. Antiinfect. Drug Discov.* **2006**, *1*, 201–207.

Miller, M. B.; Bassler, B. L. Quorum Sensing in Bacteria. *Annu. Rev. Microbiol.* **2001**, *55*, 165-199.

Mishra, C.; Reiling, S.; Zarena, D.; Wang, G. Host Defense Antimicrobial Peptides as Antibiotics: Design and Application Strategies. *Curr. Opin. Chem. Biol.* **2017**, *38*, 87-96.

Monk, A. B.; Rees, C. D.; Barrow, P.; Hagens, S.; Harper, D. R. Bacteriophage Applications: Where are we now? *Lett. Appl. Microbiol.* **2010**, *51*, 363-369.

Monte, J.; Abreu, C. A.; Borges, A.; Simões, C. L.; Simões, M. Antimicrobial Activity of Selected Phytochemicals Against *Escherichia coli* and *Staphylococcus aureus* and Their Biofilms. *Pathogens* **2014**, *3*, 473–498.

Morales, E.; Cots, F.; Sala, M.; Comas, M.; Belvis, F.; Riu, M.; Salvadó, M.; Grau, S.; Horcajada, J. P.; Montero, M. M.; Castells, X. Hospital Costs of Nosocomial Multidrug-Resistant *Pseudomonas aeruginosa* Acquisition. *BMC Health Serv. Res.* **2012**, *12*, 122–129.

Morar, M.; Wright, G. D. The Genomic Enzymology of Antibiotic Resistance. *Annu. Rev. Genet.* **2010**, *44*, 25-51.

Mosqueda, G.; Ramos, J. L. A Set of Genes Encoding a Second Toluene Efflux System in *Pseudomonas Putida* DOT-T1E is Linked to the Tod Genes for Toluene Metabolism. *J. Bacteriol.* **2000**, *182*, 937-943.

- Mosti, G.; Labichella, M. L.; Picerni, P.; Magliaro, A.; Mattaliano, V. The Debridement of Hard to Heal Leg Ulcers by Means of a New Device Based on Fluidjet Technology. *Int. Wound J.* **2005**, *2*, 307-314.
- Mowery, B. P. *et al.* Mimicry of antimicrobial host-defense peptides by random copolymers. *J. Am. Chem. Soc.* **2007**, *129*, 15474–15476.
- Moyano, D. F. *et al.* Immunomodulatory Effects of Coated Gold Nanoparticles in LPS-Stimulated In Vitro and In Vivo Murine Model Systems. *Chem.* **2016**, *1*, 320–327.
- Mulcahy, H.; Charron-Mazenod, L.; Lewenza, S. Extracellular DNA Chelates Cations and Induces Antibiotic Resistance in *Pseudomonas aeruginosa* Biofilms. *PLoS Pathog.* **2008**, *4*, e1000213.
- Muñoz-Bonilla, A. & Fernández-García, M. Polymeric materials with antimicrobial activity. *Prog. Polym. Sci.* **2012**, *37*, 281–339.
- Nathwani, D.; Raman, G.; Sulham, K.; Gavaghan, M.; Menon, V. Clinical and Economic Consequences of Hospital-Acquired Resistant and Multidrug-Resistant *Pseudomonas aeruginosa* Infections: A Systematic Review and Meta-Analysis. *Antimicrob. Resist. Infect. Control* **2014**, *3*, 32–47.
- Nazzaro, F.; Fratianni, F.; De Martino, L.; Coppola, R.; De Feo, V. Effect of Essential Oils on Pathogenic Bacteria. *Pharmaceuticals* **2013**, *6*, 1451–1474.
- Nederberg, F. *et al.* Biodegradable nanostructures with selective lysis of microbial membranes. *Nat. Chem.* **2011**, *3*, 409–414.
- Norman, A.; Hansen, L. H.; Sorensen, S. J. Conjugative Plasmids: Vessels of the Communal Gene Pool. *Philos. Trans. R. Soc. Lond. B. Biol. Sci.* **2009**, *364*, 2275-2289.
- O’Connell, K. M. G.; Hodgkinson, J. T.; Sore, H. F.; Welch, M.; Salmond, G. P. C.; Spring, D. R. Combating Multidrug-Resistant Bacteria: Current Strategies for the Discovery of Novel Antibacterials. *Angew. Chemie Int. Ed.* **2013**, *52*, 10706–10733.
- Olsen, I. Biofilm-Specific Antibiotic Tolerance and Resistance. *Eur. J. Clin. Microbiol. Infect. Dis.* **2015**, *34*, 877-886.
- O’Reilly, E.; Lanza, J. Fluorescamine: A Rapid and Inexpensive Method for Measuring Total Amino Acids in Nectars. *Ecology* **1995**, *76*, 2656-2660.
- Oussalah, M.; Caillet, S.; Saucier, L.; Lacroix, M. Inhibitory Effects of Selected Plant Essential Oils on the Growth of Four Pathogenic Bacteria: *E. coli* O157:H7, *Salmonella typhimurium*, *Staphylococcus aureus* and *Listeria monocytogenes*. *Food Control* **2007**, *18*, 414-420.
- Palermo, E. F. & Kuroda, K. Structural determinants of antimicrobial activity in polymers which mimic host defense peptides. *Appl. Microbiol. Biotechnol.* **2010**, *87*, 1605–1615.

- Pantos, A.; Tsogas, I.; Paleos, C. M. Guanidinium Group: A Versatile Moiety Inducing Transport and Multicompartmentalization in Complementary Membranes. *Biochim. Biophys. Acta* **2008**, *1778*, 811-823.
- Parameswaran, N., & Patial S. Necrosis Factor- α Signaling In Macrophages. *Crit. Rev. Eukaryot. Gene Expr.* **2010**, *20*, 87-103.
- Patch, J. A. & Barron, A. E. Helical Peptoid Mimics of Magainin-2 Amide. *J. Am. Chem. Soc.* **2003**, *125*, 12092–12093.
- Patravale, V. B.; Mandawgade, S. D. Novel Cosmetic Delivery Systems: An Application Update. *Int. J. Cosmet. Sci.* **2008**, *30*, 19-33.
- Piddock, L. J. Multidrug-Resistance Efflux Pumps – Not Just for Resistance. *Nat. Rev. Microbiol.* **2006**, *4*, 629-636.
- Poirel, L.; Rodriguez-Martinez, J. M.; Mammeri, H.; Liard, A.; Nordmann, P. Origin of Plasmid-Mediated Quinolone Resistance Determinant QnrA. *Antimicrob. Agents Chemother.* **2005**, *49*, 3523-3525.
- Poole, K. Efflux-Mediated Multiresistance in Gram-Negative Bacteria. *Clin. Microbiol. Infect.* **2004**, *10*, 12-26.
- Pounder, R. J.; Stanford, M. J.; Brooks, P.; Richards, S. P.; Dove, A. P. Metal Free Thiol-Maleimide ‘Click’ Reaction as a Mild Functionalisation Strategy for Degradable Polymers. *Chem. Commun.* **2008**, *0*, 5158–5160.
- RD, W. & GD, E. Biofilms and chronic infections. *JAMA* **2008**, *299*, 2682–2684.
- Reichert, J. M. Antibodies to Watch in 2015. *MAbs* **2015**, *7*, 1-8.
- Reuter, K.; Steinbach, A.; Helms, V. Interfering with Bacterial Quorum Sensing. *Perspectives in Medicinal Chemistry* **2016**, *8*, 1-15.
- Richards, M. J.; Edwards, J. R.; Culver, D. H.; Gaynes, R. P. Nosocomial Infections in Combined Medical-Surgical Intensive Care Units in the United States. *Infect. Control Hosp. Epidemiol.* **2000**, *21*, 510–515.
- Rodriguez-Martinez, J. M.; Cano, M. E.; Velasco, C.; Martinez-Martinez, L.; Pascual, A. Plasmid-Mediated Quinolone Resistance: an Update. *J. Infect. Chemother.* **2011**, *17*, 149-182.
- Romling, U.; Balsalobre, C. Biofilm Infections, Their Resilience to Therapy and Innovative Treatment Strategies. *J. Intern. Med.* **2012**, *272*, 541-561.
- Roy, S.; Elgharably, H.; Sinha, M.; Ganesh, K.; Chaney, S.; Mann, E.; Miller, C.; Khanna, S.; Bergdall, V. K.; Powell, H. M.; Cook, C. H.; Gordillo, G. M.; Wozniak, D. J.; Sen, C.

K. Mixed-species Biofilm Compromises Wound Healing by Disrupting Epidermal Barrier Function. *J. Pathol.* **2014**, *233*, 331-343.

Saha, K.; Rahimi, M.; Yazdani, M.; Kim, S. T.; Moyano, D. F.; Hou, S.; Das, R.; Mout, R.; Rezaee, F.; Mahmoudi, M.; Rotello, V. M. Regulation of Macrophage Recognition through the Interplay of Nanoparticle Surface Functionality and Protein Corona. *ACS Nano* **2016**, *10*, 4421–4430.

Sambhy, V.; Peterson, B. R.; Sen, A. Antibacterial and Hemolytic Activities of Pyridinium Polymers as a Function of the Spatial Relationship Between the Positive Charge and the Pendant Alkyl Tail. *Angew. Chem. Int. Ed.* **2008**, *47*, 1250-1254.

Samperio, C.; Boyer, R.; Eigel III, W. N.; Holland, K. W.; McKinney, J. S.; O’Keefe, S. F.; Smith, R.; Marcy, J. E. Enhancement of Plant Essential Oils’ Aqueous Solubility and Stability Using Alpha and Beta Cyclodextrin. *J. Agric. Food Chem.* **2010**, *58*, 12950-12956.

Sanchez, C. J.; Mende, K.; Beckius, M. L.; Akers, K. S.; Romano, D. R.; Wenke, J. C.; Murray, C. K. Biofilm Formation by Clinical Isolates and the Implications in Chronic Infections. *BMC Infect. Dis.* **2013**, *13*, 47–58.

Sanchez-Moreno, P.; Buzon, P.; Boulaiz, H.; Peula-Garcia, J. M.; Ortega-Vinuesa, J. L.; Luque, I.; Salvati, A.; Marchal, J. A. Balancing the Effect of Corona on Therapeutic Efficacy and Macrophage Uptake of Lipid Nanocapsules. *Biomaterials* **2015**, *61*, 266-278.

Sanchez-Moreno, P.; Ortega-Vinuesa, J. L.; Martin-Rodriguez, A.; Boulaiz, H.; Marchal-Corrales, J. A.; Peula-Garcia, J. M. Characterization of Different Functionalized Lipidic Nanocapsules as Potential Drug Carriers. *Int. J. Mol. Sci.* **2012**, *13*, 2405-2424.

Sanson, C.; Schatz, C.; Le Meins, J.-F.; Brûlet, A.; Soum, A.; Lecommandoux, S. Biocompatible and Biodegradable Poly(trimethylene carbonate)-b-Poly(L-glutamic acid) Polymersomes: Size Control and Stability. *Langmuir* **2010**, *26*, 2751–2760.

Sauer, K.; Camper, A. K.; Ehrlich, G. D.; et al. *Pseudomonas aeruginosa* Displays Multiple Phenotypes During Development as a Biofilm. *J. Bacteriol.* **2002**, *184*, 1140-1154.

Saviuc, C.-M.; Drumea, V.; Olariu, L.; Chifiriuc, M.-C.; Bezirtzoglou, E.; Lazar, V. Essential Oils with Microbicidal and Antibiofilm Activity. *Curr. Pharm. Biotechnol.* **2015**, *16*, 137-151.

Schierle, C. F.; De la Garza, M.; Mustoe, T. A.; Galiano, R. D. *Staphylococcal* Biofilms Impair Wound Healing by Delaying Reepithelialization in a Murine Cutaneous Wound Model. *Wound Repair Regen.* **2009**, *17*, 354–359.

Schulz, M.; Iwersen-Bergmann, S.; Andresen, H.; Schmoldt, A. Therapeutic and Toxic Blood Concentrations of Nearly 1,000 Drugs and Other Xenobiotics. *Crit. Care* **2012**, *16*, R136-R139.

- Scotta, C.; Juan, C.; Cabot, G.; Oliver, A.; Lalucat, J.; Bennasar, A.; Alberti, S. Environmental Microbiota Represents a Natural Reservoir for Dissemination of Clinically Relevant Metallo-beta-Lactamases. *Antimicrob. Agents Chemother.* **2011**, *55*, 5376-5379.
- Scutera, S.; Zucca, M.; Savoia, D. Novel Approaches for the Design and Discovery of Quorum-Sensing Inhibitors. *Expert Opin. Drug. Discov.* **2014**, *9*, 353-366.
- Seo, M. -D.; Won, H. -S.; Kim, J. -H.; Mishig-Ochir, T.; Lee, B. -J. Antimicrobial Peptides for Therapeutic Applications: A Review. *Molecules* **2012**, *17*, 12276-12286.
- Serra, R.; Grande, R.; Butrico, L.; Rossi, A.; Settimio, U. F.; Caroleo, B.; Amato, B.; Gallelli, L.; de Franciscis, S. Chronic Wound Infections: The Role of *Pseudomonas aeruginosa* and *Staphylococcus aureus*. *Expert Rev. Anti. Infect. Ther.* **2015**, *13*, 605-613.
- Shah, N. S.; Wright, A.; Bai, G. H.; Barrera, L.; Boulahbal, F.; et al. Worldwide Emergence of Extensively Drug-Resistant Tuberculosis. *Emerg. Infect. Dis.* **2007**, *13*, 380-387.
- Sharifi-Rad, J.; Sharifi-Rad, M.; Hoseini-Alfatemi, S. M.; Iriti, M. Composition, Cytotoxic and Antimicrobial Activities of Satureja Intermedia C.A.Mey Essential Oil. *Int. J. Mol. Sci.* **2015**, *16*, 17812-17825.
- Shi, Y.; Huang, J.; Zeng, G.; Gu, Y.; et al. Exploiting Extracellular Polymer Substances (EPS) Controlling Strategies for Performance Enhancement of Biological Wastewater Treatments: An Overview. *Chemosphere* **2017**, *180*, 396-411.
- Sieprawska-Lupa, M. *et al.* Degradation of human antimicrobial peptide LL-37 by *Staphylococcus aureus*-derived proteinases. *Antimicrob. Agents Chemother.* **2004**, *48*, 4673-4679.
- Simoes, M.; Bennett, R. N.; Rosa, E. A. S. Understanding Antimicrobial Activities of Phytochemicals Against Multidrug-Resistant Bacteria and Biofilms. *Nat. Prod. Rep.* **2009**, *26*, 746-757.
- Simone, E. A.; Dziubla, T. D.; Muzykantov, V. R.; Eric A Simone, Thomas D Dziubla, V. R. M. Polymeric Carriers: Role of Geometry in Drug Delivery. *Expert Opin. Drug Deliv.* **2008**, *5*, 1283-1300.
- Singh, A.; Halder, S.; Menon, G.R.; et al. Meta-analysis of Randomized Controlled Trials on Hydrocolloid Occlusive Dressing Versus Conventional Gauze Dressing in the Healing of Chronic Wounds. *Asian J. Surg.* **2004**, *27*, 326-332.
- Singh, P.; Shukla, R.; Prakash, B.; Kumar, A.; et al. Chemical Profile, Antifungal, Antiaflatoxigenic and Antioxidant Activity of *Citrus maxima* Burm. And *Citrus sinensis* (L.) Osbeck Essential Oils and their Cyclic Monoterpene, DL-Limonene. *Food Chem. Toxicol. Int. J. Publ. Br. Ind. Biol. Res. Assoc.* **2010**, *48*, 1734-1740.

- Singh, R.; Ray, P.; Das, A.; et al. Penetration of Antibiotics Through *Staphylococcus aureus* and *Staphylococcus epidermidis* Biofilms. *J. Antimicrob. Chemoth.* **2010**, *65*, 1955-1958.
- Song, Z.; Borgwardt, L.; Hoiby, N.; Wu, H.; Sorensen, T. S.; Borgwardt, A. Prosthesis Infections After Orthopedic Joint Replacement: The Possible Role of Bacterial Biofilms. *Orthop. Rev. (Pavia)* **2013**, *5*, 65-71.
- Stewart, P. S.; William Costerton, J. Antibiotic Resistance of Bacteria in Biofilms. *Lancet* **2001**, *358*, 135–138.
- Štimac, A.; Šekutor, M.; Mlinarić-Majerski, K.; Frkanec, L.; Frkanec, R. Adamantane in Drug Delivery Systems and Surface Recognition. *Molecules*, **2017**, *22*, 297.
- Stone, G.; Wood, P.; Dixon, L.; et al. Tetracycline Rapidly Reaches all the Constituent Cells of Uropathogenic *Escherichia coli* Biofilms. *Antimicrob. Agents. Ch.* **2002**, *46*, 2458-2461.
- Suci, P. A.; Mittelman, M. W.; Yu, F. P.; et al. Investigation of Ciprofloxacin Penetration into *Pseudomonas aeruginosa* Biofilms. *Antimicrob. Agents. Ch.* **1994**, *38*, 2125-2133.
- Sukegawa, T.; Masuko, I.; Oyaizu, K.; Nishide, H. Expanding the Dimensionality of Polymers Populated with Organic Robust Radicals Toward Flow Cell Application: Synthesis of TEMPO-Crowded Bottlebrush Polymers using Anionic Polymerization and ROMP. *Macromolecules* **2014**, *47*, 8611–8617.
- Sun, B. K.; Siphraşvili, Z.; Khavari, P. A. Advances in Skin Grafting and Treatment of Cutaneous Wounds. *Science* **2014**, *346*, 941-945.
- Sun, Y.; Sun, T.-L.; Huang, H. W. Mode of Action of Antimicrobial Peptides on *E. coli* Spheroplasts. *Biophys. J.* **2016**, *111*, 132-139.
- Szomolay, B.; Klapper, I.; Dockery, J.; Stewart, P. S. Adaptive Responses to Antimicrobial Agents in Biofilms. *Environ. Microbiol.* **2005**, *7*, 1186–1191.
- Tackling Drug-Resistant Infections Globally: Final Report and Recommendations, May 19, 2016, <https://amr-review.org/Publications> (accessed Aug 2018).
- Talelli, M.; Rijcken, C. J. F.; Lammers, T.; Seevinck, P. R.; Storm, G.; et al. Superparamagnetic Iron Oxide Nanoparticles Encapsulated in Biodegradable Thermosensitive Polymer Micelles: Toward a Targeted Nanomedicine Suitable for Image-Guided Drug Delivery. *Langmuir* **2009**, *25*, 2060-2067.
- Tam, V. H.; Rogers, C. A.; Chang, K.-T.; Weston, J. S.; Caeiro, J.-P.; Garey, K. W. Impact of Multidrug-Resistant *Pseudomonas aeruginosa* Bacteremia on Patient Outcomes. *Antimicrob. Agents Chemother.* **2010**, *54*, 3717–3722.

Tashiro, T. Antibacterial and Bacterium Adsorbing Macromolecules. *Macromol. Mater. Eng.* **2001**, *286*, 63–87.

Tetz, G.; Tetz, V. Bacteriophage Infections of Microbiota can Lead to Leaky Gut in an Experimental Rodent Model. *Gut Pathog.* **2016**, *8*, 33.

Trautner, B. W.; Darouiche, R. O. Role of Biofilm in Catheter-Associated Urinary Tract Infection. *Am. J. Infect. Control* **2004**, *32*, 177-183.

Tseng, B. S.; Zhang, W.; Harrison, J. J.; Quach, T. P.; Song, J. L.; Penterman, J.; Singh, P. K.; Chopp, D. L.; Packman, A. I.; Parsek, M. R. The Extracellular Matrix Protects *Pseudomonas aeruginosa* Biofilms by Limiting the Penetration of Tobramycin. *Environ. Microbiol.* **2013**, *15*, 2865–2878.

Turek, C.; Stintzing, F. C. Stability of Essential Oils: A Review. *Compr. Rev. Food. Sci. Food Saf.* **2013**, *12*, 40-53.

Udenfriend, S.; Stein, S.; Bohlen, P.; Dairman, W.; Leimgruber, W.; Weigele, M. Fluorescamine: A Reagent for Assay of Amino Acids, Peptides, Proteins, and Primary Amines in the Picomole Range. *Science* **1972**, *178*, 871-872.

Van Amersfoort, E. S., Van Berkel, T. J. C. & Kuiper, J. Receptors, mediators, and mechanisms involved in bacterial sepsis and septic shock. *Clin. Microbiol. Rev.* **2003**, *16*, 379–414.

Veerachamy, S.; Yarlagadda, T.; Manivasagam, G.; Yarlagadda, P. K. Bacterial Adherence and Biofilm Formation on Medical Implants: A Review. *P. I. Mech. Eng. H* **2014**, *228*, 1083-1099.

Veldhuizen, E. J. A.; Creutzberg, T. O.; Burt, S. A.; Haagsman, H. P. Low Temperature And Binding To Food Components Inhibit The Antibacterial Activity Of Carvacrol Against *Listeria Monocytogenes* In Steak Tartare. *J. Food. Prot.* **2007**, *70*, 2127-2132.

Vergis, J.; Gokulakrishnan, P.; Agarwal, R. K.; Kumar, A. Essential Oils as Natural Food Antimicrobial Agents: A Review. *Crit Rev Food Sci Nutr* **2015**, *55*, 1320-1383.

Vian, M. A.; Fernandez, X.; Visinoni, F.; Chemat, F. Microwave Hydrodiffusion and Gravity, a New Technique for Extgraction of Essential Oils. *J. Chromatogr. A* **2008**, *1190*, 14-17.

Vroom, J. M.; De Grauw, K. J.; Gerritsen, H. C.; Bradshaw, D. J.; Marsh, P. D.; Watson, G. K.; Birmingham, J. J.; Allison, C. Depth Penetration and Detection of pH Gradients in Biofilms by Two-Photon Excitation Microscopy. *Appl. Environ. Microbiol.* **1999**, *65*, 3502-3511.

Walters, M. C.; Roe, F.; Bugnicourt, A.; Franklin, M. J.; Stewart, P. S. Contributions of Antibiotic Penetration, Oxygen Limitation, and Low Metabolic Activity to Tolerance of

Pseudomonas aeruginosa Biofilms to Ciprofloxacin and Tobramycin. *Antimicrob. Agents Chemother.* **2003**, *47*, 317–323.

Wang, G.; Li, X.; Wang, Z. APD3: The Antimicrobial Peptide Database as a tool for Research and Education. *Nucleic Acids Res.* **2016**, *44*, D1087-D1093.

Wang, H.; Khor, T. O.; Shu, L.; Su, Z.; Fuentes, F.; Lee, J.-H.; Kong, A.-N. T. Plants Against Cancer: A Review on Natural Phytochemicals in Preventing and Treating Cancers and Their Druggability. *Anticancer Agents Med. Chem.* **2012**, *12*, 1281-1305.

Wang, H.; Wu, H.; Ciofu, O.; Song, Z.; Høiby, N. In Vivo Pharmacokinetics/Pharmacodynamics of Colistin and Imipenem in *Pseudomonas aeruginosa* Biofilm Infection. *Antimicrob. Agents Chemother.* **2012**, *56*, 2683-2690.

Wang, L.; Weller, C. L. Recent Advances in Extraction of Nutraceuticals from Plants. *Trends Food Sci. Technol.* **2006**, *17*, 300-312.

Wang, L.-S.; Gupta, A.; Rotello, V. M. Nanomaterials for the Treatment of Bacterial Biofilms. *ACS Infect. Dis.* **2015**, *2*, 3-4.

Wiegand, I., Hilpert, K. & Hancock, R. E. W. Agar and broth dilution methods to determine the minimal inhibitory concentration (MIC) of antimicrobial substances. *Nat. Protoc.* **2008**, *3*, 163–75.

Wilton, M.; Charron-Mazenod, L.; Moore R.; et al. Extracellular DNA Acidifies Biofilms and Induces Aminoglycoside Resistance in *Pseudomonas aeruginosa*. *Antimicrob. Agents Ch.* **2015**, *60*, 544-553.

Wittebole, X.; De Roock, S.; Opal, S. M. A Historical Overview of Bacteriophage Therapy as an Alternative to Antibiotics for the Treatment of Bacterial Pathogens. *Virulence* **2014**, *5*, 226-235.

Wolfram, J.; Yang, Y.; Shen, J.; Moten, A.; Chen, C.; Shen, H.; Ferrari, M.; Zhao, Y. The Nano-plasma Interface: Implications of the Protein Corona. *Colloids Surf. B Biointerfaces* **2014**, *124*, 17-24.

Wu, H.; Moser, C.; Wang, H.; Høiby, N.; Song, Z.-J.; Hoiby, N.; Song, Z.-J. Strategies for Combating Bacterial Biofilm Infections. *Int. J. Oral Sci.* **2014**, *7*, 1–7.

Xu, C.; Li, J.; Yang, L.; Shi, F.; Yang, L.; Ye, M. Antibacterial Activity and a Membrane Damage Mechanism of *Lachnum* YM30 Melanin Against *Vibrio parahaemolyticus* and *Staphylococcus aureus*. *Food Control* **2017**, *73*, 1445-1451.

Yang, J.; Liu, F.; Yang, L.; Li, S. Hydrolytic and Enzymatic Degradation of Poly(trimethylene carbonate-co-D,L-lactide) Random Copolymers With Shape Memory Behavior. *Eur. Polym. J.* **2010**, *46*, 783–791.

Yin, L. M., Edwards, M. A., Li, J., Yip, C. M. & Deber, C. M. Roles of hydrophobicity and charge distribution of cationic antimicrobial peptides in peptide-membrane interactions. *J. Biol. Chem.* **2012**, *287*, 7738–7745.

Zeeb, B.; Gibis, M.; Fischer, L.; Weiss, J. Influence of Interfacial Properties on Ostwald Ripening in Crosslinked Multilayered Oil-in-water Emulsions. *J. Colloid Interface Sci.* **2012**, *387*, 65-73.

Zhou, Z.; Zheng, A.; Zhong, J., Interactions of Biocidal Guanidine Hydrochloride Polymer Analogs with Model Membranes: A Comparative Biophysical Study. *Acta Biochim Biophys Sin (Shanghai)* **2011**, *43*, 729-737.

Zhu, D. Y.; Guo, J. W.; Xian, J. X.; Fu, S. Q. Novel Sulfonate-Containing Halogen-Free Flame-Retardants: Effect of Ternary and Quaternary Sulfonates Centered on Adamantane on the Properties of Polycarbonate Composites. *RSC Adv.* **2017**, *7*, 39270-39278.

Ziani, K.; Chang, Y.; McLandsborough, L.; McClements, D. J. Influence of Surfactant Charge on Antimicrobial Efficacy of Surfactant-Stabilized Thyme Oil Nanoemulsions. *J. Agric. Food Chem.* **2011**, *59*, 6247-6255.